

GRAPHOMNI: A COMPREHENSIVE AND EXTENSIBLE BENCHMARK FRAMEWORK FOR LARGE LANGUAGE MODELS ON GRAPH-THEORETIC TASKS

000
001
002
003
004
005
006
007
008
009
010
011
012
013
014
015
016
017
018
019
020
021
022
023
024
025
026
027
028
029
030
031
032
033
034
035
036
037
038
039
040
041
042
043
044
045
046
047
048
049
050
051
052
053
Anonymous authors
Paper under double-blind review

ABSTRACT

This paper introduces GRAPHOMNI, a comprehensive benchmark designed to evaluate the reasoning capabilities of LLMs on graph-theoretic tasks articulated in natural language. GRAPHOMNI spans diverse graph types, serialization formats, and prompting schemes, substantially extending upon prior efforts in both scope and depth. Through systematic evaluation, we uncover critical interactions among these dimensions, revealing their decisive impact on model performance. Our experiments show that state-of-the-art closed-source models such as Claude-3.5 and o4-mini consistently lead overall, yet still leave considerable headroom, while open-source models display pronounced sensitivity to various design choices. Beyond the standard scope, larger graphs, real-world graphs, and additional NP-hard tasks are further discussed. We further analyze efficiency via output token usage, highlighting cost-accuracy trade-offs, and introduce a reinforcement learning-based optimizer that adaptively selects factor combinations, reducing evaluation cost by 75% while retaining strong accuracy. This flexible and extensible benchmark not only deepens understanding of LLM performance on structured graph reasoning but also establishes a robust foundation for advancing model design and evaluation. The code and datasets are available at <https://anonymous.4open.science/r/ID-14092>.

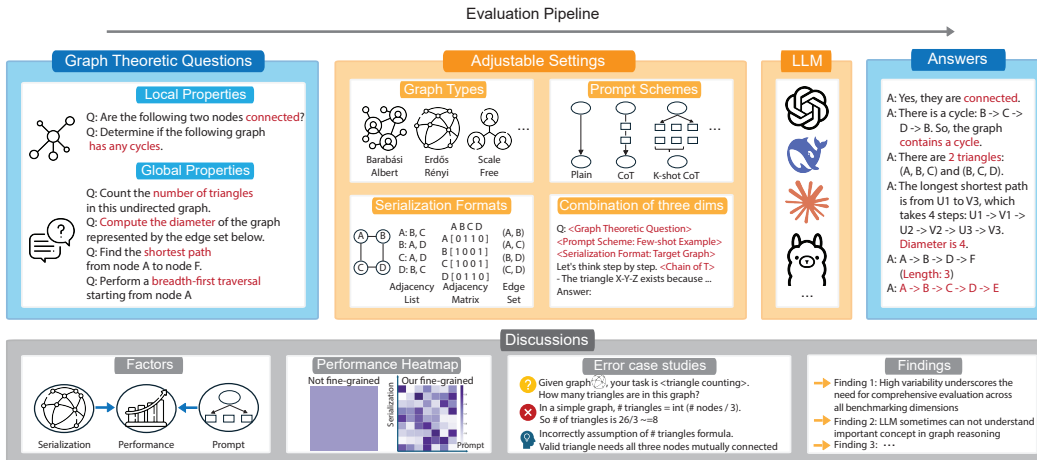


Figure 1: **GRAPHOMNI Evaluation Pipeline.** We convert graph-theoretic tasks into text-based questions about local and global properties. In the adjustable settings, we vary three dimensions, i.e., graph type, serialization format, and prompt scheme, and then generate every possible combination.

1 INTRODUCTION

Large Language Models (LLMs) have emerged as a transformative force in natural language processing (NLP), demonstrating state-of-the-art performance in tasks such as open-ended text generation, summarization, and problem-solving (Radford et al., 2019; Brown et al., 2020; Raffel et al., 2020;

Lewis et al., 2020). However, their application to structured reasoning on graph-based data remains relatively underexplored. Graphs, defined by their nodes and edges, encapsulate complex relationships that are crucial to many real-world applications, including social network analysis (Easley et al., 2010), recommendation systems (Wu et al., 2022), out-of-distribution detection (Fang et al., 2025a), and drug discovery (Gaudelot et al., 2021).

Traditional approaches to graph analysis primarily rely on Graph Neural Networks (GNNs) that are designed with specialized representations and training paradigms tailored for tasks such as node classification (Wu et al., 2020), link prediction (Zhang & Chen, 2018), and community detection (Su et al., 2022). In contrast, LLMs are trained on vast quantities of unstructured or semi-structured text and excel at reasoning about entities and relationships described linguistically, as evidenced by benchmarks like MMLU (Hendrycks et al., 2021a) and MATH (Hendrycks et al., 2021b). This discrepancy raises a pivotal question: **Can LLMs be effectively harnessed to understand and manipulate graph-theoretic concepts when graphs are articulated in natural language?**

To address this question, a multi-dimensional evaluation is required rather than tuning a single knob. Prior work has examined individual components in isolation, including prompting strategies (Wang et al., 2023; Fatemi et al., 2024), textual graph serialization (Xypolopoulos et al., 2024), or specific graph families (Zhang et al., 2024b), but this piecemeal view obscures how these choices interact. We therefore vary three interacting dimensions jointly. First, **graph type**: different graph types exhibit distinct structures, so we use synthetic generators (ER, BA, scale-free, bipartite) to produce them, which in turn affects how readily a text description can capture these structures. Second, **serialization format**: the same graph written as an adjacency list or matrix, an edge set, or a richer schema can help or hinder model reading. Third, **prompt scheme**: the way the question is posed (zero-shot, few-shot, instructive, algorithmic, chain-of-thought) can shift answers even with identical inputs. As summarized in Table 1, previous studies do not vary these dimensions together, so they cannot determine whether gains come from the model, the representation, or the instruction, nor explain why a setting that benefits one model may harm another. Consequently, we still lack a comprehensive and robust understanding of LLM capabilities in graph reasoning.

Table 1: Comparison of existing graph-related benchmarks for LLM with our GRAPHOMNI. We evaluate their inclusion of different types of graphs, serialization formats, and prompt schemes, noting a gap between recent works and ours. Additionally, GRAPHOMNI is the only work with a random baseline as well as a modularized and expandable framework design. More related works are included in Detailed Related Works in Appendix F.

Benchmarks	Graph Sources			Serializations		Prompt Schemes		Evaluation Framework	
	# Samples	# Graph Types [*]	Node Size	Multiple Types	# Types	Multiple Types	# Types	Random Baseline	Modularized
LLM4DyG (Zhang et al., 2024b)	900 (100 per task)	4	5 to 20	✗	1	✓	4	✓	✗
GraphInstruct (Luo et al., 2024b)	N/A	3	5 to 35	✓	3	✗	1	✗	✓
MAGMA (Taylor et al., 2024)	~ 400	1	5 to 50	✗	1	✗	1	✗	✗
NLGraph (Wang et al., 2023)	5,902	1	5 to 35	✗	1	✓	5	✓	✗
GPC (Dai et al., 2024)	350	1	5 to 35	✓	2	✗	N/A	✗	✗
GraphWiz (Chen et al., 2024a)	3,600	1	2 to 100	✗	1	✗	1	✗	✗
GPT4Graph (Gu et al., 2024a)	N/A	1	10 to 20	✓	4	✓	6	✗	✗
GraphArena (Tang et al., 2025)	10,000	N/A	5 to 30 [†]	✗	1	✗	1	✗	✗
GraphQA (Fatemi et al., 2024)	2,300	7	5 to 20	✗ (only via text)	1	✓	6	✗	✓
NLGif (Zhang et al., 2024a)	37,000	2	3 to 25	✗	1	✗	1	✗	✗
GraphWild (Zhang et al., 2025)	49,224	5	N/A	✗	1	✗	1	N/A	N/A
GRAPHOMNI	241,726	7	5 to 30	✓	7	✓	9	✓	✓

^{*} Note that # Graph Types is targeted for synthetic datasets and reflects the number of types of random graph generators.

[†] The range is for all non-trivial tasks, excluding nearest neighbor and shortest distance.

To address this gap, we propose GRAPHOMNI, a unified benchmark with an extensible framework, summarized in Figure 1. It represents the most comprehensive graph-theory-based evaluation framework developed to date, compared with all related works in Table 1. It spans various graph types, serialization formats, and prompt schemes, surpassing previous works in scope and granularity. Furthermore, our framework is designed as an extensible and flexible evaluation system. Researchers can easily incorporate new graph generators, serialization methods, and prompt strategies, thereby ensuring that the benchmark remains current with evolving methodologies in both LLM research and graph theory. A random baseline is then implemented to ensure a fair evaluation.

With the help of GRAPHOMNI we clearly demonstrate that no single serialization or prompt works best for all models and accuracy varies widely across graph types, serializations, and prompts, which validates the need for our multi-dimensional design and per-task configuration. Additionally, model

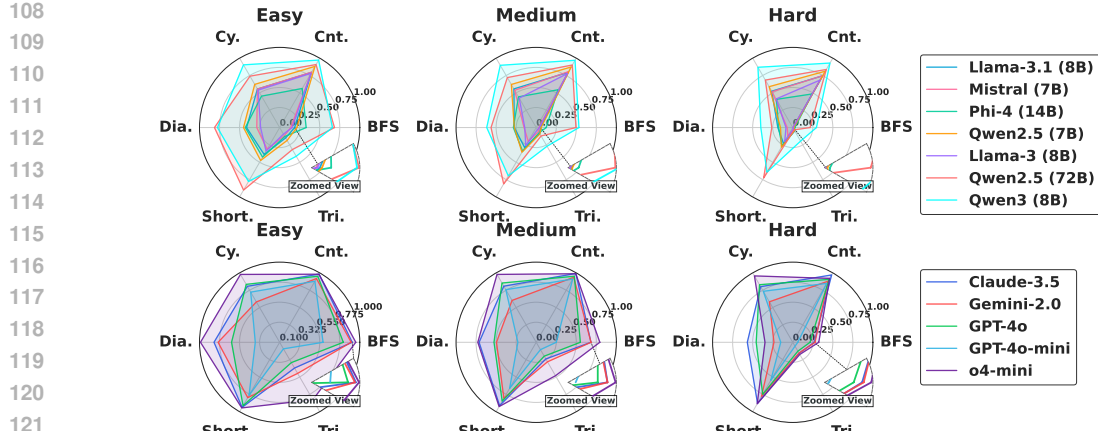


Figure 2: Radar charts comparing the performance of open-source (top row) and closed-source (bottom row) LLMs across six canonical graph reasoning tasks at three difficulty levels.

performance requires further improvement overall: Claude-3.5 and o4-mini lead across tasks and difficulty levels, yet even they fall short of the near-perfect accuracy a non-specialist human evaluator could achieve on 5–30 node problems given sufficient time. To verify the robustness of the evaluation results, we extend the analysis to larger graphs, NP-hard tasks, and conduct a representativeness check on real-world graphs, all of which yield the same trends. Motivated by these results, we introduce a simple RL-inspired selector that chooses the optimal settings (prompt + serialization) for each task, thereby improving accuracy at a minimal extra cost. We summarize our contributions as:

* **Novel benchmark:** We introduce GRAPHOMNI, the most comprehensive benchmark to our knowledge for evaluating graph-theoretic reasoning in LLMs, covering a wide range of synthetic graph types, diverse serialization formats, and varied prompt schemes.

* **Comprehensive evaluation framework:** We design a flexible and extensible evaluation framework that allows for the seamless addition or removal of graph generators, serialization methods, and prompt schemes, ensuring adaptability to future research developments. We also include extended studies on larger graphs (30–50 nodes), real-world datasets, and NP-Hard tasks, which together confirm the robustness and transferability of our conclusions.

* **Insightful empirical observations:** State-of-the-art models still exhibit considerable room for improvement overall. Our experiments reveal substantial performance variance, with notable accuracy differences across different serialization and prompting configurations, emphasizing the need for comprehensive evaluation across all dimensions to provide fair and trustworthy understandings.

* **Practical methods inspired by observations:** Motivated by the above observations, we develop an RL-based adaptive mechanism that dynamically selects the optimal factors, achieving near-optimal performance with only a small exploration cost.

2 GRAPHOMNI

Overview and Statistics. GRAPHOMNI rigorously evaluates LLM performance on graph reasoning by examining the interplay between graph structure, textual representation, and prompt formulation. It comprises four key components: **Benchmark Tasks**, **Graph Types**, **Prompt Schemes**, and **Serialization Formats**. Figure 1 illustrates how these four components form our end-to-end evaluation pipeline. **Benchmark Tasks** cover canonical graph problems that test both local and global reasoning. **Graph Types** are defined by diverse synthetic datasets generated by different random graph generators, including stochastic, scale-free, and bipartite models. **Prompt Schemes** incorporate various query designs such as algorithmic, chain-of-thought, k-shot, instructive, and zero-shot approaches. **Serialization Formats** convert graph data into text using methods like adjacency lists, matrices, and the GMoL. Moreover, we have designed three difficulty modes for all graph-related tasks, determined by the number of nodes: Easy (5–10 nodes), Medium (10–20 nodes), and Hard (20–30 nodes). This unified and extensible framework distinguishes itself by integrating multiple dimensions of graph reasoning into a single evaluation platform, thereby providing comprehensive insights into LLM

162 performance on complex, structured data. The basic statistics of GRAPHOMNI are presented in
 163 Table 2, while token statistics for different combinations are shown in Figure 3. In summary, our
 164 dataset contains a total of 241,726 queries. More detailed statistics are in Appendix B.
 165

166 **Graph Tasks.** We consider **6 canonical tasks** that cap-
 167 ture both local and global properties of graphs, thereby
 168 requiring diverse reasoning capabilities from LLMs.
 169 Connectivity involves determining whether a path exists
 170 between two designated nodes, testing the model’s under-
 171 standing of local linkages. Cycle detection requires veri-
 172 fying the presence of any cycle, which probes the model’s
 173 ability to recognize recurring patterns in connectivity.
 174 Diameter calculation demands calculating the max-
 175 imum distance between any two nodes, thereby challeng-
 176 ing the model to grasp the global network structure. BFS
 177 order tests the ability to generate an ordered sequence
 178 of nodes as encountered in a breadth-first search, assess-
 179 ing sequential output and structured reasoning. Triangle
 180 counting requires precise numerical enumeration of 3-
 181 cycles, blending quantitative precision with structural in-
 182 sight. Shortest path tasks compel the model to identify
 183 the most efficient route between two nodes. Collectively,
 184 these tasks provide a robust measure of performance across
 185 both binary decisions and nuanced numerical analyses. For
 186 more details on the design of the graph task, please refer to Appendix A.3, where we further discuss
 187 the rationale behind the task selection and analyze the distinct capability demands of each task in
 188 Appendix A.3.1. We also include NP-hard tasks for extended discussion, elaborated in Appendix C.4.

189 **Graph Generators (Types of Graphs).** To mirror the diversity found in real-world net-
 190 works, our benchmark incorporates a broad array of graph families of **7 types**, each pre-
 191 senting unique structural characteristics that challenge LLM reasoning. ER Graphs are gen-
 192 erated by random sampling from the space of all graphs with n vertices. Within this fam-
 193 ily, ERM employs a fixed edge count m , randomly chosen between 1 and $\frac{n(n-1)}{2}$, while
 194 ERP uses a probability-based approach with an edge probability drawn uniformly from $[0, 1]$.
 195 Extending these models to capture structured varia-
 196 tions, Bipartite ER Graphs (denoted as BERM and BERP)
 197 impose bipartite constraints that yield additional topo-
 198 logical diversity. To reflect the power-law distribu-
 199 tions prevalent in real-world networks, we include
 200 Barabási-Albert Graphs (BAG), generated by ini-
 201 tializing a complete graph of m_0 vertices (with m_0
 202 randomly chosen up to $\frac{n}{3}$) and sequentially adding
 203 nodes that form $m = m_0 + 1$ connections via pre-
 204 ferential attachment. Recognizing that many practical
 205 networks are hierarchical or tree-like, we extend BAG
 206 to Barabási-Albert Forests (BAF) by enforcing an acyclic topology. Moreover, our framework
 207 features Scale-Free (SF) Graphs generated via a degree-weighted random connection strategy,
 208 which can yield multiple disconnected components, offering a complementary perspective to BAG.
 209 A detailed description of each type of graph can be found in Appendix A.4, where we also provide
 210 the detailed rationale for this selection and empirical evidence showing that even within the 5–30
 211 node range, the chosen generators yield statistically distinct and representative structural regimes in
 212 Appendix A.4.1.

213 **Prompt Schemes.** Recognizing that the formulation of query prompts critically influences LLM
 214 reasoning, our benchmark systematically evaluates **9 distinct prompt schemes** that vary in the degree
 215 of explicit guidance provided. The k-Shot prompts supply multiple exemplars from simpler graph
 216 instances to prime the model with relevant examples. The Algorithm prompts (Wang et al., 2023)
 217 explicitly delineate a well-known algorithm (such as BFS or Dijkstra), offering clear procedural
 218 instructions. In contrast, Chain-of-Thought (CoT) prompts (Wei et al., 2022) encourage the model to
 219 articulate intermediate reasoning steps, thereby exposing its internal thought process. The Instruct

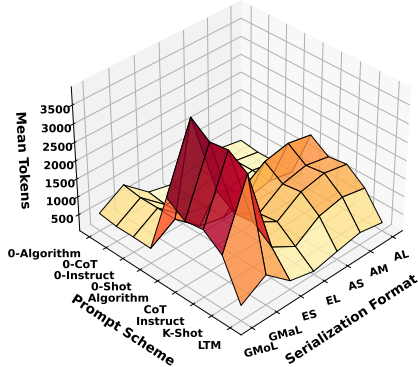


Figure 3: **Token usage for prompt-serializ-
 ation combinations by GPT-4 tokenizer.** More detailed statistics are included in Figures 6a and 6b.

Table 2: **Statistical summary of
 GRAPHOMNI over tasks at all difficulty
 levels.** More statistics are in Table 7.

Difficulty	Easy	Medium	Hard
Numbers	88956	87318	65452
Avg. Nodes	8.01	14.70	26.61
Avg. Edges	11.70	34.51	77.60

216 prompts use directive language tailored for instruction-based models to elicit focused responses.
 217 All three types above come with few-shot examples. For cases requiring minimal intervention, the
 218 0-Shot (i.e., plain) prompts pose bare questions without supplementary cues. To further investigate
 219 the impact of reasoning visibility, we also include variants without few-shot examples, such as 0-CoT,
 220 0-Instruct, and 0-Algorithm, which deliberately restrict the exposure of intermediate solution
 221 steps, as well as LTM prompts that employ least-to-most prompting. The detailed design process and
 222 some examples of the prompt program are shown in Appendix A.5.

223 **Serialization Formats.** Since LLMs operate on textual inputs, the method by which graphs are
 224 serialized has a profound impact on the clarity and accessibility of structural information. Our
 225 benchmark examines **7 distinct serialization formats** that offer varied representations of graph
 226 topology. The Graph Modeling Language (GMoL) provides a structured, tag-based representation
 227 that mirrors hierarchical data organization. In contrast, the Adjacency Set and Edge Set formats
 228 offer succinct listings of node neighbors and edges, respectively, emphasizing compactness. The
 229 Edge List format, which may incorporate additional details such as edge weights, serves as a more
 230 verbose alternative. Moreover, the Adjacency Matrix and Adjacency List formats balance detail
 231 and conciseness differently depending on the graph density, and the Graph Markup Language (GMaL)
 232 (Brandes et al., 2013) is an XML-based file format used to describe graph structures, including nodes,
 233 edges, and their attributes. Specific examples of graph serialization formats are in Appendix A.6.

237 3 EXPERIMENTAL SETTING

242 We evaluate the graph reasoning capabilities of various LLMs on a diverse set of tasks and difficulty
 243 levels. Our protocol highlights the impact of different dimensions in Section 2 on model performance.

244 **Random Baselines.** To assess the intrinsic graph reasoning ability of our models, we include a
 245 random baseline for each task. Appendix A.2 shows its detailed design process. These baselines
 246 provide a clear reference point for evaluating how much the LLMs improve upon chance performance
 247 when reasoning about graph-theoretic properties expressed in natural language.

248 **Models and Configurations.** We evaluate a diverse suite of LLMs spanning both open-source
 249 and closed-source categories. Our open-source models include Llama-3, Llama-3.1, Mistral,
 250 Phi-4, Qwen-2.5, and Qwen-3, while our closed-source models consist of Claude-3.5, Gemini-2.0,
 251 GPT-4o, GPT-4o-mini and o4-mini (versions and sources of the LLMs applied can be found in
 252 Appendix A.1). The model selection here is designed to provide coverage of the widely used LLMs
 253 of different sizes, reasoning types, and whether they are open-sourced or not, based on the budget
 254 and availability of models at the time of the work. We also try our best to include models with better
 255 performance on GRAPHOMNI than comparable alternatives to make our conclusion convincing. In
 256 all experiments related to few-shot examples, five exemplars are prepended to the prompt (i.e., k=5).
 257 More implementation details can be found in Appendix A.

258 **Evaluation Metrics.** Evaluation of LLM responses is conducted using predefined binary accuracy
 259 metrics, assigning an output of 1 for correct responses and 0 for incorrect responses. For qualitative
 260 tasks, such as Connectivity verification and Cycle detection, correctness is determined by
 261 identifying and verifying key phrases in the model’s output (e.g., “yes, there is a cycle” or “yes, there
 262 is a path”) against the ground truth (GT). For numerical tasks, such as Triangle counting and
 263 Diameter calculation, correctness is assessed by extracting numerical values that follow specific
 264 key phrases (e.g., “the number of triangles is” or “the diameter is”) and directly comparing these
 265 numerical outputs to the corresponding ground truth values. For tasks with multiple valid solutions,
 266 specifically BFS order and Shortest path, evaluation is conducted using a rule-based function.
 267 This evaluation process involves identifying key phrases, such as “The BFS traversal starting from
 268 node X is” or “The shortest path from node X to node Y is,” to extract the model’s response. Based
 269 on this extraction, we evaluate the model’s response using a task-specific rule-based algorithm that
 verifies solutions for tasks and assigns a score of 1 when the response matches one of the correct
 answers. The detailed rationale for the choice of the metrics is included in Appendix C.6.

270 Table 3: Benchmark Results of Representative LLMs Across Tasks (Mean \pm 95% CI Margin).
271 **Bold orange** / Underlined blue / **Light purple** highlights indicate best/second-best/third-best per-
272 formance in its category. The complete results are included in Table 13.
273

Task	Difficulty	Open-source Models						Closed-source Models				Random
		Llama-3.1 (8B)	Mistral (7B)	Phi-4 (14B)	Qwen-2.5 (72B)	Qwen-2.5 (7B)	Qwen-3 (8B)	Claude-3.5	GPT-4o	Gemini-2.0	o4-mini	
BFS order	E	18.69 \pm 3.02	13.75 \pm 1.44	33.03 \pm 7.32	71.41\pm3.45	21.46 \pm 4.26	65.87 \pm 5.59	91.42 \pm 1.65	81.48 \pm 3.22	90.31 \pm 2.30	95.46\pm0.78	0.00
	M	5.27 \pm 0.93	3.36 \pm 0.44	12.49 \pm 3.24	<u>47.82\pm5.30</u>	6.05 \pm 1.41	<u>53.30\pm5.42</u>	68.25 \pm 2.96	55.07 \pm 4.50	68.40 \pm 3.95	79.37\pm2.08	0.00
	H	0.63 \pm 0.19	0.34 \pm 0.14	2.65 \pm 0.80	<u>22.03\pm4.39</u>	1.38 \pm 0.37	<u>29.53\pm4.25</u>	26.80 \pm 2.64	21.58 \pm 3.69	<u>27.77\pm3.34</u>	<u>32.45\pm3.88</u>	0.00
Connectivity	E	79.53 \pm 2.03	79.90 \pm 1.89	56.29 \pm 8.58	<u>90.24\pm1.89</u>	88.10 \pm 1.46	97.47\pm1.29	98.38\pm0.60	95.63 \pm 1.30	92.61 \pm 1.42	98.23 \pm 0.63	67.49
	M	79.47 \pm 2.00	80.60 \pm 1.92	54.38 \pm 7.99	<u>89.68\pm1.56</u>	87.23 \pm 1.60	96.87\pm1.16	<u>99.11\pm0.39</u>	95.12 \pm 1.37	93.60 \pm 1.10	98.72 \pm 0.52	70.75
	H	74.58 \pm 2.67	74.77 \pm 2.46	48.39 \pm 7.50	<u>84.09\pm1.98</u>	81.19 \pm 2.02	92.89\pm2.07	96.99\pm1.48	90.59 \pm 2.19	87.99 \pm 1.67	92.02 \pm 3.99	66.36
Cycle	E	55.49 \pm 0.90	55.44 \pm 0.96	45.25 \pm 5.90	<u>74.02\pm3.34</u>	62.19 \pm 1.85	90.30\pm2.33	82.56 \pm 3.89	<u>85.08\pm2.27</u>	62.30 \pm 3.32	97.97\pm0.71	50.00
	M	55.69 \pm 1.08	53.71 \pm 0.72	44.26 \pm 5.43	<u>71.99\pm3.34</u>	62.07 \pm 1.80	89.66\pm2.07	80.80 \pm 3.99	82.35 \pm 2.30	60.29 \pm 3.22	97.75\pm0.76	50.00
	H	52.40 \pm 1.47	51.64 \pm 1.02	40.64 \pm 4.97	<u>68.40\pm2.73</u>	58.88 \pm 2.14	86.81\pm2.27	80.10 \pm 3.97	82.96 \pm 2.55	58.30 \pm 2.80	95.61\pm1.23	50.00
Diameter	E	41.27 \pm 5.37	28.55 \pm 4.28	42.81 \pm 5.06	78.50\pm1.16	45.08 \pm 4.17	77.56\pm2.77	<u>83.71\pm1.26</u>	63.99 \pm 2.19	79.14 \pm 1.94	98.88\pm0.15	11.20
	M	27.29 \pm 4.20	15.17 \pm 2.57	28.49 \pm 4.09	<u>52.32\pm2.00</u>	27.31 \pm 3.16	61.71\pm2.28	71.22 \pm 1.30	52.64 \pm 3.05	49.52 \pm 2.14	72.84\pm1.82	6.70
	H	18.63 \pm 3.27	6.97 \pm 1.26	17.71 \pm 3.02	<u>29.59\pm2.48</u>	15.27 \pm 2.47	<u>39.83\pm2.67</u>	56.70\pm2.02	45.60 \pm 3.24	23.45 \pm 2.97	34.61 \pm 2.84	3.72
Shortest	E	38.75 \pm 5.81	31.18 \pm 4.43	42.61 \pm 8.88	90.03\pm2.27	47.46 \pm 8.76	77.69\pm5.17	94.35 \pm 2.93	92.17 \pm 1.91	81.75 \pm 4.70	95.08\pm3.06	50.00
	M	28.84 \pm 4.56	19.89 \pm 3.05	33.92 \pm 7.68	81.17\pm3.03	35.53 \pm 6.80	69.60 \pm 5.50	91.27 \pm 2.84	84.84 \pm 2.93	80.67 \pm 4.15	92.60\pm3.49	50.00
	H	23.03 \pm 3.85	12.21 \pm 1.95	26.60 \pm 6.26	72.53\pm4.29	28.31 \pm 5.50	64.28 \pm 5.60	87.88 \pm 3.36	74.98 \pm 4.17	78.16 \pm 4.55	88.63\pm4.44	50.00
Triangle	E	14.97 \pm 1.53	11.87 \pm 1.32	12.88 \pm 2.05	36.57\pm4.40	18.56 \pm 1.24	41.36\pm4.63	43.41 \pm 1.64	36.32 \pm 1.54	<u>50.33\pm2.31</u>	84.54\pm0.56	2.13
	M	8.56 \pm 0.92	5.86 \pm 0.73	7.54 \pm 1.33	<u>14.52\pm2.63</u>	9.18 \pm 0.73	26.95\pm2.44	24.00 \pm 0.77	20.00 \pm 0.72	<u>28.12\pm1.65</u>	48.13\pm1.46	1.62
	H	4.95\pm0.69	2.55 \pm 0.44	4.38 \pm 1.04	4.73 \pm 1.58	4.45 \pm 0.58	19.54\pm1.34	15.92 \pm 0.72	12.81 \pm 0.88	15.55 \pm 1.29	<u>17.53\pm1.43</u>	1.82

4 RESULTS AND ANALYSIS

4.1 MAIN RESULTS

We evaluate model performance comprehensively across four main dimensions: model overall capability, graph type, effectiveness of prompting strategy, and impact of serialization format. This multifaceted evaluation offers a comprehensive understanding of the most effective approaches for graph algorithm tasks. Our analysis systematically considers each task at varying difficulty levels (*easy/medium/hard*). To isolate each dimension, we control for other variables when assessing a particular aspect and calculate the mean accuracy with a 95% confidence interval (Mean \pm 95% CI Margin) across all combinations of the remaining factors. For example, when evaluating model capability, we compute statistics across all combinations of graph types, prompts, and serialization formats while holding the model constant. The evaluation results from the model capability perspective are presented in Table 3 and Figure 2. To provide a comprehensive view, we present additional experimental results in Appendix E.1 examining prompt schemes, serialization formats, and graph types across collective results (Tables 14, 15, 16), open-source models (Tables 17, 18, 19), and closed-source models (Tables 20, 21, 22). These controlled evaluations yield complementary insights summarized across multiple perspectives. Additionally, example input/output pairs are provided for clarity in Appendix E.5.

Result 1: High variability underscores the need for comprehensive evaluation across all benchmarking dimensions. Detailed analysis reveals substantial variability in LLM performance across different combinations of serialization formats, prompting schemes, and graph types. This variability highlights the need for a comprehensive evaluation across all benchmarking dimensions. The performance heatmaps, presented in Appendix E.2, illustrate the accuracy of different prompt schemes and serialization formats across tasks, models, and difficulty levels. The performance heatmaps show that no single serialization or prompting strategy consistently outperforms others across all tasks and difficulty levels. Instead, optimal results require careful and adaptive selection of serialization-prompt combinations, explicitly tailored to task characteristics such as structured graph-theoretic reasoning tasks. For instance, in the case of GPT-4o, depicted in Figure 4, accuracy gaps of up to 40% occur when varying input representations within the same task and model, indicating a significant sensitivity to input formatting, which is also observed in other domains, like evaluation of vision language models (VLMs) (Feizi et al., 2025). These observations emphasize that evaluating LLMs comprehensively across interconnected dimensions, i.e., serialization formats and prompting schemes, is essential for fairly assessing their capabilities in graph reasoning tasks.

Result 2: Model performance still has considerable room for improvement. Models generally demonstrate reasonable performance across tasks, underscoring their inherent potential in graph reasoning when appropriately guided. Notably, o4-mini delivers remarkable performance, frequently surpassing other closed-source models across most tasks and setting a new benchmark overall. However, the performance gap remains large on the *hard* difficulty tasks, particularly BFS order, Diameter calculation, and Triangle counting, which require full, global information of the graph. Here, even o4-mini’s performance drops to as low as 32.45% on BFS order (*Hard*), 34.61%

on Diameter calculation (*Hard*), and 17.53% on Triangle counting (*Hard*), underscoring the remaining challenge in holistic graph reasoning. Therefore, substantial room for improvement persists relative to ideal human-level outcomes, primarily due to the scarcity of structured graph-theoretic content in typical web corpora used for LLM pretraining. Among open-source alternatives, Qwen-3 remains the top performer but continues to lag behind leading closed-source models, such as o4-mini and Claude-3.5, suggesting a meaningful room for advancement in open-source solutions.

Result ③: Common Errors Reveal Fundamental Gaps in Graph Reasoning. Our error analysis highlights representative categories of errors commonly observed in incorrect LLM responses: **A. Misinterpretation of serialization formats:** Models occasionally struggled to accurately interpret serialized graph representations, resulting in misunderstandings of the underlying graph structure, such as [BFS order case 1](#), [Connectivity case 1](#), and [Triangle counting case 2](#) in the Appendix; **B. Incorrect reasoning about graph-theoretic concepts:** LLMs frequently exhibited fundamental misunderstandings of basic graph definitions and problem-solving methods. In the error cases [Triangle counting case 1](#), incorrect responses inaccurately estimated the number of triangles as approximately one-third of the number of nodes. For the error cases [Diameter calculation case 1](#), some models erroneously identified the diameter as the length of the longest path, rather than correctly defining it as the length of the longest shortest path between any two nodes. These representative errors underscore critical areas for improvement in the graph reasoning capabilities of current LLMs. Additional error cases and analyses are provided in Appendix E.4.

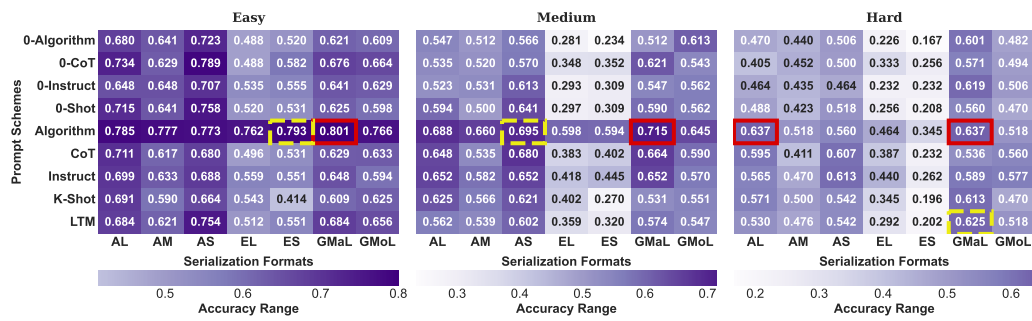


Figure 4: **Performance heatmaps for different prompt schemes and serialization formats on Diameter calculation of GPT-4o.** The color intensity represents the accuracy, with darker colors indicating better performance. The red solid and yellow dashed line indicates Best and Second Best Performance, respectively.

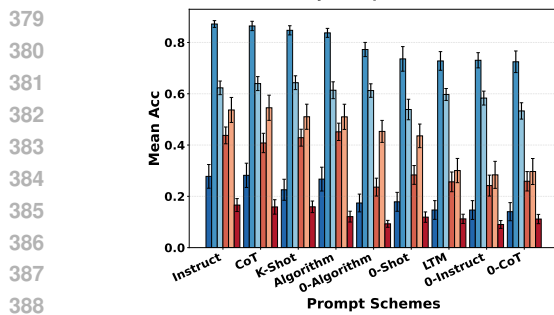
4.2 FINE-GRAINED EMPIRICAL FINDINGS ON MODEL PERFORMANCE

In this section, we dive deeper into our empirical results, identifying detailed performance patterns and revealing nuanced interactions across various evaluation dimensions. We present here the two most critical findings, while additional observations are available in Appendix E.6.

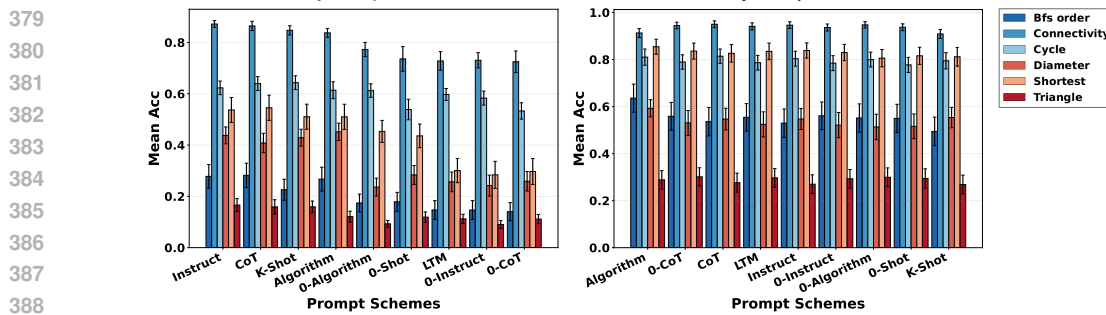
Finding ①: Domain-specific knowledge significantly improves model performance on graph-theoretic tasks. Algorithm-based prompts, explicitly detailing graph-theoretic algorithms, consistently improved model accuracy in structured reasoning tasks such as BFS order and Diameter calculation (Table 14). This result highlights the value of incorporating explicit domain knowledge into prompts, particularly when tasks require step-by-step algorithmic reasoning. From [Diameter calculation case 1](#) and [Triangle counting case 1](#), it shows that when employing plain prompts, the LLM’s response does not accurately reflect the appropriate method for solving the relevant task.

Finding ②: Scaling raises the floor, while reasoning lifts the ceiling. A targeted comparison of Qwen-2.5 (7B), Qwen-2.5 (72B), and Qwen-3 (8B) (Table 11) highlights complementary effects. Scaling within the same family (7B to 72B) yields consistent improvements on easier tasks and splits, such as BFS order, Shortest path, and Diameter calculation (*Easy/Medium*). By contrast, a reasoning model at a comparable size, i.e., Qwen-3 (8B), delivers larger gains on the hardest regimes that require multi-step exploration and combinatorial checks, including BFS order, Diameter calculation, and Triangle counting (*Hard*). Together, these results indicate that scaling predominantly improves robustness on simpler instances, while reasoning-centric design is more effective for pushing the upper bound of graph reasoning ability (details in Appendix C.5).

378



(a) Open-source models.



(b) Closed-source models.

Figure 5: **Accuracy of open-source versus closed-source models with different prompt schemes.** (a) and (b) show the average performance with a 95% confidence interval for open/closed-source models across various prompt schemes and tasks, with x -axis sorted by mean accuracy.

Finding ③: Divergent impacts of prompt schemes – Open-source models benefit from multi-shot exemplars, whereas they do not help closed-source models much. In Figures 5a and 5b, the open-source model achieves the highest average accuracy with prompt schemes that incorporate shots. However, for the closed-source model, prompt schemes show more complexity. Only considering prompt patterns, 0-CoT performs second to best, 0-Algorithm worst, but both surpass k-shot. However, adding shots improves Algorithm’s overall accuracy, suggesting that shots enhance the model’s understanding of Algorithm-based prompts. Yet, this effect is not universal: shots may hinder comprehension in particularly challenging tasks, as noted in Finding ⑤ Appendix E.6.

4.3 EXTENDED STUDY AND DISCUSSION

Scaling to Larger Graphs (Beyond 30 Nodes). We extend the evaluation to graphs with 30–50 nodes, sampling 50 graphs per generator and ~ 3 k test cases overall (details in Appendix C.1). As the results in Table 8 show, the performance degrades as graph size increases, particularly for tasks with sequential or combinatorial requirements: accuracy on BFS order and Triangle counting drops sharply, reflecting the added difficulty of maintaining frontiers or enumerating subgraphs over longer horizons. By contrast, tasks such as Connectivity and Cycle detection remain relatively stable, consistent with their reliance on local connectivity checks. Importantly, despite the absolute drop in scores, the **relative ranking of models and the performance gap between open- and closed-source systems remain nearly identical to the 5–30 node Hard split**, confirming that the benchmark’s conclusions are robust under further scaling of graph size.

Representative Check on Real-World Graphs. We further test whether our synthetic setup transfers to real data by evaluating on two representative domains: IMDB-MULTI (social/interaction) and ogbg-molhiv (molecular), yielding ~ 3.6 k samples across six tasks (details in Appendix C.2). Results in Table 9 corroborate our findings: (i) Connectivity and Cycle detection are consistently easiest; (ii) ordered-path tasks (BFS order, Shortest path, Diameter calculation) remain substantially harder, dominated by serialization and memory errors; and (iii) Triangle counting is the most challenging. However, because many public graphs are sparse and connected, specific tasks become easier than in our synthetic regime (e.g., Connectivity saturates near 100% for strong models). This shows that **real-world graphs alone can under-stress graph reasoning**. Together with prior works that adopt synthetic-only designs (Fatemi et al., 2024; Chen et al., 2024a; Luo et al., 2024b), our results validate real graphs as a sound check, but reaffirm that synthetic graphs provide a systematic evaluation with balanced structural coverage, controllability, and contamination-free conditions. The detailed rationale is elaborated in Appendix C.3.

Exploration on NP-Hard Tasks. As a complementary stress test, we also consider two classical NP-hard problems, Hamiltonian cycle detection and Max-Cut (details in Appendix C.4). Results in Table 10 show accuracy patterns aligned with our six canonical tasks: open-source models remain near random, while closed-source reasoning-oriented models attain noticeably higher but still imperfect scores. This indicates that the core conclusions of GRAPHOMNI naturally extend to NP-hard problems. Interestingly, however, LLMs do not exhibit the same graded difficulty separation between polynomial-time and NP-hard tasks as human solvers: accuracy tends to collapse uniformly

432 across NP-hard regimes just like polynomial tasks. Thus, while useful as a complementary check,
 433 NP-hard tasks do not add progressive challenge in the same way as our tractable yet demanding suite,
 434 reinforcing why the latter remain the centerpiece of GRAPHOMNI.

435 **Efficiency–accuracy trade-off.** Besides accuracy, we also analyze inference efficiency by measuring
 436 the number of output tokens produced across models (details in Appendix E.7). The results reveal
 437 a clear trade-off: accuracy gains often come at the cost of longer responses, but models navigate
 438 this balance differently. Closed-source models (e.g., GPT-4o, Claude-3.5) reach high accuracy with
 439 compact generations under 300 tokens, while o4-mini relies on very long chains of thought (over
 440 1.6K tokens) to achieve similar accuracy (Figure 32). By contrast, open-source models such as Llama-
 441 3.1 and Qwen-2.5 (7B) must generate substantially longer outputs to achieve high performance,
 442 whereas shorter responses are correlated with lower accuracy. These trends persist across difficulty
 443 levels, task types, serialization formats, and prompt schemes (Tables 23–26). Overall, efficiency,
 444 measured by output length, emerges as an additional axis of divergence across LLMs, reinforcing the
 445 importance of evaluating not only correctness but also the cost of achieving it.

446 4.4 REINFORCEMENT LEARNING (RL)-BASED PROMPT SEARCH INSPIRED BY GRAPHOMNI

447 Our benchmark evaluates three key dimensions, *graph type*, *serialization format*, and *prompt scheme*,
 448 to underscore the critical role of transforming graph structures into textual inputs for LLM inference.
 449 While GraphOmni provides comprehensive insights into how different dimensions affect LLM
 450 inference, we still face a concrete, actionable question: Given many interacting dimensions, which
 451 prompt configuration is best for a specific graph reasoning task? In this section, we want to identify
 452 the optimal combination strategies (serialization format; prompt scheme, etc.) that enhance the
 453 effectiveness of textual representations, thereby improving LLM performance in graph reasoning
 454 and understanding tasks. We define the process of converting graph structures into textual inputs
 455 tailored to a specific task as the **serialization process**. To operationalize this serialization process, we
 456 introduce an RL-based search method as a diagnostic tool within our benchmark, enabling automatic
 457 selection of effective serialization strategies.

458 Specifically, RL transforms optimizing the serialization process into a sequential decision-making
 459 problem for each type and difficulty of the task. There are T decision epochs, and each decision
 460 epoch determines one component of the serialization strategy. Then we provide a predetermined
 461 order to specify a sequence of **action spaces** $\{\mathcal{A}_t\}_{t=1,\dots,T}$ (e.g., \mathcal{A}_t can be all candidate prompts).
 462 We set the initial state s_0 as the specific type and difficulty of the task. Then at decision epoch
 463 $t = 1, \dots, T$, we choose an action $a_t \in \mathcal{A}_t$ based on the previous actions a_1, \dots, a_{t-1} . Then the
 464 **state** s_t consists of the task type and difficulty (initial state s_0) together with the previously selected
 465 serialization components. This corresponds to a policy $\pi_t : \mathcal{S}_0 \times \mathcal{A}_1 \times \dots \times \mathcal{A}_{t-1} \mapsto \mathcal{A}_t$, where \mathcal{S}_0 is
 466 the state space of the initial state s_0 . For any instance s (e.g., a query for Connectivity task in easy
 467 mode for a specific graph), a **binary reward**, denoted by $r(s, a_1, \dots, a_T)$, is incurred at the end of the
 468 decision epoch, which is set to 1 if the LLM correctly answers the specific query under the selected
 469 serialization strategy (a_1, \dots, a_T) and to 0 otherwise. For each type and difficulty of the task, our
 470 **objective** is to maximize the expected reward of choosing the serialization strategy a_1, \dots, a_T :

$$471 \max_{\{\pi_t\}_{t=1,\dots,T}} \mathbb{E}[r(s, a_1, \dots, a_T) | s_0],$$

472 where the expectation is taken with respect to the problem instance s and the (random) answer output
 473 by an LLM (affected by the randomness of the LLM, e.g., the temperature parameter). Note that (i)
 474 s_0 is part of the instance information s , and (ii) we fix the type and difficulty of the task, and the
 475 only randomness in terms of s is from graph generation. To approximate this objective function,
 476 we generate N different graphs for each type of query. We assess the performance of RL using the
 477 **average reward** across the N graphs, which essentially is the accuracy of the serialization strategy for
 478 a specific graph-related task across these N graphs.

479 Consider the problem of dealing with high-dimensional, complex state spaces in serialization process,
 480 we employ the Deep Q -Network (DQN) (Mnih et al., 2013) to implement RL, which employs a
 481 neural network as a function approximator for the Q -function. Specifically, we use a neural network
 482 $\hat{Q}_t(s_0, a_1, \dots, a_t; \theta_t)$ parameterized by θ_t to approximate the corresponding $Q_t(s_0, a_1, \dots, a_t)$ for
 483 the actions or factors considered in serialization process. Each Q -network is modeled as a three-layer
 484 multilayer perceptron with ReLU activations. Training minimizes the mean squared error loss, and

486 action selection follows an ϵ -greedy policy, where ϵ linearly decays from 1.0 to a minimum of 0.01.
 487 Then we design the **RL-Opt** (RL-guided Optimal Serialization Selection) experiment, where we
 488 leverage existing benchmark data to apply RL for evaluating computational cost and validating
 489 the effectiveness of the derived optimal strategy. Additionally, we introduce the **RL-Scale** (RL
 490 Scalability in Serialization Expansion) experiment to analyze how RL’s computational cost scales
 491 when incorporating additional factors in the serialization process. All detailed information can be
 492 found in Appendix D.

493 In **RL-Opt**, the serialization process involved three key factors based on our benchmark’s results:
 494 serialization format, prompt scheme, and the choice of open-source language models. To evaluate the
 495 effectiveness of RL in identifying the optimal combination, we employ two key metrics: Cost and
 496 Rate. To evaluate RL’s effectiveness in finding the optimal combination, we use two metrics: (a) Cost
 497 is the ratio of explored combinations: $\text{Cost} = \frac{k}{K}$, where k is the number of explored combinations,
 498 and K is the total number of combinations; (b) Rate = $\frac{\text{acc}_*}{\text{acc}_{\max}}$, where acc_* is the accuracy of RL’s
 499 best-found combination and acc_{\max} is the highest accuracy in the benchmark data. Results are in
 500 Table 4. The results demonstrate that, at only 25% of the original cost, the RL-based method is still
 501 able to maintain an average success rate of 0.9, indicating its capability to significantly reduce the
 502 time required to search for optimal combinations while preserving the quality of the outcomes.

503 Table 4: **Performance summary of RL-Opt**, averaged across all instances of a specific experimental
 504 case, reducing the cost to about 25% of the original, maintaining an average success rate of 0.9.
 505

Task	Mode	Avg Cost	Avg Rate	Task	Mode	Avg Cost	Avg Rate
BFS order	Easy	0.2203	0.9740	Connectivity	Easy	0.2244	0.9883
	Medium	0.2251	0.9045		Medium	0.2263	0.9875
	Hard	0.2279	0.7812		Hard	0.2238	0.9871
Cycle	Easy	0.2229	0.9757	Diameter	Easy	0.2263	0.9728
	Medium	0.2263	0.9833		Medium	0.2181	0.9541
	Hard	0.2203	0.9584		Hard	0.2235	0.9471
Shortest path	Easy	0.2244	0.9636	Triangle	Easy	0.2276	0.9061
	Medium	0.2159	0.9856		Medium	0.2206	0.8456
	Hard	0.2187	0.9073		Hard	0.2235	0.7321

5 CONCLUSION

518 We introduced GRAPHOMNI, a comprehensive benchmark framework for systematically evaluating
 519 the graph reasoning capabilities of LLMs. By analyzing critical dimensions, including graph types,
 520 serialization formats, and prompt schemes, we provided extensive insights into the strengths and
 521 limitations of current LLMs. Our empirical findings emphasize that no single serialization or
 522 prompting strategy consistently outperforms others. Motivated by these insights, we propose a
 523 reinforcement learning-based approach that dynamically selects the optimal serialization-prompt
 524 pairings, leading to significant improvements in accuracy. GRAPHOMNI’s modular and extensible
 525 design establishes a robust foundation for future research, facilitating advances toward general-
 526 purpose graph reasoning models.

527
 528
 529
 530
 531
 532
 533
 534
 535
 536
 537
 538
 539

540 **Ethics Statement** We confirm that this research complies with all applicable ethical guidelines and
 541 does not present any ethical issues.
 542

543 **Reproducibility Statement** We have taken extensive measures to ensure the reproducibility of our
 544 work. The source code and data resources are released at <https://anonymous.4open.science/r/ID-14092>
 545 and <https://huggingface.co/datasets/GoodAIResearch/GraphOmni-anon>, respectively.

546 Our experimental setup, including model configurations and evaluation protocols, is fully described in
 547 Section 3 in the main content and Section A in Appendix. For transparency, we provide comprehensive
 548 coverage of input–output examples (Section E.5) and error cases (Section E.4) in Appendix, enabling
 549 a thorough understanding and verification of the reported results.
 550

551 Together, these resources support faithful reproduction and further exploration of our findings.
 552

553 REFERENCES

554 W. Aiello, F. Chung, and L. Lu. A random graph model for massive graphs. In *Proceedings of*
 555 *the 32nd Annual ACM Symposium on Theory of Computing (STOC)*, pp. 171–180, 2000. doi:
 556 10.1145/335305.335326.
 557

558 R. Albert and A.-L. Barabási. Emergence of scaling in random networks. *Science*, 286(5439):
 559 509–512, 1999. doi: 10.1126/science.286.5439.509.
 560 Ulrik Brandes, Markus Eiglsperger, Jürgen Lerner, and Christian Pich. Graph markup language
 561 (graphml). 2013.
 562

563 Tom B. Brown, Benjamin Mann, Nick Ryder, Melanie Subbiah, Jared Kaplan, Prafulla Dhariwal,
 564 Arvind Neelakantan, Pranav Shyam, Girish Sastry, Amanda Askell, Sandhini Agarwal, Ariel
 565 Herbert-Voss, Gretchen Krueger, Tom Henighan, Rewon Child, Aditya Ramesh, Daniel M. Ziegler,
 566 Jeffrey Wu, Clemens Winter, Christopher Hesse, Mark Chen, Eric Sigler, Mateusz Litwin, Scott
 567 Gray, Benjamin Chess, Jack Clark, Christopher Berner, Sam McCandlish, Alec Radford, Ilya
 568 Sutskever, and Dario Amodei. Language models are few-shot learners. In *Proceedings of the 34th*
 569 *International Conference on Neural Information Processing Systems, NIPS '20*, Red Hook, NY,
 570 USA, 2020. Curran Associates Inc. ISBN 9781713829546.
 571

571 Ziwei Chai, Tianjie Zhang, Liang Wu, Kaiqiao Han, Xiaohai Hu, Xuanwen Huang, and Yang
 572 Yang. Graphilm: Boosting graph reasoning ability of large language model. *arXiv preprint*
 573 *arXiv:2310.05845*, 2023.
 574

575 Deepayan Chakrabarti and Christos Faloutsos. Graph mining: Laws, generators, and algorithms.
 576 *ACM Comput. Surv.*, 38(1):2–es, June 2006. ISSN 0360-0300. doi: 10.1145/1132952.1132954.
 577 URL <https://doi.org/10.1145/1132952.1132954>.
 578

579 Nuo Chen, Yuhang Li, Jianheng Tang, and Jia Li. Graphwiz: An instruction-following language model
 580 for graph computational problems. In *Proceedings of KDD 2024*, 2024a. doi: 10.1145/3637528.
 581 3672010.
 582

583 Runjin Chen, Tong Zhao, Ajay Jaiswal, Neil Shah, and Zhangyang Wang. Lлага: Large language and
 584 graph assistant. *arXiv preprint arXiv:2402.08170*, 2024b.
 585

586 Xinnan Dai, Haohao Qu, Yifen Shen, Bohang Zhang, Qihao Wen, Wenqi Fan, Dongsheng Li, Jiliang
 587 Tang, and Caihua Shan. How do large language models understand graph patterns? a benchmark
 588 for graph pattern comprehension. *arXiv preprint arXiv:2410.05298*, 2024.
 589

590 Debarati Das, Ishaan Gupta, Jaideep Srivastava, and Dongyeop Kang. Which modality should
 591 i use - text, motif, or image? : Understanding graphs with large language models, 2024.
 592 arXiv:2311.09862v2.
 593

594 David Easley, Jon Kleinberg, et al. *Networks, crowds, and markets: Reasoning about a highly*
 595 *connected world*, volume 1. Cambridge university press Cambridge, 2010.
 596

597 P. Erdős and A. Rényi. On the evolution of random graphs. *Publications of the Mathematical Institute*
 598 *of the Hungarian Academy of Sciences*, 5:17–61, 1960.

594 Xiang Fang, Arvind Easwaran, Blaise Genest, and Ponnuthurai Nagaratnam Suganthan. Adaptive
 595 hierarchical graph cut for multi-granularity out-of-distribution detection. *IEEE Transactions on*
 596 *Artificial Intelligence*, 2025a.

597

598 Yi Fang, Dongzhe Fan, Sirui Ding, Ninghao Liu, and Qiaoyu Tan. Uniglm: Training one unified
 599 language model for text-attributed graph embedding. In *Proceedings of the Eighteenth ACM*
 600 *International Conference on Web Search and Data Mining (WSDM)*, 2025b. doi: 10.1145/3701551.
 601 3703586.

602 Bahare Fatemi, Jonathan Halcrow, and Bryan Perozzi. Talk like a graph: Encoding graphs for large
 603 language models. In *Proceedings of ICLR 2024*, 2024.

604

605 Aarash Feizi, Sai Rajeswar, Adriana Romero-Soriano, Reihaneh Rabbany, Spandana Gella, Valentina
 606 Zantedeschi, and João Monteiro. Pairbench: A systematic framework for selecting reliable judge
 607 vlms. *arXiv preprint arXiv:2502.15210*, 2025.

608 Yifan Feng, Chengwu Yang, Xingliang Hou, Shaoyi Du, Shihui Ying, Zongze Wu, and Yue Gao.
 609 Beyond graphs: Can large language models comprehend hypergraphs? In *The Thirteenth Inter-*
 610 *national Conference on Learning Representations*, 2025. URL <https://openreview.net/forum?id=28qOQwjuma>.

611

612 Thomas Gaudelot, Ben Day, Arian R Jamasb, Jyothish Soman, Cristian Regep, Gertrude Liu,
 613 Jeremy BR Hayter, Richard Vickers, Charles Roberts, Jian Tang, et al. Utilizing graph ma-
 614 chine learning within drug discovery and development. *Briefings in bioinformatics*, 22(6):bbab159,
 615 2021.

616

617 E. N. Gilbert. Random graphs. *The Annals of Mathematical Statistics*, 30(4):1141–1144, 1959. doi:
 618 10.1214/aoms/1177706098.

619

620 Jiayan Guo, Lun Du, Hengyu Liu, Mengyu Zhou, Xinyi He, and Shi Han. Gpt4graph: Can large
 621 language models understand graph structured data? an empirical evaluation and benchmarking,
 622 2024a. *arXiv:2305.15066v2*.

623

624 Kai Guo, Zewen Liu, Zhikai Chen, Hongzhi Wen, Wei Jin, Jiliang Tang, and Yi Chang. Learning
 625 on graphs with large language models (llms): A deep dive into model robustness. *arXiv preprint*
 626 *arXiv:2407.12068*, 2024b.

627

628 Xiaoxin He, Yijun Tian, Yifei Sun, Nitesh Chawla, Thomas Laurent, Yann LeCun, Xavier Bresson,
 629 and Bryan Hooi. G-retriever: Retrieval-augmented generation for textual graph understanding and
 630 question answering. *Advances in Neural Information Processing Systems*, 37:132876–132907,
 631 2024.

632

633 Dan Hendrycks, Collin Burns, Steven Basart, Andy Zou, Mantas Mazeika, Dawn Song, and Jacob
 634 Steinhardt. Measuring massive multitask language understanding. In *International Conference on*
 635 *Learning Representations*, 2021a. URL <https://openreview.net/forum?id=d7KBjmI3GmQ>.

636

637 Dan Hendrycks, Collin Burns, Saurav Kadavath, Akul Arora, Steven Basart, Eric Tang, Dawn Song,
 638 and Jacob Steinhardt. Measuring mathematical problem solving with the MATH dataset. In
 639 *Thirty-fifth Conference on Neural Information Processing Systems Datasets and Benchmarks Track*
 640 *(Round 2)*, 2021b. URL <https://openreview.net/forum?id=7Bywt2mQsCe>.

641

642 Weihua Hu, Matthias Fey, Marinka Zitnik, Yuxiao Dong, Hongyu Ren, Bowen Liu, Michele Catasta,
 643 and Jure Leskovec. Open graph benchmark: datasets for machine learning on graphs. In *Proceed-*
 644 *ings of the 34th International Conference on Neural Information Processing Systems, NIPS '20*,
 645 Red Hook, NY, USA, 2020. Curran Associates Inc. ISBN 9781713829546.

646

647 Yunlong Hu, Zheng Zhang, and Liang Zhao. Beyond text: A deep dive into large language models'
 648 ability on understanding graph data. *arXiv preprint arXiv:2310.04944*, 2023.

649

650 Bowen Jin, Gang Liu, Chi Han, Meng Jiang, Heng Ji, and Jiawei Han. Large language models on
 651 graphs: A comprehensive survey. In *Transactions on Knowledge and Data Engineering (TKDE)*,
 652 2024a.

648 Bowen Jin, Chulin Xie, Jiawei Zhang, Kashob Kumar Roy, Yu Zhang, Zheng Li, Ruirui Li, Xianfeng
 649 Tang, Suhang Wang, Yu Meng, and Jiawei Han. Graph chain-of-thought: Augmenting large
 650 language models by reasoning on graphs. In *Findings of the Association for Computational
 651 Linguistics: ACL 2024*, pp. 163–184, 2024b. ACL 2024.

652 Lecheng Kong, Jiarui Feng, Hao Liu, Chengsong Huang, Jiaxin Huang, Yixin Chen, and Muhan
 653 Zhang. Gofa: A generative one-for-all model for joint graph language modeling. *arXiv preprint
 654 arXiv:2407.09709*, 2024.

655 M. Latapy, C. Magnien, and N. Del Vecchio. Basic notions for the analysis of large two-mode
 656 networks. *Social Networks*, 30(1):31–48, 2008. doi: 10.1016/j.socnet.2007.04.006.

658 Mike Lewis, Yinhan Liu, Naman Goyal, Marjan Ghazvininejad, Abdelrahman Mohamed, Omer Levy,
 659 Veselin Stoyanov, and Luke Zettlemoyer. BART: Denoising sequence-to-sequence pre-training for
 660 natural language generation, translation, and comprehension. In Dan Jurafsky, Joyce Chai, Natalie
 661 Schluter, and Joel Tetreault (eds.), *Proceedings of the 58th Annual Meeting of the Association for
 662 Computational Linguistics*, pp. 7871–7880, Online, July 2020. Association for Computational
 663 Linguistics. doi: 10.18653/v1/2020.acl-main.703. URL <https://aclanthology.org/2020.acl-main.703/>.

665 Shilong Li, Yancheng He, Hangyu Guo, Xingyuan Bu, Ge Bai, Jie Liu, Jiaheng Liu, Xingwei
 666 Qu, Yangguang Li, Wanli Ouyang, et al. Graphreader: Building graph-based agent to enhance
 667 long-context abilities of large language models. *arXiv preprint arXiv:2406.14550*, 2024a.

668 Xin Li, Weize Chen, Qizhi Chu, Haopeng Li, Zhaojun Sun, Ran Li, Chen Qian, Yiwei Wei, Zhiyuan
 669 Liu, Chuan Shi, Maosong Sun, and Cheng Yang. Can large language models analyze graphs like
 670 professionals? a benchmark, datasets and models. In *Proceedings of the 38th Conference on
 671 Neural Information Processing Systems (NeurIPS 2024) - Track on Datasets and Benchmarks*,
 672 2024b. URL: <https://github.com/BUPT-GAMMA/ProGraph>.

674 Yuhang Li, Zhixun Li, Peisong Wang, Jia Li, Xiangguo Sun, Hong Cheng, and Jeffrey Xu Yu. A
 675 survey of graph meets large language model: Progress and future directions. *arXiv preprint
 676 arXiv:2311.12399*, 2023.

677 Yuhang Li, Peisong Wang, Zhixun Li, Jeffrey Xu Yu, and Jia Li. Zerog: Investigating cross-dataset
 678 zero-shot transferability in graphs. In *Proceedings of the KDD Conference*, 2024c. doi: 10.1145/
 679 3637528.3671982.

680 Yuhang Li, Peisong Wang, Xiao Zhu, Aochuan Chen, Haiyun Jiang, Deng Cai, Victor W Chan, and
 681 Jia Li. Glbench: A comprehensive benchmark for graph with large language models. *Advances in
 682 Neural Information Processing Systems*, 37:42349–42368, 2024d.

684 Yuankai Luo, Hongkang Li, Qijiong Liu, Lei Shi, and Xiao-Ming Wu. Node identifiers: Compact,
 685 discrete representations for efficient graph learning. *arXiv preprint arXiv:2405.16435*, 2024a.

686 Zihan Luo, Xiran Song, Hong Huang, Jianxun Lian, Chenhao Zhang, Jinqi Jiang, and Xing Xie.
 687 Graphinstruct: Empowering large language models with graph understanding and reasoning
 688 capability, 2024b. *arXiv:2403.04483v2*.

690 Haitao Mao, Zhikai Chen, Wenzhuo Tang, Jianan Zhao, Yao Ma, Tong Zhao, and Neil Shah. Position:
 691 Graph foundation models are already here. In *Proceedings of the International Conference on
 692 Machine Learning (ICML)*, 2024.

693 Volodymyr Mnih, Koray Kavukcuoglu, David Silver, Alex Graves, Ioannis Antonoglou, Daan
 694 Wierstra, and Martin Riedmiller. Playing atari with deep reinforcement learning. *arXiv preprint
 695 arXiv:1312.5602*, 2013.

696 Christopher Morris, Nils M. Kriege, Franka Bause, Kristian Kersting, Petra Mutzel, and Marion
 697 Neumann. Tudataset: A collection of benchmark datasets for learning with graphs, 2020. URL
 698 <https://arxiv.org/abs/2007.08663>.

700 Bryan Perozzi, Bahareh Fatemi, Dustin Zelle, Anton Tsitsulin, Mehran Kazemi, Rami Al-Rfou, and
 701 Jonathan Halcrow. Let your graph do the talking: Encoding structured data for llms. *arXiv preprint
 702 arXiv:2402.05862*, 2024.

702 Alec Radford, Jeff Wu, Rewon Child, David Luan, Dario Amodei, and Ilya Sutskever. Language
 703 models are unsupervised multitask learners. 2019.

704

705 Colin Raffel, Noam Shazeer, Adam Roberts, Katherine Lee, Sharan Narang, Michael Matena, Yanqi
 706 Zhou, Wei Li, and Peter J. Liu. Exploring the limits of transfer learning with a unified text-to-text
 707 transformer. *J. Mach. Learn. Res.*, 21(1), January 2020. ISSN 1532-4435.

708 Clayton Sanford, Bahareh Fatemi, Ethan Hall, Anton Tsitsulin, Mehran Kazemi, Jonathan Halcrow,
 709 Bryan Perozzi, and Vahab Mirrokni. Understanding transformer reasoning capabilities via graph
 710 algorithms. *Advances in Neural Information Processing Systems*, 37:78320–78370, 2024.

711

712 Melanie Sclar, Yejin Choi, Yulia Tsvetkov, and Alane Suhr. Quantifying language models' sensitivity
 713 to spurious features in prompt design or: How i learned to start worrying about prompt formatting.
 714 *arXiv preprint arXiv:2310.11324*, 2023.

715 Melanie Sclar, Yejin Choi, Yulia Tsvetkov, and Alane Suhr. Quantifying language models' sensitivity
 716 to spurious features in prompt design. In *International Conference on Learning Representations*
 717 (*ICLR*), 2024.

718 Chengshuai Shi, Kun Yang, Zihan Chen, Jundong Li, Jing Yang, and Cong Shen. Efficient prompt
 719 optimization through the lens of best arm identification. *arXiv preprint arXiv:2402.09723*, 2024.

720

721 Rok Sosic and Jure Leskovec. Large scale network analytics with snap: Tutorial at the world
 722 wide web 2015 conference. In *Proceedings of the 24th International Conference on World*
 723 *Wide Web*, WWW '15 Companion, pp. 1537–1538, New York, NY, USA, 2015. Association
 724 for Computing Machinery. ISBN 9781450334730. doi: 10.1145/2740908.2744708. URL
 725 <https://doi.org/10.1145/2740908.2744708>.

726 Xing Su, Shan Xue, Fanzhen Liu, Jia Wu, Jian Yang, Chuan Zhou, Wenbin Hu, Cecile Paris, Surya
 727 Nepal, Di Jin, et al. A comprehensive survey on community detection with deep learning. *IEEE*
 728 *transactions on neural networks and learning systems*, 35(4):4682–4702, 2022.

729

730 Yanchao Tan, Zihao Zhou, Hang Lv, Weiming Liu, and Carl Yang. Walklm: A uniform language
 731 model fine-tuning framework for attributed graph embedding. In *Proceedings of NeurIPS 2023*,
 732 2023.

733 Yanchao Tan, Hang Lv, Xinyi Huang, Jiawei Zhang, Shiping Wang, and Carl Yang. Musegraph:
 734 Graph-oriented instruction tuning of large language models for generic graph mining. *arXiv*
 735 *preprint arXiv:2403.04780*, 2024.

736

737 Jiabin Tang, Yuhao Yang, Wei Wei, Lei Shi, Lixin Su, Suqi Cheng, Dawei Yin, and Chao Huang.
 738 Graphgpt: Graph instruction tuning for large language models. In *Proceedings of the 47th*
 739 *International ACM SIGIR Conference on Research and Development in Information Retrieval*, pp.
 740 491–500, 2024.

741 Jianheng Tang, Qifan Zhang, Yuhan Li, Nuo Chen, and Jia Li. Grapharena: Evaluating and exploring
 742 large language models on graph computation. In *The Thirteenth International Conference on*
 743 *Learning Representations*, 2025. URL <https://openreview.net/forum?id=Y1r9yCMzeA>.

744 Alexander K. Taylor, Anthony Cuturro, Vishal Yathish, Mingyu Derek Ma, and Wei Wang. Are
 745 large-language models graph algorithmic reasoners?, 2024. *arXiv:2410.22597v1*.

746

747 Heng Wang, Shangbin Feng, Tianxing He, Zhaoxuan Tan, Xiaochuang Han, and Yulia Tsvetkov.
 748 Can language models solve graph problems in natural language? *Advances in Neural Information*
 749 *Processing Systems*, 36:30840–30861, 2023.

750 Jianing Wang, Junda Wu, Yupeng Hou, Yao Liu, Ming Gao, and Julian McAuley. Instructgraph:
 751 Boosting large language models via graph-centric instruction tuning and preference alignment.
 752 *arXiv preprint arXiv:2402.08785*, 2024a.

753

754 Yu Wang, Ryan A Rossi, Namyong Park, Huiyuan Chen, Nesreen K Ahmed, Puja Trivedi, Franck
 755 Dernoncourt, Danai Koutra, and Tyler Derr. Large generative graph models. *arXiv preprint*
arXiv:2406.05109, 2024b.

756 Jason Wei, Xuezhi Wang, Dale Schuurmans, Maarten Bosma, Fei Xia, Ed Chi, Quoc V Le, Denny
 757 Zhou, et al. Chain-of-thought prompting elicits reasoning in large language models. *Advances in*
 758 *neural information processing systems*, 35:24824–24837, 2022.

759

760 Shiwen Wu, Fei Sun, Wentao Zhang, Xu Xie, and Bin Cui. Graph neural networks in recommender
 761 systems: a survey. *ACM Computing Surveys*, 55(5):1–37, 2022.

762

763 Zonghan Wu, Shirui Pan, Fengwen Chen, Guodong Long, Chengqi Zhang, and Philip S Yu. A
 764 comprehensive survey on graph neural networks. *IEEE transactions on neural networks and*
 765 *learning systems*, 32(1):4–24, 2020.

766

767 Lianghao Xia, Ben Kao, and Chao Huang. Opengraph: Towards open graph foundation models.
 768 *arXiv preprint arXiv:2403.01121*, 2024.

769

770 Yuhao Xu, Xinqi Liu, Keyu Duan, Yi Fang, Yu-Neng Chuang, Daochen Zha, and Qiaoyu
 771 Tan. Graphfm: A comprehensive benchmark for graph foundation model. *arXiv preprint*
 772 *arXiv:2406.08310*, 2024.

773

774 Christos Xypolopoulos, Guokan Shang, Xiao Fei, Giannis Nikolentzos, Hadi Abdine, Iakovos Evdai-
 775 mon, Michail Chatzianastasis, Giorgos Stamou, and Michalis Vazirgiannis. Graph linearization
 776 methods for reasoning on graphs with large language models. *arXiv preprint arXiv:2410.19494*,
 777 2024.

778

779 Hao Yan, Chaozhuo Li, Ruosong Long, Chao Yan, Jianan Zhao, Wenwen Zhuang, Jun Yin, Peiyan
 780 Zhang, Weihao Han, Hao Sun, et al. A comprehensive study on text-attributed graphs: Bench-
 781 marking and rethinking. *Advances in Neural Information Processing Systems*, 36:17238–17264,
 782 2023.

783

784 Muhan Zhang and Yixin Chen. Link prediction based on graph neural networks. *Advances in neural*
 785 *information processing systems*, 31, 2018.

786

787 Qifan Zhang, Xiaobin Hong, Jianheng Tang, Nuo Chen, Yuhan Li, Wenzhong Li, Jing Tang, and Jia
 788 Li. Gcoder: Improving large language model for generalized graph reasoning. In *Proceedings*
 789 *of the 34th ACM International Conference on Information and Knowledge Management*, CIKM
 790 ’25, pp. 4149–4159, New York, NY, USA, 2025. Association for Computing Machinery. ISBN
 9798400720406. doi: 10.1145/3746252.3761066. URL <https://doi.org/10.1145/3746252.3761066>.

791

792 Yizhuo Zhang, Heng Wang, Shangbin Feng, Zhaoxuan Tan, Xiaochuang Han, Tianxing He, and Yulia
 793 Tsvetkov. Can llm graph reasoning generalize beyond pattern memorization? In *Findings of the*
 794 *Association for Computational Linguistics: EMNLP 2024*, pp. 2289–2305, 2024a.

795

796 Zeyang Zhang, Xin Wang, Ziwei Zhang, Haoyang Li, Yijian Qin, and Wenwu Zhu. Llm4dyg: Can
 797 large language models solve spatial-temporal problems on dynamic graphs? In *Proceedings of*
 798 *the 30th ACM SIGKDD Conference on Knowledge Discovery and Data Mining (KDD ’24)*. ACM,
 799 2024b. doi: 10.1145/3637528.3671709.

800

801 Jianan Zhao, Le Zhuo, Yikang Shen, Meng Qu, Kai Liu, Michael Bronstein, Zhaocheng Zhu, and
 802 Jian Tang. Graphtext: Graph reasoning in text space. *arXiv preprint arXiv:2310.01089*, 2023.

803

804

805

806

807

808

809

810 Table of Contents for Appendix

	Page	
811		
812		
813		
814	A. Experimental Details	17
815	A.1 LLM Versions	17
816	A.2 Parameter and Random Baseline Settings	17
817	A.3 Graph Tasks	18
818	A.3.1 Rationale for Selection of Tasks	18
819	A.4 Graph Types	19
820	A.4.1 Rationale for Generator Selection	20
821	A.5 Prompt Format	21
822	A.6 Serialization Format	21
823	A.7 Data Examples	23
824		
825	B. Benchmark Statistics	26
826	B.1 Basic Statistics of GRAPHOMNI	26
827	B.2 Token Statistics of GRAPHOMNI	28
828		
829	C. Extended Discussion and Ablation Study of GRAPHOMNI	28
830	C.1 Study on Larger Graph (Beyond 30 Nodes)	28
831	C.2 Study on Real-World Graphs: Representative Check	29
832	C.3 Considerations on Real-World Graphs vs. Synthetic Graphs	30
833	C.4 Exploration on NP-Hard Tasks	30
834	C.5 Scaling vs. Reasoning: Disentangling Their Effects on Graph Reasoning	31
835	C.6 Rationale for Binary Metric over Partial Score	33
836		
837	D. RL-based Prompt Search Inspired by GRAPHOMNI	33
838	D.1 Background and Serialization Process	33
839	D.2 Details for RL-Opt Setting	34
840		
841	E. Comprehensive Experimental Results	37
842	E.1 Fine-grained Results Across Dimension	37
843	E.2 Performance Heatmaps across Tasks	41
844	E.2.1 Heatmaps for BFS order	41
845	E.2.2 Heatmaps for Connectivity	46
846	E.2.3 Heatmaps for Cycle detection	49
847	E.2.4 Heatmaps for Diameter calculation	52
848	E.2.5 Heatmaps for Shortest path	55
849	E.2.6 Heatmaps for Triangle counting	58
850	E.3 Graph Type Sensitivity Analysis	61
851	E.4 Error Analysis	68
852	E.5 Input/Output Examples	76
853	E.6 More Findings from Evaluation Results	101
854	E.7 Analysis on Efficiency via Number of Output Tokens	102
855		
856	F. Detailed Related Works	104
857	F.1 LLM Applications on Graph Data	105
858	F.2 Benchmarks on LLM Application to Graph Data	106
859		
860	G. Limitations and Future Directions of GRAPHOMNI	106
861		
862	H. Additional Ablation Studies	107
863	H.1 Performance v.s. Time Complexity of Tasks	107
	H.2 Scaling Beyond 50 Nodes	109
	H.3 Robustness Check under Prompt Noise (Perturbation)	109

864 **A EXPERIMENTAL DETAILS**
865866 **A.1 LLM VERSIONS**
867868
869 Table 5 provides an overview of the diverse suite of large language models (LLMs) evaluated in our
870 study. Open-source models are hyperlinked to their respective documentation, while closed-source
871 models are identified by their version numbers. Note that we only uniformly sample 25% of data
872 when evaluating Qwen-3 due to the limited time after its release, so its result will be only included in
873 the model-wise statistics, i.e. Table 3 for refernce.
874875 Table 5: Overview of evaluated LLMs. Open-source models are linked, while closed-source models
876 list their version.
877

878 Model	879 Model Link/Version
879 Llama-3	880 Meta-Llama-3-8B (Link)
880 Llama-3.1	881 Llama-3.1-8B (Link)
881 Mistral	882 Mistral-7B-v0.3 (Link)
882 Phi-4	883 Phi-4-14B (Link)
883 Qwen-2.5 (7B)	884 Qwen-2.5-7B-Instruct (Link)
884 Qwen-2.5 (72B)	885 Qwen-2.5-72B-Instruct (Link)
885 Qwen-3 (8B)	886 Qwen-3-8B (Link)
887 Claude-3.5	888 claude-3-5-sonnet-20241022
888 Gemini-2.0	889 gemini-2.0-flash-001 (Version 1)
889 GPT-4o	890 gpt-4o-2024-08-06
890 GPT-4o-mini	891 gpt-4o-mini-2024-07-18
891 o4-mini	892 o4-mini-2025-04-16

893 **A.2 PARAMETER AND RANDOM BASELINE SETTINGS**
894895
896 **Parameter setting.** We have studied various methods of representing graphs as text based on a
897 diverse set of basic graph problems. This appendix details the parameter setting and the design of
898 the graph input text. For the parameter setting, the temperature is set to 0.7, following the parameter
899 selection in [Wang et al. \(2023\)](#). The nucleus sampling (top-p) is set to 0.9 for open-source models,
900 while for closed-source models, the default top-p value is used.
901902 **Random Baselines setting.** For Cycle detection, the random baseline simply selects an answer
903 from {True, False}—yielding an expected accuracy of 50%. Since the GT obtained through the
904 design function has a high proportion of True labels, we iterate through all queries, assuming the
905 given answer is True. We then use GT for evaluation, leading to the final baseline based on this
906 assumption. For tasks that require generating numerical outputs (e.g., Diameter calculation
907 and Triangle counting), the random baseline corresponds to randomly choosing one of the valid
908 numerical solutions derived from the graph’s structure. For the Diameter calculation task, the
909 random baseline is determined based on the number of nodes in the graph for each query. Specifically,
910 we sample a random integer from the range $[1, N]$, where N is the number of nodes in the graph, and
911 compare it with the ground truth to compute the baseline performance. For the Triangle counting
912 task, the random baseline is derived from the estimated upper bound on the number of triangles in the
913 graph. We compute the maximum possible number of triangles based on the number of nodes and the
914 task difficulty level, take the smaller value between these estimates, and sample a random integer
915 from the range $[1, M]$, where M is the determined upper bound. The sampled value is then compared
916 against the ground truth to obtain the random baseline performance. In contrast, for tasks that require
917 generating sequences (e.g., BFS order), the number of possible combinations is combinatorially
918 large, so a random baseline would yield an accuracy that is approximately 0%.

918 A.3 GRAPH TASKS
919920 We conducted a comprehensive study on a diverse set of fundamental graph problems, including
921 BFS order, Cycle detection, Connectivity, Diameter calculation, Shortest path, and
922 Triangle counting. The input text for each task is provided below, where the italicized variables X ,
923 Y denote generic node numbers corresponding to the specific problem under consideration.924
925 **Graph Tasks**
926

- **BFS-ORDER:** Give the bfs traversal order starting from node X .
- **CYCLE:** Is there a cycle in this graph?
- **CONNECTIVITY:** Is there a path between node X and node Y ?
- **DIAMETER:** What is the diameter of this graph?
- **SHORTEST PATH:** Give the shortest path from node X to node Y .
- **TRIANGLE:** How many triangles are in this graph?

926
927
928
929
930
931933 A.3.1 RATIONALE FOR SELECTION OF TASKS
934935 The six core tasks in GRAPHOMNI are deliberately selected to span qualitatively different reasoning
936 capacities. Their difficulty increases as the model must move from local checks to global traversals,
937 maintain more intermediate states in working memory, or perform exhaustive combinatorial enu-
938 meration. Beyond **reasoning capacities**, variation also arises from how well LLMs internalize **task**
939 **definitions** and from the complexity of **output formats**. Together, these factors explain the accuracy
940 gaps observed in Table 3 and highlight why the chosen tasks form a balanced and challenging suite.941 **Aspect 1: Reasoning capacities required.** These tasks are grouped according to the type and depth
942 of reasoning they demand, ranging from simple global checks to multi-layered traversals and full
943 combinatorial enumeration.944 Here follows a detailed elaboration on these three aspects.
945946 1. *Reachability verification* (Connectivity, Cycle detection). These tasks require a global
947 traversal but only a simple decision condition, such as whether the graph is connected or
948 whether a cycle is present. Most errors stem from serialization misunderstandings (e.g.,
949 assuming a missing edge exists, in Appendix E.4.3). Once the format is parsed correctly,
950 accuracy is high.
951 2. *Ordered-path reasoning* (BFS order, Shortest path, Diameter calculation).
952 These tasks demand that the model keep a frontier or distance map and then output or
953 compare those ordered distances. For BFS order, the model must list nodes level-by-level.
954 In the error case in Appendix E.4.7, failures occur when it forgets whether two previously
955 visited nodes are connected. Shortest path and Diameter calculation add a final
956 aggregation step: the former selects the minimum path, the latter the maximum among
957 all shortest paths. The common mistakes are also mostly about losing track of some vital
958 information while exploring the graph. Like the one in Appendix E.4.2 for Diameter
959 calculation, the model forgets two important edges, so the path length is wrong. Accuracy
960 here for those three tasks is lower than the first type of tasks because the model must track
961 ordering information across multiple expansion layers.
962 3. *Combinatorial enumeration* (Triangle counting).
963 Triangle counting is the most challenging: the model must evaluate every three-node
964 subset and make sure each sub-traverse is correct. Even given correct execution of the enu-
965 meration, the counting should be accurate to produce the correct final result. Appendix E.4.6
966 and E.4.8 document the dominant errors on enumeration over each possible triangle in the
967 graph (like missing an edge or wrongly assuming one). We also spotted cases that fail on
968 the counting at the end, too. In sum, performance is strongest when only reachability is
969 tested, drops when ordered path reasoning is required, and falls sharply when complete
970 combinatorial enumeration comes into play.971 **Aspect 2: Task understanding and definition knowledge.** LLMs sometimes rely on heuristics rather
972 than precise textbook definitions, particularly for less common tasks. For example, some models

972 confuse diameter with the longest simple path, producing inflated results (Appendix E.4.1). Others
 973 apply shortcuts such as “triangles $\approx n/3$ ” (Appendix E.4.5), ignoring the need for all three edges to
 974 be present. Such misinterpretations highlight that accuracy depends not only on raw reasoning ability
 975 but also on task comprehension. Our coverage of tasks enable the evaluation on these knowledge of
 976 each model and it does reflect in the results as the error cases mentioned.

977 **Aspect 3: Output format.** The output formats of the tasks chosen are also very diverse. Some tasks
 978 here need only a short answer, i.e., “Yes/No” for Connectivity or a single number for Triangle
 979 counting, so there is little room for formatting errors. Meanwhile, BFS order is different: the model
 980 must print a long, strictly level-by-level list of node IDs, and one extra or missing node makes the
 981 whole response wrong. The coverage of different output formats brings challenges to the models.
 982

983 In summary, these systematic differences validate that the GRAPHOMNI task suite probes diverse
 984 reasoning skills over graphs and exposes where current LLMs struggle most.
 985

986 A.4 GRAPH TYPES

987 A primary distinguishing aspect of our benchmark is the inclusion of multiple graph families, each
 988 possessing unique structural properties. All 7 types of graph are highlighted in **bold**:

990 **1. Erdős–Rényi (ER)** Graphs are randomly sampled from the space of all possible graphs with
 991 n vertices, making them well-suited for capturing a wide range of topological and connectivity
 992 properties within a fixed number of vertices.

993 To enhance the diversity of random graphs, we consider two sampling methods: m -edge sampling
 994 and probability-based sampling, referred to as **Erdős–Rényi M-Edges (ERM)** (Erdős & Rényi,
 995 1960) and **Erdős–Rényi Probability (ERP)** (Gilbert, 1959) respectively.

- 997 • **ERM:** Generates graphs with n vertices and a fixed number of edges m , where m is ran-
 998 domly chosen between 1 and $\frac{n(n-1)}{2}$, ensuring that all possible edge counts are considered.
- 999 • **ERP:** Constructs graphs with n vertices but an unfixed number of edges, where the edge
 1000 probability is randomly sampled as a floating-point value between 0 and 1.

1001 Additionally, we extend these models to bipartite settings:

- 1003 • **Bipartite Erdős–Rényi M-Edges (BERM)** and **Bipartite Erdős–Rényi Probability**
 1004 (**BERP**) graphs (Latapy et al., 2008) are generated using the ERM and ERP sampling
 1005 strategies but constrained to bipartite structures.
- 1006 • These bipartite graphs introduce additional variations in topology and connectivity that
 1007 standard ERM and ERP graphs, which are inherently undirected, may not capture.

1009 **2. Barabási–Albert Graphs (BAG)** (Albert & Barabási, 1999) exhibit a power-law degree distri-
 1010 bution, where a small number of nodes (hubs) have significantly higher degrees, while most nodes
 1011 have relatively few connections. Such structures frequently appear in real-world networks, including
 1012 social and biological systems.

1013 While ER graphs, being randomly sampled, may occasionally exhibit power-law degree distributions,
 1014 BAGs explicitly model this phenomenon due to their practical prevalence.

- 1016 • BAGs are constructed by starting with a complete graph of m_0 vertices and incrementally
 1017 adding nodes.
- 1018 • Each new node forms m connections, where m is proportional to the degrees of existing
 1019 nodes (preferential attachment).
- 1020 • In our dataset, m_0 is randomly sampled with an upper bound of $\frac{n}{3}$, and m is set to $m_0 + 1$.

1022 Although BAGs generally capture power-law degree distributions, they do not always represent
 1023 tree-like structures such as citation networks or hierarchical systems. To address this, we introduce
 1024 **Barabási–Albert Forests (BAF)** (Albert & Barabási, 1999), which follow the same generation
 1025 process as BAGs but enforce an acyclic structure, ensuring that the result is a forest (a set of trees)
 rather than a single connected graph.

1026 **3. Scale-Free (SF) Graphs** (Aiello et al., 2000) Another class of power-law networks that BAGs
 1027 may not fully capture is general scale-free (SF) networks. While all BAGs are SF, not all SF graphs
 1028 are BA.

1029

- 1030 • BAGs typically consist of a single connected component, whereas SF graphs can contain
 1031 multiple disconnected components.
- 1032 • To represent SF graphs more comprehensively, we introduce a distinct SF graph generation
 1033 process, different from BAGs.

1034

1035 Unlike BAGs, which are constructed through incremental growth and preferential attachment, SF
 1036 graphs are generated using a degree-weighted random connection strategy:

1037

- 1038 • All vertices are created at once.
- 1039 • Edges are formed probabilistically, where the probability of a connection is proportional to
 1040 node degrees.

1041

1042 These fundamental differences in growth dynamics and edge formation result in SF graphs and BAGs
 1043 capturing distinct topological properties. By including both, we enhance the diversity of our dataset.

1044 These families challenge LLMs to adapt their reasoning across numerous topological extremes,
 1045 from sparse bipartite graphs to highly connected ones. Although future expansions may include
 1046 small-world graphs or others, this current selection already covers a rich array of structural profiles as
 1047 elaborated in the next section.

1048 **A.4.1 RATIONALE FOR GENERATOR SELECTION**

1049

1050 The seven generators in GRAPHOMNI are deliberately selected to provide the most comprehensive
 1051 structural coverage possible within the 5–30 node range. Each generator encodes a distinct motif/structure
 1052 observed in real-world networks, i.e. random connectivity, scale-free growth, bipartite
 1053 affiliation, hierarchical trees or other tendencies, ensuring that the benchmark spans all major regimes
 1054 of graph organization. Even at this scale, the underlying generative biases remain evident and produce
 1055 meaningful differences in task difficulty and model behavior. By relying on controlled synthetic
 1056 generators, GRAPHOMNI achieves balanced representation across families while isolating structural
 1057 effects without the confounding noise of empirical data.

1058 To be specific, the selected generators cover a wide range of canonical structures:

1059

- 1060 **1. Erdős–Rényi M-Edges (ERM) & Probability (ERP).** Serve as canonical baselines for
 1061 random connectivity, yielding binomial/Poisson degree distributions used extensively in the
 1062 study of biological and technological networks.
- 1063 **2. Bipartite ERM (BERM) & Bipartite ERP (BERP).** Capture two-mode affiliation struc-
 1064 tures, such as author–paper and user–item systems, which exhibit realistic clustering and
 1065 degree properties.
- 1066 **3. Barabási–Albert Graphs (BAG).** Model scale-free networks with hubs emerging via
 1067 preferential attachment, mirroring the structure of the Internet, citation graphs, and social
 1068 networks.
- 1069 **4. Barabási–Albert Forests (BAF).** A specialization of the BA process that produces acyclic
 1070 scale-free trees, modeling hierarchical taxonomies such as phylogenies and organizational
 1071 charts.
- 1072 **5. Scale-Free (SF) Graphs.** Configuration-style models generate prescribed power-law de-
 1073 gree sequences, often producing disconnected components akin to regional transport or
 1074 communication subnetworks.

1075

1076 To further validate that these generators produce graphs with statistically distinct and meaningful
 1077 properties, we conduct two empirical studies. First, we sample 1,000 graphs of 30 nodes each from
 1078 the same Barabási–Albert (BAG) and Erdős–Rényi (ERP) generators used in GRAPHOMNI. As
 1079 summarized in Table 6, the two models exhibit clearly different structural characteristics: BA graphs
 form hubs with high maximum degree and short paths, while ER graphs display uniform randomness

1080 with lower clustering and longer paths. Second, as shown in Table 7 in Appendix B.1, even when
 1081 node counts are fixed, the edge counts (and thus average degrees) vary substantially across generators,
 1082 providing strong statistical evidence that the structural characteristics of these graph families are
 1083 fundamentally distinct. Together, these results confirm that the design of GRAPHOMNI captures the
 1084 essential structural diversity needed to probe LLM reasoning.

1085
 1086 Table 6: Comparison of structural statistics for 1,000 sampled graphs with 30 nodes. BAG graphs
 1087 exhibit hub formation with high maximum degree and short paths, while ERP graphs display more
 1088 uniform randomness.

Type	Max Degree	Clustering Coefficient	Avg Path Length
Barabási–Albert (BAG)	19.28 ± 2.15	0.397 ± 0.042	1.76 ± 0.014
Erdős–Rényi (ERP)	10.43 ± 1.35	0.199 ± 0.044	2.07 ± 0.099

1096 A.5 PROMPT SCHEMES

1097
 1098 The process of converting a graph into a textual representation is referred to as the serialization
 1099 process, which involves two primary considerations in our study: the choice of serialization format
 1100 and the selection of the prompting method. we employ a total of nine distinct prompting methods:
 1101 Algorithm, CoT, k-shot, Instruct, 0-Shot(i.e. plain), 0-CoT, 0-Instruct, 0-Algorithm, and
 1102 LTM. As outlined in the main text, the pairs Algorithm and 0-Algorithm, CoT and 0-CoT, k-shot
 1103 and 0-Shot, and Instruct and 0-Instruct share a common structural format, with the first element
 1104 in each pair incorporating additional 5 examples. A detailed description of the design for each of
 1105 these prompting methods is provided below. In particular, for the algorithmic description components
 1106 of Algorithm and 0-Algorithm, we primarily draw upon established methodologies in Wang et al.
 1107 (2023) and illustrate them with an example derived from the BFS-order task.

Prompt format

- **0-CoT:** Let's think step by step:
- **LTM:** Let's break down this problem:
- **0-INSTRUCT:** Let's construct a graph with the nodes and edges first:
- **0-ALGORITHM:** To determine the BFS (Breadth-First Search) traversal order, you need to follow these steps: 1. Initialize: Start by choosing a starting node and enqueue it into a queue. 2. Mark visited: Mark the starting node as visited to avoid reprocessing. 3. Traverse: While the queue is not empty: Dequeue a node and add it to the traversal order. For each unvisited neighboring node of the dequeued node, enqueue it and mark it as visited. 4. Continue the process until all reachable nodes are visited.

1119 A.6 SERIALIZATION FORMATS

1120
 1121 This study utilizes seven distinct yet commonly used graph representation formats: Adjacency
 1122 Matrix, Adjacency List, Adjacency Set, Edge Set, Edge List, Graph Modeling Language
 1123 (GMoL), and Graph Markup Language (GML). For the same graph, even when the underlying
 1124 information remains consistent, the representation varies across different serialization formats in
 1125 textual form. The following section presents specific examples of the same graph depicted in various
 1126 serialization formats.

1127 Adjacency Set

1128 {0: {1}, 1: {0, 2}, 2: {1}, 3: {4}, 4: {3, 5}, 5: {4}}

1131 Edge Set

1132 {(0, 1), (4, 5), (1, 2), (3, 4)}

```

1134
1135     Edge List
1136     0 1
1137     1 2
1138     3 4
1139     4 5
1140
1141
1142
1143
1144
1145
1146
1147     Adjacency Matrix
1148     [[0 1 0 0 0 0]
1149     [1 0 1 0 0 0]
1150     [0 1 0 0 0 0]
1151     [0 0 0 0 1 0]
1152     [0 0 0 1 0 1]
1153     [0 0 0 0 1 0]]
1154
1155
1156
1157
1158
1159
1160
1161     Adjacency List
1162     {0: [1], 1: [0, 2], 2: [1], 3: [4], 4: [3, 5], 5: [4]}
1163
1164
1165
1166
1167
1168
1169
1170
1171     GMaL
1172
1173     <?xml version='1.0' encoding='utf-8'?>
1174     <GMaL xmlns="http://GMaL.graphdrawing.org/xmlns"
1175         xmlns:xsi="http://www.w3.org/2001/XMLSchema-instance"
1176         xsi:schemaLocation="http://GMaL.graphdrawing.org/xmlns
1177         http://GMaL.graphdrawing.org/xmlns/1.0/GMaL.xsd">
1178     <graph edgedefault="undirected">
1179         <node id="0" />
1180         <node id="1" />
1181         <node id="2" />
1182         <node id="3" />
1183         <node id="4" />
1184         <node id="5" />
1185         <edge source="0" target="1" />
1186         <edge source="1" target="2" />
1187         <edge source="3" target="4" />
1188         <edge source="4" target="5" />
1189     </graph>
1190     </GMaL>

```

```

1188 GMoL
1189
1190 graph [
1191   node [
1192     id 0
1193     label "0"
1194   ]
1195   node [
1196     id 1
1197     label "1"
1198   ]
1199   node [
1200     id 2
1201     label "2"
1202   ]
1203   node [
1204     id 3
1205     label "3"
1206   ]
1207   node [
1208     id 4
1209     label "4"
1210   ]
1211   node [
1212     id 5
1213     label "5"
1214   ]
1215   edge [
1216     source 0
1217     target 1
1218   ]
1219   edge [
1220     source 1
1221     target 2
1222   ]
1223   edge [
1224     source 3
1225     target 4
1226   ]
1227   edge [
1228     source 4
1229     target 5
1230   ]
1231 ]

```

A.7 DATA EXAMPLES

1231 In order to better show the input example, we select the BFS order task in the serialization format
1232 is the Adjacency List of the complete prompt example, due to space reasons, the middle of the
1233 excessively long part we will use "...". Each of the following examples is randomly selected from the
1234 source data.

1235

1236

1237

1238

1239

1240

1241

0-Shot

Given a graph, your task is to determine the bfs traversal order of this graph starting at node 4. And the graph representation of: Adjacency List is {0: [1], 1: [0, 2, 3, 5, 6], 2: [1, 4], 3: [1], 4: [2], 5: [1, 7], 6: [1], 7: [5, 8], 8: [7]}

Q: Give the bfs traversal order starting from node 4.

A:

1242

1243

1244

1245

1246

1247

1248

1249

1250

1251

1252

1253

1254

1255

1256

1257

1258

1259

1260

1261

1262

1263

1264

1265

1266

1267

1268

1269

1270

1271

1272

1273

1274

1275

1276

1277

1278

1279

1280

1281

1282

1283

1284

1285

1286

1287

1288

1289

1290

1291

1292

1293

1294

1295

0-CoT

Given a graph, your task is to determine the bfs traversal order of this graph starting at node 7. And the graph representation of: Adjacency List is {1: [0, 2], 0: [1, 3, 4, 5, 6], 2: [1], 3: [0], 4: [0, 8], 5: [0, 7], 6: [0], 7: [5], 8: [4]}

Q: Give the bfs traversal order starting from node 7.

A:

Let's think step by step:

0-Instruct

Given a graph, your task is to determine the bfs traversal order of this graph starting at node 6. And the graph representation of: Adjacency List is {1: [0, 2], 0: [1, 3, 4, 7, 8], 2: [1], 3: [0], 4: [0, 5], 5: [4, 6], 6: [5], 7: [0], 8: [0]}

Q: Give the bfs traversal order starting from node 6.

A:

Let's construct a graph with the nodes and edges first:

0-Algorithm

To determine the BFS (Breadth-First Search) traversal order, you need to follow these steps:

1. Initialize: Start by choosing a starting node and enqueue it into a queue.

2. Mark visited: Mark the starting node as visited to avoid reprocessing.

3. Traverse: While the queue is not empty: Dequeue a node and add it to the traversal order. For each unvisited neighboring node of the dequeued node, enqueue it and mark it as visited.

4. Continue the process until all reachable nodes are visited.

Given a graph, your task is to determine the bfs traversal order of this graph starting at node 7. And the graph representation of: Adjacency List is {0: [7, 3, 2, 6, 1, 8, 5], 1: [4, 6, 3, 5, 0, 2], 2: [5, 0, 1, 7], 3: [7, 0, 8, 1, 6, 4], 4: [1, 8, 5, 7, 3, 6], 5: [2, 6, 7, 8, 4, 1, 0], 6: [1, 8, 5, 3, 0, 4], 7: [0, 3, 5, 4, 8, 2], 8: [4, 6, 5, 3, 7, 0]}

Q: Give the bfs traversal order starting from node 7.

A:

LTM

Given a graph, your task is to determine the bfs traversal order of this graph starting at node 4. And the graph representation of: Adjacency List is {0: [4, 5, 7], 1: [2, 3, 4, 5, 6], 2: [1, 3, 4, 6], 3: [1, 2, 5, 6], 4: [0, 1, 2, 5, 6], 5: [0, 1, 3, 4, 6, 7], 6: [1, 2, 3, 4, 5], 7: [0, 5]}

Q: Give the bfs traversal order starting from node 4.

A:

Let's break down this problem:

1296
1297**Algorithm**1298
1299
1300
1301

To determine the BFS (Breadth-First Search) traversal order, you need to follow these steps: 1. Initialize: Start by choosing a starting node and enqueue it into a queue. 2. Mark visited: Mark the starting node as visited to avoid reprocessing. 3. Traverse: While the queue is not empty: Dequeue a node and add it to the traversal order. For each unvisited neighboring node of the dequeued node, enqueue it and mark it as visited. 4. Continue the process until all reachable nodes are visited.

1302
1303
1304

Given a graph, your task is to determine the BFS traversal order of this graph starting at node 7. And the graph representation of Adjacency List is : {0: [1, 2, 3, 4, 6], 1: [0, 2, 8], 2: [0, 1, 5], 3: [0], 4: [0, 7], 5: [2], 6: [0], 7: [4], 8: [1]}

1305
1306
1307
1308
1309
1310
1311
1312

Q: Give the BFS traversal order starting from node 7.

A: Dequeue node 7. The neighbors are [4], so enqueue node 4. Dequeue node 4. The neighbors of 4 are [7, 0]. Node 7 is visited, so enqueue node 0. Dequeue node 0. The neighbors of 0 are [1, 2, 3, 6, 4]. Node 4 is already visited, so enqueue node 1, 2, 3, and 6. Dequeue node 1. The neighbors of 1 are [0, 2, 8]. Nodes 0 and 2 are visited, so enqueue node 8. Dequeue node 2. The neighbors of 2 are [0, 5]. Node 0 is visited, so enqueue node 5. Dequeue node 3. The neighbors of 3 are [0]. Node 0 is visited, so no new nodes. Dequeue node 6. The neighbors of 6 are [0]. Node 0 is visited, so no new nodes. Dequeue node 8. The neighbors of 8 are [1]. Node 1 is visited, so no new nodes. Dequeue node 5. The neighbors of 5 are [2]. Node 2 is visited, so no new nodes. All its neighbors have been visited, so the traversal ends. The BFS traversal order starting from node 7 is 7, 4, 0, 1, 2, 3, 6, 8, 5.

1313
1314
1315
1316
1317

Given a graph, your task is to determine the bfs traversal order of this graph starting at node 3. And the graph representation of: Adjacency List is {0: [3, 7, 8, 5, 6, 1, 4], 1: [4, 10, 0, 3, 9, 5, 2], 2: [10, 9, 4, 8, 7, 3, 6, 1], 3: [0, 5, 1, 4, 10, 7, 8, 2], 4: [2, 9, 1, 10, 6, 3, 0], 5: [9, 3, 0, 6, 7, 8, 1, 10], 6: [10, 0, 5, 7, 4, 9, 2], 7: [8, 10, 0, 5, 6, 2, 3], 8: [9, 7, 0, 5, 2, 3, 10], 9: [8, 10, 2, 5, 4, 1, 6], 10: [9, 6, 7, 2, 4, 1, 3, 8, 5]} Q

Q: Give the bfs traversal order starting from node 3.

1318

A:

1319
1320
1321
1322
1323
1324
1325
1326
1327
13281329
1330**CoT**

Given a graph, your task is to determine the BFS traversal order of this graph starting at node 7. And the graph representation of Adjacency List is : {0: [1, 2, 3, 4, 6], 1: [0, 2, 8], 2: [0, 1, 5], 3: [0], 4: [0, 7], 5: [2], 6: [0], 7: [4], 8: [1]}

1333
1334
1335
1336
1337
1338
1339
1340
1341

Q: Give the BFS traversal order starting from node 7.

A: The BFS traversal starts at node 7. In BFS, we visit each node level by level, starting from the node we begin at (node 7). Here's the step-by-step breakdown: Start at node 7. The first node in the BFS traversal is 7. Visit the neighbors of 7. The neighbors of node 7 are just node 4 (since 7 4 is an edge). So, we enqueue node 4. Visit the neighbors of node 4. The neighbors of node 4 are node 0 (4 0), so we enqueue node 0. Visit the neighbors of node 0. The neighbors of node 0 are nodes 1, 2, 3, 4 and 6. Since node 4 has already been visited, we enqueue nodes 1, 2, 3, and 6 in that order. Visit the neighbors of nodes 1, 2, 3, 6. From this point, the BFS continues by visiting any remaining unvisited neighbors of these nodes in the same manner, reaching node 8 last. Thus, the BFS traversal order starting from node 7 is 7, 4, 0, 1, 2, 3, 6, 8, 5. The BFS traversal order starting from node 7 is 7,4,0,1,2,3,6,8,5.

1342
1343
1344
1345
1346
1347
1348
1349

Given a graph, your task is to determine the bfs traversal order of this graph starting at node 28. And the graph representation of: Adjacency List is {0: [1, 2, 3, 4, 31], 1: [0], 2: [0, 17, 22, 33], 3: [0, 5, 7, 8, 9, 10, 13, 15, 16, 19, 22, 23, 24, 26, 27, 28, 31], 4: [0, 6, 8, 10, 14, 15, 24, 27, 30], 5: [3, 8], 6: [4], 7: [3, 11, 12, 25], 8: [3, 4, 5, 10, 29], 9: [3], 10: [3, 4, 8, 33], 11: [7, 18, 20], 12: [7, 21], 13: [3], 14: [4], 15: [3, 4, 28, 33], 16: [3], 17: [2, 19, 24], 18: [11, 32], 19: [3, 17], 20: [11], 21: [12], 22: [2, 3], 23: [3], 24: [3, 4, 17], 25: [7], 26: [3], 27: [3, 4, 33], 28: [3, 15], 29: [8], 30: [4], 31: [0, 3], 32: [18], 33: [2, 10, 15, 27]}

Q: Give the bfs traversal order starting from node 28.

A:

1350

K-Shot

1351

Given a graph, your task is to determine the BFS traversal order of this graph starting at node 7. And the graph representation of Adjacency List is : {0: [1, 2, 3, 4, 6], 1: [0, 2, 8], 2: [0, 1, 5], 3: [0], 4: [0, 7], 5: [2], 6: [0], 7: [4], 8: [1]}

1354

Q: Give the BFS traversal order starting from node 7.

1355

A: The BFS traversal order starting from node 7 is 7,4,0,1,2,3,6,8,5

1356

...

Given a graph, your task is to determine the bfs traversal order of this graph starting at node 2. And the graph representation of: Adjacency List is 0: [6], 1: [6], 2: [6], 3: [6], 4: [6], 5: [6], 6: [0, 1, 2, 3, 4, 5]

1358

Q: Give the bfs traversal order starting from node 2.

1359

A:

1360

1361

Instruct

1362

Given a graph, your task is to determine the BFS traversal order of this graph starting at node 7. And the graph representation of Adjacency List is : {0: [1, 2, 3, 4, 6], 1: [0, 2, 8], 2: [0, 1, 5], 3: [0], 4: [0, 7], 5: [2], 6: [0], 7: [4], 8: [1]}

1363

Let's construct a graph with the nodes and edges first.

1364

Q: Give the BFS traversal order starting from node 7.

1365

A: The BFS traversal starts at node 7. In BFS, we visit each node level by level, starting from the node we begin at (node 7). Here's the step-by-step breakdown: Start at node 7. The first node in the BFS traversal is 7. Visit the neighbors of 7. The neighbors of node 7 are just node 4 (since 7 4 is an edge). So, we enqueue node 4. Visit the neighbors of node 4. The neighbors of node 4 are node 0 (4 0), so we enqueue node 0. Visit the neighbors of node 0. The neighbors of node 0 are nodes 1, 2, 3, 4 and 6. Since node 4 has already been visited, we enqueue nodes 1, 2, 3, and 6 in that order. Visit the neighbors of nodes 1, 2, 3, 6. From this point, the BFS continues by visiting any remaining unvisited neighbors of these nodes in the same manner, reaching node 8 last. Thus, the BFS traversal order starting from node 7 is 7, 4, 0, 1, 2, 3, 6, 8, 5. The BFS traversal order starting from node 7 is 7,4,0,1,2,3,6,8,5.

1366

...

Given a graph, your task is to determine the bfs traversal order of this graph starting at node 10. And the graph representation of: Adjacency List is {0: [4, 14, 1, 11, 5, 13, 2, 12], 1: [12, 4, 10, 2, 0, 3, 14, 11], 2: [8, 9, 1, 13, 11, 12, 15, 5, 0], 3: [10, 1, 11, 7, 8], 4: [0, 1, 15, 11, 6, 10], 5: [14, 6, 11, 0, 2, 7], 6: [5, 4, 11, 10, 14], 7: [14, 12, 9, 13, 3, 8, 5], 8: [2, 15, 14, 12, 10, 3, 7, 13], 9: [2, 7, 15, 12, 14, 13], 10: [3, 1, 8, 15, 4, 11, 6], 11: [14, 2, 0, 12, 4, 3, 5, 6, 10, 1, 13], 12: [1, 13, 7, 2, 14, 11, 9, 8, 0], 13: [12, 2, 7, 9, 0, 11, 8], 14: [7, 0, 11, 5, 12, 8, 9, 1, 6], 15: [4, 9, 8, 2, 10]}

1367

Let's construct a graph with the nodes and edges first.

1368

Q: Give the bfs traversal order starting from node 10.

1369

A:

1370

1371

1372

1373

1374

B BENCHMARK STATISTICS

1375

This section presents the statistical characteristics of GRAPHOMNI, focusing on the graph families and token usage. We first detail the statistical properties of graph families used in our benchmark in Section B.1, followed by an overview of token consumption associated with various prompt schemes and serialization formats in Section B.2.

1376

1377

1378

1379

1380

1381

1382

B.1 BASIC STATISTICS OF GRAPHOMNI

1383

1384

1385

1386

1387

Table 7 offers a detailed statistical overview of the diverse graph families employed in GRAPHOMNI. The table reports the average number of nodes and edges for each graph family across tasks such as BFS order, Connectivity, Cycle detection, Diameter calculation, Shortest path, and Triangle counting. These statistics are presented for three difficulty levels: easy, medium, and hard, which reveal the inherent structural complexity differences introduced by the various synthetic graph generators. The selection of graph families is guided by their unique topological properties so that each task is evaluated on graphs that best reflect the challenges encountered in practical applications. In addition, some graph families are omitted from certain tasks because of their intrinsic structural characteristics; for instance, graphs produced by the BAF and all bipartite graphs are excluded from triangle detection when they are structurally incapable of forming triangles.

1404
1405
1406
1407
1408
1409
1410
1411
1412

Table 7: Statistics of Different Graph Types

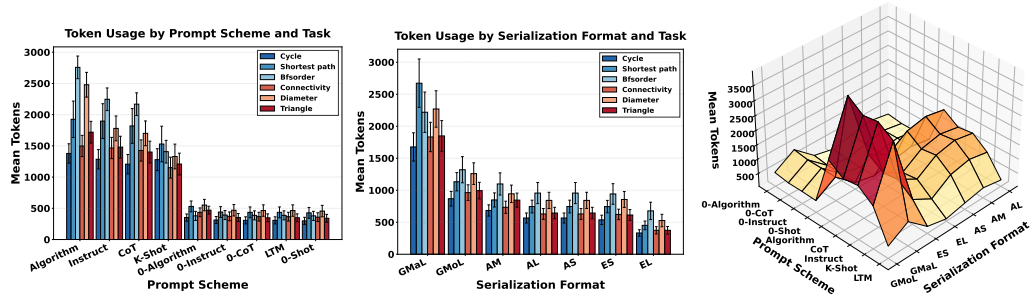
Task	Graph Type	Easy		Medium		Hard	
		#Avg Nodes	#Avg Edges	#Avg Nodes	#Avg Edges	#Avg Nodes	#Avg Edges
BFS-order	BAF	8.11	5.78	15.14	11.06	27.86	20.14
	BAG	8.19	11.36	13.92	23.28	26.55	82.14
	Bipartite-ERM	8.03	6.50	14.44	19.28	27.23	59.36
	Bipartite-ERP	7.94	5.44	14.42	16.72	28.86	57.82
	ERM	8.22	16.06	13.72	51.92	25.32	135.09
	ERP	8.03	13.14	14.33	50.17	24.59	121.77
	SF	8.11	9.00	14.81	19.00	27.73	38.00
Connectivity	BAF	8.14	6.21	13.83	10.67	31.17	27.00
	Bipartite-ERM	8.07	7.43	15.33	23.00	30.83	63.00
	Bipartite-ERP	8.14	7.57	13.67	20.00	28.17	59.33
	ERM	8.07	9.71	13.83	36.67	27.50	102.17
	ERP	8.11	10.56	17.83	66.17	26.33	98.00
Cycle	BAG	7.93	9.90	14.12	25.10	27.82	59.04
	Bipartite-ERM	8.12	7.60	15.62	20.38	28.54	57.96
	Bipartite-ERP	8.29	7.12	15.17	17.55	30.25	44.89
	ERM	8.19	11.43	15.10	36.43	26.46	58.21
	ERP	8.07	9.71	15.40	26.36	26.07	71.18
	SF	8.05	8.07	12.71	14.24	25.04	29.71
Diameter	BAG	7.98	9.73	14.30	29.91	26.81	92.24
	ERM	8.00	19.73	15.22	65.48	25.90	139.79
	ERP	8.16	18.61	15.17	70.36	25.19	130.79
	SF	7.95	9.14	15.41	19.91	28.48	39.10
Shortest-Path	BAF	7.83	6.11	14.17	11.56	25.62	21.71
	BAG	7.97	10.72	14.72	31.19	25.29	88.33
	Bipartite-ERM	8.06	8.97	14.61	30.58	25.50	94.71
	Bipartite-ERP	8.11	9.72	14.61	28.86	25.58	89.00
	ERM	8.00	17.42	15.47	67.89	25.96	179.21
	ERP	8.03	18.92	15.42	63.14	25.25	165.46
	SF	8.03	9.42	15.50	20.03	25.54	35.21
Triangle	BAG	8.16	13.12	14.09	25.48	27.72	55.65
	ERM	8.06	17.44	13.39	30.81	28.80	62.60
	ERP	7.94	16.05	14.16	31.11	27.22	55.28
	SF	8.14	9.59	15.61	20.88	28.35	38.58

Note: Graph types are selectively excluded from certain tasks based on their structural properties: (1) Connectivity excludes BAG as they are inherently connected by construction; (2) Diameter calculation task excludes BAF and Bipartite-ER graphs due to potentially disconnected components leading to infinite distances; (3) Triangle counting excludes BAF and Bipartite graphs as they are structurally incapable of forming triangles; (4) Cycle detection excludes BAF as they are acyclic by definition.

1451
1452
1453
1454
1455
1456
1457

B.2 TOKEN STATISTICS OF GRAPHOMNI

Figure 6 offers an overview of token consumption across different dimensions. We use GPT-4 tokenizer here. Token usage is impacted by the choice of prompt scheme and graph serialization format, interactions between them can further influence the overall token count.



(a) Token usage across different prompt schemes and tasks. (b) Token usage across different serialization formats and tasks (c) Token usage for prompt-serialization format combinations.

Figure 6: Analysis of token usage patterns across different dimensions. (a) shows how token usage varies across different prompt schemes for each task. (b) illustrates token consumption patterns for different serialization formats across tasks. (c) provides a 3D surface visualization of the interaction between prompt schemes and serialization formats regarding token usage. Error bars in (a) and (b) represent the standard error of the mean.

C EXTENDED STUDY AND DISCUSSION OF GRAPHOMNI

C.1 STUDY ON LARGER GRAPH (BEYOND 30 NODES)

Our benchmark design centers on graphs with 5–30 nodes. While modest compared to real-world networks, this range is both deliberate and effective. First, it aligns with the context length limits of current LLMs and matches the scale used in nearly all recent graph reasoning benchmarks (see Table 3), ensuring comparability. Also, the scale enables us to generate tens of thousands of diverse queries per task, providing statistically robust performance estimates and clearly separating different models apart, like open-source from closed-source models. In this sense, the 5–30 node regime is not a limitation, but a well-calibrated testbed for probing the boundaries of LLM graph reasoning.

To further validate our considerations, we conduct additional experiments on graphs with 30–50 nodes. We sample 50 graphs evenly across all seven generators and evaluate four representative models, yielding approximately 3k new test cases with varied prompt and serialization settings. Results are reported in Table 8. As expected, larger graphs further stress performance, especially on BFS order and Triangle counting. Nevertheless, the relative ranking and accuracy patterns remain consistent with the 5–30 node Hard split, reinforcing the robustness of our findings.

Table 8: Preliminary results on 30–50 node graphs (EH = Extra Hard). Results on the 5–30 node Hard split are shown in parentheses. **Bold orange** / Underlined blue / Light blue highlights indicate best/second-best/third-best performance in its category.

Task	Difficulty	Open-source Models				Closed-source Models	
		Llama-3.1 (8B)	Mistral (7B)	Phi-4 (14B)	Qwen-2.5 (7B)	Claude-3.5	o4-mini
BFS order	EH	0.70±0.36(0.63)	0.27±0.23 (0.34)	2.55±1.08 (2.65)	1.19±0.52 (1.38)	16.07±2.48 (26.80)	35.39±12.61 (32.43)
Connectivity	EH	80.33±3.24(74.58)	84.11±3.26 (74.77)	51.82±8.23 (48.39)	85.01±3.06 (81.19)	97.92±1.18 (96.99)	91.48±7.80 (92.08)
Cycle	EH	56.62±3.16 (52.40)	52.62±2.32 (51.64)	49.38±8.09 (40.64)	61.38±2.61 (62.27)	68.53±5.14 (78.22)	71.66±11.33 (93.06)
Diameter	EH	15.39±3.87 (18.63)	6.89±2.06 (6.97)	16.44±2.89 (17.71)	11.67±2.31 (15.27)	48.78±4.76 (56.70)	37.89±6.56 (34.61)
Shortest	EH	15.56±6.76 (23.03)	1.48±2.03 (12.21)	16.30±7.66 (26.60)	11.85±6.62 (28.31)	57.04±4.46 (87.88)	58.08±4.52 (88.62)
Triangle	EH	3.19±0.92(4.95)	2.41±0.65(2.55)	4.35±1.40 (4.38)	4.40±0.80 (4.45)	12.31±0.82 (15.92)	8.28±4.35 (17.53)

1512

C.2 STUDY ON REAL-WORLD GRAPHS: REPRESENTATIVE CHECK

1513

1514

To assess whether our synthetic design translates to real data, we run a focused representative check on two widely used real-world graph suites from complementary domains: a social/interaction dataset IMDB-MULTI (Morris et al., 2020) and a molecular graph dataset (ogbg-molhiv) (Hu et al., 2020). We sample 20 graphs per difficulty per dataset (60 graphs per task in total and thus $\sim 3.6k$ evaluated samples across tasks with prompt/serialization variants) and test four representative open-source models plus two closed-source models. Table 9 reports the experimental results.

1519

1520

Finding 1: Conclusions remain consistent. Across all six tasks and difficulty levels, accuracy patterns on IMDB-MULTI and ogbg-molhiv closely track the synthetic results: (i) reachability (Connectivity, Cycle detection) is the easiest regime and exhibits high accuracy once serialization is parsed; (ii) ordered-path tasks (BFS order, Shortest path, Diameter calculation) remain substantially harder, with error modes dominated by lost ordering or forgotten edges; and (iii) Triangle counting remains the most difficult due to exhaustive enumeration and arithmetic reliability. The *relative ranking* of models is stable, and the *gap structure* between open- and closed-source models mirrors the results from standard GRAPHOMNI. In short, the representative real-world runs perfectly corroborate our synthetic-only conclusions rather than overturning them.

1521

1522

1523

1524

1525

1526

1527

1528

Finding 2: Real graphs often simplify certain tasks. Because many public real graphs are connected and sparse within the selected ranges, some tasks become easier than in our synthetic distribution. For example, connectivity saturates for strong models (near 100% on Easy/Medium in Table 9), and cycle detection displays uniformly higher means than in matched synthetic settings. This is because the uneven data distribution of real graphs means that nearly all graphs are connected and contain at least one cycle. This ease does not invalidate the benchmark, but it shows that *using real-world graphs alone can under-stress* the tasks that are critical to graph reasoning.

1529

1530

1531

1532

1533

1534

1535

1536

In sum, we include IMDB-MULTI and ogbg-molhiv as a *representative check*, which validates that our conclusions persist on real graphs from two major application families (social interaction and molecular science). However, consistent with both our evidence and prior community practice, we retain synthetic graphs in GRAPHOMNI as the default for *comprehensive structural coverage, fine-grained interpretability and control, and contamination-free* evaluation.

1537

1538

1539

1540

1541

1542

1543

Table 9: Benchmark results of LLMs across tasks (Mean \pm 95% CI Margin) on real-world graphs. Results on the standard setting (i.e. GRAPHOMNI) are shown in parentheses.

Bold orange / Underlined blue / Light purple highlights indicate best/second-best/third-best performance in its category.

1544

1545

1546

1547

Task	Difficulty	Open-source Models				Closed-source Models	
		Llama-3.1 (8B)	Mistral (7B)	Phi-4 (14B)	Qwen-2.5 (7B)	Claude-3.5	o4-mini
BFS order	E	45.63 \pm 5.22 (18.69)	47.06\pm3.18 (13.75)	41.90 \pm 8.66 (33.03)	41.98 \pm 7.40 (21.46)	97.14\pm0.91 (91.42)	96.46 \pm 1.37 (95.46)
	M	12.14 \pm 2.11 (5.27)	10.24 \pm 1.85 (3.36)	17.86\pm3.89 (12.49)	10.32 \pm 2.49 (6.05)	76.98 \pm 2.79 (68.25)	86.89\pm3.94 (79.37)
	H	2.94 \pm 0.90 (0.63)	0.24 \pm 0.27 (0.34)	4.76\pm1.77 (2.65)	0.95 \pm 0.76 (1.38)	41.35 \pm 3.76 (26.80)	44.65\pm9.89 (32.45)
Connectivity	E	94.21 \pm 1.47 (79.53)	93.57 \pm 1.89 (79.90)	61.59 \pm 9.07 (56.29)	96.35\pm0.92 (88.10)	99.92 \pm 0.16 (98.38)	100.00\pm0.00 (98.23)
	M	88.73 \pm 2.37 (79.47)	88.81 \pm 2.98 (80.60)	53.25 \pm 8.09 (54.38)	93.10\pm1.67 (87.23)	99.92\pm0.16 (99.11)	99.83 \pm 0.23 (98.72)
	H	89.44 \pm 2.01 (74.58)	87.30 \pm 3.32 (74.77)	55.24 \pm 7.67 (48.39)	89.76\pm2.04 (81.19)	98.65\pm0.67 (96.99)	95.63 \pm 3.04 (92.02)
Cycle	E	56.75 \pm 2.62 (55.49)	51.43 \pm 1.56 (55.44)	51.03 \pm 6.82 (45.25)	59.37\pm2.00 (62.19)	80.48 \pm 4.81 (82.56)	94.51\pm2.14 (97.97)
	M	54.05 \pm 2.46 (55.69)	49.92 \pm 1.18 (53.71)	48.17 \pm 5.83 (44.26)	55.63\pm1.79 (62.07)	76.51 \pm 5.06 (80.80)	92.19\pm3.78 (97.75)
	H	51.03 \pm 2.21 (52.40)	49.84 \pm 1.31 (51.64)	44.68 \pm 5.27 (40.64)	54.05\pm2.20 (58.88)	71.75 \pm 3.87 (80.10)	89.65\pm3.40 (95.61)
Diameter	E	25.48 \pm 4.20 (41.27)	20.95 \pm 4.18 (28.55)	50.48\pm5.69 (42.81)	47.86 \pm 3.57 (45.08)	83.33 \pm 1.13 (83.71)	97.30\pm0.90 (98.88)
	M	15.48 \pm 3.51 (27.29)	8.81 \pm 2.24 (15.17)	25.16\pm3.92 (28.49)	23.02 \pm 3.29 (27.31)	58.33 \pm 2.82 (71.22)	84.37\pm3.89 (72.84)
	H	8.97 \pm 3.00 (18.63)	6.19 \pm 2.58 (6.97)	14.21\pm2.36 (17.71)	12.86 \pm 1.89 (15.27)	43.02 \pm 2.52 (56.70)	64.12\pm7.27 (34.61)
Shortest	E	39.21 \pm 5.87 (38.75)	28.65 \pm 4.69 (31.18)	43.89 \pm 8.80 (42.61)	50.08\pm9.17 (47.46)	98.49 \pm 1.29 (94.35)	98.59\pm1.44 (95.08)
	M	30.16 \pm 4.57 (28.84)	21.83 \pm 3.61 (19.89)	34.44 \pm 7.92 (33.92)	37.14\pm7.44 (35.53)	95.71 \pm 2.09 (91.27)	98.39\pm1.72 (92.60)
	H	22.06 \pm 3.73 (23.03)	14.05 \pm 2.51 (12.21)	30.16\pm6.43 (26.60)	29.68 \pm 5.65 (28.31)	92.14 \pm 1.80 (87.88)	95.79\pm2.91 (88.63)
Triangle	E	11.19 \pm 3.03 (14.97)	5.32 \pm 1.69 (11.87)	23.81 \pm 5.33 (12.88)	24.44\pm3.65 (18.56)	63.89 \pm 3.16 (43.41)	81.30\pm4.10 (84.54)
	M	6.51 \pm 2.03 (8.56)	1.83 \pm 0.84 (5.86)	14.44\pm3.61 (7.54)	11.83 \pm 2.51 (9.18)	47.30 \pm 2.74 (24.00)	82.20\pm3.86 (48.13)
	H	5.95 \pm 2.17 (4.95)	1.35 \pm 0.64 (2.55)	9.60\pm3.21 (4.38)	9.52 \pm 2.40 (4.45)	34.84 \pm 2.80 (15.92)	65.29\pm8.75 (17.53)

1564

1565

1566
1567

C.3 CONSIDERATIONS ON REAL-WORLD GRAPHS VS. SYNTHETIC GRAPHS

1568
1569
1570

In designing our benchmark, we considered several possible choices of evaluation substrate, including both real-world and synthetic graphs. After careful consideration, we opted to primarily use synthetic graphs, for the following methodological reasons:

1571
1572
1573
1574
1575
1576
1577
1578
1579
1580
1581
1582
1583
1584
1585
1586

1. *Coverage and controllability.* Our seven classic generators are selected to span the principal structural motifs (random/Poisson, scale-free, bipartite, hierarchical, small-world), and they support fine-grained parameter control (e.g., p in Erdős–Rényi, attachment in BA) (Chakrabarti & Faloutsos, 2006). This control enables balanced, modular ablations and isolates causal factors of failure, which typical public real-graph suites do not provide.
2. *Representativeness vs. noise in public repositories.* Real-graph repositories such as SNAP (Sosic & Leskovec, 2015) skew toward specific domains (social/web) with narrow size and density bands. Also, many graphs are connected and share similar sparsity patterns. This induces *structural narrowness* and *domain bias*, and it can *reduce task hardness* (e.g., connectivity becomes trivial). Mixing such graphs into a general-purpose reasoning benchmark, therefore, risks adding noise without broadening structural regimes.
3. *Zero contamination.* Fully synthetic construction guarantees no overlap with pretraining corpora, avoiding inflated scores due to memorization or leakage (Hendrycks et al., 2021a). Given rapidly evolving LLMs and opaque training mixtures, contamination-free evaluation is essential for credible comparisons.

1587
1588
1589
1590
1591
1592
1593
1594
1595
1596
1597

Meanwhile, **synthetic-only evaluation is also standard in prior work.** This design choice is not unique to GRAPHOMNI. Several foundational studies adopt the same “synthetic only” paradigm to ensure interpretability and controlled analysis: GraphQA (Fatemi et al., 2024) and GraphInstruct (Luo et al., 2024b) both rely solely on synthetic graphs to probe LLM reasoning, while GraphWiz (Chen et al., 2024a) demonstrates that synthetic graphs can even serve as effective fine-tuning data. These precedents highlight that synthetic construction is widely accepted in the community as the most principled way to study graph reasoning in LLMs. At the same time, we note that the real-graph domains we choose (IMDB-MULTI and ogbg-molhiv) align with recent works such as LLM4Hypergraph (Feng et al., 2025), which employ citation networks and protein structures, respectively. Thus, our real-graph ablation covers representative application families, while our synthetic benchmark remains the default for comprehensive coverage and methodological clarity.

1598
1599

C.4 EXPLORATION ON NP-HARD TASKS

1600
1601
1602
1603

To complement our six canonical tasks, we further probe LLM performance on two classical NP-hard graph problems: Hamiltonian cycle detection and Max-Cut. This evaluation serves as an ablation rather than a core component of GRAPHOMNI, allowing us to test whether the conclusions from tractable tasks extend to settings of higher computational complexity.

1604
1605
1606
1607
1608
1609
1610
1611
1612
1613
1614

Experimental setup. We retain the three difficulty splits by node size: Easy ($n \in [0, 10]$), Medium ($n \in (10, 20]$), and Hard ($n \in (20, 25]$). Compared to the main benchmark, the Hard regime uses slightly smaller graphs due to the exponential growth in search space. For *Hamiltonian cycle*, structural imbalance makes several generators unsuitable (e.g., SF, Bipartite-ERM, BAF, and Bipartite-ERP rarely admit cycles). We therefore restrict the task to ERM, ERP, and BAG, with ground-truth labels balanced 50/50 between existence and non-existence of a Hamiltonian cycle. For clarity, we also report Hamiltonian cycle results on the positive cases separately, since these are strictly harder: a correct answer must not only assert existence but also return a complete and valid tour (metric mentioned below). For *Max-Cut*, all seven graph families are included (SF, ERM, ERP, BAG, BERP, BAF, and BERM). We sample 18 graphs per split for Hamiltonian cycle and 14 per split for Max-Cut, yielding just over 6,000 queries across prompt and serialization variants.

1615
1616
1617
1618
1619

Evaluation metrics. As with the canonical tasks, we apply strict binary scoring. For *Hamiltonian cycle*, a prediction is marked correct only if: (i) the model explicitly affirms or denies the existence of a cycle in line with the ground truth, and (ii) when the ground truth is True, the model additionally outputs a concrete cycle, which we verify with a dedicated checker. Omitting an explicit decision or producing a non-verifiable tour results in 0. For *Max-Cut*, we extract both the predicted maximum cut size and the corresponding bipartition (from phrases such as “the maximum cut size is ...”). A

1620 custom validation function checks whether the reported cut matches the ground truth. Full correctness
 1621 requires both size and partition to be correct, while partial matches or non-extractable answers are
 1622 scored 0.

1623 **Results and insights.** As summarized in Table 10, performance patterns closely resemble those of the
 1624 six canonical tasks: open-source models hover near random, while closed-source reasoning models
 1625 achieve substantially higher, but still imperfect, scores. Thus, the core conclusions of GRAPHOMNI
 1626 generalize naturally to NP-hard settings. More interestingly, these results highlight how LLMs
 1627 perceive task difficulty differently from humans. Whereas human solvers experience a sharp jump in
 1628 difficulty between polynomial-time and NP-hard problems, current LLMs instead exhibit a nearly
 1629 uniform collapse in accuracy across NP-hard tasks. In other words, scaling to NP-hard does not
 1630 introduce a progressive “step up” in challenge for models as it does for humans. This suggests that
 1631 including NP-hard tasks may not meaningfully enrich the evaluation landscape, and reinforces our
 1632 focus on tractable yet diverse tasks as the primary design of GRAPHOMNI.

1633 Table 10: Benchmark Results of LLMs Across Tasks (Mean \pm 95% CI Margin).
 1634 **Bold orange** / Underlined blue / **Light purple** highlights indicate best/second-best/third-best
 1635 performance in its category.

Task	Difficulty	Open-source Models					Closed-source Models o4-mini
		Llama-3.1 (8B)	Mistral (7B)	Phi-4 (14B)	Qwen2.5 (7B)	qwen38	
Hamilton cycle	E	57.14 \pm 2.97	55.47 \pm 2.85	57.67 \pm 6.25	73.02 \pm 2.87	93.74\pm1.45	97.09\pm0.88
	M	54.94 \pm 3.40	46.03 \pm 3.05	50.09 \pm 6.59	<u>60.14\pm2.93</u>	<u>84.83\pm2.38</u>	71.08 \pm 2.39
	H	54.94 \pm 3.61	46.38 \pm 3.04	51.85 \pm 6.98	<u>60.23\pm3.05</u>	79.98\pm2.64	55.56 \pm 2.48
Hamilton cycle (Positive Samples)	E	45.68 \pm 4.96	63.67 \pm 7.09	54.67 \pm 6.04	<u>73.02\pm5.14</u>	89.59\pm2.51	95.24\pm1.54
	M	50.62 \pm 6.90	64.73 \pm 7.61	60.85 \pm 8.39	<u>71.60\pm5.30</u>	79.37\pm4.15	49.56 \pm 4.32
	H	47.09 \pm 6.88	58.38 \pm 6.81	55.73 \pm 8.13	<u>61.55\pm6.36</u>	70.90\pm4.61	18.46 \pm 3.64
Max cut	E	15.10 \pm 3.29	11.63 \pm 2.44	<u>23.88\pm4.69</u>	18.37 \pm 2.71	27.96\pm4.56	61.94\pm4.27
	M	5.20 \pm 1.66	5.10 \pm 1.43	6.43 \pm 1.81	<u>10.41\pm1.26</u>	16.94\pm2.33	28.16 \pm 1.80
	H	1.22 \pm 0.70	0.61 \pm 0.47	<u>2.04\pm1.03</u>	1.12 \pm 0.61	9.08\pm2.17	34.74 \pm 3.64

1648 C.5 SCALING VS. REASONING: DISENTANGLING THEIR EFFECTS ON GRAPH REASONING

1649 To contrast model *scaling* with *reasoning-centric* improvements, we isolate three Qwen variants:
 1650 **Qwen-2.5 (7B)** as the baseline, **Qwen-2.5 (72B)** to represent scaling up within the same family, and
 1651 **Qwen-3 (8B)** as a reasoning model at a comparable parameter budget. Table 11 subsets the main
 1652 results (Table 3) to these three columns.

1653 **Finding 1: Scaling lifts the floor.** Relative to Qwen-2.5 (7B), Qwen-2.5 (72B) yields consistent
 1654 improvements across nearly all tasks, particularly on the easier splits. For example, accuracy on
 1655 BFS order (Easy) rises from 21.46 to 71.41, an absolute gain of nearly 50%, while Shortest path
 1656 (Easy) improves from 47.46% to 90.03%, a margin of over 42%. Similarly, Diameter calculation
 1657 (Easy) increases by more than 33% (45.08% \rightarrow 78.50%). Even on Connectivity, which is already
 1658 near-saturated, scaling provides modest yet consistent lifts (E/M/H: +2.14%, +2.45%, +2.90%,
 1659 respectively). In contrast, on the most combinatorial regime, Triangle counting (Hard), the gain
 1660 is negligible (4.45% \rightarrow 4.73%), suggesting that sheer scale does little to overcome the inherent
 1661 difficulty of exhaustive enumeration.

1662 **Finding 2: Reasoning lifts the ceiling.** When holding parameter count roughly constant, Qwen-3
 1663 (8B) substantially outperforms both Qwen-2.5 (7B) and, on several hard splits, even Qwen-2.5 (72B).
 1664 For instance, on BFS order (Hard), performance improves from 22.03% to 29.53% compared to
 1665 Qwen-2.5 (72B), a relative advantage of more than 7%. On Diameter calculation (Hard), the
 1666 margin widens further: 39.83% versus 29.59%, an absolute gain of over 10%. The effect is most
 1667 striking on Triangle counting (Hard), where Qwen-3 (8B) achieves 19.54%, far surpassing the
 1668 4.73% of Qwen-2.5 (72B). These results indicate that architectural and optimization changes targeted
 1669 at reasoning are more effective in extending the *upper bound* of graph reasoning ability than scaling
 1670 alone.

1671 **Implication.** Scaling and reasoning improve different aspects of performance. Larger models
 1672 predominantly strengthen robustness on easier instances, lifting the floor, whereas reasoning-oriented
 1673 models better capture multi-hop dependencies and complex subgraph structures, lifting the ceiling. A

1674
1675
1676
1677
1678
1679
1680
1681
1682
1683

1684 Table 11: Isolating scaling vs. reasoning effects. Baseline: Qwen-2.5 (7B). Scaling: Qwen-2.5
1685 (72B). Reasoning: Qwen-3 (8B). **Bold orange** / Underlined blue / Light blue highlights indicate
1686 best/second-best/third-best performance.

Task	Difficulty	Open-source Models		
		Qwen2.5 (72B)	Qwen2.5 (7B)	Qwen3 (8B)
BFS order	E	71.41±3.45	21.46±4.26	<u>65.87±5.59</u>
	M	<u>47.82±5.30</u>	6.05±1.41	53.30±5.42
	H	<u>22.03±4.39</u>	1.38±0.37	29.53±4.25
Connectivity	E	<u>90.24±1.89</u>	88.10±1.46	97.17±1.29
	M	<u>89.68±1.56</u>	87.23±1.60	96.87±1.16
	H	<u>84.09±1.98</u>	81.19±2.02	92.89±2.07
Cycle	E	<u>74.02±3.34</u>	62.19±1.85	90.30±2.33
	M	<u>71.99±3.34</u>	62.07±1.80	89.66±2.07
	H	<u>68.40±2.73</u>	58.88±2.14	86.81±2.27
Diameter	E	78.50±1.16	45.08±4.17	<u>77.56±2.77</u>
	M	<u>52.32±2.00</u>	27.31±3.16	61.71±2.28
	H	<u>29.59±2.48</u>	15.27±2.47	39.83±2.67
Shortest	E	90.03±2.27	47.46±8.76	<u>77.69±5.17</u>
	M	81.17±3.03	35.53±6.80	<u>69.60±5.50</u>
	H	72.53±4.29	28.31±5.50	<u>64.28±5.60</u>
Triangle	E	<u>36.57±4.40</u>	18.56±1.24	41.36±4.63
	M	<u>14.52±2.63</u>	9.18±0.73	26.95±2.44
	H	<u>4.73±1.58</u>	4.45±0.58	19.54±1.34

1719
1720
1721
1722
1723
1724
1725
1726
1727

1728 balanced recipe, i.e. moderate scaling *combined with* reasoning-oriented objectives, appears most
 1729 promising for closing the persistent gaps in BFS order, Diameter calculation, and Triangle
 1730 counting.

1732 C.6 RATIONALE FOR BINARY METRIC OVER PARTIAL SCORE

1734 Evaluating graph reasoning outputs with partial credit is appealing in theory, but defining a consistent
 1735 and objective scheme across six tasks, seven graph types, seven serializations, and nine prompt
 1736 schemes is exceptionally difficult. In practice, two approaches exist: assigning credit based on the
 1737 degree of correctness in the final answer, or rewarding intermediate steps and sub-outputs. Both
 1738 approaches introduce major challenges. For final answers, it is often ambiguous how to compare
 1739 partially correct results (e.g., is overcounting triangles by one preferable to undercounting by one?).
 1740 Such ambiguity undermines the credibility of fine-grained scoring. For intermediate steps, reliably
 1741 extracting and interpreting model outputs at scale is infeasible, since formatting and reasoning styles
 1742 vary widely across models and prompts.

1743 By contrast, binary accuracy against a known ground truth provides a clear and unambiguous
 1744 evaluation signal. With the extensive and diverse evaluation set in GRAPHOMNI, binary scoring
 1745 captures performance gaps robustly and fairly across models and tasks. While finer-grained metrics
 1746 such as edit distance, subtask scoring, or partial correctness may be valuable for training objectives
 1747 like reinforcement learning, they extend beyond the present study’s evaluation focus. Incorporating
 1748 such measures represents a promising avenue for future work.

1749 D RL-BASED PROMPT SEARCH INSPIRED BY GRAPHOMNI

1750 D.1 BACKGROUND AND SERIALIZATION PROCESS

1753 Our benchmark evaluates three key dimensions—*graph type*, *serialization format*, and *prompt*
 1754 *scheme*—to underscore the critical role of transforming graph structures into textual inputs for LLM
 1755 inference. In this section, *We want to identify the optimal combination strategies (serialization format;*
 1756 *prompt scheme, etc.) that enhance the effectiveness of textual representations*, thereby improving
 1757 LLM performance in graph reasoning and understanding tasks. Prior research indicates that while a
 1758 particular serialization format or prompt scheme may yield optimal performance in isolation, their
 1759 combination does not necessarily lead to the best results, highlighting complex interactions among
 1760 various factors. Furthermore, the final performance of LLMs may be influenced by additional factors
 1761 that were not systematically examined in our benchmark (e.g., those in Appendix D.3), underscoring
 1762 the intricate nature of the graph-to-text transformation process, which extends beyond the scope of
 1763 single-factor analysis. This makes finding the optimal serialization strategy complex. We define the
 1764 process of converting graph structures into textual inputs tailored to a specific task as the **serialization**
 1765 **process**. Similar prompt processes are used in NLP. For example, [Shi et al. \(2024\)](#) formulated *prompt*
 1766 *formatting* as a multi-armed bandit problem; [Sclar et al. \(2023\)](#) employed Thompson sampling
 1767 to determine the optimal strategies. For LLM-based graph reasoning, however, previous studies
 1768 predominantly focused on single-factor variations. The multiple factor considered in our study
 1769 significantly complicates the serialization process—once a particular factor is determined, others are
 1770 influenced in complex and often unpredictable ways.

1771 Due to these complexities, it is computationally enormous to find the optimal serialization strategy
 1772 by enumerating all possible combinations (termed as *grid search* in our study). To mitigate this
 1773 computational challenge, we propose using RL to find a high-quality serialization strategy under a
 1774 limited LLM cost, because of RL’s ability to learn near-optimal strategies in high-dimensional spaces
 1775 through exploration and feedback. In the context of RL, we assume that all benchmarking results
 1776 (e.g., those in Section 4.1 and 4.2) are not available. Instead, we will repeatedly choose various
 1777 serialization strategies, test their performance, and use the results for RL.

1778 Specifically, RL transforms optimizing the serialization process strategy into a sequential decision-
 1779 making problem for each type and difficulty of the task. There are T decision epochs, and each
 1780 decision epoch determines one component of the serialization strategy. For example, the decision
 1781 horizon is $T = 3$ when we aim to identify the optimal combination of the serialization format, prompt
 1782 scheme, and LLM. In the $T = 3$ decision epochs, we sequentially determine the prompt scheme,
 1783 serialization format, and LLM. Such an order of optimizing the components of a serialization strategy

is predetermined, and we will investigate its impact on the optimization results in future studies. This predetermined order specifies a sequence of action spaces $\{\mathcal{A}_t\}_{t=1,\dots,T}$ (e.g., \mathcal{A}_t can be all candidate LLMs). We set the initial state s_0 as the specific type and difficulty of the task.

Then at decision epoch $t = 1, \dots, T$, we choose an action $a_t \in \mathcal{A}_t$ based on the previous actions a_1, \dots, a_{t-1} . This corresponds to a policy $\pi_t : \mathcal{S}_0 \times \mathcal{A}_1 \times \dots \times \mathcal{A}_{t-1} \mapsto \mathcal{A}_t$, where \mathcal{S}_0 is the state space of the initial state s_0 . For any instance s (e.g., a query for Connectivity task in easy mode for a specific graph), a binary reward, denoted by $r(s, a_1, \dots, a_T)$, is incurred at the end of the decision epoch, which is set to 1 if the LLM correctly answers the specific query under the selected serialization strategy (a_1, \dots, a_T) and to 0 otherwise. For each type and difficulty of the task, our objective is to maximize the expected reward of choosing the serialization strategy a_1, \dots, a_T :

$$\max_{\{\pi_t\}_{t=1,\dots,T}} \mathbb{E}[r(s, a_1, \dots, a_T) | s_0],$$

where the expectation is taken with respect to the problem instance s and the (random) answer output by an LLM (affected by the randomness of the LLM, e.g., the temperature parameter). Note that (i) s_0 is part of the instance information s , and (ii) we fix the type and difficulty of the task, and the only randomness in terms of s is from graph generation. To approximate this objective function, we generate N different graphs for each type of query. We assess the performance of RL using the average reward across the N graphs, which essentially is the accuracy of the serialization strategy for a specific graph-related task across these N graphs.

We use the Q -learning approach to solve this optimization problem. Let $Q_t(s_0, a_1, \dots, a_t)$ be the Q -function at decision epoch $t = 1, \dots, T$, which represents the optimal reward-to-go if actions a_1, \dots, a_t have been determined at decision epoch t given the initial state s_0 . These functions satisfy the Bellman recursion:

$$Q_t(s_0, a_1, \dots, a_t) = \max_{a_{t+1} \in \mathcal{A}_{t+1}} Q_{t+1}(s_0, a_1, \dots, a_{t+1}), \quad t = 1, \dots, T-1$$

with terminal condition

$$Q_T(s_0, a_1, \dots, a_T) = \mathbb{E}[r(s, a_1, \dots, a_T) | s_0],$$

This terminal Q -function can be approximated by the accuracy of the LLM answer across the N generated graphs.

Consider the problem of dealing with high-dimensional, complex state spaces in serialization process, we employ the Deep Q -Network (DQN) (Mnih et al., 2013) to implement RL, which employs a deep neural network as a function approximator for the Q -function. Specifically, we use a neural network $\hat{Q}_t(s_0, a_1, \dots, a_t; \theta_t)$ parameterized by θ_t to approximate the corresponding $Q_t(s_0, a_1, \dots, a_t)$ for the actions or factors considered in serialization process. Each Q -network is modeled as a three-layer multilayer perceptron with ReLU activations. Training minimizes the mean squared error loss, and action selection follows an ϵ -greedy policy, where ϵ linearly decays from 1.0 to a minimum of 0.01. The detailed algorithm for each initial state s_0 is provided in Algorithm 1.

We design two experimental settings, **RL-Opt** and **RL-Scale**, to assess the effectiveness of our approach. **RL-Opt** focuses on a $T = 3$ serialization process—selecting the serialization format, prompt scheme, and LLM model—and evaluates both LLM cost and the accuracy of identifying the optimal configuration. **RL-Scale** extends the scope to include additional factors beyond those in GRAPHOMNI, investigating the scalability of the RL method for more complex serialization tasks, with an emphasis on LLM cost.

D.2 DETAILS FOR RL-OPT SETTING

In **RL-Opt**, we apply RL to find a high-quality serialization strategy under a limited LLM cost. The serialization process in this case involved three key factors: serialization formats (in total 7), nine prompt schemes (in total 9), and five open-source language models (including LLaMA3, LLaMA 3.1, Mistral, Phi-4, and Qwen-2.5). The total number of possible combinations in our search space is given by $E = 7 \times 9 \times 5 = 315$. To find a high-quality serialization strategy, we set the total training episodes to $M = 80$ and initial learning rate to 0.001 during RL training. We evaluate the RL performance on 6 tasks in three different modes, resulting in a total of 18 experimental cases.

1836 **Algorithm 1** RL Framework of GRAPHOMNI

1837 **Input:** Action spaces $\{\mathcal{A}_t\}_{t=1}^T$; number of training episodes M ; exploration rate ϵ ; initial state s_0

1838 **Initialization:**

1839 Generate N graphs according to the initial state s_0

1840 Initialize Q -networks $\{\hat{Q}_t(s_0, a_1, \dots, a_t; \theta_t)\}_{t=1}^T$ with random initialized weights θ_t

1841 **for** episode = 1 to M **do**

1842 **for** t = 1 to T **do**

1843 **Choose action:**

1844 With probability ϵ , select a random action $a_t \in \mathcal{A}_t$

1845 Otherwise, set $a_t \leftarrow \arg \max_{a \in \mathcal{A}_t} \hat{Q}_t(s_0, a_1, \dots, a_{t-1}, a; \theta_t)$

1846 **Execute action and obtain new state:**

1847 Update state: $\{s_0, a_1, \dots, a_t\} \leftarrow \{s_0, a_1, \dots, a_{t-1}\} \cup \{a_t\}$

1848 **Q-network update:**

1849 If $t = T$, set y to be the accuracy of the LLM answer across the N generated graphs

1850 Otherwise, set $y \leftarrow \max_{a \in \mathcal{A}_{t+1}} \hat{Q}_{t+1}(a_1, \dots, a; \theta_{t+1})$

1851 Perform a gradient descent step on $(y - \hat{Q}_t(a_1, \dots, a_t; \theta_t))^2$ with respect to θ_t

1852 **end for**

1853 Decay exploration rate: $\epsilon \leftarrow \epsilon \cdot \text{decay rate}$

1854 **end for**

1857

1858

1859

1860

1861 For each case, based on our numerical results in Sections 4.1 and 4.2, we know which combination

1862 (serialization format; prompt scheme; LLM) performs the best for each specific graph-related task.

1863 Hence, we can compare the serialization strategy obtained by RL with the ground-truth optimal

1864 strategy.

1865 Specifically, we employ two key metrics. **Search Cost:** Given that RL explores k different combi-

1866 nations during the training process, we define $\text{Cost} = \frac{k}{K}$, where k depends on the number of training

1867 episodes and K is the total number of combinations. **Rate:** Let acc_* be the accuracy achieved by

1868 the best combination found by RL, and acc_{\max} be the highest accuracy in Sections 4.1 and 4.2.

1869 Then we define $\text{Rate} = \frac{\text{acc}_*}{\text{acc}_{\max}}$. The results are displayed in Table 4. It can be seen that, with an

1870 approximate 25% reduction in cost, the RL method still maintains an average rate of around 0.9,

1871 indicating its ability to significantly shorten the time required for the search for optimal combinations

1872 while ensuring the quality of the results. This outcome underscores the notable advantages of RL in

1873 the serialization process problem—it can rapidly find high-quality solutions, thereby substantially

1874 reducing computational resources and time costs. Moreover, this approach does not rely heavily on

1875 extensive manual expertise, enhancing the automation of the optimization process. As a result, it

1876 is not only applicable to the factors considered in this study but also adaptable to other factors that

1877 warrant further investigation.

1878

1879

1880

1881 D.3 RL-SCALE

1882

1883

1884 In **RL-Scale**, we examine the scalability of our RL method by incorporating additional four factors

1885 into the serialization process. Different from **RL-Opt** that optimizes the LLM model, we fix the

1886 model as **Qwen-2.5** and test the performance on the Diameter calculation task in **easy** mode. The

1887 additional four factors are inspired by [Sclar et al. \(2023\)](#), which are the delimiters between sentences,

1888 the capitalization style of each sentence, the delimiter used to introduce questions and answers, and

1889 the delimiter between words. As before, we still optimize the prompt scheme and the serialization

format. Details of the 6 factors implemented in the serialization process are shown below.

1890

1891

1892

1893

1894

1895

1896

1897

1898

1899

1900

1901

1902

1903

1904

1905

1906

1907

1908

1909

1910

1911

1912

1913

1914

1915

1916

1917

1918

1919

1920

1921

1922

1923

1924

1925

1926

1927

1928

1929

1930

1931

1932

1933

1934

1935

1936

1937

1938

1939

1940

1941

1942

1943

6 factors implemented in serialization process

- **SPACES1**: delimiter between sentences, include: ' - ', ' <sep> ', ' , ' , ' \n ', ' \n ', ' \t ', ' ; \n ', ' , ' . ' , ' || '
- **CS**: the delimiter used to introduce questions and answers, include: ' \n \t ', ' \n ', ' : ', ' : ', ' \t ', ' :: ', ' , ' - ', ' : ', ' :: '
- **SPACES2**: delimiter between words, include: ' , ' , ' \t '
- **CASE FUNCTION**: the overall capitalization mode of each sentences, include: no change, title, upper, lower
- **PROMPTS SCHEME**: include: 0-shot, 0-CoT, 0-Instruct, 0-Algorithm, LTM, Algorithm, CoT, k-shot, Instruct
- **SERIALIZATION FORMAT**: include: GMoL, Adjacency Set, Edge Set, Edge List, Adjacency Matrix, Adjacency List, GMaL

Since the optimal combination in RL-Scale is unknown, we only focus on the cost of RL finding the near optimal combination. In addition, taking into account the LLM cost problem and the performance stability, for each combination, we took a fixed evaluation of 30 samples to get accuracy and set the temperature to 0. Ultimately, we compare the costs of RL and grid search under conditions where the serialization process involves 2–6 factors, with the results presented in Figure 7. For step counts of 2, 3, 4, 5, and 6, the number of combinations explored for RL is 40, 121, 182, 300, and 632, respectively. In contrast, the number of combinations for Grid Search is 100, 300, 1200, 8400, and 75600 for the same step counts. It shows that RL exhibits a highly promising trend in terms of the cost associated with searching for optimal combinations.

When considering two-step factors, the cost of RL is comparable to that of grid search. However, as factors or steps increase, the cost growth of RL is significantly lower than that of grid search. This finding suggests that for serialization process tasks, RL can adaptively adjust its strategy to better accommodate complex environments, highlighting its broader potential for application.

Table 12: 2–6 factors, top-3 combinations and corresponding reward from **RL-Scale**.

Grid research	Rank	Combination Parameters	Reward
100	1	Edge List,0-shot, Q:, A:,,\n\t,no	0.3000
	2	Edge List,0-shot, Q:, A:,\n,,no	0.2667
	3	Edge List,0-shot, Q:, A:,,no	0.2000
300	1	Edge List,0-shot, Q:, A:,,\n\t,no	0.3667
	2	Edge List,0-shot, Q:, A:,-,\n\t,\n\t,no	0.3333
	3	Edge List,0-shot, Q:, A:,-,\n\t,-,no	0.3333
1200	1	Edge List,0-shot, Q:, A:,-,,\n,upper	0.4000
	2	Edge List,0-shot, Q:, A:,\n,,lower	0.4000
	3	Edge List,0-shot, Q:, A:,-,\n,,upper	0.3667
8400	1	Adjacency Matrix,0-shot, Q:, A:,<sep>,,\n,title	0.5667
	2	GMoL,0-shot, Q:, A:,\n,\n,,upper	0.5333
	3	GMoL,0-shot, Q:, A:,\n,\n,,upper	0.5333
75600	1	Adjacency Set,Algorithm, Q:, A:,\n,,lower	0.6333
	2	Adjacency Set,Algorithm, Q:, A:,\n,,no	0.6333
	3	Adjacency Matrix,0-shot, Q:, A:,\n,,title	0.6000

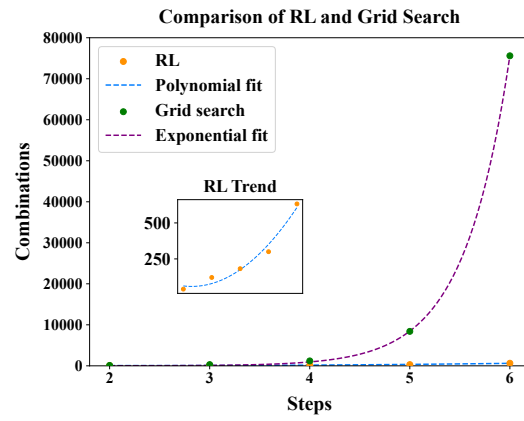


Figure 7: RL and Grid Search

1944 E COMPREHENSIVE EXPERIMENTAL RESULTS

1946 In this section, we include all the experimental results and additional analysis of the GRAPHOMNI as
 1947 a reference to support our claims and findings mentioned in Section 4.1. We first present fine-grained
 1948 experimental results broken down across main evaluation dimensions in Appendix E.1, followed
 1949 by detailed performance heatmaps for all tasks and models in Appendix E.2. Finally, we provide a
 1950 comprehensive error analysis with representative cases in Appendix E.4.

1952 E.1 FINE-GRAINED RESULTS ACROSS DIMENSION

1954 In this subsection, we present detailed performance results across model capability, graph type,
 1955 prompting schemes, and serialization format impact. Based on the complete evaluation results in
 1956 Table 13, we further analyze the results from multiple perspectives, including overall performance
 1957 across all models, separate analyses for open-source models, and specific results for closed-source
 1958 models. These comprehensive results provide additional evidence supporting our main findings
 1959 discussed in Section 4.1.

1960 Table 13: Benchmark Results of LLMs Across Tasks (Mean \pm 95% CI Margin).
 1961 **Bold orange** / Underlined blue / **Light purple** highlights indicate best/second-best/third-best
 1962 performance in its category.

Task	Difficulty	Open-source Models						Closed-source Models						Random
		Llama-3 (8B)	Llama-3.1 (8B)	Mistral (7B)	Phi-3 (14B)	Qwen-2.5 (72B)	Qwen-2.5 (7B)	Qwen-3 (8B)	Claude-3.5	GPT-4o	GPT-4o-mini	Gemini-2.0	o4-mini	
BFS order	E	15.62 \pm 2.94	18.69 \pm 3.02	13.75 \pm 1.44	33.03 \pm 3.22	71.41\pm3.45	21.46 \pm 4.26	<u>65.87\pm5.59</u>	<u>91.42\pm1.65</u>	81.48 \pm 3.22	58.75 \pm 4.22	90.31 \pm 2.30	95.46\pm0.78	0.00
	M	4.04 \pm 0.81	5.27 \pm 0.93	3.36 \pm 0.44	12.49 \pm 3.24	<u>47.82\pm5.30</u>	6.05 \pm 1.41	53.30\pm5.42	68.25 \pm 2.96	55.07 \pm 4.50	25.03 \pm 3.11	<u>68.40\pm3.95</u>	79.37\pm2.08	0.00
	H	0.39 \pm 0.15	0.63 \pm 0.19	0.34 \pm 0.14	2.65 \pm 0.80	22.03 \pm 4.39	1.38 \pm 0.37	29.53 \pm 4.25	26.80 \pm 0.90	21.58 \pm 3.69	6.28 \pm 0.90	27.77\pm3.34	<u>32.45\pm3.88</u>	0.00
Connectivity	E	78.01 \pm 2.28	79.53 \pm 2.03	79.90 \pm 1.88	56.29 \pm 8.55	90.24 \pm 1.89	88.10 \pm 1.46	97.17\pm1.29	<u>98.38\pm0.60</u>	95.63 \pm 1.30	89.10 \pm 2.32	92.61 \pm 1.42	<u>98.23\pm0.63</u>	67.49
	M	77.78 \pm 2.78	79.47 \pm 2.00	80.60 \pm 1.92	54.38 \pm 7.99	89.68 \pm 1.56	87.23 \pm 1.60	96.87\pm1.16	<u>99.11\pm0.39</u>	95.12 \pm 1.37	91.07 \pm 1.42	93.60 \pm 1.10	<u>98.72\pm0.52</u>	70.75
	H	68.49 \pm 4.49	74.58 \pm 2.67	74.77 \pm 2.46	48.39 \pm 7.50	84.09 \pm 1.98	81.19 \pm 2.02	92.89\pm2.07	<u>96.99\pm1.49</u>	90.59 \pm 2.19	84.82 \pm 2.17	87.99 \pm 1.67	<u>92.02\pm3.99</u>	66.36
Cycle	E	53.84 \pm 1.75	55.49 \pm 0.90	55.44 \pm 0.96	45.25 \pm 5.90	74.02 \pm 3.34	62.19 \pm 1.85	90.30\pm2.33	82.56 \pm 3.89	<u>85.08\pm2.27</u>	75.04 \pm 2.83	62.30 \pm 3.32	97.97\pm0.71	50.00
	M	42.38 \pm 1.13	55.69 \pm 1.08	53.71 \pm 0.72	44.26 \pm 5.43	71.99 \pm 3.4	62.07 \pm 1.80	89.66\pm2.07	80.80 \pm 3.94	<u>85.35\pm2.30</u>	75.79 \pm 2.96	60.29 \pm 3.22	97.75\pm0.76	50.00
	H	41.24 \pm 1.53	52.40 \pm 1.47	51.64 \pm 1.02	40.64 \pm 4.97	68.40 \pm 2.73	58.88 \pm 2.14	86.81\pm2.27	80.10 \pm 3.97	<u>82.96\pm2.55</u>	73.46 \pm 3.30	58.30 \pm 2.80	95.61\pm1.23	50.00
Diameter	E	23.78 \pm 4.17	41.27 \pm 5.37	28.55 \pm 4.28	42.81 \pm 5.0	78.50\pm1.16	45.08 \pm 4.17	77.56\pm2.77	<u>83.71\pm1.26</u>	63.99 \pm 2.19	37.36 \pm 2.62	79.14 \pm 1.94	98.88\pm0.15	11.20
	M	14.29 \pm 2.66	27.29 \pm 4.20	15.17 \pm 2.57	28.94 \pm 4.09	<u>52.32\pm2.00</u>	27.31 \pm 3.16	61.71\pm2.28	71.22 \pm 3.0	52.64 \pm 3.05	22.85 \pm 2.97	49.52 \pm 2.14	72.84\pm1.82	6.70
	H	8.48 \pm 1.75	18.63 \pm 3.27	6.97 \pm 1.26	17.71 \pm 3.02	29.59\pm2.48	15.27 \pm 2.47	39.83\pm2.67	<u>56.70\pm2.03</u>	45.60\pm3.24	14.98 \pm 2.54	23.45 \pm 2.97	34.61 \pm 2.84	3.72
Shortest	E	33.93 \pm 4.44	38.75 \pm 5.81	31.18 \pm 4.43	42.61 \pm 8.88	90.03\pm2.27	47.46 \pm 8.76	<u>77.69\pm5.17</u>	94.35 \pm 2.93	92.17 \pm 1.91	78.69 \pm 4.24	81.75 \pm 4.70	95.08\pm3.06	50.00
	M	26.07 \pm 4.96	28.84 \pm 4.56	19.89 \pm 3.05	33.92 \pm 7.68	<u>81.17\pm3.03</u>	35.53 \pm 6.80	<u>69.60\pm5.50</u>	91.27 \pm 2.84	84.84 \pm 2.93	66.31 \pm 3.36	80.67 \pm 4.15	92.60\pm3.49	50.00
	H	20.00 \pm 3.97	23.03 \pm 3.85	12.21 \pm 1.95	26.60 \pm 2.6	72.53\pm4.29	28.31 \pm 5.50	64.28 \pm 5.60	87.88 \pm 3.36	74.98 \pm 4.17	54.73 \pm 4.54	78.16 \pm 4.55	<u>88.63\pm4.44</u>	50.00
Triangle	E	9.49 \pm 1.02	14.97 \pm 1.53	11.87 \pm 1.32	12.88 \pm 2.05	<u>36.57\pm4.40</u>	18.56 \pm 1.24	41.36\pm4.63	43.41 \pm 1.64	36.32 \pm 1.54	18.51 \pm 1.39	<u>50.33\pm2.31</u>	84.54\pm0.56	2.13
	M	3.06 \pm 0.39	8.56 \pm 0.92	5.86 \pm 0.73	7.54 \pm 1.33	<u>14.52\pm2.63</u>	9.18 \pm 0.73	26.95\pm2.44	24.04 \pm 0.77	20.00 \pm 0.72	10.62 \pm 0.81	<u>28.12\pm1.65</u>	48.13\pm1.46	1.62
	H	1.82 \pm 0.36	4.95\pm0.69	2.55 \pm 0.44	4.38 \pm 1.04	4.73 \pm 1.58	4.45 \pm 0.58	19.54\pm1.34	15.92 \pm 0.72	12.81 \pm 0.88	5.65 \pm 0.71	15.55 \pm 1.29	17.53\pm1.43	1.82

E.1.1 OVERALL RESULTS

Here we present a comprehensive analysis of the overall performance across all evaluation dimensions. While our main findings in Result 1 highlight the moderate performance of models with considerable room for improvement, the detailed results in Tables 14, 15, and 16 reveal several noteworthy patterns:

Task-specific Performance Variation: The performance varies significantly across different tasks and difficulty levels. For instance, in Connectivity tasks, models generally achieve higher accuracy (80%–90% for easy level) compared to more complex tasks like Triangle counting (20%–30% for hard level). This suggests that while LLMs can handle basic graph properties well, they struggle with tasks requiring more sophisticated reasoning and counting.

Difficulty Level Impact: There is a consistent and non-linear sharp decline in performance as task difficulty increases. With larger graphs, models face challenges in both processing longer contexts and conducting more complex reasoning tasks, which typically require longer reasoning paths, more precise intermediate steps, and more comprehensive exploration of the graph structure. The sharp performance drop on larger graphs suggests that current LLMs struggle to maintain reliable reasoning capabilities when faced with extended multi-step graph operations.

Model Type Performance Gap: The performance gap between closed-source and open-source models is particularly evident in complex tasks. For instance, GPT-4o and Claude-3.5 consistently outperform other models by a significant margin (15%–20%) in tasks like Diameter calculation and Triangle counting especially at higher difficulty levels. This reinforces our observation about the current limitations of open-source models in complex graph reasoning tasks.

Graph Type Impact: The evaluation reveals distinct performance patterns across different graph types, with certain structures showing clear advantages for specific tasks. Our analysis shows that

bipartite graphs (BERM, BERP) tend to exhibit higher performance in connectivity and clustering-related tasks (Connectivity), potentially due to their explicit partitioning of node sets, which simplifies certain connectivity relationships for LLMs. For shortest-path (Shortest path) tasks, hierarchical structures like BAF often show higher accuracy, as the tree-like paths may align well with reasoning processes for pathfinding. In local pattern identification tasks such as triangle counting (Triangle counting), simpler graph structures like SF often perform better, possibly because they reduce the complexity of identifying local patterns. These observations suggest that the interplay between graph types and task characteristics can significantly influence LLM reasoning behaviors.

Table 14: Benchmark Results of Prompt Schemes Across Tasks (Mean \pm 95% CI Margin of All Models). **Bold orange** / Underlined blue highlights indicate best/second-best performance.

Task	Difficulty	0-Algorithm	0-CoT	0-Instruct	0-Shot	Algorithm	CoT	Instruct	K-Shot	LTM
BFS order	E	52.20 \pm 7.28	46.54 \pm 8.20	48.42 \pm 8.22	51.49 \pm 7.34	63.39\pm7.10	<u>63.33\pm6.23</u>	62.93 \pm 6.16	56.51 \pm 6.45	48.12 \pm 8.15
	M	33.63 \pm 6.46	33.37 \pm 6.89	33.36 \pm 6.76	33.94 \pm 6.72	43.48\pm7.23	<u>38.99\pm6.37</u>	38.61 \pm 6.20	33.08 \pm 6.09	32.89 \pm 6.67
	H	13.57 \pm 3.45	14.46 \pm 3.58	13.98 \pm 3.50	14.58 \pm 3.71	19.37\pm4.46	14.01 \pm 3.42	13.27 \pm 3.27	11.68 \pm 3.01	13.95 \pm 3.50
Connectivity	E	85.51 \pm 3.01	83.27 \pm 5.06	86.86 \pm 2.45	82.79 \pm 5.40	88.79 \pm 2.32	92.35\pm1.88	92.37\pm1.57	87.46 \pm 2.34	83.00 \pm 4.70
	M	86.34 \pm 3.34	83.30 \pm 4.89	83.80 \pm 3.28	83.36 \pm 5.45	88.98 \pm 2.05	<u>91.98\pm1.94</u>	92.07\pm1.45	89.24 \pm 2.05	83.65 \pm 4.17
	H	81.76 \pm 3.99	78.34 \pm 4.87	74.21 \pm 4.90	79.80 \pm 5.35	82.89 \pm 2.52	<u>85.68\pm2.70</u>	86.41\pm2.19	85.16 \pm 2.57	78.35 \pm 4.41
Cycle	E	71.75 \pm 3.91	64.73 \pm 5.07	70.23 \pm 3.67	64.93 \pm 5.34	71.28 \pm 4.34	73.01\pm3.62	71.66 \pm 3.77	73.12\pm3.62	68.89 \pm 3.90
	M	69.16 \pm 4.07	64.50 \pm 4.73	67.75 \pm 3.99	63.94 \pm 5.37	70.02 \pm 4.77	71.59\pm4.06	69.86 \pm 4.11	<u>70.40\pm4.24</u>	67.58 \pm 3.85
	H	66.27 \pm 4.04	62.75 \pm 4.47	62.14 \pm 4.60	62.54 \pm 5.20	67.38 \pm 4.79	69.12\pm4.20	67.95 \pm 4.13	<u>68.35\pm4.14</u>	66.35 \pm 3.73
Diameter	E	51.52 \pm 6.46	52.66 \pm 6.81	52.55 \pm 7.06	53.65 \pm 6.46	70.28\pm3.10	62.32 \pm 4.95	64.42 \pm 4.01	64.65\pm4.09	53.41 \pm 6.66
	M	34.41 \pm 5.35	36.65 \pm 5.50	34.34 \pm 5.62	37.54 \pm 5.07	50.69\pm2.97	46.65 \pm 4.66	<u>48.00\pm4.06</u>	47.64 \pm 3.93	35.83 \pm 5.37
	H	19.53 \pm 3.90	22.28 \pm 3.81	20.59 \pm 4.16	22.92 \pm 3.71	<u>32.13\pm3.29</u>	30.80 \pm 3.78	32.54\pm3.49	31.89 \pm 3.29	21.19 \pm 4.09
Shortest	E	67.58 \pm 5.64	57.06 \pm 8.17	55.89 \pm 8.48	67.18 \pm 6.33	<u>74.79\pm6.01</u>	74.73 \pm 6.10	75.62\pm5.76	72.75 \pm 6.37	57.17 \pm 7.99
	M	59.32 \pm 6.24	50.97 \pm 8.02	50.60 \pm 8.14	58.52 \pm 6.58	65.09 \pm 6.39	66.73\pm6.09	<u>66.02\pm6.19</u>	63.98 \pm 6.26	51.80 \pm 7.73
	H	53.14 \pm 6.66	48.40 \pm 7.89	46.88 \pm 8.05	52.54 \pm 6.82	56.18 \pm 6.72	57.27\pm6.41	<u>57.10\pm6.38</u>	54.03 \pm 6.43	47.97 \pm 7.67
Triangle	E	28.81 \pm 4.95	29.95 \pm 5.04	28.00 \pm 5.04	31.22 \pm 5.08	32.39 \pm 4.75	<u>34.81\pm5.10</u>	35.03\pm4.68	33.39 \pm 4.57	30.52 \pm 4.95
	M	16.01 \pm 2.92	17.07 \pm 2.83	15.88 \pm 2.93	16.97 \pm 3.10	16.62 \pm 2.86	18.07 \pm 3.15	18.67\pm2.77	<u>18.52\pm2.78</u>	17.11 \pm 2.89
	H	8.85 \pm 1.53	10.14\pm1.68	8.55 \pm 1.56	9.42 \pm 1.63	8.21 \pm 1.56	9.48 \pm 1.81	9.12 \pm 1.53	<u>9.54\pm1.58</u>	9.10 \pm 1.47

Table 15: Benchmark Results of Serialization Formats Across Tasks (Mean \pm 95% CI Margin of All Models). **Bold orange** / Underlined blue highlights indicate best/second-best performance.

Task	Difficulty	AL	AM	AS	EL	ES	GMaL	GMoL
BFS order	E	63.27\pm6.63	49.10 \pm 7.02	<u>62.54\pm6.63</u>	50.40 \pm 6.27	51.68 \pm 6.37	58.86 \pm 6.42	47.54 \pm 5.57
	M	47.13\pm6.74	27.55 \pm 5.27	<u>45.18\pm6.56</u>	31.39 \pm 5.17	29.57 \pm 4.96	39.55 \pm 5.88	29.56 \pm 4.91
	H	23.92\pm4.37	5.19 \pm 1.16	<u>23.59\pm4.24</u>	11.40 \pm 2.17	9.06 \pm 1.69	15.58 \pm 2.75	11.50 \pm 2.31
Connectivity	E	<u>89.49\pm3.25</u>	80.92 \pm 3.10	89.57\pm3.20	87.02 \pm 3.42	88.50 \pm 3.21	88.44 \pm 2.96	84.58 \pm 2.31
	M	<u>88.75\pm3.23</u>	82.63 \pm 2.85	89.04\pm3.09	86.51 \pm 3.48	86.72 \pm 3.31	88.27 \pm 3.04	86.87 \pm 2.52
	H	<u>85.52\pm3.48</u>	68.37 \pm 2.46	85.68\pm3.38	82.49 \pm 3.65	81.03 \pm 3.52	83.83 \pm 3.70	82.87 \pm 3.09
Cycle	E	64.30 \pm 3.53	65.75 \pm 3.61	64.41 \pm 3.50	71.54 \pm 3.59	<u>75.38\pm3.40</u>	76.09\pm4.26	72.22 \pm 3.38
	M	63.35 \pm 3.58	62.90 \pm 3.51	63.23 \pm 3.52	70.55 \pm 3.81	<u>72.51\pm3.64</u>	73.93\pm4.43	71.70 \pm 3.94
	H	61.00 \pm 3.59	59.06 \pm 2.94	60.20 \pm 3.52	69.64 \pm 3.95	68.82 \pm 3.68	71.42\pm4.32	<u>70.96\pm4.24</u>
Diameter	E	58.31 \pm 5.29	58.63 \pm 4.95	<u>61.33\pm5.09</u>	54.95 \pm 5.24	54.51 \pm 5.33	62.28\pm4.87	58.68 \pm 5.18
	M	42.89 \pm 4.77	39.67 \pm 3.83	45.69\pm4.68	37.78 \pm 4.05	35.60 \pm 4.18	<u>44.52\pm4.38</u>	42.98 \pm 4.48
	H	27.68 \pm 4.00	23.65 \pm 3.01	<u>29.61\pm3.82</u>	23.26 \pm 2.76	20.03 \pm 2.70	29.77\pm3.63	27.90 \pm 3.49
Shortest	E	75.89\pm5.76	54.14 \pm 5.97	76.60\pm5.61	72.00 \pm 5.63	68.99 \pm 5.81	52.85 \pm 7.49	68.35 \pm 5.23
	M	69.65\pm6.00	40.94 \pm 5.24	<u>69.14\pm5.68</u>	64.57 \pm 5.83	58.30 \pm 5.90	52.38 \pm 7.34	59.60 \pm 5.25
	H	<u>65.31\pm6.09</u>	28.22 \pm 4.13	65.79\pm5.96	55.82 \pm 5.90	52.05 \pm 5.83	47.88 \pm 7.06	53.20 \pm 5.42
Triangle	E	32.03 \pm 4.41	27.61 \pm 4.08	31.82 \pm 4.48	31.70 \pm 4.21	30.64 \pm 4.06	34.30\pm4.44	<u>32.89\pm4.61</u>
	M	17.50 \pm 2.56	13.50 \pm 1.94	17.61 \pm 2.60	<u>18.65\pm2.66</u>	16.45 \pm 2.40	18.83\pm2.71	17.95 \pm 2.89
	H	8.78 \pm 1.42	6.61 \pm 1.05	10.35\pm1.51	9.77 \pm 1.38	8.75 \pm 1.22	<u>10.34\pm1.48</u>	9.50 \pm 1.59

E.1.2 RESULTS OF OPEN-SOURCE MODELS

Open-source models exhibit several distinct characteristics compared to the overall results. In terms of prompting schemes (Table 17), more structured approaches show clear advantages: CoT and

Table 16: Benchmark Results of Graph Type Across Tasks (Mean \pm 95% CI Margin). **Bold orange** / Underlined blue highlights indicate best/second-best performance. “-” indicates the graph type is not applicable for that task.

Task	Difficulty	BAF	BAG	BERM	BERP	ERM	ERP	SF
BFS order	E	43.82 \pm 3.13	44.93 \pm 3.06	53.30\pm2.77	52.68 \pm 2.75	43.49 \pm 2.76	47.82 \pm 2.88	48.20 \pm 3.08
	M	35.06\pm3.03	29.38 \pm 2.68	24.96 \pm 2.33	<u>34.56\pm2.58</u>	21.76 \pm 1.97	22.48 \pm 2.05	26.63 \pm 2.57
	H	27.58\pm2.66	7.17 \pm 1.17	6.67 \pm 0.95	<u>13.79\pm1.34</u>	4.03 \pm 0.70	8.40 \pm 1.06	7.40 \pm 1.24
Connectivity	E	77.04 \pm 1.68	-	88.03\pm1.48	84.29 \pm 1.52	<u>87.02\pm1.49</u>	86.97 \pm 1.54	-
	M	78.99 \pm 1.62	-	<u>86.31\pm1.52</u>	86.60\pm1.54	84.61 \pm 1.51	86.11 \pm 1.56	-
	H	65.93 \pm 1.75	-	<u>84.18\pm1.75</u>	82.12 \pm 1.67	80.68 \pm 1.74	85.28\pm1.70	-
Cycle	E	-	64.90 \pm 1.60	65.98 \pm 1.49	65.02 \pm 1.39	<u>68.32\pm1.70</u>	69.25\pm1.57	61.08 \pm 1.40
	M	-	60.18 \pm 1.73	67.21\pm1.66	61.41 \pm 1.54	65.23 \pm 1.86	<u>66.08\pm1.70</u>	59.10 \pm 1.53
	H	-	55.20 \pm 1.56	<u>64.66\pm1.91</u>	65.58\pm1.72	61.97 \pm 1.82	62.99 \pm 1.81	54.98 \pm 1.45
Diameter	E	-	47.35 \pm 2.10	-	-	44.95 \pm 2.25	<u>48.96\pm2.23</u>	56.82\pm2.08
	M	-	33.38 \pm 1.79	-	-	30.64 \pm 2.04	<u>35.81\pm2.21</u>	37.41\pm1.65
	H	-	<u>22.78\pm1.81</u>	-	-	20.70 \pm 1.92	26.76\pm2.11	22.10 \pm 1.15
Shortest path	E	66.73\pm2.98	60.06 \pm 2.82	57.52 \pm 2.82	61.01 \pm 2.88	55.12 \pm 2.80	59.53 \pm 2.87	<u>61.12\pm2.86</u>
	M	58.11\pm3.01	52.88 \pm 2.84	48.95 \pm 2.76	48.72 \pm 2.72	45.83 \pm 2.73	51.55 \pm 2.75	<u>57.08\pm2.88</u>
	H	55.62\pm3.15	46.19 \pm 2.97	42.47 \pm 2.69	39.67 \pm 2.85	39.54 \pm 2.65	43.36 \pm 2.62	<u>48.93\pm2.89</u>
Triangle	E	-	<u>25.25\pm1.53</u>	-	-	12.54 \pm 0.79	17.17 \pm 1.08	41.20\pm2.03
	M	-	<u>16.75\pm1.11</u>	-	-	7.38 \pm 0.45	9.55 \pm 0.56	18.30\pm1.12
	H	-	8.99\pm0.77	-	-	5.48 \pm 0.42	7.56 \pm 0.56	<u>8.22\pm0.58</u>

Instruct prompts consistently outperform simpler schemes like 0-Shot and LTM across most tasks. This is particularly evident in Connectivity tasks, suggesting that open-source models benefit more from explicit reasoning guidance.

For serialization formats (Table 18), open-source models show a strong preference for concise representations. Adjacency List (AL) and Adjacency Set (AS) formats consistently perform better than more complex formats like GMaL and GMoL. This contrasts with the overall results.

Regarding graph types (Table 19), while the general pattern of task-specific advantages remains similar to overall results, open-source models show more pronounced performance gaps between optimal and sub-optimal graph types. For instance, in Triangle counting tasks, SF significantly outperforms other graph types with a wider margin compared to the overall results.

Table 17: Benchmark Results of Prompt Schemes Across Tasks of Open-source Models (Mean \pm 95% CI Margin). **Bold orange** / Underlined blue highlights indicate best/second-best performance.

Task	Difficulty	0-Algorithm	0-CoT	0-Instruct	0-Shot	Algorithm	CoT	Instruct	K-Shot	LTM
BFS order	E	29.72 \pm 5.04	20.25 \pm 5.44	22.19 \pm 5.76	29.64 \pm 5.43	44.34 \pm 6.33	49.24\pm6.00	<u>48.84\pm5.85</u>	41.62 \pm 5.48	22.50 \pm 5.82
	M	15.25 \pm 4.15	14.05 \pm 4.83	14.56 \pm 4.88	15.98 \pm 4.70	25.31 \pm 5.94	25.88\pm5.78	<u>25.34\pm5.56</u>	19.52 \pm 4.83	14.26 \pm 4.73
	H	7.26 \pm 3.03	7.76 \pm 3.14	7.24 \pm 3.04	7.98 \pm 3.11	10.51\pm3.54	<u>9.47\pm3.53</u>	9.18 \pm 3.40	6.55 \pm 2.61	7.28 \pm 3.05
Connectivity	E	78.11 \pm 2.96	74.21 \pm 5.84	81.31 \pm 2.35	74.83 \pm 6.44	85.70 \pm 2.46	<u>89.23\pm2.10</u>	89.46\pm1.64	84.83 \pm 2.42	74.19 \pm 5.33
	M	79.13 \pm 3.60	74.08 \pm 5.58	75.56 \pm 3.19	74.54 \pm 6.48	85.39 \pm 2.12	<u>88.40\pm2.16</u>	88.98\pm1.42	86.52 \pm 2.17	75.15 \pm 4.56
	H	74.52 \pm 4.29	69.13 \pm 5.34	62.30 \pm 4.72	71.41 \pm 6.22	80.14 \pm 2.19	81.68 \pm 2.63	83.14\pm1.86	<u>82.85\pm2.48</u>	69.05 \pm 4.51
Cycle	E	64.31 \pm 3.28	53.62 \pm 4.73	63.66 \pm 3.11	55.38 \pm 5.41	64.32 \pm 4.01	<u>66.89\pm3.33</u>	64.67 \pm 3.40	67.48\pm3.19	60.90 \pm 3.26
	M	61.02 \pm 3.52	53.61 \pm 4.13	59.75 \pm 3.36	53.78 \pm 5.41	61.55 \pm 4.57	<u>63.81\pm3.73</u>	62.44 \pm 3.63	64.06\pm3.88	59.66 \pm 3.12
	H	58.42 \pm 3.61	52.68 \pm 3.84	51.53 \pm 3.83	52.42 \pm 5.14	58.25 \pm 4.44	<u>61.20\pm3.71</u>	59.80 \pm 3.51	61.39\pm3.53	58.60 \pm 2.91
Diameter	E	36.41 \pm 5.49	37.12 \pm 5.95	37.36 \pm 6.51	40.67 \pm 5.67	66.33\pm2.63	56.63 \pm 4.76	<u>60.39\pm3.27</u>	59.93 \pm 3.51	39.13 \pm 5.92
	M	22.68 \pm 3.90	25.26 \pm 4.68	22.36 \pm 4.68	27.65 \pm 4.24	44.44\pm2.65	40.30 \pm 4.44	<u>42.93\pm3.59</u>	41.45 \pm 3.45	24.25 \pm 4.38
	H	11.69 \pm 2.25	15.25 \pm 2.78	12.84 \pm 3.17	16.71 \pm 2.83	24.70 \pm 2.52	25.50 \pm 3.29	27.98\pm3.00	<u>27.22\pm2.93</u>	13.57 \pm 3.00
Shortest	E	55.81 \pm 5.40	34.34 \pm 7.21	32.39 \pm 7.55	52.73 \pm 6.28	62.03 \pm 6.43	65.72\pm6.36	<u>64.55\pm6.34</u>	63.04 \pm 6.48	34.38 \pm 6.84
	M	43.89 \pm 5.43	28.21 \pm 6.58	28.25 \pm 6.95	42.44 \pm 5.92	50.31 \pm 6.24	53.78\pm6.20	<u>52.94\pm6.29</u>	50.08 \pm 6.15	29.44 \pm 6.13
	H	36.26 \pm 5.51	26.51 \pm 6.31	24.50 \pm 6.42	35.58 \pm 5.60	40.67 \pm 6.12	44.11\pm6.18	<u>43.56\pm6.04</u>	39.99 \pm 5.93	26.35 \pm 5.73
Triangle	E	14.74 \pm 1.98	16.91 \pm 3.09	14.22 \pm 2.52	19.88 \pm 3.43	21.98 \pm 3.28	<u>27.32\pm4.52</u>	28.14\pm3.84	26.35 \pm 3.34	17.79 \pm 3.07
	M	7.98 \pm 1.39	10.24 \pm 1.73	8.37 \pm 1.58	9.86 \pm 1.87	9.57 \pm 1.97	12.94 \pm 2.81	14.13\pm2.43	<u>13.91\pm2.23</u>	10.28 \pm 1.82
	H	5.14 \pm 1.22	6.28 \pm 1.48	4.50 \pm 1.19	5.96 \pm 1.31	4.71 \pm 1.31	7.35 \pm 1.99	7.53\pm1.70	<u>7.49\pm1.57</u>	5.57 \pm 1.08

Table 18: Benchmark Results of Serialization Formats Across Tasks of Open-source Models (Mean \pm 95% CI Margin). **Bold orange** / Underlined blue highlights indicate best/second-best performance.

Task	Difficulty	AL	AM	AS	EL	ES	GMaL	GMoL
BFS order	E	42.12\pm5.89	25.68 \pm 5.21	<u>41.02\pm5.77</u>	30.04 \pm 4.94	30.01 \pm 4.73	39.54 \pm 5.84	31.41 \pm 4.67
	M	27.55\pm5.90	11.92 \pm 3.59	<u>24.79\pm5.40</u>	15.90 \pm 3.81	14.02 \pm 3.31	22.74 \pm 4.95	15.40 \pm 3.31
	H	15.45\pm4.36	1.99 \pm 0.72	<u>14.60\pm4.10</u>	5.87 \pm 1.72	4.63 \pm 1.27	8.99 \pm 2.41	5.41 \pm 1.55
Connectivity	E	<u>83.33\pm3.84</u>	74.63 \pm 3.50	83.54\pm3.79	80.79 \pm 3.99	82.76 \pm 3.78	82.97 \pm 3.43	81.23 \pm 2.45
	M	82.36 \pm 3.78	76.85 \pm 3.22	82.90\pm3.60	79.50 \pm 4.01	79.40 \pm 3.71	<u>82.89\pm3.56</u>	82.11 \pm 2.83
	H	<u>78.43\pm3.98</u>	66.16 \pm 2.66	78.89\pm3.86	74.26 \pm 4.04	72.53 \pm 3.73	77.01 \pm 4.25	77.11 \pm 3.48
Cycle	E	58.72 \pm 3.30	59.20 \pm 3.30	59.18 \pm 3.31	62.89 \pm 3.39	66.65\pm3.27	<u>65.24\pm4.14</u>	64.64 \pm 3.20
	M	57.70 \pm 3.29	55.73 \pm 3.00	57.82 \pm 3.24	60.81 \pm 3.56	63.40\pm3.40	<u>62.44\pm4.28</u>	61.86 \pm 3.81
	H	54.64 \pm 3.29	52.54 \pm 2.56	54.50 \pm 3.25	58.80 \pm 3.54	<u>59.95\pm3.40</u>	60.04\pm4.00	59.54 \pm 3.85
Diameter	E	47.25 \pm 5.10	49.01 \pm 4.53	<u>49.78\pm4.91</u>	45.06 \pm 4.89	43.82 \pm 4.78	53.68\pm4.95	48.95 \pm 5.18
	M	32.28 \pm 4.19	31.91 \pm 3.38	<u>34.83\pm4.23</u>	30.61 \pm 3.72	28.06 \pm 3.68	35.40\pm4.09	33.50 \pm 4.16
	H	18.13 \pm 3.07	19.70 \pm 2.24	<u>20.57\pm3.23</u>	19.65 \pm 2.70	16.12 \pm 2.39	22.44\pm2.89	19.87 \pm 2.82
Shortest	E	<u>61.38\pm6.13</u>	39.46 \pm 5.99	62.90\pm6.02	57.99 \pm 5.93	54.26 \pm 5.99	30.52 \pm 5.96	55.14 \pm 5.54
	M	<u>52.45\pm5.93</u>	27.69 \pm 4.83	54.63\pm5.79	47.29 \pm 5.55	41.24 \pm 5.35	25.75 \pm 5.41	45.99 \pm 5.22
	H	<u>47.79\pm5.86</u>	18.72 \pm 3.74	48.52\pm5.72	38.00 \pm 5.16	34.34 \pm 4.78	22.69 \pm 5.10	36.89 \pm 4.81
Triangle	E	20.03 \pm 3.02	17.87 \pm 2.49	18.98 \pm 2.82	20.52 \pm 2.70	21.13 \pm 2.77	24.76\pm3.74	<u>22.42\pm3.50</u>
	M	10.37 \pm 1.79	8.81 \pm 1.35	10.41 \pm 1.83	11.17 \pm 1.65	10.72 \pm 1.70	12.92\pm2.19	<u>11.28\pm2.06</u>
	H	5.37 \pm 1.34	5.45 \pm 1.07	<u>6.76\pm1.52</u>	5.84 \pm 1.13	6.44 \pm 1.25	7.07\pm1.39	5.50 \pm 1.28

Table 19: Benchmark Results of Graph Type Across Tasks of Open-source Models (Mean \pm 95% CI Margin). **Bold orange** / Underlined blue highlights indicate best/second-best performance. “-” indicates the graph type is not applicable for that task.

Task	Difficulty	BAF	BAG	BERM	BERP	ERM	ERP	SF
BFS order	E	31.18 \pm 2.30	31.34 \pm 2.18	41.92\pm2.08	<u>41.16\pm2.04</u>	30.59 \pm 1.90	34.53 \pm 2.01	34.43 \pm 2.24
	M	<u>23.15\pm2.23</u>	19.97 \pm 1.90	17.92 \pm 1.79	24.76\pm1.87	14.89 \pm 1.41	15.08 \pm 1.41	18.27 \pm 1.86
	H	18.06\pm2.00	7.31 \pm 1.11	6.36 \pm 0.99	<u>10.85\pm1.16</u>	4.08 \pm 0.83	6.70 \pm 1.00	7.38 \pm 1.13
Connectivity	E	72.16 \pm 1.43	-	86.82\pm1.41	81.79 \pm 1.41	<u>84.65\pm1.40</u>	84.10 \pm 1.45	-
	M	74.84 \pm 1.43	-	<u>83.02\pm1.42</u>	84.28\pm1.45	80.99 \pm 1.38	82.86 \pm 1.44	-
	H	60.68 \pm 1.43	-	82.25\pm1.62	79.76 \pm 1.55	75.94 \pm 1.55	<u>81.89\pm1.59</u>	-
Cycle	E	-	60.70 \pm 1.34	62.16 \pm 1.36	63.53 \pm 1.36	<u>63.61\pm1.44</u>	64.51\pm1.39	59.65 \pm 1.33
	M	-	56.82 \pm 1.36	62.69\pm1.43	59.75 \pm 1.40	60.91 \pm 1.48	<u>62.21\pm1.44</u>	57.42 \pm 1.33
	H	-	52.15 \pm 1.27	<u>59.50\pm1.52</u>	61.04\pm1.48	57.73 \pm 1.49	59.09 \pm 1.46	53.36 \pm 1.23
Diameter	E	-	45.50 \pm 1.84	-	-	45.74 \pm 2.04	<u>48.57\pm1.99</u>	53.09\pm1.83
	M	-	<u>32.72\pm1.52</u>	-	-	28.87 \pm 1.60	31.85 \pm 1.76	36.16\pm1.45
	H	-	19.95 \pm 1.26	-	-	16.46 \pm 1.24	<u>20.54\pm1.33</u>	20.90\pm1.04
Shortest	E	59.63\pm2.63	51.54 \pm 2.37	49.30 \pm 2.39	52.61 \pm 2.46	46.04 \pm 2.32	50.04 \pm 2.37	52.97 \pm 2.46
	M	49.10\pm2.53	42.32 \pm 2.25	38.87 \pm 2.22	39.58 \pm 2.23	36.20 \pm 2.12	41.70 \pm 2.18	46.98 \pm 2.36
	H	46.37\pm2.59	34.28 \pm 2.16	33.36 \pm 2.10	30.18 \pm 2.18	30.50 \pm 1.99	33.90 \pm 2.06	38.55 \pm 2.22
Triangle	E	-	<u>19.17\pm1.27</u>	-	-	11.68 \pm 0.95	13.80 \pm 1.02	35.37\pm1.73
	M	-	<u>11.15\pm0.85</u>	-	-	7.62 \pm 0.72	8.66 \pm 0.87	15.28\pm1.05
	H	-	5.00 \pm 0.49	-	-	5.67 \pm 0.66	<u>5.78\pm0.53</u>	8.13\pm0.79

2160 E.1.3 RESULTS OF CLOSED-SOURCE MODELS
2161

2162 Closed-source models exhibit notably different characteristics compared to their open-source counterparts.
2163 For prompting schemes (Table 20), these models show more robust performances across
2164 different prompting methods, with even simple prompts like 0-Shot achieving competitive results.
2165 This is particularly evident in Connectivity tasks, where performance remains consistently high
2166 across most prompting schemes, suggesting less reliance on explicit reasoning guidance.

2167 The serialization format results (Table 21) reveal another key distinction: closed-source models handle
2168 complex formats more effectively. While they perform well with concise formats like AL and AS,
2169 they also show strong performance with structured formats like GMaL, especially in tasks requiring
2170 sophisticated reasoning like Cycle detection and Diameter calculation. This contrasts sharply
2171 with open-source models' preference for simpler formats.

2172 Regarding graph types (Table 22), closed-source models demonstrate more balanced performance
2173 across different graph structures. For instance, in Triangle counting tasks, while SF still performs
2174 best, the performance gap between different graph types is notably smaller than in open-source
2175 models, suggesting more robust graph structure processing capabilities.

2176 Table 20: Benchmark Results of Prompt Schemes Across Tasks of Closed-source Models (Mean \pm 95%
2177 CI Margin). **Bold orange** / Underlined blue highlights indicate best/second-best performance.

Task	Difficulty	0-Algorithm	0-CoT	0-Instruct	0-Shot	Algorithm	CoT	Instruct	K-Shot	LTM
BFS order	E	83.66 \pm 3.70	83.34 \pm 3.61	<u>85.15\pm3.08</u>	82.07 \pm 3.81	90.06\pm3.02	83.07 \pm 3.53	82.66 \pm 3.60	77.35 \pm 4.92	83.99 \pm 3.24
	M	59.37 \pm 4.92	<u>60.42\pm4.91</u>	59.67 \pm 4.68	59.09 \pm 5.30	68.91\pm5.06	57.33 \pm 4.97	57.17 \pm 4.72	52.05 \pm 5.35	58.98 \pm 4.71
	H	22.41 \pm 3.11	<u>23.85\pm3.19</u>	23.41 \pm 3.10	23.82 \pm 3.61	31.79\pm4.30	20.38 \pm 2.78	19.01 \pm 2.68	18.86 \pm 2.90	23.29 \pm 3.12
Connectivity	E	95.86 \pm 1.05	95.95 \pm 1.18	94.64 \pm 1.41	93.92 \pm 1.60	93.10 \pm 1.77	96.72\pm0.94	<u>96.43\pm0.92</u>	91.15 \pm 2.01	95.34 \pm 1.27
	M	<u>96.43\pm0.87</u>	96.22 \pm 1.01	95.34 \pm 1.08	95.71 \pm 0.96	94.01 \pm 1.35	96.99\pm0.74	96.39 \pm 0.86	93.06 \pm 1.54	95.56 \pm 1.26
	H	91.90\pm2.12	91.24 \pm 2.07	90.89 \pm 2.19	<u>91.55\pm2.04</u>	86.76 \pm 2.74	91.28 \pm 2.34	90.98 \pm 2.27	88.40 \pm 2.57	91.37 \pm 2.23
Cycle	E	82.17\pm3.67	80.28 \pm 3.42	79.43 \pm 3.52	78.30 \pm 3.73	81.03 \pm 3.95	<u>81.58\pm3.22</u>	81.44 \pm 3.27	81.01 \pm 3.54	80.08 \pm 3.46
	M	80.54 \pm 3.54	79.75 \pm 3.45	78.96 \pm 3.56	78.15 \pm 3.55	<u>81.87\pm3.83</u>	82.49\pm3.33	80.25 \pm 3.73	79.27 \pm 4.03	78.67 \pm 3.54
	H	77.26 \pm 3.40	76.84 \pm 3.45	76.99 \pm 3.62	76.70 \pm 3.54	<u>80.15\pm3.87</u>	80.20\pm3.71	79.35 \pm 3.73	78.08 \pm 4.07	77.19 \pm 3.54
Diameter	E	72.68 \pm 4.82	<u>74.42\pm5.02</u>	73.82 \pm 5.02	71.82 \pm 5.47	75.80\pm3.36	70.29 \pm 4.77	70.07 \pm 4.65	71.25 \pm 4.47	73.39 \pm 5.17
	M	50.83 \pm 5.17	52.60 \pm 4.72	51.12 \pm 4.85	51.37 \pm 4.68	59.43\pm2.32	55.54 \pm 4.35	55.09 \pm 4.23	<u>56.29\pm3.86</u>	52.05 \pm 4.71
	H	30.49 \pm 4.51	32.11 \pm 4.10	31.43 \pm 4.30	31.62 \pm 4.03	42.53\pm2.94	38.21 \pm 3.90	<u>38.93\pm3.70</u>	38.44 \pm 3.31	31.85 \pm 4.34
Shortest	E	84.07 \pm 3.82	88.87 \pm 2.80	88.79 \pm 2.82	87.42 \pm 3.00	92.65\pm2.03	87.34 \pm 4.55	<u>91.11\pm2.21</u>	86.34 \pm 4.99	89.08 \pm 2.76
	M	80.93 \pm 3.96	82.83 \pm 3.74	81.91 \pm 3.79	81.03 \pm 3.90	85.77\pm3.19	<u>84.86\pm3.11</u>	84.34 \pm 3.27	83.45 \pm 3.41	83.09 \pm 3.71
	H	76.76 \pm 4.53	79.05\pm4.48	78.22 \pm 4.56	76.28 \pm 4.86	77.90 \pm 4.42	75.69 \pm 4.35	76.05 \pm 4.32	73.70 \pm 4.50	<u>78.23\pm4.84</u>
Triangle	E	48.50\pm4.79	48.20 \pm 4.65	47.29 \pm 4.80	47.11 \pm 5.09	46.96 \pm 4.77	45.29 \pm 5.08	44.68 \pm 5.02	43.25 \pm 5.25	<u>48.33\pm4.58</u>
	M	27.25\pm2.82	26.62 \pm 2.82	26.38 \pm 2.91	<u>26.92\pm3.24</u>	26.47 \pm 2.58	25.25 \pm 2.98	25.02 \pm 2.66	24.98 \pm 2.90	26.67 \pm 2.88
	H	14.04 \pm 1.22	15.54\pm1.20	14.23 \pm 1.14	<u>14.27\pm1.47</u>	13.11 \pm 1.26	12.46 \pm 1.29	11.34 \pm 1.11	12.41 \pm 1.38	14.04 \pm 1.28

2196 E.2 PERFORMANCE HEATMAPS ACROSS TASKS
2197

2198 In this section, we provide detailed visualizations of model performance through heatmaps, extending
2199 the example shown in Figure 4. These heatmaps illustrate the interaction between prompting schemes
2200 and serialization formats across different tasks and difficulty levels, offering a comprehensive view of
2201 how various methodological combinations affect model performance.

2202 E.2.1 HEATMAPS FOR BFS order TASK
2203

2204 As shown in Figure 8 (featuring Claude-3.5, GPT-4o, GPT-4o-mini, Gemini-2.0), Figure 9 (featuring
2205 Llama-3 (8B), Llama-3.1 (8B), Mistral (7B), Phi-4 (14B)), Figure 10 (featuring Qwen-2.5 (7B),
2206 o4-mini), the heatmaps compare different prompt strategies and graph serialization formats under
2207 easy, medium, and hard difficulties for the BFS order task. The color intensity encodes accuracy
2208 (darker = higher), and solid/dashed boxes highlight best/second-best combinations, respectively.
2209

2214
2215
2216
2217
2218
2219Table 21: Benchmark Results of Serialization Formats Across Tasks of Closed-source Models (Mean \pm 95% CI Margin). **Bold orange** / Underlined blue : best performance, Underlined and blue highlight: second best performance

Task	Difficulty	AL	AM	AS	EL	ES	GMaL	GMoL
BFS order	E	92.88\pm1.83	81.89 \pm 3.82	<u>92.68\pm1.81</u>	78.90 \pm 3.23	82.02 \pm 3.12	85.90 \pm 2.55	70.12 \pm 3.57
	M	74.53\pm3.82	49.43 \pm 4.43	<u>73.71\pm3.56</u>	53.07 \pm 3.89	51.34 \pm 3.83	63.09 \pm 3.86	49.39 \pm 4.33
	H	<u>35.79\pm3.30</u>	9.67 \pm 1.14	36.16\pm3.18	19.14 \pm 1.89	15.26 \pm 1.50	24.81 \pm 2.21	20.02 \pm 2.24
Connectivity	E	98.11\pm0.54	89.74 \pm 1.12	<u>98.03\pm0.54</u>	95.74 \pm 1.13	96.53 \pm 0.99	96.11 \pm 1.00	89.27 \pm 1.78
	M	97.70\pm0.54	90.73 \pm 0.99	<u>97.63\pm0.59</u>	96.32 \pm 0.89	96.96 \pm 0.83	95.81 \pm 1.00	93.53 \pm 1.20
	H	95.46\pm0.98	71.48 \pm 2.03	<u>95.19\pm1.08</u>	94.01 \pm 1.09	92.93 \pm 1.27	93.39 \pm 1.48	90.94 \pm 1.44
Cycle	E	72.12 \pm 3.34	74.92 \pm 3.33	71.72 \pm 3.33	83.66 \pm 2.45	<u>87.60\pm1.93</u>	91.29\pm2.34	82.83 \pm 2.51
	M	71.27 \pm 3.45	72.94 \pm 3.32	70.82 \pm 3.43	84.19 \pm 2.40	85.26 \pm 2.40	90.03\pm2.39	<u>85.48\pm2.35</u>
	H	69.91 \pm 3.34	68.19 \pm 2.55	68.17 \pm 3.35	84.81 \pm 2.42	81.23 \pm 2.64	87.34\pm2.64	86.94 \pm 2.62
Diameter	E	73.80 \pm 4.05	72.10 \pm 4.41	77.50\pm3.57	68.80 \pm 4.60	69.47 \pm 4.79	<u>74.33\pm3.76</u>	72.30 \pm 3.99
	M	<u>57.75\pm4.10</u>	50.53 \pm 3.49	60.91\pm3.70	47.82 \pm 3.74	46.15 \pm 4.07	57.28 \pm 3.59	56.24 \pm 3.66
	H	<u>41.04\pm3.81</u>	29.17 \pm 3.62	42.25\pm3.30	28.32 \pm 2.59	25.52 \pm 2.79	40.03 \pm 3.70	39.15 \pm 3.24
Shortest	E	96.21\pm1.37	74.70 \pm 3.14	<u>95.78\pm1.55</u>	91.61 \pm 1.89	89.61 \pm 2.27	84.10 \pm 5.04	86.86 \pm 1.44
	M	93.72\pm1.32	59.50 \pm 3.52	89.45 \pm 2.34	88.76 \pm 1.72	82.18 \pm 2.96	<u>89.66\pm1.81</u>	78.67 \pm 2.45
	H	<u>89.85\pm2.04</u>	41.52 \pm 3.27	89.97\pm1.92	80.77 \pm 2.87	76.84 \pm 3.50	83.15 \pm 2.67	76.04 \pm 2.49
Triangle	E	<u>48.83\pm4.09</u>	41.24 \pm 4.50	49.80\pm4.18	47.36 \pm 4.18	43.95 \pm 4.27	47.65 \pm 4.15	47.53 \pm 4.59
	M	27.47 \pm 2.30	20.06 \pm 1.98	<u>27.69\pm2.33</u>	29.13\pm2.55	24.48 \pm 2.43	27.10 \pm 2.61	27.28 \pm 2.98
	H	13.56 \pm 0.96	8.24 \pm 0.96	15.38\pm0.86	<u>15.28\pm0.98</u>	11.97 \pm 0.88	14.92 \pm 1.15	15.11 \pm 1.38

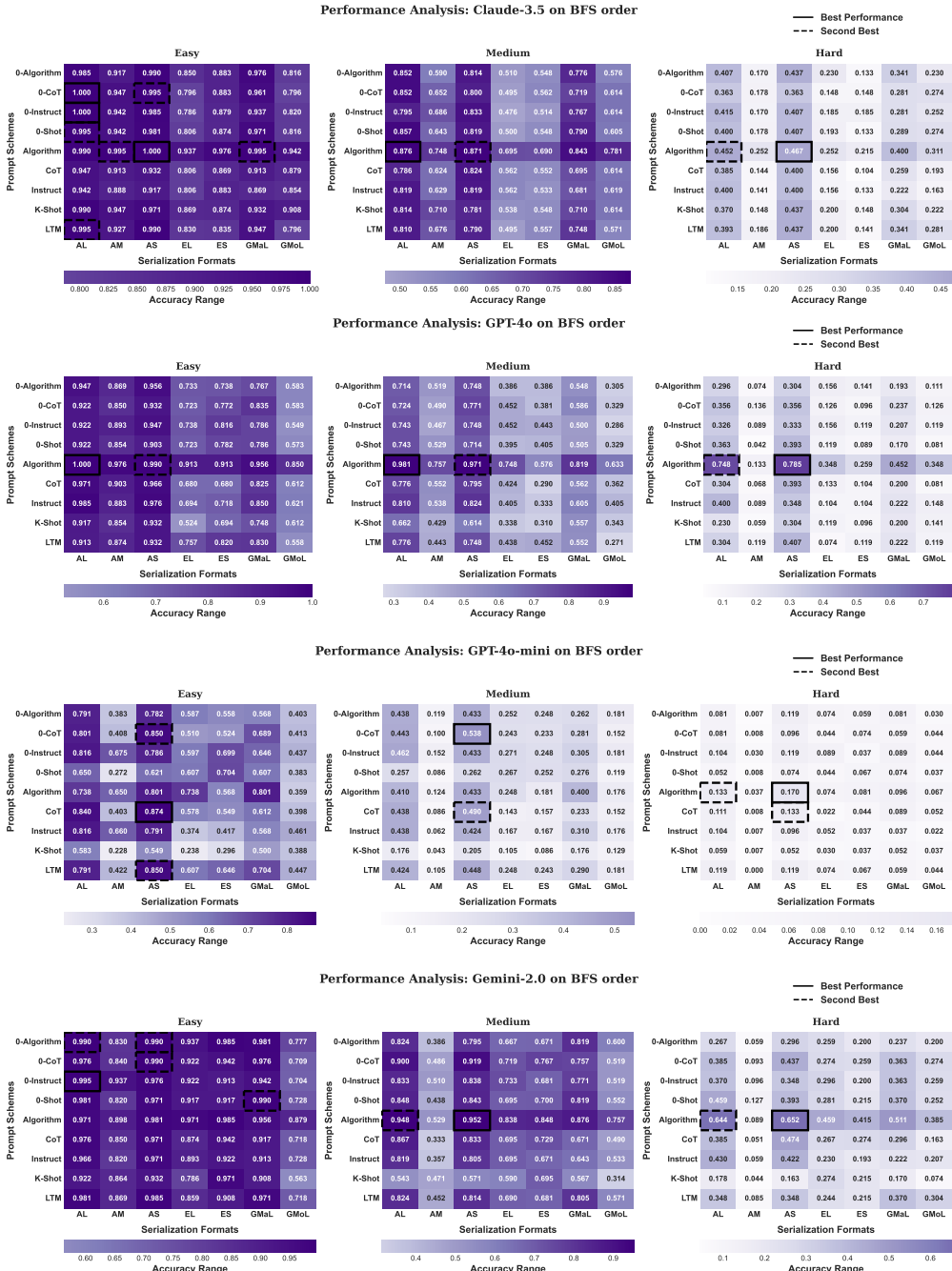
2239
2240
2241
2242
2243Table 22: Benchmark Results of Graph Type Across Tasks of Closed-source Models (Mean \pm 95% CI Margin). **Bold orange** / Underlined blue highlights indicate best/second-best performance. “-” indicates the graph type is not applicable for that task.

Task	Difficulty	BAF	BAG	BERM	BERP	ERM	ERP	SF
BFS order	E	83.62 \pm 1.34	83.41 \pm 1.40	84.98 \pm 1.23	<u>85.73\pm1.17</u>	77.72 \pm 1.50	83.45 \pm 1.29	86.16\pm1.29
	M	75.54\pm1.65	63.93 \pm 1.91	55.38 \pm 1.81	67.58\pm1.67	45.67 \pm 1.68	48.93 \pm 1.68	60.08 \pm 1.96
	H	61.08\pm1.79	18.36 \pm 1.33	16.07 \pm 1.06	<u>28.99\pm1.18</u>	10.62 \pm 0.91	20.46 \pm 1.22	19.04 \pm 1.41
Connectivity	E	92.90 \pm 0.74	-	95.59 \pm 0.47	94.17 \pm 0.57	<u>96.03\pm0.40</u>	96.18\pm0.42	-
	M	93.29 \pm 0.66	-	97.06\pm0.32	<u>96.53\pm0.39</u>	95.53 \pm 0.40	95.92 \pm 0.45	-
	H	83.06 \pm 1.27	-	92.36 \pm 0.87	91.62 \pm 0.88	<u>92.49\pm0.74</u>	95.46\pm0.49	-
Cycle	E	-	81.22 \pm 1.34	81.07 \pm 1.20	78.68 \pm 1.23	<u>82.18\pm1.40</u>	83.77\pm1.20	76.63 \pm 1.32
	M	-	77.94 \pm 1.39	83.95\pm1.17	77.45 \pm 1.27	82.07 \pm 1.41	<u>82.82\pm1.14</u>	75.76 \pm 1.32
	H	-	71.11 \pm 1.49	<u>83.02\pm1.19</u>	83.38\pm1.14	79.35 \pm 1.36	80.67 \pm 1.33	70.99 \pm 1.41
Diameter	E	-	<u>72.16\pm1.69</u>	-	-	67.11 \pm 1.89	71.21 \pm 1.76	79.98\pm1.25
	M	-	53.15 \pm 1.69	-	-	48.55 \pm 1.74	57.07\pm1.55	<u>56.48\pm1.47</u>
	H	-	34.07 \pm 1.62	-	-	<u>34.54\pm1.74</u>	42.31\pm1.77	29.36 \pm 0.94
Shortest	E	<u>90.09\pm1.26</u>	89.28 \pm 1.17	85.05 \pm 1.24	88.66 \pm 1.23	86.36 \pm 1.20	90.60\pm1.09	88.84 \pm 1.20
	M	85.09 \pm 1.50	<u>85.51\pm1.26</u>	80.90 \pm 1.17	80.35 \pm 1.19	79.25 \pm 1.45	83.96 \pm 1.26	86.53\pm1.31
	H	<u>80.55\pm2.03</u>	80.74\pm1.66	74.31 \pm 1.54	75.11 \pm 1.75	71.53 \pm 1.69	75.63 \pm 1.48	80.21 \pm 1.67
Triangle	E	-	<u>51.58\pm1.78</u>	-	-	29.68 \pm 1.53	37.19 \pm 1.69	68.04\pm1.80
	M	-	<u>34.13\pm1.01</u>	-	-	14.28 \pm 0.59	18.81 \pm 0.75	37.47\pm1.66
	H	-	17.97\pm0.62	-	-	8.48 \pm 0.38	13.06 \pm 0.48	<u>14.45\pm0.60</u>

2266
2267

2268
2269
2270
2271
2272
2273
2274
2275
2276
2277
2278
2279
2280
2281
2282
2283
2284
2285
2286
2287
2288
2289
2290
2291
2292
2293
2294
2295
2296
2297
2298
2299
2300
2301
2302
2303
2304
2305
2306
2307
2308
2309
2310
2311
2312
2313
2314
2315
2316
2317
2318
2319
2320
2321

Figure 8: Performance heatmaps for prompt strategies and serialization formats on the BFS order task (Part 1). Models: Claude-3.5, GPT-4o, GPT-4o-mini, Gemini-2.0.



2322

2323

2324

2325

2326

2327

2328

2329

2330

2331

2332

2333

2334

2335

2336

2337

2338

2339

2340

2341

2342

2343

2344

2345

2346

2347

2348

2349

2350

2351

2352

2353

2354

2355

2356

2357

2358

2359

2360

2361

2362

2363

2364

2365

2366

2367

2368

2369

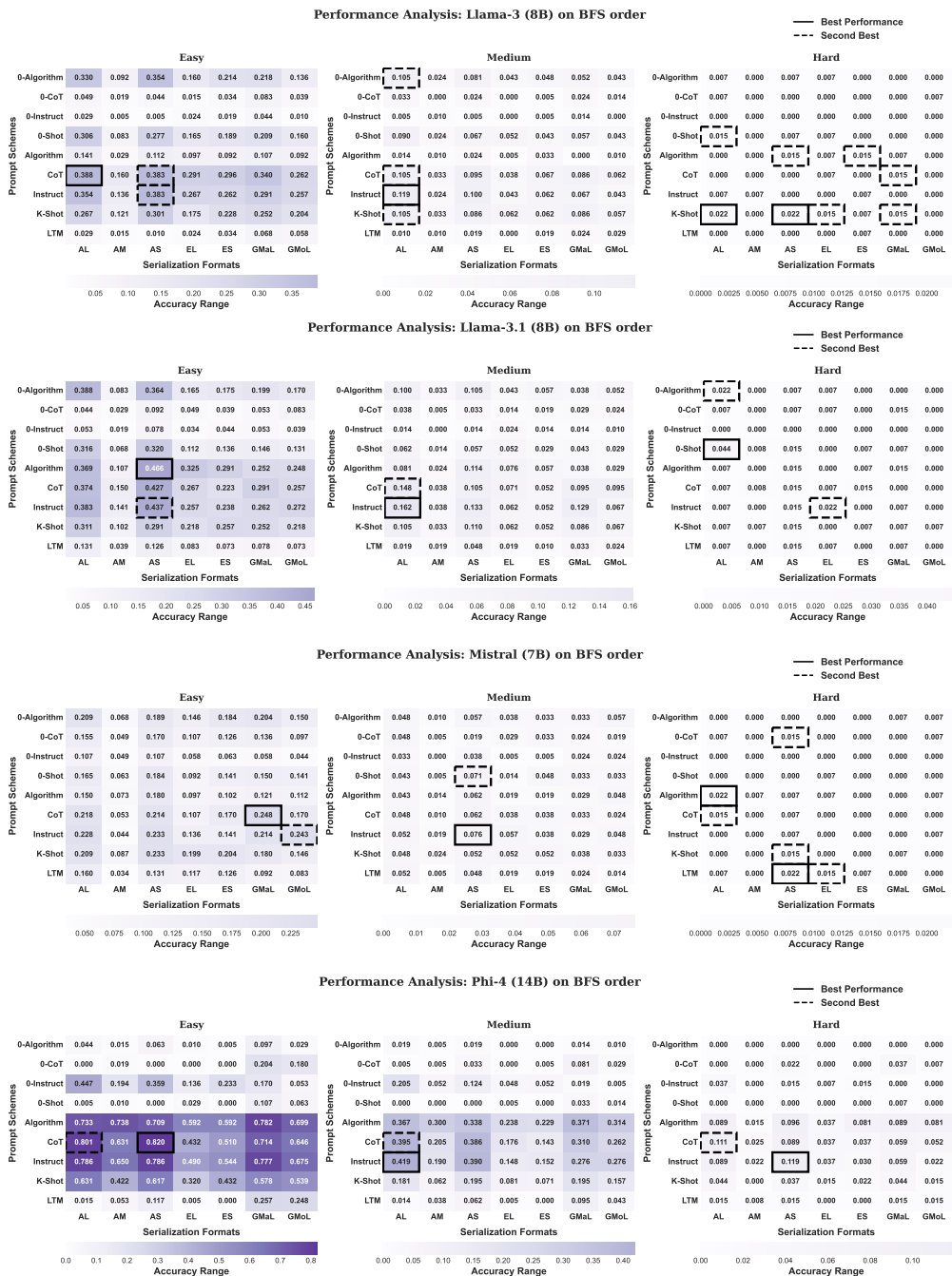


Figure 9: Performance heatmaps for prompt strategies and serialization formats on the BFS order task (Part 2). Models: Llama-3 (8B), Llama-3.1 (8B), Mistral (7B), Phi-4 (14B).

2376

2377

2378

2379

2380

2381

2382

2383

2384

2385

2386

2387

2388

2389

2390

2391

2392

2393

2394

2395

2396

2397

2398

2399

2400

2401

2402

2403

2404

2405

2406

2407

2408

2409

2410

2411

2412

2413

2414

2415

2416

2417

2418

2419

2420

2421

2422

2423

2424

2425

2426

2427

2428

2429

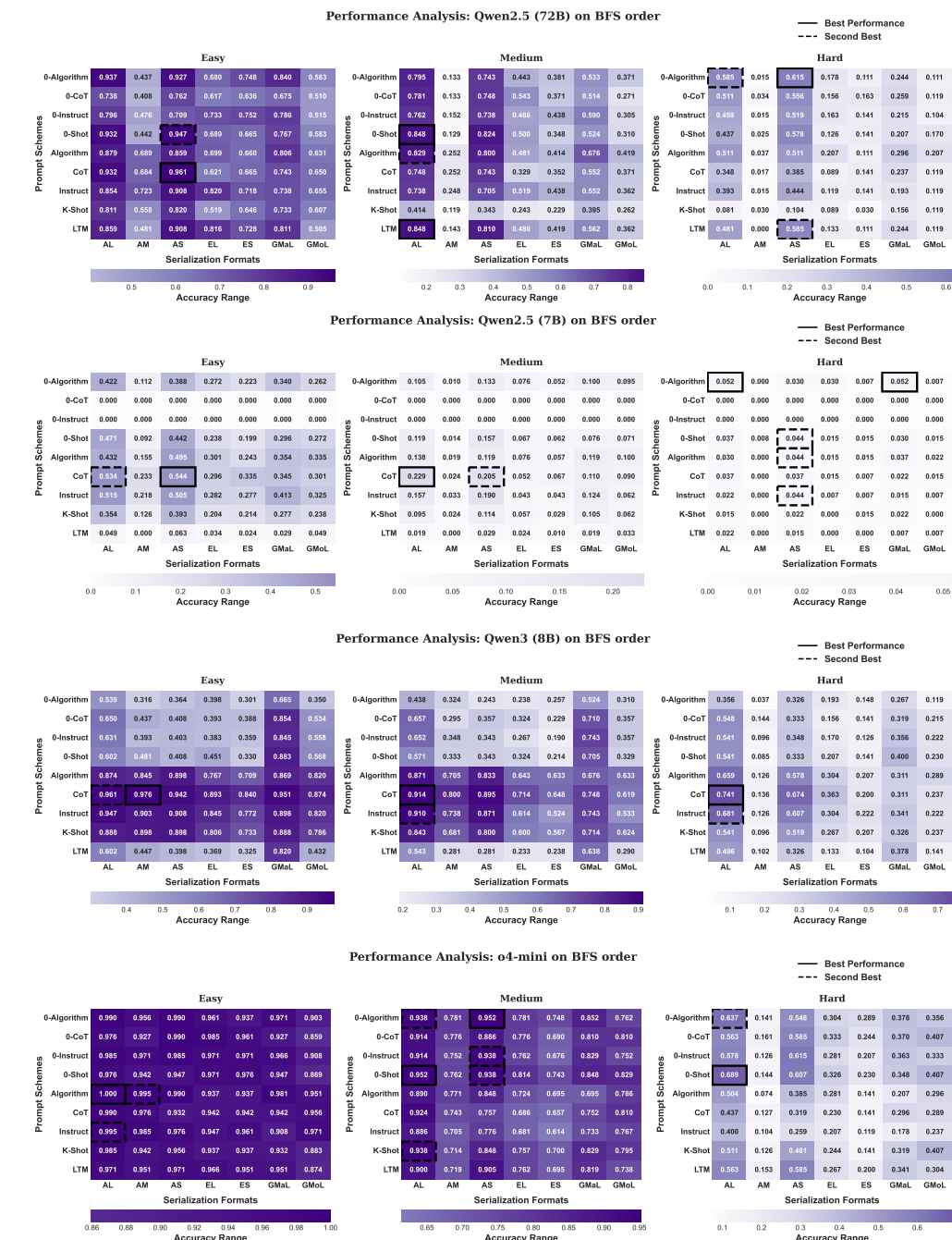
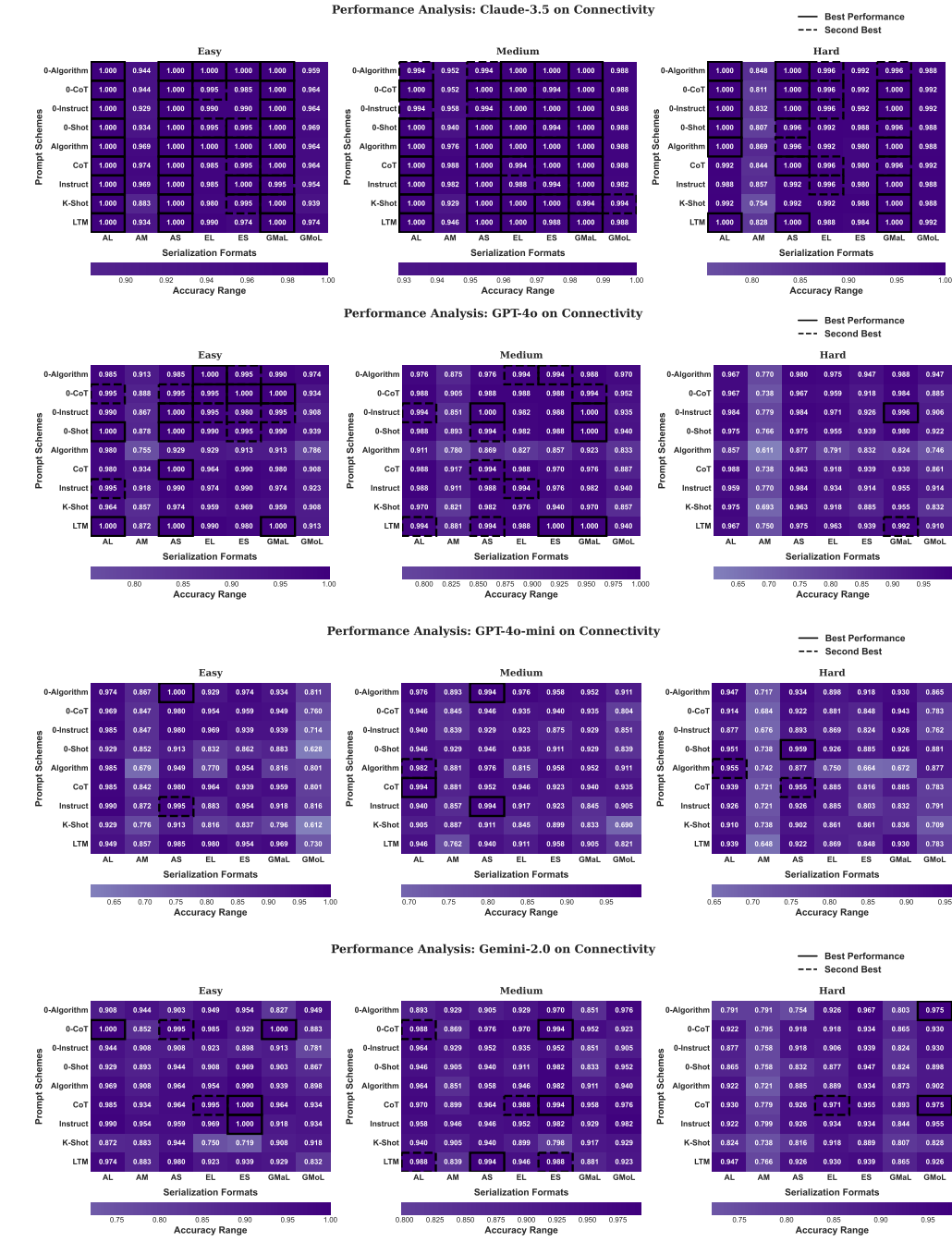


Figure 10: Performance heatmaps for prompt strategies and serialization formats on the BFS order task (Part 3). Models: Qwen-2.5 (72B), Qwen-2.5 (7B), Qwen-3 (8B), o4-mini.

2430 E.2.2 HEATMAPS FOR Connectivity TASK
2431

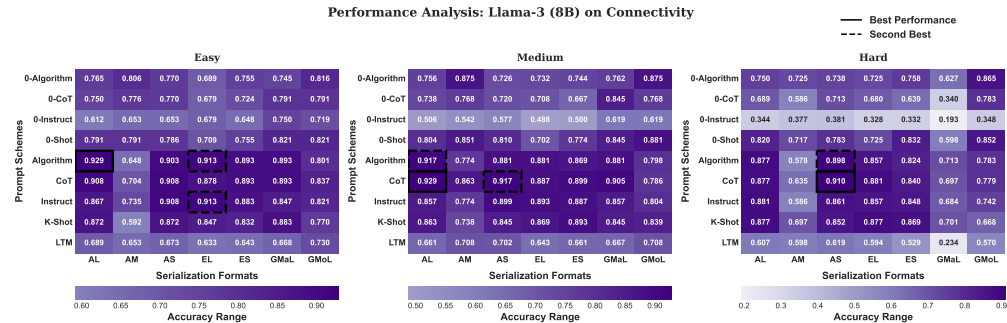
2432 As shown in Figure 11 (featuring Claude-3.5, GPT-4o, GPT-4o-mini, Gemini-2.0), Figure 12 (featuring
2433 Llama-3 (8B), Llama-3.1 (8B), Mistral (7B), Phi-4 (14B)), Figure 13 (featuring Qwen-2.5 (7B),
2434 o4-mini), the heatmaps compare different prompt strategies and graph serialization formats under
2435 easy, medium, and hard difficulties for the Connectivity task. The color intensity encodes accuracy
2436 (darker = higher), and solid/dashed boxes highlight best/second-best combinations respectively.



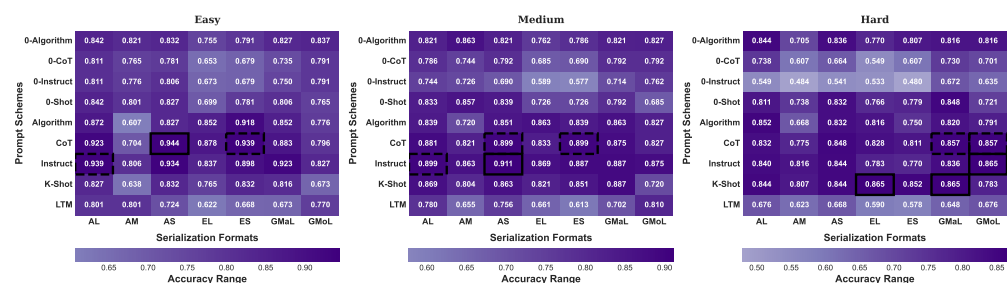
2481 Figure 11: Performance heatmaps for prompt strategies and serialization formats on the Connectivity
2482 task (Part 1). Models: Claude-3.5, GPT-4o, GPT-4o-mini, Gemini-2.0.
2483

2484
2485
2486
2487
2488
2489

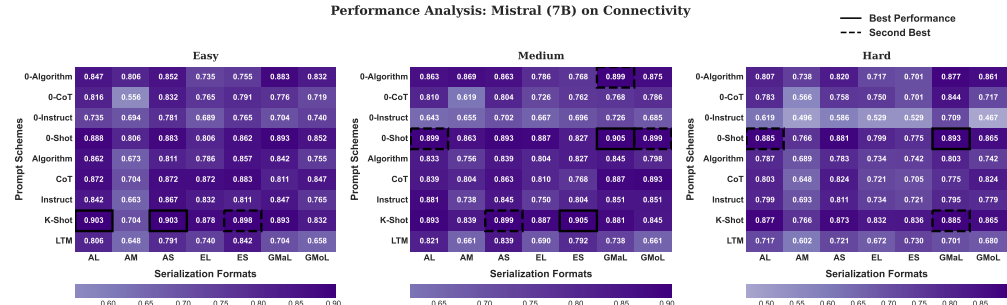
2490
2491
2492
2493
2494
2495
2496
2497
2498



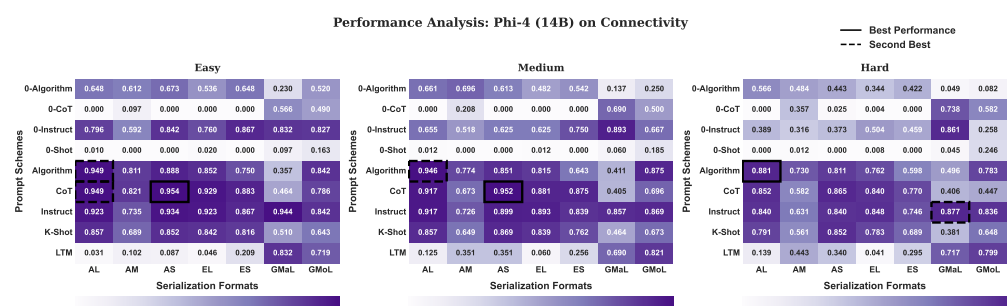
2499
2500
2501
2502
2503
2504
2505
2506
2507
2508
2509
2510
2511



2509
2510
2511
2512
2513
2514
2515
2516
2517
2518
2519



2520
2521
2522
2523
2524
2525
2526
2527
2528
2529
2530
2531



2538

2539

2540

2541

2542

2543

2544

2545

2546

2547

2548

2549

2550

2551

2552

2553

2554

2555

2556

2557

2558

2559

2560

2561

2562

2563

2564

2565

2566

2567

2568

2569

2570

2571

2572

2573

2574

2575

2576

2577

2578

2579

2580

2581

2582

2583

2584

2585

Figure 13: Performance heatmaps for prompt strategies and serialization formats on the Connectivity task (Part 3). Models: Qwen-2.5 (72B), Qwen-2.5 (7B), Qwen-3 (8B), o4-mini.

2586

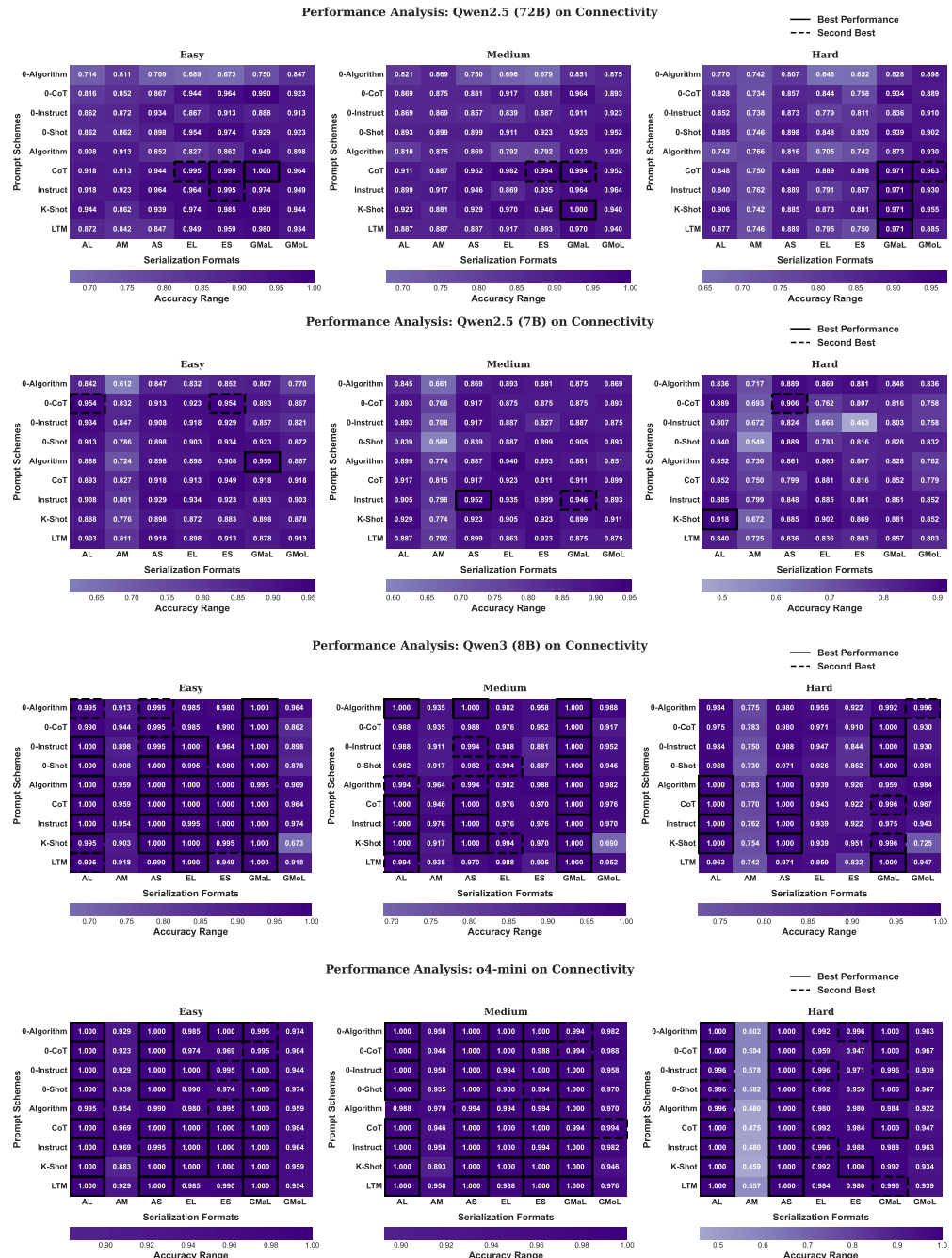
2587

2588

2589

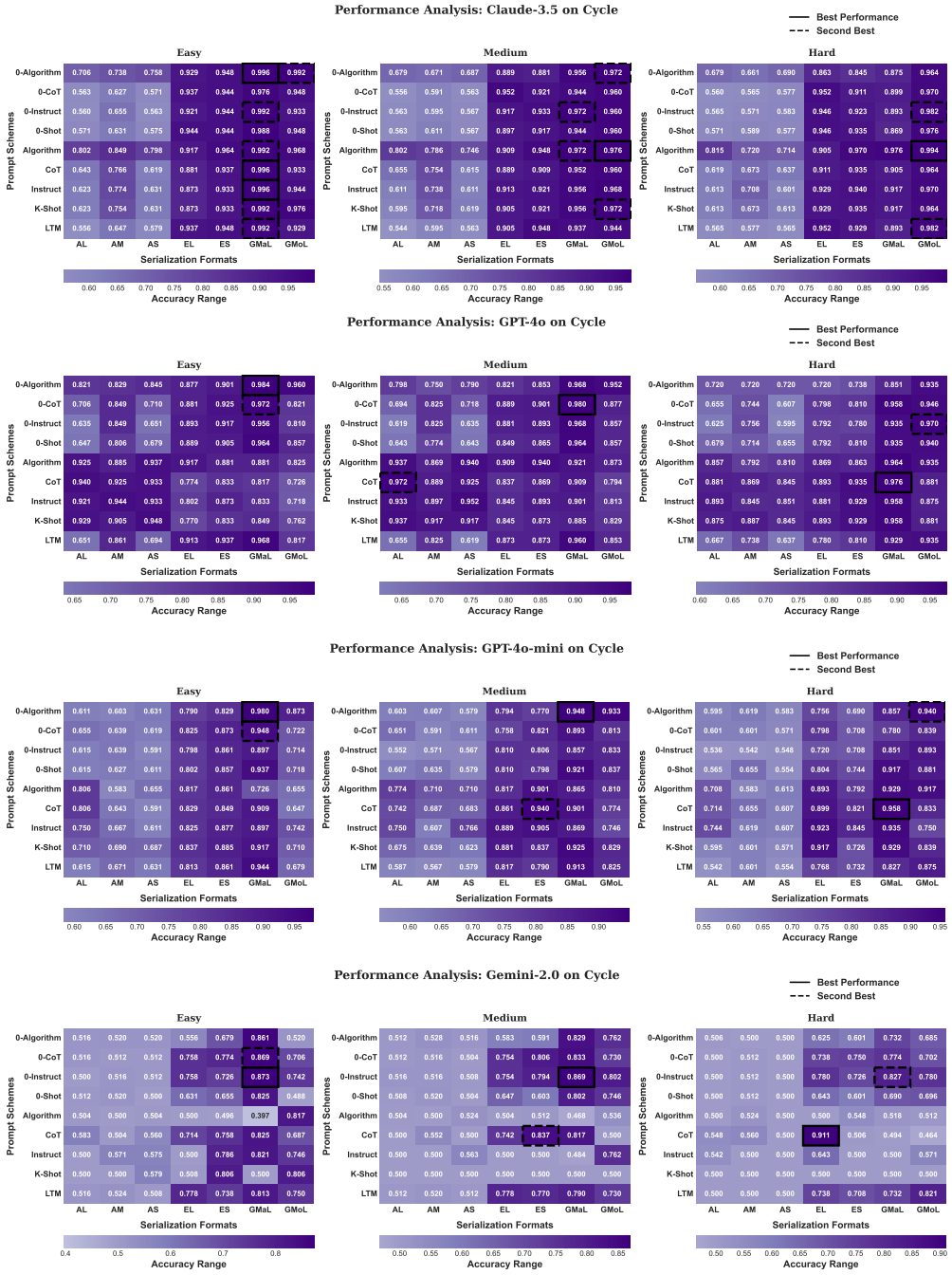
2590

2591



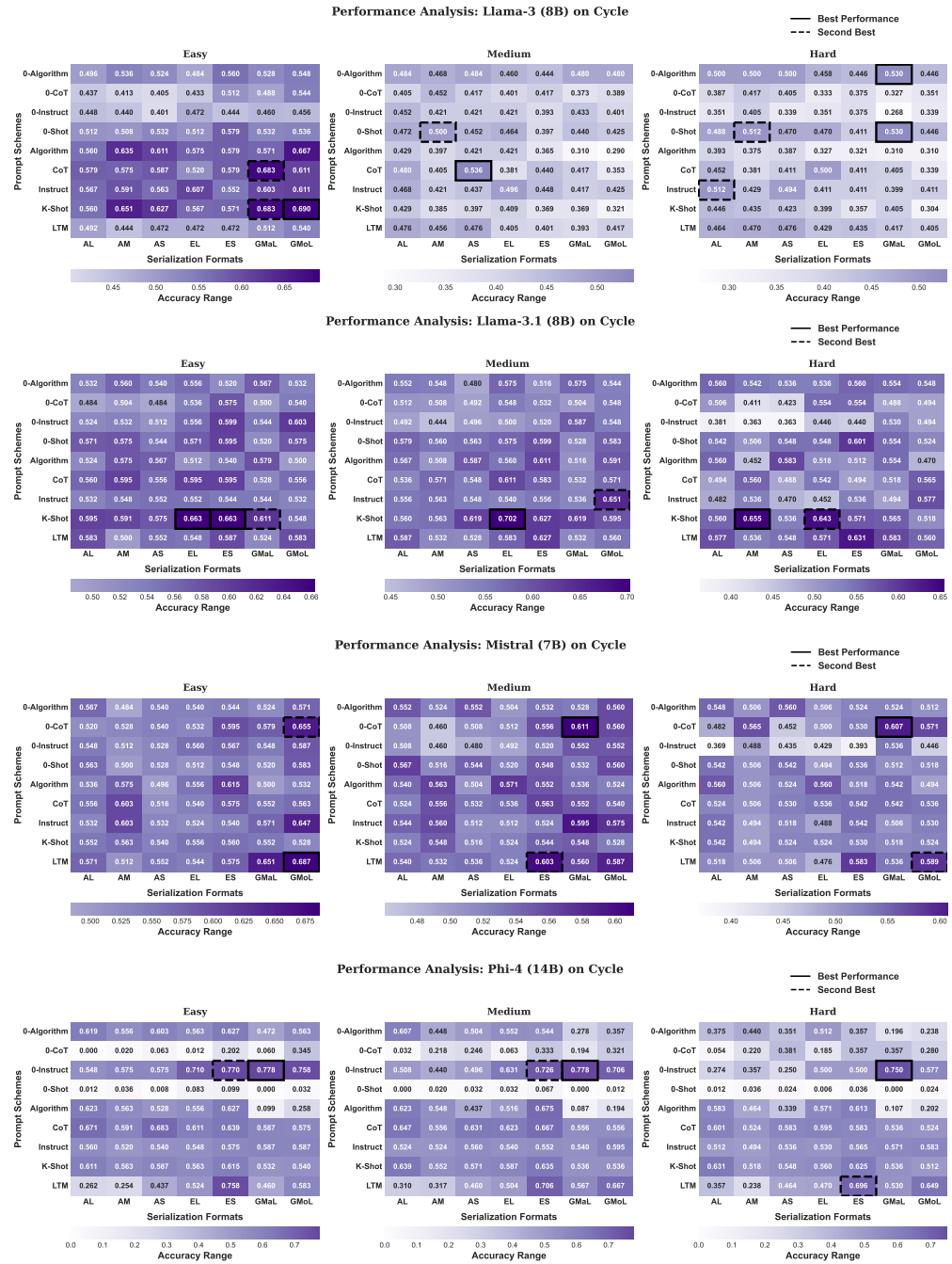
2592 E.2.3 HEATMAPS FOR Cycle detection TASK
2593

2594 As shown in Figure 14 (featuring Claude-3.5, GPT-4o, GPT-4o-mini, Gemini-2.0), Figure 15 (featuring
2595 Llama-3 (8B), Llama-3.1 (8B), Mistral (7B), Phi-4 (14B)), Figure 16 (featuring Qwen-2.5 (7B),
2596 o4-mini), the heatmaps compare different prompt strategies and graph serialization formats under easy,
2597 medium, and hard difficulties for the Cycle detection task. The color intensity encodes accuracy
2598 (darker = higher), and solid/dashed boxes highlight best/second-best combinations respectively.



2643 Figure 14: Performance heatmaps for prompt strategies and serialization formats on the Cycle task
2644 (Part 1). Models: Claude-3.5, GPT-4o, GPT-4o-mini, Gemini-2.0.
2645

2646
2647
2648
2649
2650
2651



2694 Figure 15: Performance heatmaps for prompt strategies and serialization formats on the Cycle task
2695 (Part 2). Models: Llama-3 (8B), Llama-3.1 (8B), Mistral (7B), Phi-4 (14B).

2696
2697
2698
2699

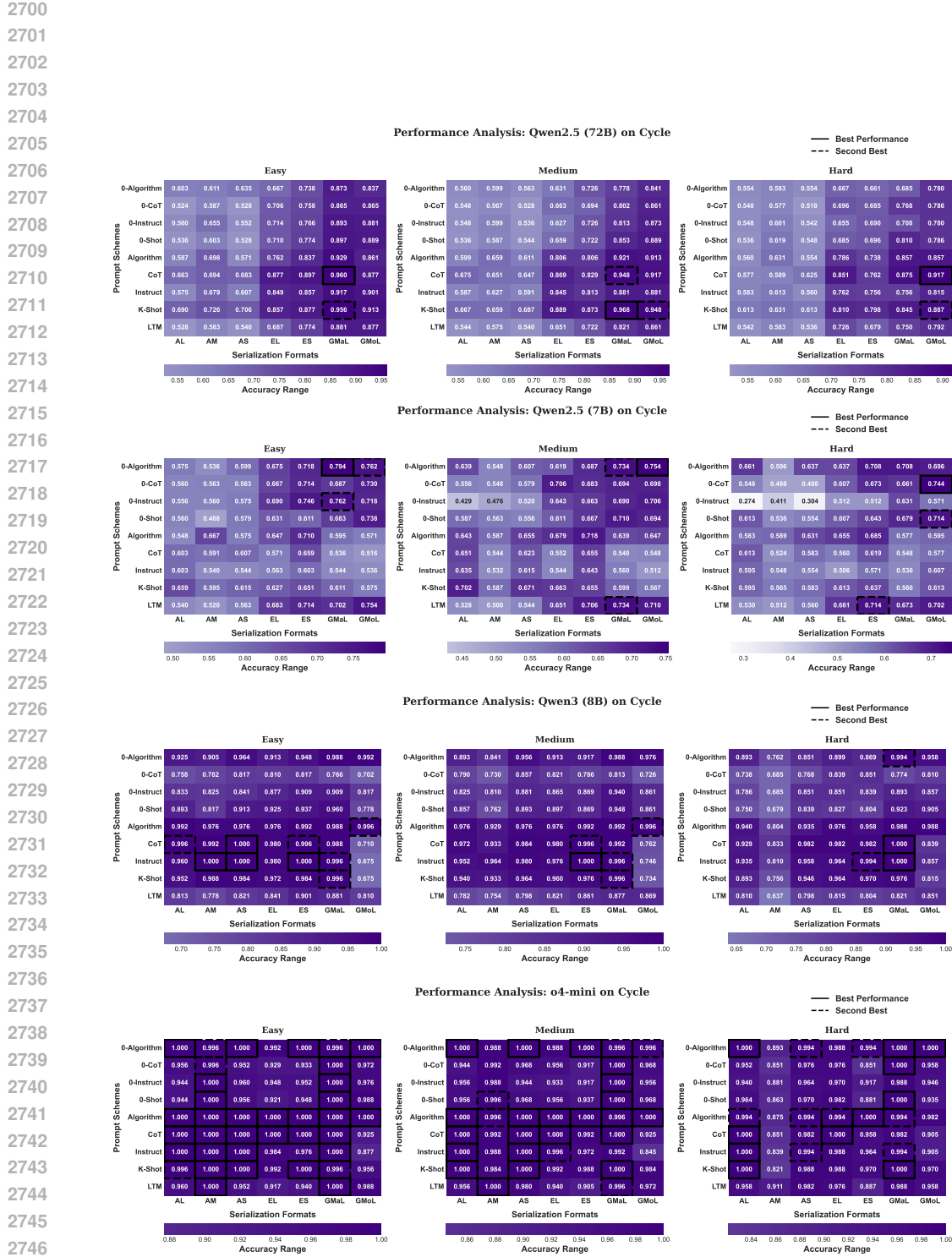


Figure 16: Performance heatmaps for prompt strategies and serialization formats on the Cycle task (Part 3). Models: Qwen-2.5 (72B), Qwen-2.5 (7B), Qwen-3 (8B), o4-mini.

E.2.4 HEATMAPS FOR Diameter calculation TASK

As shown in Figure 17 (featuring Claude-3.5, GPT-4o, GPT-4o-mini, Gemini-2.0), Figure 18 (featuring Llama-3 (8B), Llama-3.1 (8B), Mistral (7B), Phi-4 (14B)), Figure 19 (featuring Qwen-2.5 (7B), o4-mini), the heatmaps compare different prompt strategies and graph serialization formats under easy, medium, and hard difficulties for the Diameter calculation task. The color intensity encodes accuracy (darker = higher), and solid/dashed boxes highlight best/second-best combinations respectively.

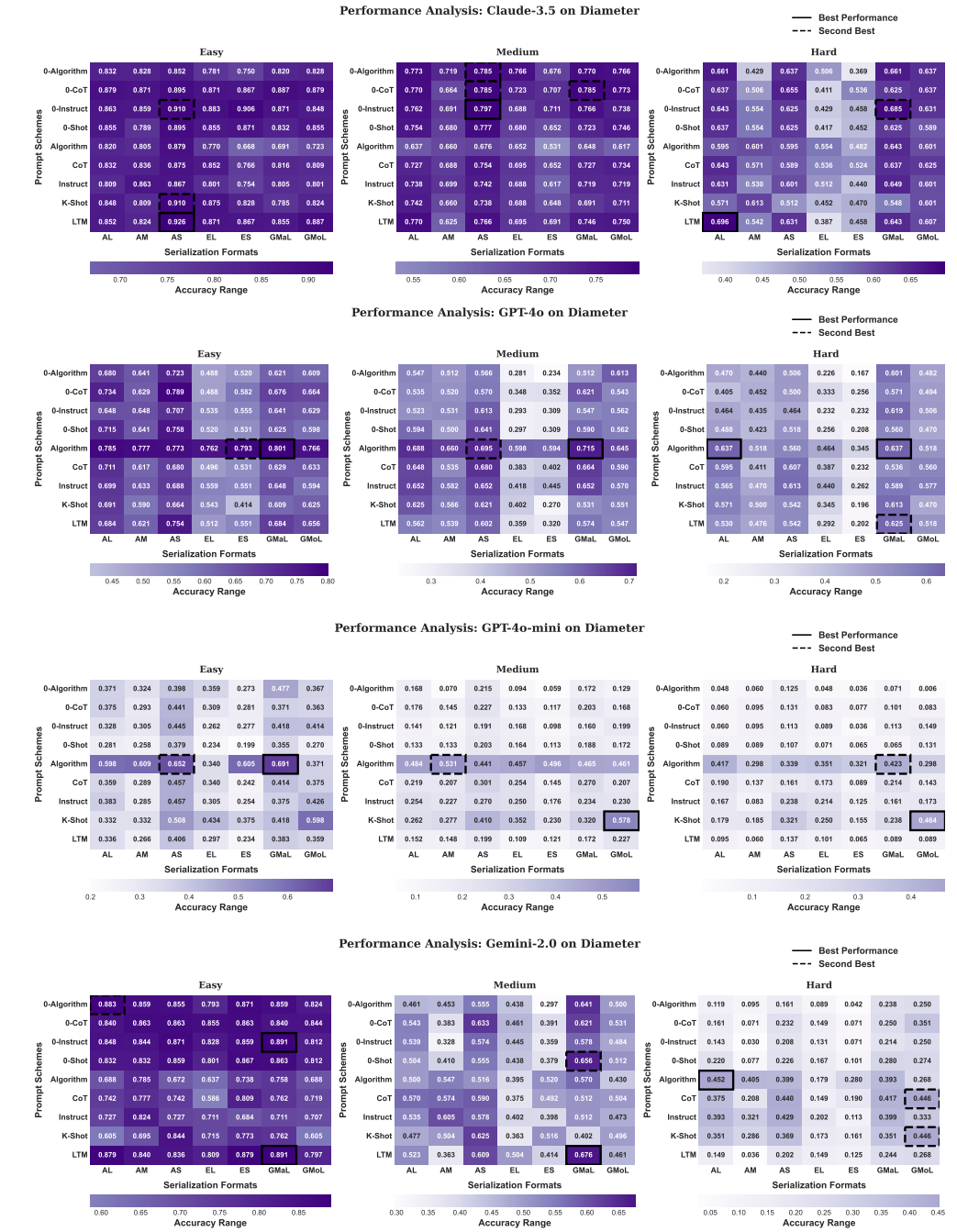


Figure 17: Performance heatmaps for prompt strategies and serialization formats on the Diameter task (Part 1). Models: Claude-3.5, GPT-4o, GPT-4o-mini, Gemini-2.0.

2808

2809

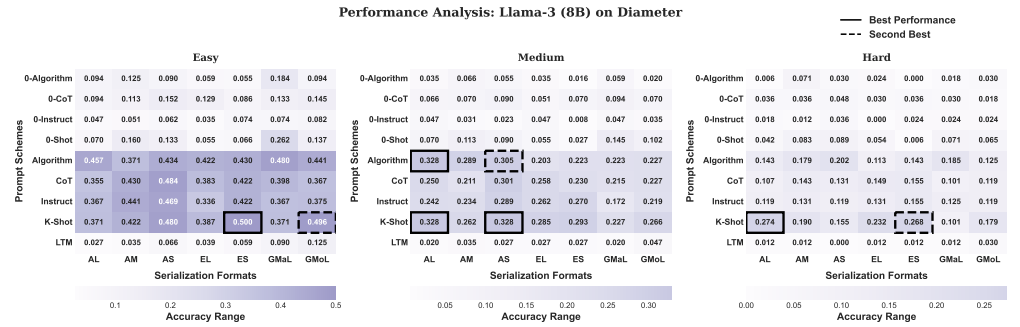
2810

2811

2812

2813

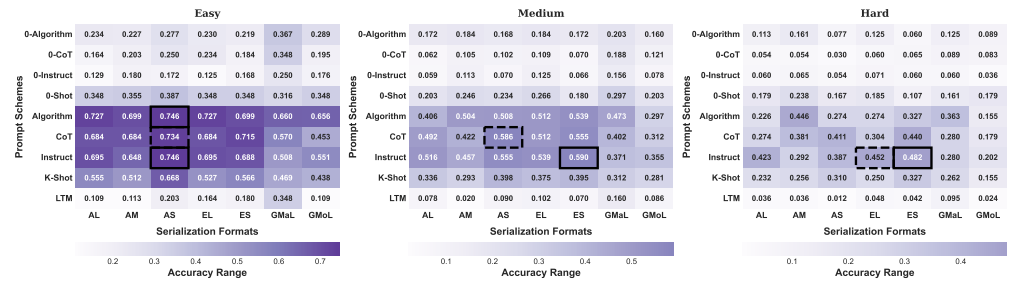
2814



2822

2823

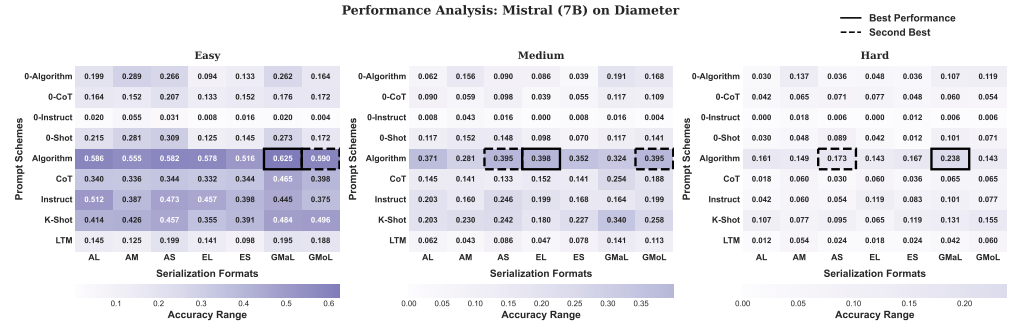
2824



2833

2834

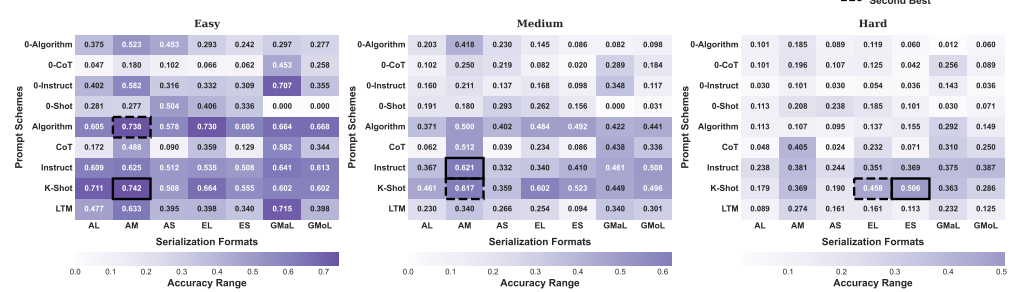
2835



2844

2845

2846



2855

Figure 18: Performance heatmaps for prompt strategies and serialization formats on the Diameter task (Part 2). Models: Llama-3 (8B), Llama-3.1 (8B), Mistral (7B), Phi-4 (14B).

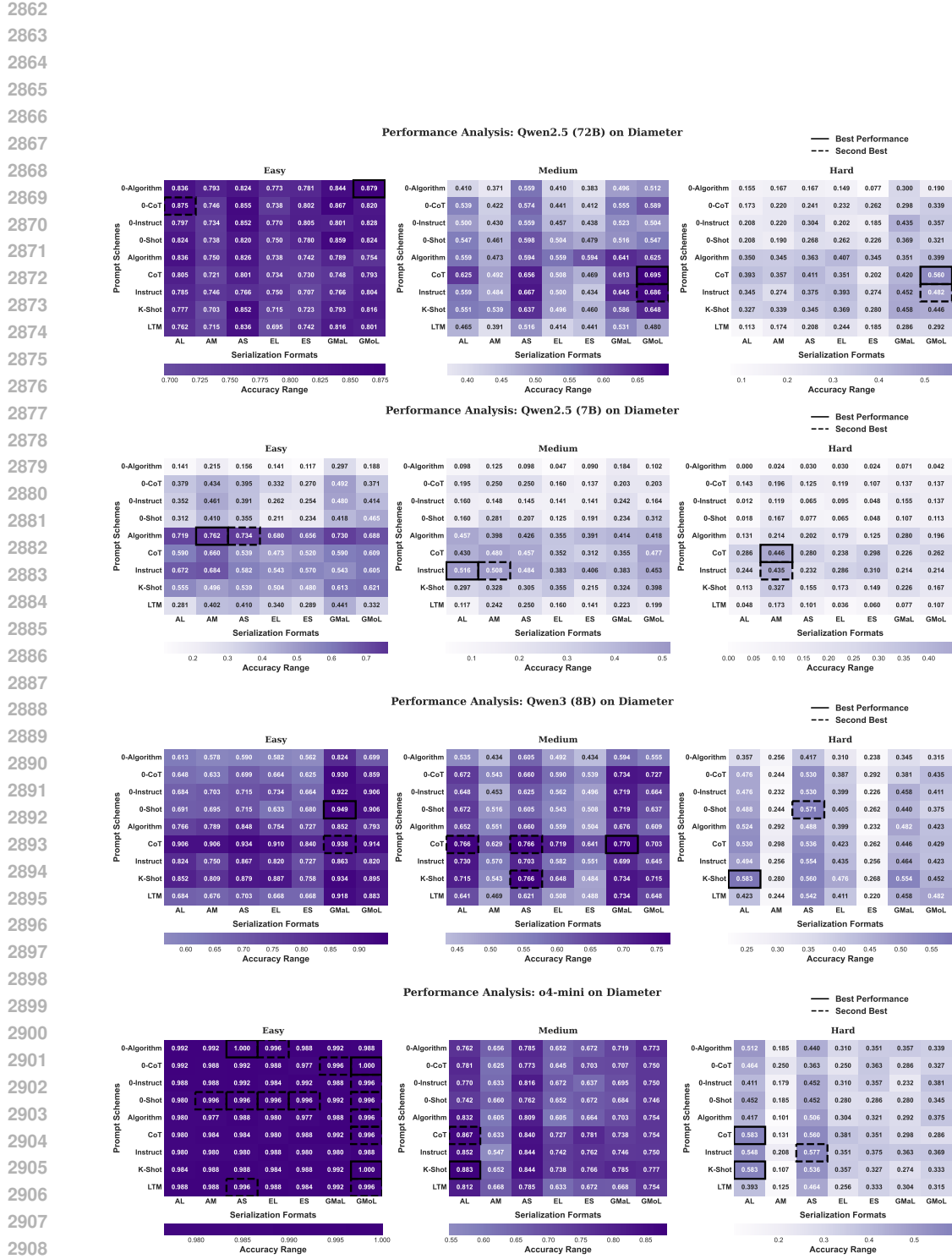
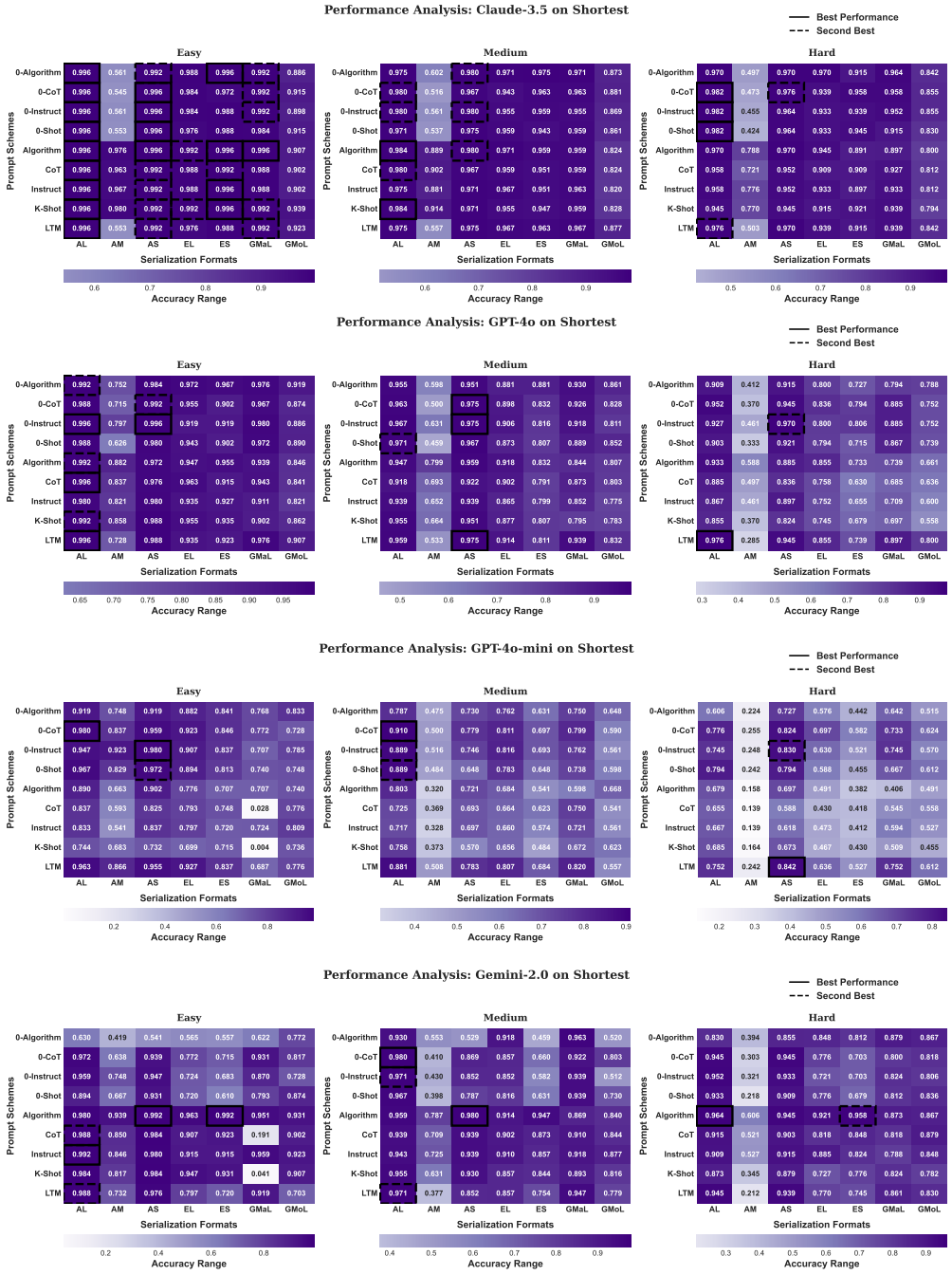


Figure 19: Performance heatmaps for prompt strategies and serialization formats on the Diameter task (Part 3). Models: Qwen-2.5 (72B), Qwen-2.5 (7B), Qwen-3 (8B), o4-mini.

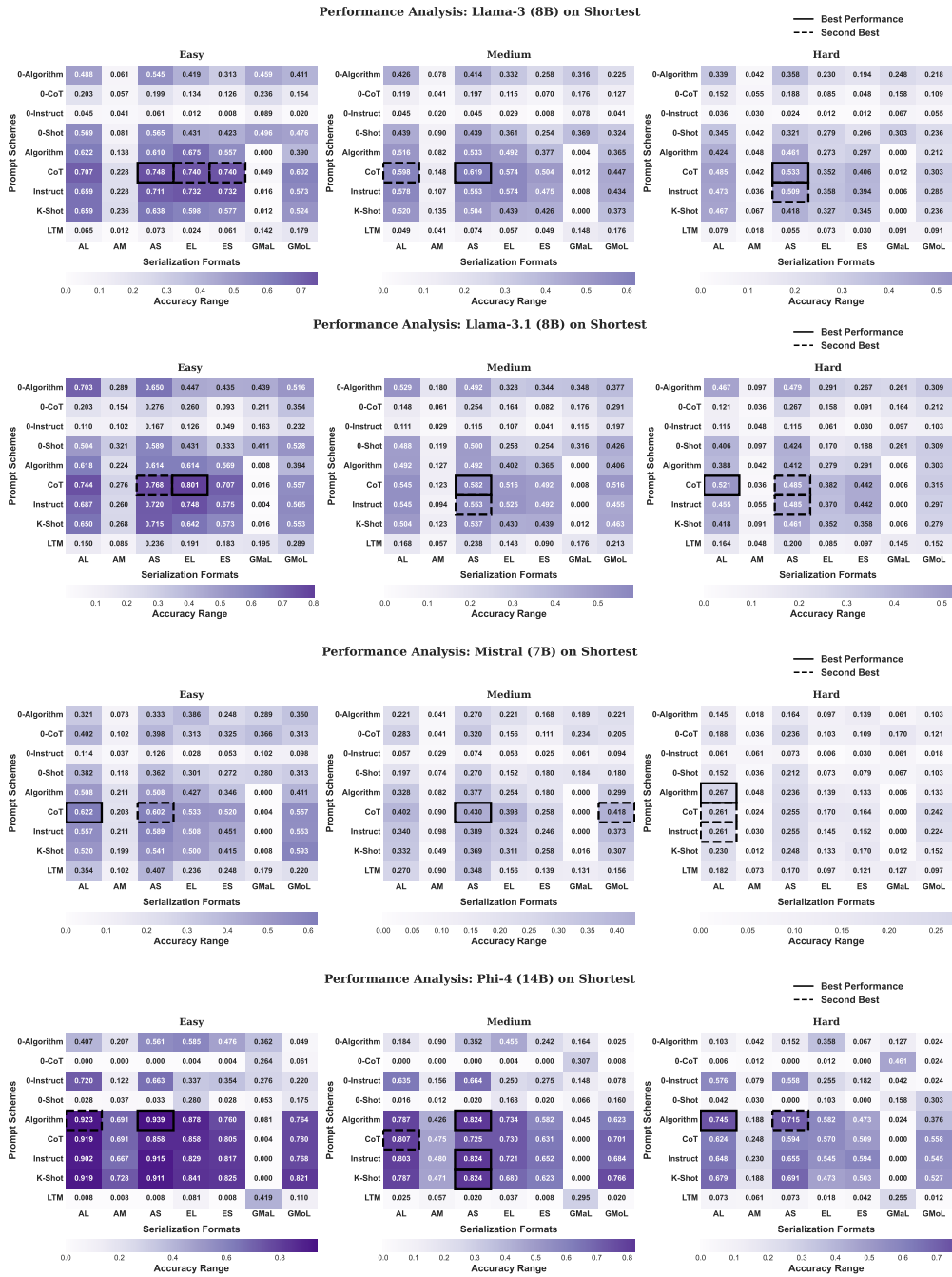
2916 E.2.5 HEATMAPS FOR Shortest path TASK
2917

2918 As shown in Figure 20 (featuring Claude-3.5, GPT-4o, GPT-4o-mini, Gemini-2.0), Figure 21 (featuring
2919 Llama-3 (8B), Llama-3.1 (8B), Mistral (7B), Phi-4 (14B)), Figure 22 (featuring Qwen-2.5 (7B),
2920 o4-mini), the heatmaps compare different prompt strategies and graph serialization formats under
2921 easy, medium, and hard difficulties for the Shortest path task. The color intensity encodes accuracy
2922 (darker = higher), and solid/dashed boxes highlight best/second-best combinations, respectively.



2967 Figure 20: Performance heatmaps for prompt strategies and serialization formats on the Shortest task
2968 (Part 1). Models: Claude-3.5, GPT-4o, GPT-4o-mini, Gemini-2.0.
2969

2970
2971
2972
2973
2974
2975
2976



3018 Figure 21: Performance heatmaps for prompt strategies and serialization formats on the Shortest task
3019 (Part 2). Models: Llama-3 (8B), Llama-3.1 (8B), Mistral (7B), Phi-4 (14B).

3020
3021
3022
3023

3024

3025

3026

3027

3028

3029

3030

3031

3032

3033

3034

3035

3036

3037

3038

3039

3040

3041

3042

3043

3044

3045

3046

3047

3048

3049

3050

3051

3052

3053

3054

3055

3056

3057

3058

3059

3060

3061

3062

3063

3064

3065

3066

3067

3068

3069

3070

3071

3072

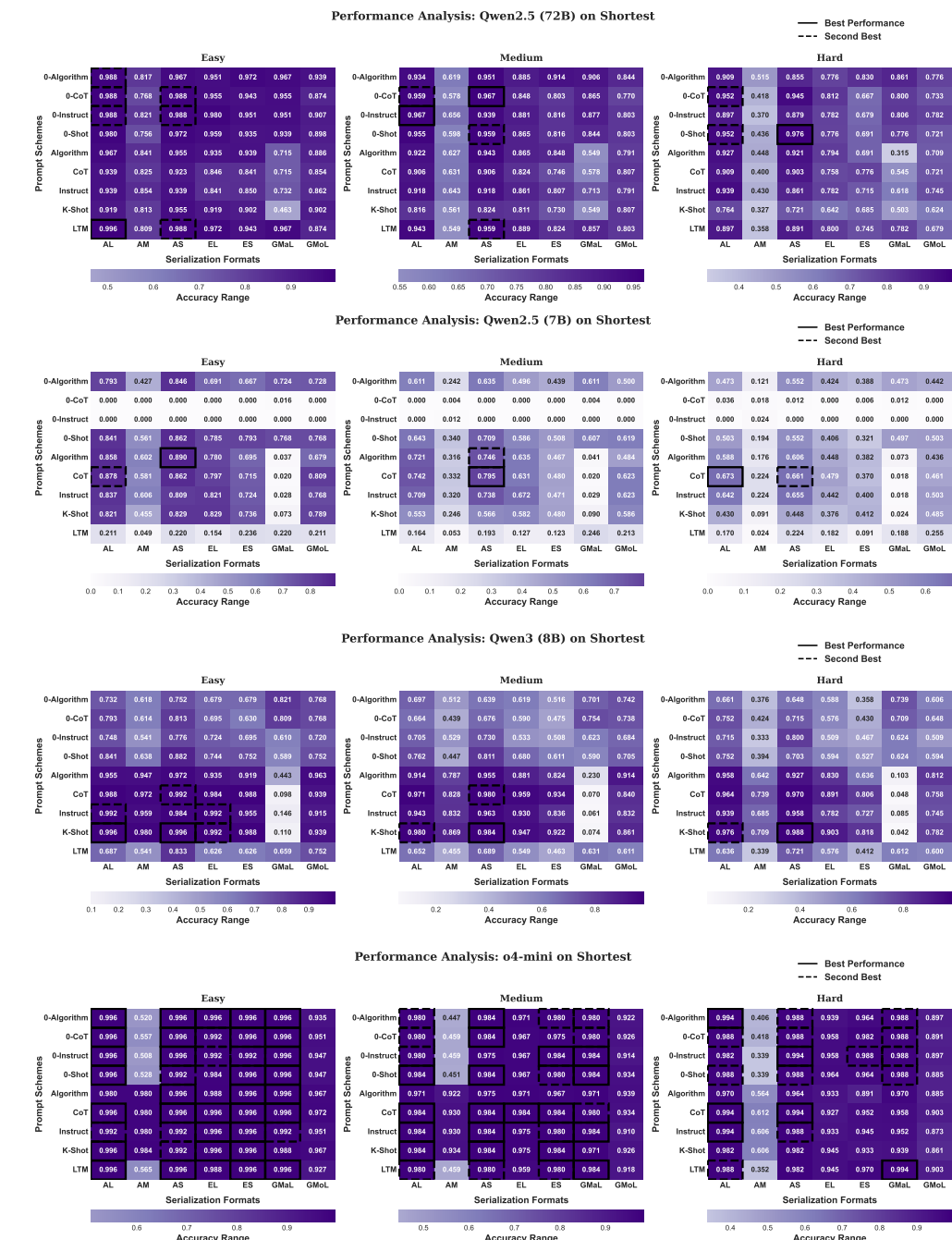
3073

3074

3075

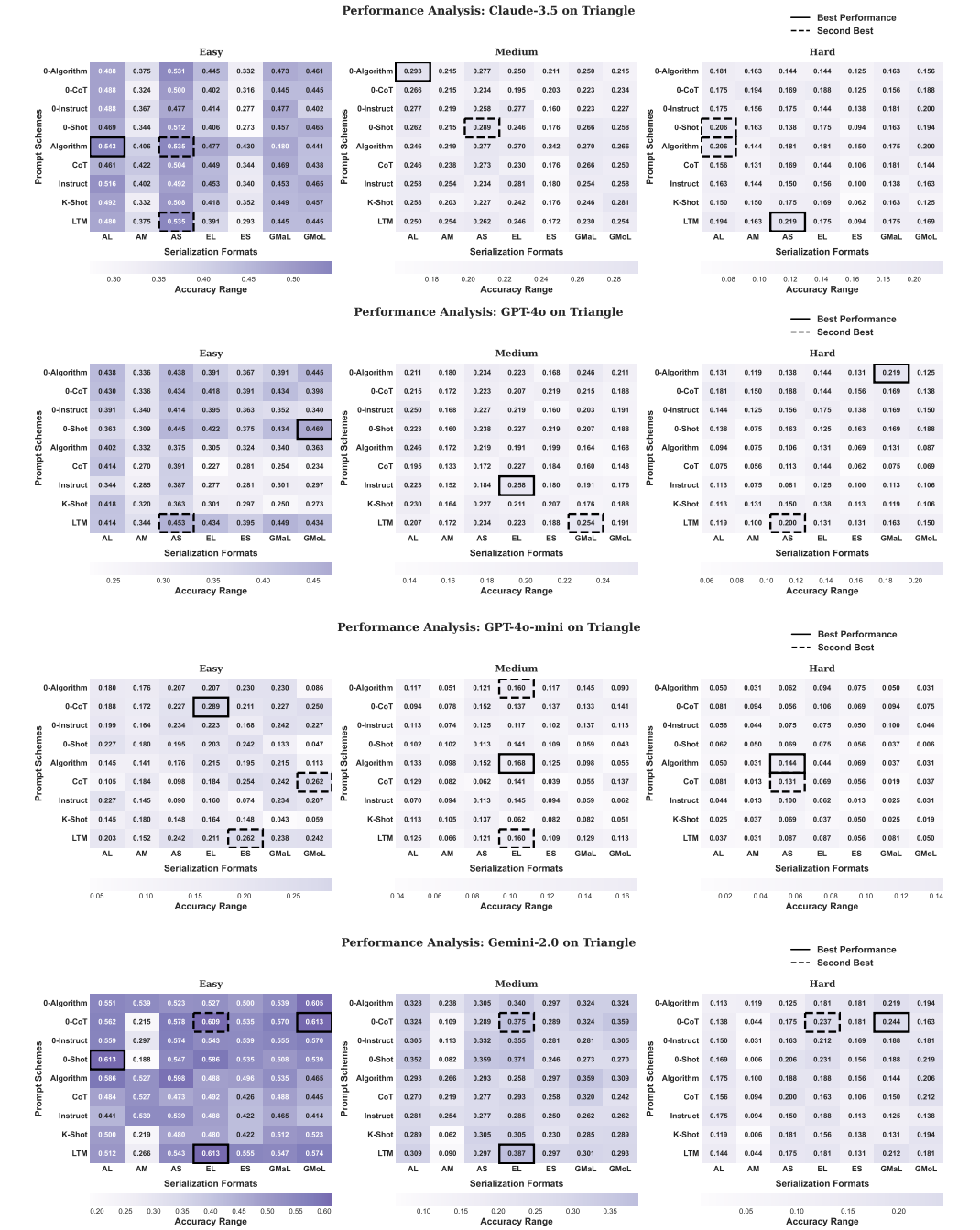
3076

3077



3078 E.2.6 HEATMAPS FOR Triangle counting TASK
3079

3080 As shown in Figure 23 (featuring Claude-3.5, GPT-4o, GPT-4o-mini, Gemini-2.0) , Figure 24
3081 (featuring Llama-3 (8B), Llama-3.1 (8B), Mistral (7B), Phi-4 (14B)), Figure 25 (featuring Qwen-2.5
3082 (7B), o4-mini), the heatmaps compare different prompt strategies and graph serialization formats
3083 under easy, medium, and hard difficulties for the Triangle counting task. The color intensity
3084 encodes accuracy (darker = higher), and solid/dashed boxes highlight best/second-best combinations
3085 respectively.



3130 Figure 23: Performance heatmaps for prompt strategies and serialization formats on the Triangle task
3131 (Part 1). Models: Claude-3.5, GPT-4o, GPT-4o-mini, Gemini-2.0.

3132

3133

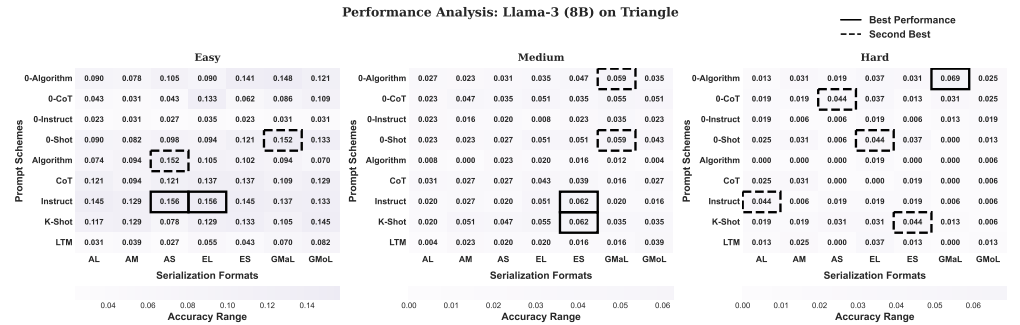
3134

3135

3136

3137

3138



3139

3140

3141

3142

3143

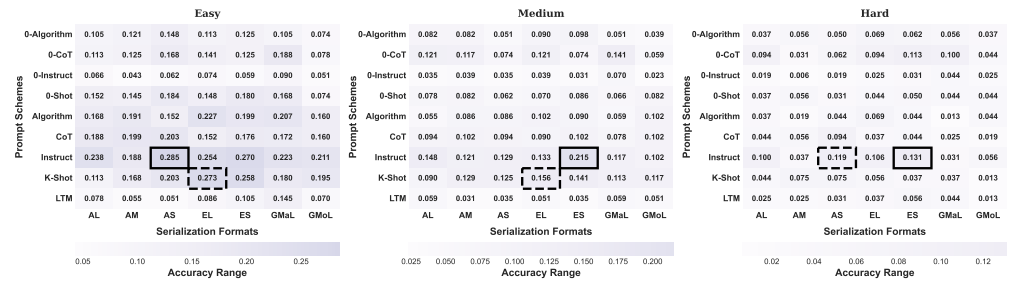
3144

3145

3146

3147

3148



3149

3150

3151

3152

3153

3154

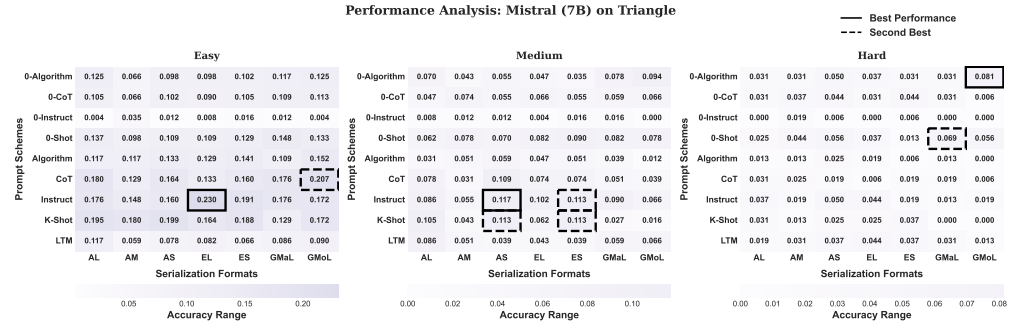
3155

3156

3157

3158

3159



3160

3161

3162

3163

3164

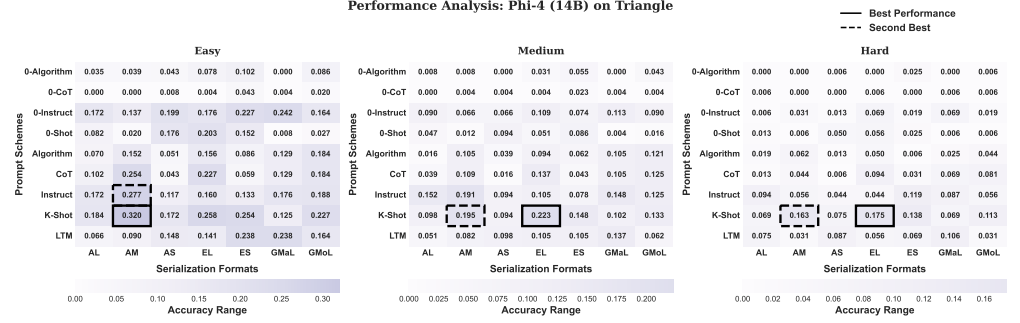
3165

3166

3167

3168

3169



3170

3171

3172

3173

3174

3175

3176

3177

3178

3179

Figure 24: Performance heatmaps for prompt strategies and serialization formats on the Triangle task (Part 2). Models: Llama-3 (8B), Llama-3.1 (8B), Mistral (7B), Phi-4 (14B).

3186

3187

3188

3189

3190

3191

3192

3193

3194

3195

3196

3197

3198

3199

3200

3201

3202

3203

3204

3205

3206

3207

3208

3209

3210

3211

3212

3213

3214

3215

3216

3217

3218

3219

3220

3221

3222

3223

3224

3225

3226

3227

3228

3229

3230

3231

3232

3233

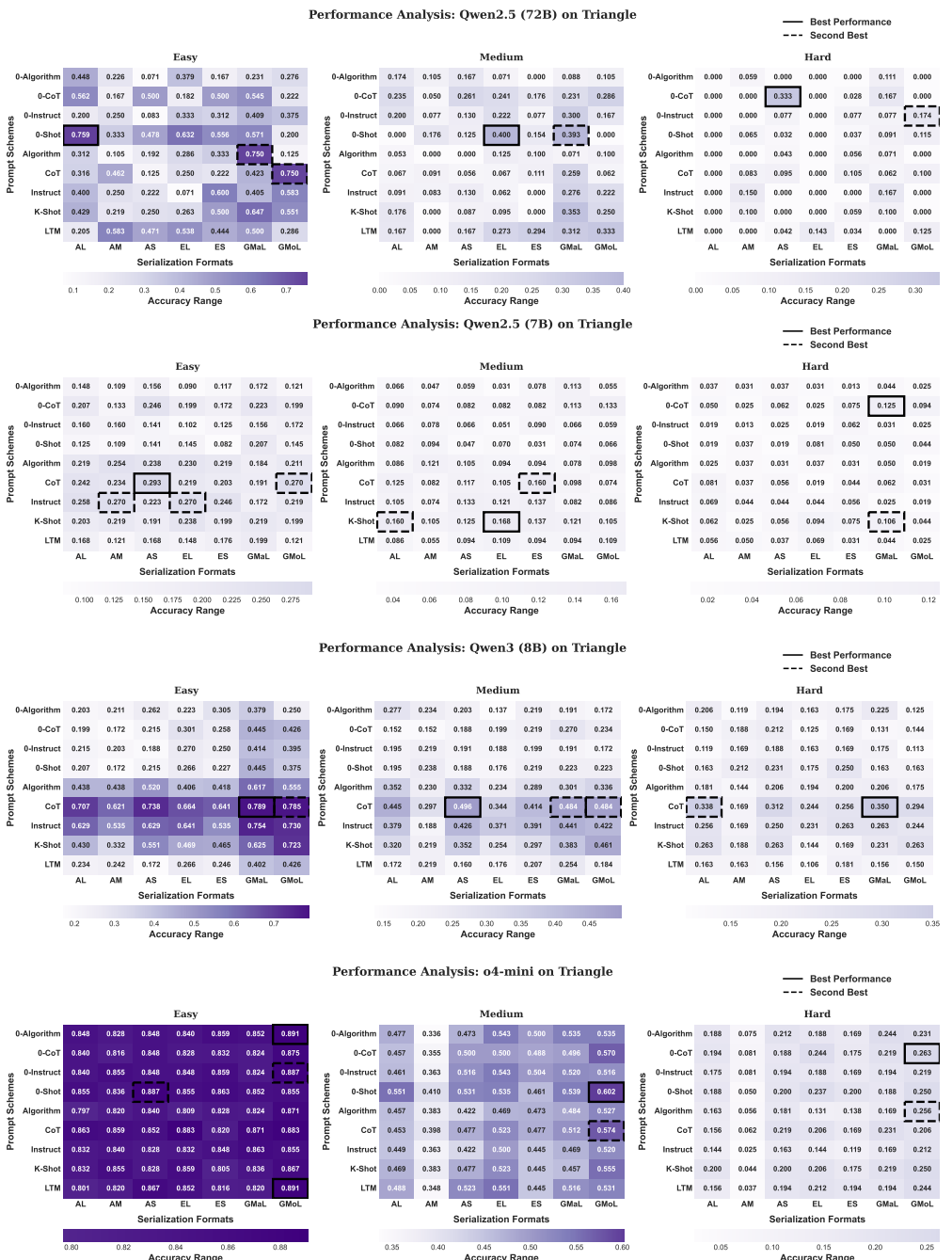


Figure 25: Performance heatmaps for prompt strategies and serialization formats on the Triangle task (Part 3). Models: Qwen-2.5 (72B), Qwen-2.5 (7B), Qwen-3 (8B), o4-mini.

3240 E.3 GRAPH TYPE SENSITIVITY ANALYSIS
3241

3242 While our main heatmaps analyze interactions between serialization formats and prompt schemes,
3243 the role of **graph types** in cross-factor analysis requires a different approach. Creating individual
3244 heatmaps for each graph type \times task \times difficulty combination would yield over 100+ visualizations,
3245 which would be comprehensive but impractical for interpretation. Instead, we introduce a sensitivity-
3246 based framework that quantifies how graph types respond to factor variations while maintaining both
3247 interpretability and extensibility.

3248 **Methodology.** For each graph type in a given task-difficulty setting, we compute two metrics by
3249 averaging across all models:

- 3250 • **Prompt Sensitivity (S_p):** For each serialization format, we calculate the standard deviation of
3251 accuracy across different prompt schemes, then average over all formats. This measures how much
3252 performance fluctuates when changing prompts.
- 3253 • **Format Sensitivity (S_f):** Symmetrically, for each prompt scheme, we calculate the standard
3254 deviation across serialization formats, then average over all prompts.

3255 We visualize each task-difficulty combination as a scatter plot in (S_p, S_f) space, where each bubble
3256 represents a graph type, and color encodes mean performance. Using median splits, we partition the
3257 space into four interpretable quadrants: *Robust* (low S_p , low S_f), *Prompt-Critical* (high S_p , low S_f),
3258 *Format-Critical* (low S_p , high S_f), and *Both Critical* (high S_p , high S_f).

3259 **Key Findings:** Figures 26–31 present plots covering all task-difficulty combinations. Based on the
3260 analysis of these data, we arrive at the following insights.
3261

- 3262 1. **Open-source models are much more prompt-sensitive than closed-source ones.** Across
3263 different tasks, the prompt sensitivity range of open-source models is consistently larger
3264 than that of closed-source models. For example, in the BFS order – Medium setting, the
3265 prompt sensitivity typically falls between 0.12 and 0.16, whereas that of open-source models
3266 ranges only from 0.02 to 0.05. This indicates that closed-source models rely more heavily
3267 on using an appropriate serialization format to achieve strong performance.
- 3268 2. **Closed-source models are more sensitive to serialization format than open-source
3269 models.** Across tasks, the format sensitivity range of closed-source models is generally
3270 higher. For instance, in the Diameter calculation – Easy setting, format sensitivity
3271 falls between 0.03 and 0.06, whereas open-source models range from 0.15 to 0.19. This
3272 suggests that open-source models depend more on advanced prompt-engineering strategies
3273 to improve performance, while closed-source models gain more from suitable serialization
3274 formatting.

3275 Notably, the difference in sensitivity between open-source and closed-source models can be explained
3276 by how LLMs typically process graph reasoning tasks, which can be viewed as involving two stages:
3277 (i) understanding the task itself, and (ii) interpreting the graph-structured input. Closed-source models,
3278 due to their stronger reasoning capabilities, encounter fewer difficulties in task understanding; as a
3279 result, they are more sensitive to the information contained in the graph data—i.e., the serialization
3280 format. In contrast, task understanding plays a more significant role for open-source models, and
3281 prompts exert a more direct influence on this stage than serialization formatting, leading to their
3282 higher prompt sensitivity. This interpretation is also consistent with our earlier finding—Finding
3283 3: Open-source models benefit from multi-shot exemplars, whereas closed-source models do not.
3284 Closed-source models do not require additional exemplars to grasp the task, whereas open-source
3285 models rely more on examples to enhance task comprehension.

3286 **Extensibility.** This framework directly supports GraphOmni’s extensible design. When adding new
3287 graph families (e.g., real-world networks), researchers can apply the same analytical pipeline to
3288 assess sensitivity profiles before conducting full evaluations. Complete implementation details and
3289 visualization scripts are available in our code repository.

3290
3291
3292
3293

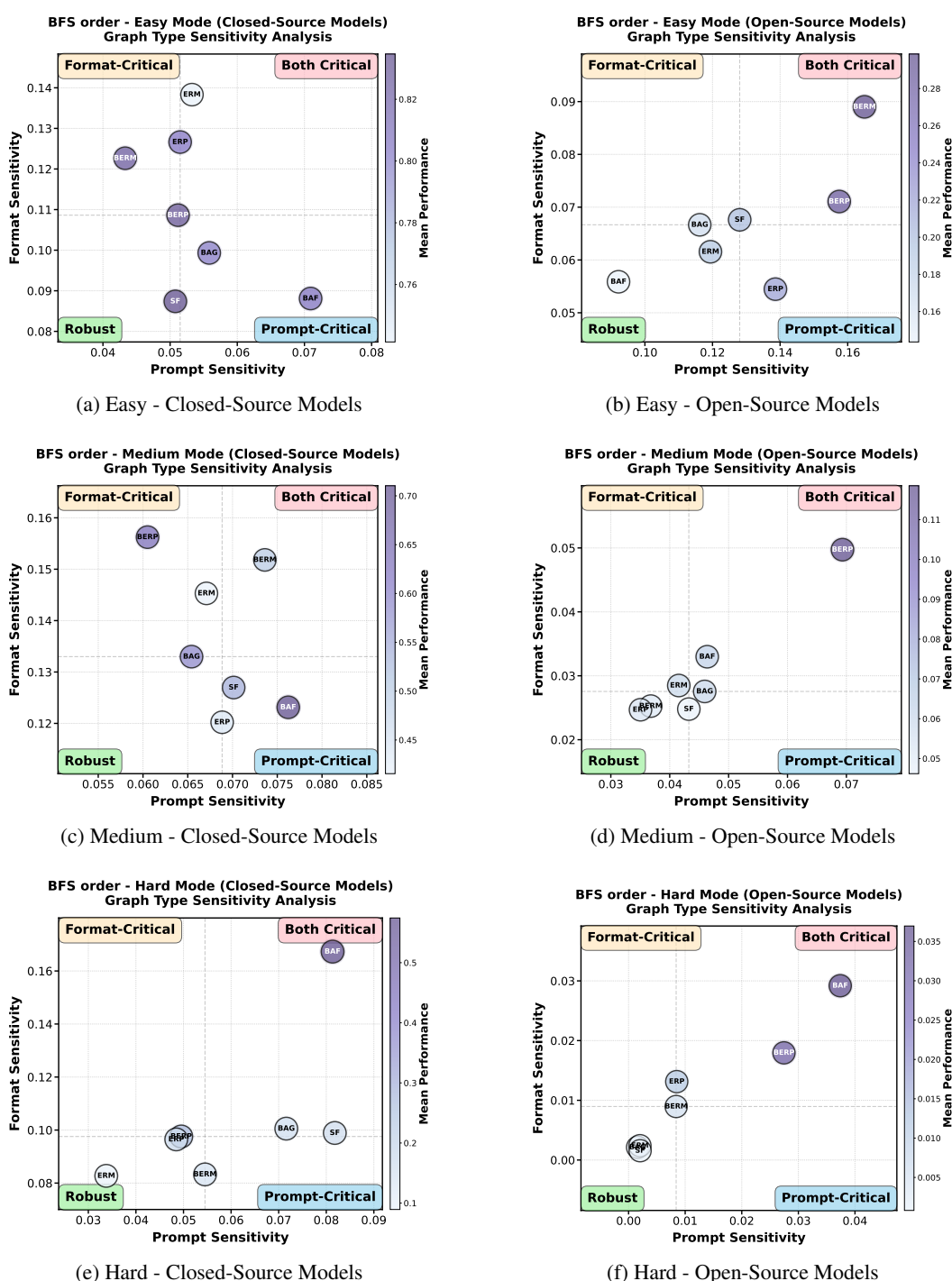


Figure 26: Graph type sensitivity analysis for BFS order task, comparing open-source and closed-source models. This comparison reveals whether sensitivity patterns are consistent across model categories.

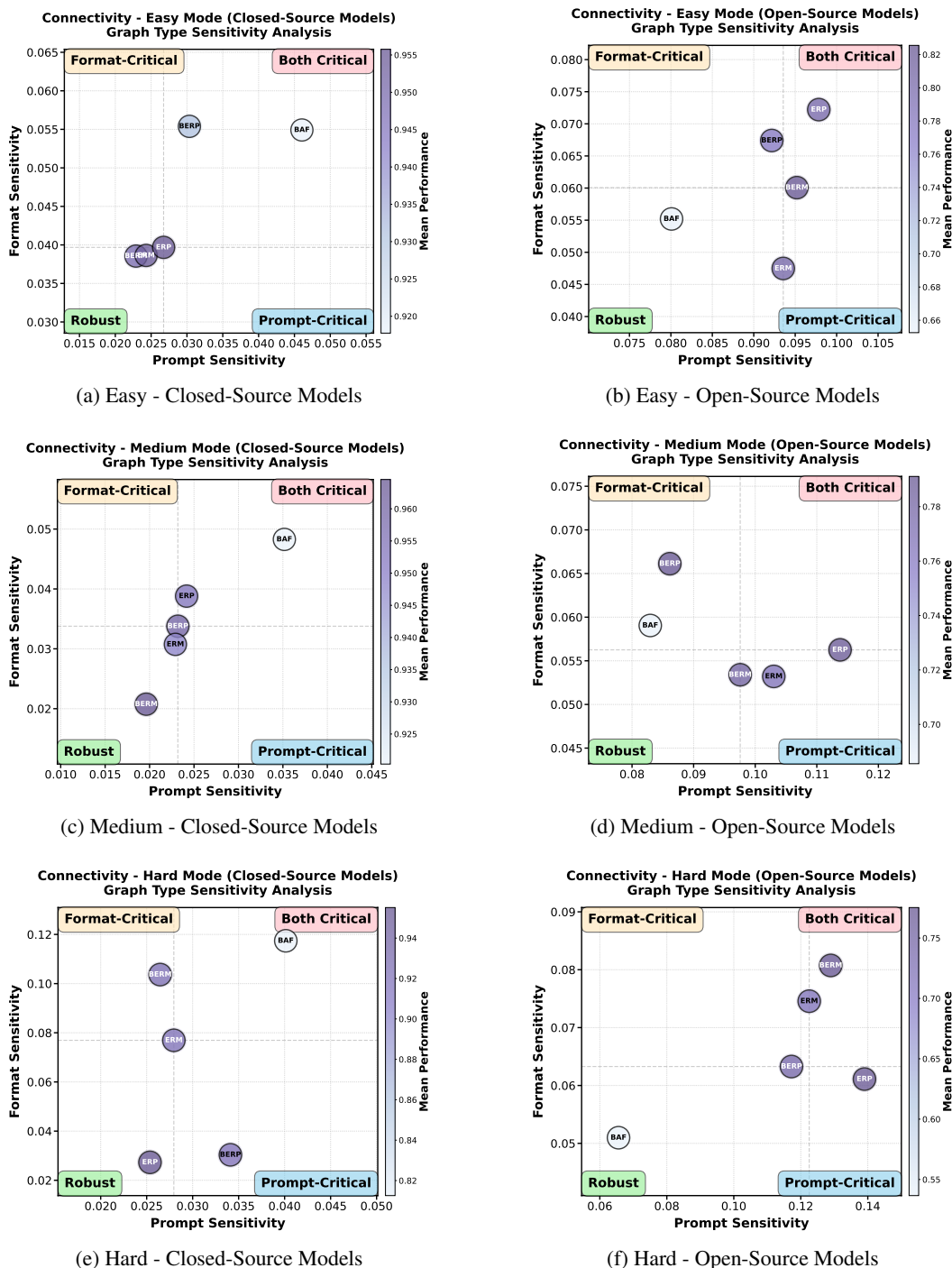


Figure 27: Graph type sensitivity analysis for Connectivity task, comparing open-source and closed-source models. This comparison reveals whether sensitivity patterns are consistent across model categories.

3402

3403

3404

3405

3406

3407

3408

3409

3410

3411

3412

3413

3414

3415

3416

3417

3418

3419

3420

3421

3422

3423

3424

3425

3426

3427

3428

3429

3430

3431

3432

3433

3434

3435

3436

3437

3438

3439

3440

3441

3442

3443

3444

3445

3446

3447

3448

3449

3450

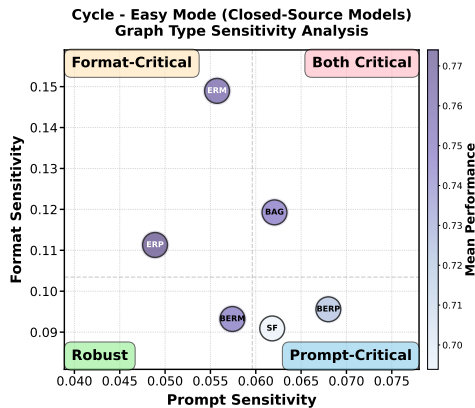
3451

3452

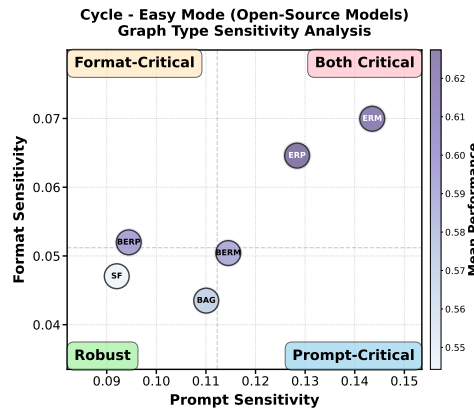
3453

3454

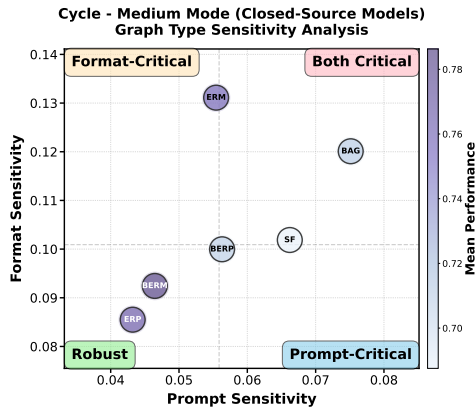
3455



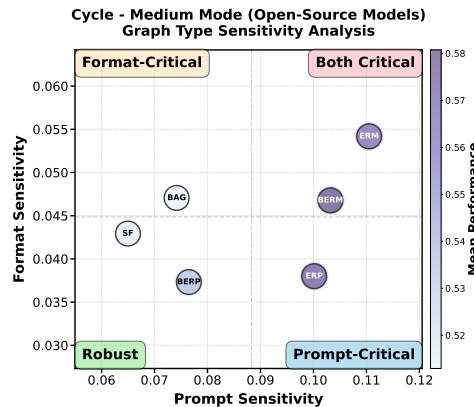
(a) Easy - Closed-Source Models



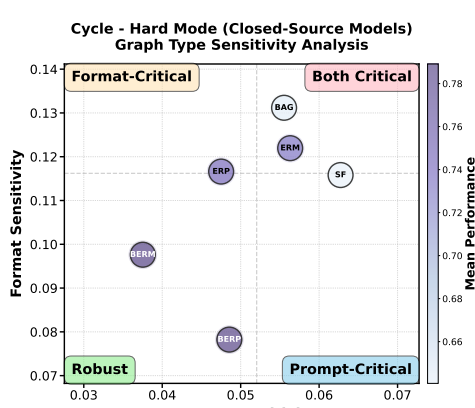
(b) Easy - Open-Source Models



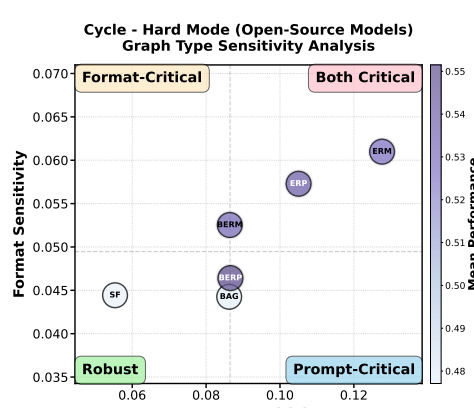
(c) Medium - Closed-Source Models



(d) Medium - Open-Source Models



(e) Hard - Closed-Source Models



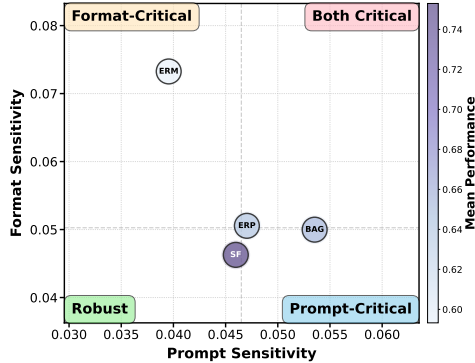
(f) Hard - Open-Source Models

Figure 28: Graph type sensitivity analysis for Cycle task, comparing open-source and closed-source models. This comparison reveals whether sensitivity patterns are consistent across model categories.

3456

3457

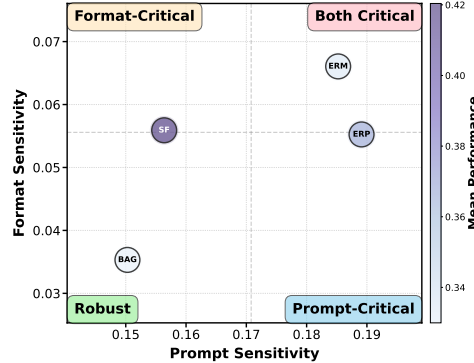
3458

3459 **Diameter - Easy Mode (Closed-Source Models)**
3460 **Graph Type Sensitivity Analysis**

3461 (a) Easy - Closed-Source Models

3462

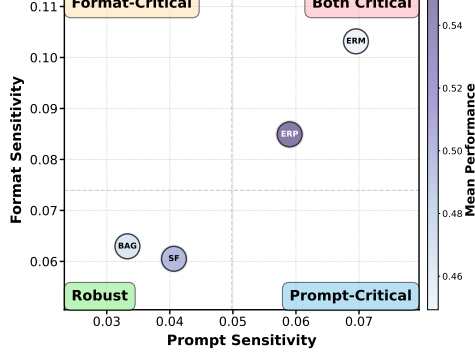
3463

3464 **Diameter - Easy Mode (Open-Source Models)**
3465 **Graph Type Sensitivity Analysis**3466 **Diameter - Easy Mode (Open-Source Models)**
3467 **Graph Type Sensitivity Analysis**

3468 (b) Easy - Open-Source Models

3469

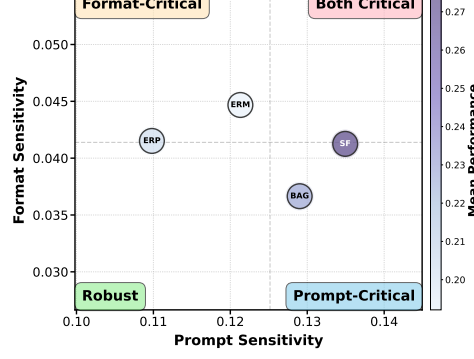
3470

3471 **Diameter - Medium Mode (Closed-Source Models)**
3472 **Graph Type Sensitivity Analysis**

3473 (c) Medium - Closed-Source Models

3474

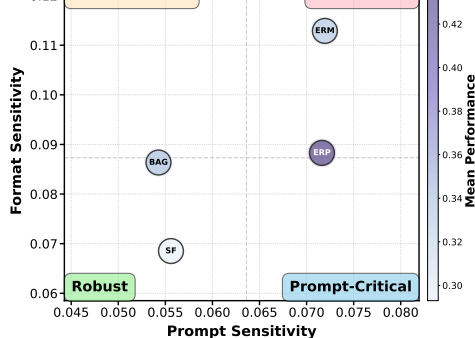
3475

3476 **Diameter - Medium Mode (Open-Source Models)**
3477 **Graph Type Sensitivity Analysis**3478 **Diameter - Medium Mode (Open-Source Models)**
3479 **Graph Type Sensitivity Analysis**

3480 (d) Medium - Open-Source Models

3481

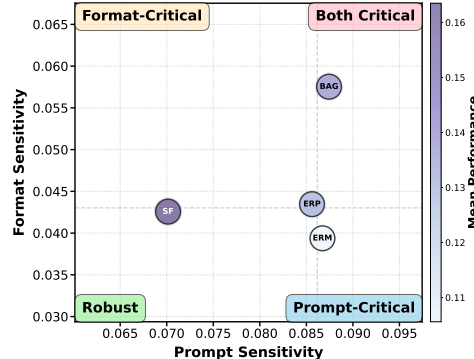
3482

3483 **Diameter - Hard Mode (Closed-Source Models)**
3484 **Graph Type Sensitivity Analysis**

3485 (e) Hard - Closed-Source Models

3486

3487

3488 **Diameter - Hard Mode (Open-Source Models)**
3489 **Graph Type Sensitivity Analysis**3490 **Diameter - Hard Mode (Open-Source Models)**
3491 **Graph Type Sensitivity Analysis**

3492 (f) Hard - Open-Source Models

3493

3494

3495

3496

3497

3498

3499

3500

3501

3502

3503

3504

3505

3506

3507

3508 **Figure 29: Graph type sensitivity analysis for Diameter task, comparing open-source and closed-source models. This comparison reveals whether sensitivity patterns are consistent across model categories.**

3509

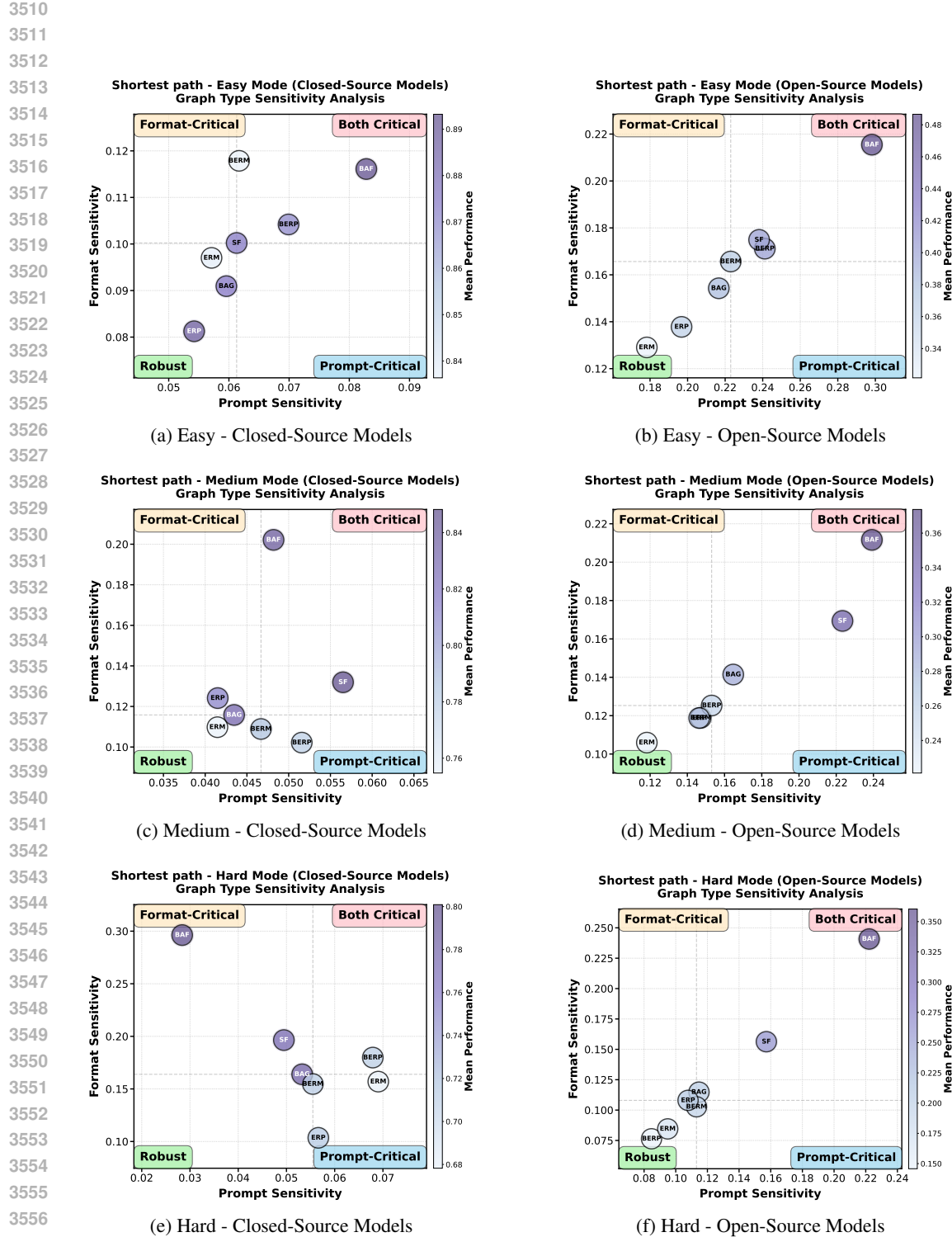
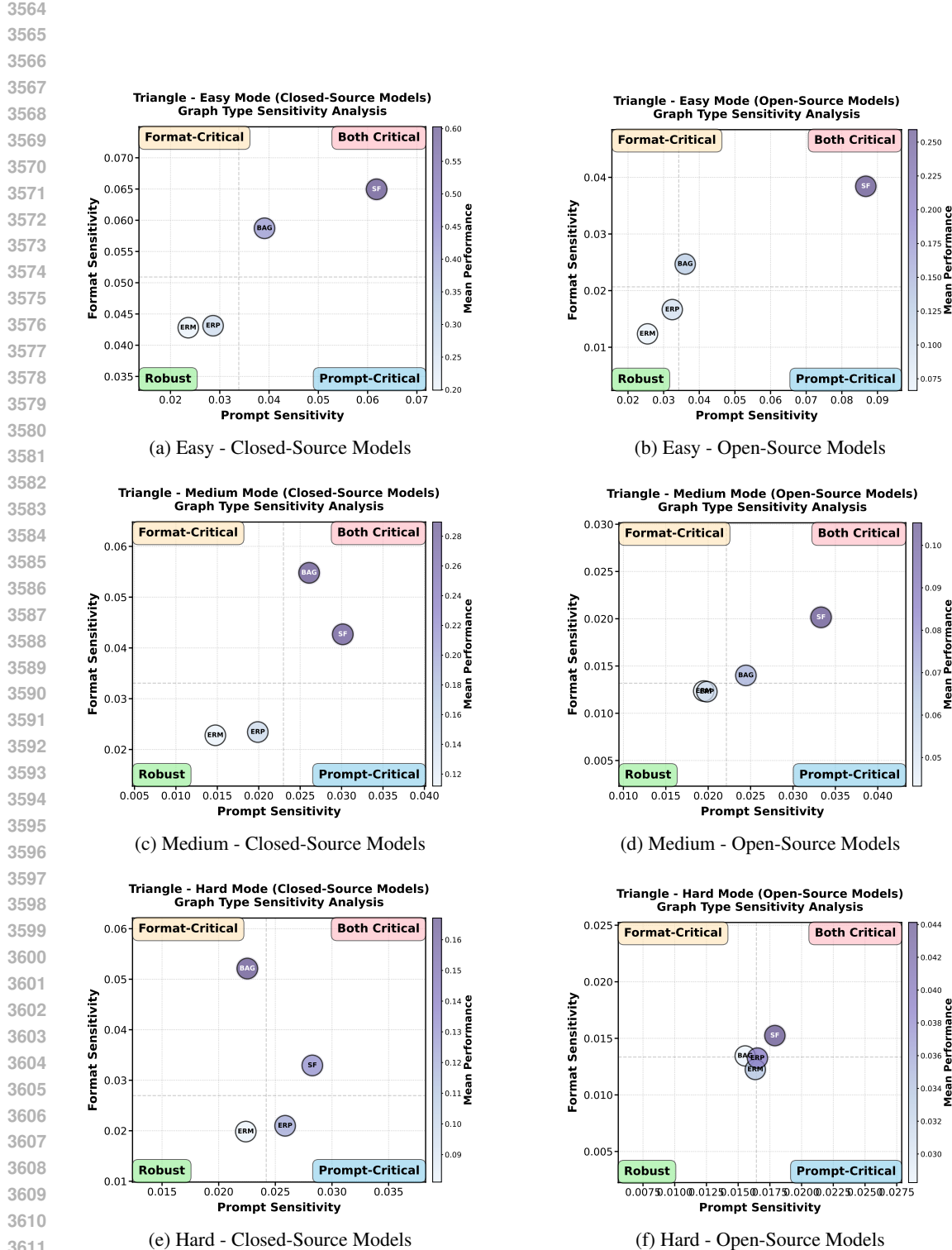


Figure 30: Graph type sensitivity analysis for Shortest path task, comparing open-source and closed-source models. This comparison reveals whether sensitivity patterns are consistent across model categories.



3618 E.4 ERROR ANALYSIS

3619

3620

3621

3622

3623

3624 This subsection presents an in-depth analysis of common error patterns observed in model responses.
 3625 We categorize representative error cases and provide concrete examples to illustrate the specific
 3626 challenges LLMs face in graph reasoning tasks. This detailed error analysis extends the brief
 3627 discussion of error categories presented in **Result ③** in Section 4.1.

3628

3629

3630

3631

3632

3633

3634

3635

3636

3637

3638

3639 E.4.1 Diameter calculation CASE 1

3640

3641

3642

3643

3644

3645

3646

3647

3648

3649

3650

3651

3652

3653

3654

3655

3656

3657

3658

3659

3660

3661

3662

3663

3664

3665

3666

3667

3668

3669

3670

3671

Diameter

- **QUERY:** Given a graph, your task is to determine the diameter of this graph. Graph: Adjacency Matrix is

```
[0 1 1 1 1 1 1 1 1]
[1 0 1 0 1 1 1 1 1]
[1 1 0 1 1 1 1 1 1]
[1 0 1 0 1 1 1 1 1]
[1 1 1 1 0 1 1 1 1]
[1 1 1 1 1 0 1 1 1]
[1 1 1 1 1 1 0 1 1]
[1 1 1 1 1 1 1 0 1]
[1 1 1 1 1 1 1 1 0]]
```

Q: What is the diameter of this graph?

A:

- **TASK INFO:** diameter,easy , 0-shot, Adjacency Matrix

- **GROUND TRUTH:** 2.0

- **MODEL:** Mistral

- **WRONG ANSWER:** the diameter of the given graph is 7.

explanation: to find the diameter of a graph, we first find the shortest path between every pair of vertices using a shortest path algorithm like dijkstra's or floyd-warshall. however, since the graph is unweighted, we can find the diameter by simply considering the longest path between any two vertices.

in this case, the longest path we can find is: - vertex 0 -> vertex 1 -> vertex 2 -> vertex 3 -> vertex 4 -> vertex 5 -> vertex 6 -> vertex 7 -> vertex 8

the number of edges in this path is $8 - 1 = 7$, so the diameter of the graph is 7.

- **ERROR CAUSE ANALYSIS:** This answer does not accurately define the concept of diameter. In the reasoning process, it mentions "first find the shortest path between every pair of vertices," which is correct. However, the final description refers to "the longest path," which can be misleading. In fact, the diameter is defined as the longest of all shortest paths rather than the longest path between any two vertices. Therefore, this explanation does not fully align with the formal definition of diameter.

3672 E.4.2 Diameter calculation CASE 2

3673

3674

3675

3676

3677

3678

3679

3680

3681

3682

3683

3684

3685

Diameter

- **QUERY:** Given a graph, your task is to determine the diameter of this graph. Graph: Adjacency List is {0: [1, 2, 3, 4, 5, 8, 10, 11, 13, 15], 1: [0, 2, 3, 4, 5, 6, 13, 15], 2: [0, 1, 3, 4, 5, 6, 7, 9, 12, 14], 3: [0, 1, 2, 4, 5, 7, 11, 13, 14], 4: [0, 1, 2, 3, 5, 6, 7, 8, 17], 5: [0, 1, 2, 3, 4, 8, 9], 6: [2, 1, 4, 9], 7: [2, 4, 3, 10, 14, 15, 16], 8: [5, 4, 0, 12, 16, 17], 9: [6, 2, 5, 10, 11, 12], 10: [0, 9, 7], 11: [3, 9, 0], 12: [2, 9, 8], 13: [3, 0, 1], 14: [2, 3, 7], 15: [7, 1, 0, 16], 16: [15, 7, 8, 17], 17: [16, 8, 4]}

Q: What is the diameter of this graph?

A: Let's break down this problem:

- **TASK INFO:** diameter, medium, LTM, Adjacency List
- **GROUND TRUTH:** 3.0
- **MODEL:** Qwen-3
- **WRONG ANSWER:**

To determine the **diameter** of a graph, we must identify the **longest shortest path** between any two nodes in the graph. This involves computing the **shortest path** between all pairs of nodes and then finding the **maximum** of these values.

—
Step 1: Understanding the Graph The graph is represented as an **adjacency list** with 18 nodes (0 through 17). The graph appears to be **connected**, which is essential for the diameter to be well-defined. We will use **Breadth-First Search (BFS)** from each node to compute the shortest paths to all other nodes.

—
Step 2: Strategy - For each node, perform BFS to find the shortest distances to all other nodes. - Keep track of the **maximum shortest distance** found across all node pairs. - The **maximum** of these distances is the **diameter**.

—
Step 3: Key Observations and Calculations Through careful inspection and BFS traversal, the **longest shortest path** was found to be between the following pairs of nodes:

- **Node 12 to Node 15:** Path: 12 → 9 → 5 → 0 → 15 (4 steps) Alternatively: 12 → 8 → 4 → 1 → 15 (4 steps)
- **Node 9 to Node 16:** Path: 9 → 2 → 4 → 8 → 16 (4 steps)
- **Node 12 to Node 15** and **Node 9 to Node 16** are two such pairs where the **shortest path** is exactly 4 steps.

Other pairs were found to have shorter distances (e.g., 2 or 3 steps). No pair was found to have a shortest path longer than 4 steps.

—
Final Result Since the **longest shortest path** in the graph is **4 steps**, the **diameter** of the graph is:

\$\$\{4\}\$\$

- **ERROR CAUSE ANALYSIS:** This result fails to find a shorter path because it ignores the two critical edges 7-15 and 7-16 in the graph. To 15 there is actually a 3-step shorter path: e.g., 12 → 2 → 7 → 15. For 9 to 16 there is a 3-step path: 9 → 10 → 7 → 16. Once these two edges are taken into account, it can be seen that no two points in the graph have a shortest path of more than 3 steps. These two edges into account, it follows that no two points in the graph have shorter paths than 3 steps. Therefore, the diameter of the graph is indeed 3, not 4.

3726 E.4.3 Connectivity CASE 1
 3727
 3728
 3729
 3730
 3731
 3732
 3733
 3734
 3735
 3736
 3737
 3738
 3739
 3740
 3741
 3742
 3743
 3744
 3745
 3746
 3747
 3748
 3749
 3750
 3751
 3752
 3753
 3754
 3755 Connectivity
 3756

- **QUERY:** Determine if there is a path between two nodes in the graph. Graph: Edge List is

3 1

4 2

5 4

6 5

7 5

3763 Q: Is there a path between node 1 and node 5?

3764 A:

3765 Let's break down this problem:

- **TASK INFO:** connectivity, easy, LTM, Edge List

- **MODEL:** Mistral

- **GROUND TRUTH:** False

- **WRONG ANSWER:**

3770 1. we have a graph with 7 nodes (1 to 7) and 6 edges.

3771 2. to find a path between two nodes, we can use depth-first search (dfs) or breadth-first search (bfs).
 3772 both algorithms will help us traverse the graph and find a path if one exists.

3773 3. in this case, we will use dfs because it is more efficient for sparse graphs like this one.

3774 4. we start at node 1. since there is an edge from node 1 to node 4, we visit node 4.

3775 5. from node 4, we find an edge to node 5, so we have found a path from node 1 to node 5.

3776 6. therefore, there is a path between nodes 1 and 5 in the graph.

3777 so the answer is: yes, there is a path between node 1 and node 5.

- **ERROR CAUSE ANALYSIS:** This answer misunderstands the EL serialization format. Although it correctly states the number of nodes and edges, it incorrectly assumes that there is an edge between nodes 1 and 4. This mistake leads to incorrect conclusions in the subsequent reasoning.

3780 E.4.4 Cycle detection CASE 1
 3781
 3782
 3783
 3784
 3785
 3786
 3787
 3788
 3789
 3790
 3791
 3792
 3793
 3794
 3795
 3796
 3797
 3798
 3799
 3800 **Cycle**
 3801 • **QUERY:** Given a graph representation, your task is determining whether the graph has a cycle Graph:
 3802 Adjacency List is
 3803 {0: [1, 2, 3, 4, 6], 1: [0, 9], 2: [0, 7, 8], 3: [0, 5], 4: [0], 5: [3], 6: [0], 7: [2], 8: [2], 9: [1]}
 3804 Q: Is there a cycle in this graph?
 3805 A:
 3806 Let's think step by step:
 3807 • **TASK INFO:** cycle, medium, 0-CoT, Adjacency List
 3808 • **MODEL:** claude-3-5-sonnet-20241022
 3809 • **GROUND TRUTH:** False
 3810 • **WRONG ANSWER:**
 3811 Let's analyze this graph to find if it contains any cycles:
 3812 1) First, let's understand the connections:
 3813 - Node 0 connects to 1,2,3,4,6
 3814 - Node 1 connects to 0,9
 3815 - Node 2 connects to 0,7,8
 3816 - Node 3 connects to 0,5
 3817 - Node 4 connects to 0
 3818 - Node 5 connects to 3
 3819 - Node 6 connects to 0
 3820 - Node 7 connects to 2
 3821 - Node 8 connects to 2
 3822 - Node 9 connects to 1
 3823 2) Looking at some paths:
 3824 - 0 → 1 → 0 (This is a cycle!)
 3825 - 0 → 2 → 0 (This is another cycle!)
 3826 - 0 → 3 → 0 (This is another cycle!)
 3827 3) The graph has multiple cycles. The simplest ones are between node 0 and its neighbors that have
 3828 return paths.
 3829 Yes, there are multiple cycles in this graph.
 3830 • **ERROR CAUSE ANALYSIS:** This answer misunderstands cycle detection in a graph. Although it
 3831 correctly lists the connections between nodes, it incorrectly assumes that a direct backtracking step
 3832 (e.g., 0 → 1 → 0) forms a cycle. In a graph, a valid cycle must involve at least three distinct nodes.
 3833 This mistake leads to incorrect conclusions about the presence of multiple cycles.

3834 E.4.5 Triangle counting CASE 1
 3835
 3836
 3837
 3838
 3839
 3840
 3841
 3842
 3843
 3844
 3845
 3846
 3847
 3848
 3849
 3850
 3851
 3852
 3853
 3854
 3855
 3856
 3857
 3858
 3859
 3860
 3861
 3862

Triangle

- **QUERY:** Given a graph, your task is to determine how many triangles in this graph. Graph: GraphML is `<?xml version='1.0' encoding='utf-8'?> <graphml xmlns="http://graphml.graphdrawing.org/xmlns" xmlns:xsi="http://www.w3.org/2001/XMLSchema-instance" xsi:schemaLocation="http://graphml.graphdrawing.org/xmlns http://graphml.graphdrawing.org/xmlns/1.0/graphml.xsd"><graph edgedefault="undirected"><node id="0"/><node id="1"/><node id="2"/>...`
- **QUERY:** Q: How many triangles are in this graph?
 A:
 - **TASK INFO:** triangle, hard, 0-shot, GraphML
 - **MODEL:** Mistral
 - **GROUND TRUTH:** 47
 - **WRONG ANSWER:** to find the number of triangles in a graph, we can use the formula for the number of triangles in a simple graph, which is given by $n / 3$, where n is the number of triples of distinct vertices that form a triangle. in this graph, we have 26 nodes, so we would calculate $26 / 3 = 8.66666666666667$, but since we cannot have a fraction of a triangle, we round down to 8. therefore, there are 8 triangles in this graph.
 - **ERROR CAUSE ANALYSIS:** This analysis misunderstands triangle counting in a graph. While it correctly identifies sets of three nodes, it incorrectly assumes that the number of triangles can be calculated as $n/3$. In a graph, a valid triangle requires all three nodes to be mutually connected. This mistake reflects a lack of proper understanding of the graph's topological structure

3888 E.4.6 Triangle counting CASE 2
 3889
 3890
 3891
 3892
 3893
 3894
 3895
 3896
 3897
 3898
 3899
 3900
 3901
 3902
 3903
 3904
 3905
 3906

Triangle

- **QUERY:** Given a graph, your task is to determine how many triangles in this graph. Graph: Adjacency List is {1: [0], 0: [1, 2, 3, 6], 2: [0, 7], 3: [0, 4, 5, 6], 4: [3, 6], 5: [3], 6: [0, 3, 4, 8], 7: [2], 8: [6]}
 Q: How many triangles are in this graph?
 A:
- **TASK INFO:** triangle, easy, 0-shot, Adjacency List
- **MODEL:** Qwen-2.5
- **GROUND TRUTH:** 2
- **WRONG ANSWER:**
 to determine the number of triangles in the graph, we need to find sets of three vertices where each pair of vertices is connected by an edge. given the adjacency list, we can go through each vertex and check all possible combinations of its neighbors to see if they form a triangle.
 here's the adjacency list for reference: `` 1: [0], 0: [1, 2, 3, 6], 2: [0, 7], 3: [0, 4, 5, 6], 4: [3, 6], 5: [3], 6: [0, 3, 4, 8], 7: [2], 8: [6] ``
 let's go through the vertices and their neighbors to find triangles:
 1. **vertex 0:** - neighbors: [1, 2, 3, 6] - check combinations: - (1, 2): not connected - (1, 3): not connected - (1, 6): not connected - (2, 3): not connected - (2, 6): not connected - (3, 6): yes, connected (forms triangle (0, 3, 6))
 2. **vertex 1:** - neighbors: [0] - only one neighbor, so no triangles.
 3. **vertex 2:** - neighbors: [0, 7] - check combinations: - (0, 7): yes, connected (forms triangle (0, 2, 7))
 4. **vertex 3:** - neighbors: [0, 4, 5, 6] - check combinations: - (0, 4): yes, connected (forms triangle (0, 3, 4)) - (0, 5): not connected - (0, 6): yes, connected (forms triangle (0, 3, 6)) - (4, 5): not connected - (4, 6): yes, connected (forms triangle (3, 4, 6)) - (5, 6): not connected
 5. **vertex 4:** - neighbors: [3, 6] - check combinations: - (3, 6): yes, connected (forms triangle (3, 4, 6))
 6. **vertex 5:** - neighbors: [3] - only one neighbor, so no triangles.
 7. **vertex 6:** - neighbors: [0, 3, 4, 8] - check combinations: - (0, 3): yes, connected (forms triangle (0, 3, 6)) - (0, 4): yes, connected (forms triangle (3, 4, 6)) - (0, 8): not connected - (3, 4): yes, connected (forms triangle (3, 4, 6)) - (3, 8): not connected - (4, 8): not connected
 8. **vertex 7:** - neighbors: [2] - only one neighbor, so no triangles.
 9. **vertex 8:** - neighbors: [6] - only one neighbor, so no triangles.
 summarizing the triangles found: - (0, 3, 6) - (0, 2, 7) - (0, 3, 4) - (3, 4, 6)
 thus, the number of triangles in the graph is **4**.
- **ERROR CAUSE ANALYSIS:** The understanding of the serialization format is incorrect in this answer. Even though it successfully prints out the AL serialization format, in its reasoning process, it incorrectly assumes that node 7 and node 0 are connected, and that node 4 and node 0 are connected, which ultimately leads to an incorrect result.

3942 E.4.7 BFS order CASE 1

3943

3944

3945

3946

3947

3948

3949

3950

3951

3952

3953

3954

3955

3956

3957

3958

3959

3960

3961

3962

3963

3964

3965

3966

3967

3968

3969

3970

3971

3972

3973

3974

3975

3976

3977

3978

3979

3980

3981

3982

3983

3984

3985

3986

3987

3988

3989

3990

3991

3992

3993

3994

3995

BFS order

- **QUERY:** Given a graph, your task is to determine the bfs traversal order of this graph starting at node 2. And the graph representation of: Adjacency Matrix is

```
[[0 1 1 1 1 0 1]
 [1 0 1 1 1 1 1]
 [1 1 0 0 0 0 0]
 [1 1 0 0 0 1 0]
 [1 1 0 0 0 0 0]
 [0 1 0 1 0 0 0]
 [1 1 0 0 0 0 0]]
```

Q: Give the bfs traversal order starting from node 2.

A:

- **TASK INFO:** bfsorder, easy, 0-shot, Adjacency Matrix

- **MODEL:** Qwen-2.5

- **STARTING NODE:** 2

- **WRONG ANSWER:**

to determine the bfs traversal order starting from node 2, we follow these steps:

1. ****initialize**:** start with node 2. add it to the queue and mark it as visited.

2. ****process the queue**:** remove the first node from the queue and visit it. then, add its unvisited neighbors to the queue.

3. ****repeat**:** continue the process until the queue is empty.

given the adjacency matrix:

```
\bmatrix
 0 & 1 & 1 & 1 & 1 & 0 & 1 \\
 1 & 0 & 1 & 1 & 1 & 1 & 1 \\
 1 & 1 & 0 & 0 & 0 & 0 & 0 \\
 1 & 1 & 0 & 0 & 0 & 1 & 0 \\
 1 & 1 & 0 & 0 & 0 & 0 & 0 \\
 0 & 1 & 1 & 0 & 1 & 0 & 0 \\
 1 & 1 & 0 & 0 & 0 & 0 & 0
\end{bmatrix}
```

]

let's perform the bfs:

1. ****start at node 2**:** - queue: [2] - visited: [2]

2. ****dequeue node 2**:** - visit node 2 - add its unvisited neighbors (nodes 1, 3, 4, 6) to the queue. - queue: [1, 3, 4, 6] - visited: [2, 1, 3, 4, 6]

3. ****dequeue node 1**:** - visit node 1 - add its unvisited neighbors (nodes 2, 3, 4, 5, 6) to the queue. nodes 2 and 6 are already visited. - queue: [3, 4, 5, 6] - visited: [2, 1, 3, 4, 5, 6]

4. ****dequeue node 3**:** - visit node 3 - add its unvisited neighbors (nodes 2, 1) to the queue. nodes 2 and 1 are already visited. - queue: [4, 5, 6] - visited: [2, 1, 3, 4, 5, 6]

5. ****dequeue node 4**:** - visit node 4 - add its unvisited neighbors (nodes 2, 3, 6) to the queue. nodes 2, 3, and 6 are already visited. - queue: [5, 6] - visited: [2, 1, 3, 4, 5, 6]

6. ****dequeue node 5**:** - visit node 5 - add its unvisited neighbors (nodes 1, 4) to the queue. nodes 1 and 4 are already visited. - queue: [6] - visited: [2, 1, 3, 4, 5, 6]

7. ****dequeue node 6**:** - visit node 6 - add its unvisited neighbors (nodes 2, 4) to the queue. nodes 2 and 4 are already visited. - queue: [] - visited: [2, 1, 3, 4, 5, 6]

the bfs traversal order starting from node 2 is: **2, 1, 3, 4, 5, 6**. note that the order of visiting

- **ERROR CAUSE ANALYSIS:** The understanding of the serialization format is incorrect in this answer. Even though it successfully prints out the AM serialization format, in its reasoning process, it incorrectly assumes that node 2 and node 0 do not have connectivity, which ultimately leads to an incorrect result.

3996 E.4.8 Triangle counting CASE 3

3997

3998

3999

4000

4001 Triangle

4002 • **QUERY:** Given a graph, your task is to determine how many triangles this graph.

4003 And the graph representation of Edge Set is :

4004 $\{(0, 1), (1, 2), (0, 4), (0, 3), (1, 8), (0, 6), (0, 2), (2, 5), (4, 7)\}$

4005 Q: How many triangles are in this graph?

4006 A: The graph contains 3 nodes that form a triangle (0, 1, and 2), resulting in 1 triangle. So the number
4007 of triangles is 1.

4008 Given a graph, your task is to determine how many triangles this graph.

4009 And the graph representation of Edge Set is :

4010 $\{(0, 1), (0, 7), (0, 4), (1, 5), (0, 3), (2, 3), (0, 2), (2, 6), (0, 5)\}$

4011 Q: How many triangles are in this graph?

4012 A: This graph includes edges that connect nodes to form two distinct triangles, namely (0, 1, 5) and (0,
4013 2, 3). The graph contains two triangles: (0, 1, 5) and (0, 2, 3). So the number of triangles is 2.

4014 Given a graph, your task is to determine how many triangles this graph.

4015 And the graph representation of Edge Set is :

4016 $\{(0, 1), (3, 4), (2, 7), (1, 4), (0, 2), (5, 6), (3, 6), (2, 5), (1, 3)\}$

4017 Q: How many triangles are in this graph?

4018 A: A graph with edges forming a single triangle: (4, 1, 3). The graph contains one triangle, formed by
nodes (4, 1, 3). So the number of triangles is 1.

4019 Given a graph, your task is to determine how many triangles this graph.

4020 And the graph representation of Edge Set is :

4021 $\{(4, 3), (1, 5), (4, 6), (4, 2), (3, 0), (0, 6), (4, 5), (0, 2), (3, 6), (1, 0)\}$

4022 Q: How many triangles are in this graph?

4023 A: The edges in this graph create two triangles: (0, 3, 6) and (3, 6, 4). The graph contains two triangles:
(0, 3, 6) and (3, 6, 4). So the number of triangles is 2.

4024 Given a graph, your task is to determine how many triangles this graph.

4025 And the graph representation of Edge Set is :

4026 $\{(3, 4), (5, 1), (5, 7), (0, 2), (8, 3), (0, 5), (0, 8), (2, 5), (1, 3), (7, 4), (6, 8), (5, 6), (5, 3), (0, 7), (2, 4), (2,
4027 1), (2, 7), (6, 1), (6, 7), (5, 8), (8, 1), (1, 4), (0, 6), (2, 3), (6, 3)\}$

4028 Q: How many triangles are in this graph?

4029 A: A dense graph with many edges, resulting in 26 distinct triangles formed by various combinations of
nodes. The graph contains 26 triangles formed by various combinations of nodes. So the number of
4030 triangles is 26.

4031 Given a graph, your task is to determine how many triangles in this graph.

4032 Graph: Edge Set is

4033 $\{(4, 3), (5, 1), (5, 7), (8, 3), (8, 6), (2, 5), (7, 4), (6, 5), (5, 0), (8, 2), (0, 1), (2, 4), (2, 7), (6, 1), (7, 3), (6,
4034 7), (8, 1), (8, 7), (0, 3), (2, 0), (1, 4), (2, 6), (6, 3)\}$

4035 Q: How many triangles are in this graph?

4036 A:

4037 • **TASK INFO:**

4038 triangle, easy, CoT, Edge Set

4039 • **GROUND TRUTH:** 164040 • **MODEL:** o4-mini4041 • **WRONG ANSWER:**4042 To count triangles, list each triple i,j,k with $i < j < k$ and check all three edges. Doing so yields these 17
4043 distinct triangles:4044 $(0,1,5), (0,2,3), (0,2,5), (1,5,6), (1,6,8), (2,4,7), (2,5,6), (2,5,7), (2,6,7), (2,6,8), (2,7,8), (3,4,7), (3,6,7),$
 $(3,6,8), (3,7,8), (5,6,7), (6,7,8).$

4045 So the number of triangles is 17.

4046 • **ERROR CAUSE ANALYSIS:** This answer misinterprets the connectivity of node 2 and node 3 and ends
4047 up thinking that 0, 2, 3 forms a triangle, leading to a final error.

4050 E.5 INPUT/OUTPUT EXAMPLES

4051

4052

4053

4054

4055

4056

4057

4058 We show more model input and output examples here. **Query** is the input to the model and **Answer**
4059 is the model output. Due to space reasons, in the middle of the excessively long part we will use "...".
4060 Each of the following examples is randomly selected from the query.

4061

4062

4063

4064

4065

4066

4067

4068

4069

4070

4071

4072

4073

4074

4075

4076

Connectivity

4077 • **QUERY:** Determine if there is a path between two nodes in the graph.4078 Graph: Edge Set is $\{(6, 18), (7, 26), (3, 22), (5, 19), (9, 17), (9, 26), (0, 23), (1, 15), (6, 11),$
4079 $(7, 10), (6, 20), (7, 19), (5, 12), (8, 11), (9, 10), (3, 24), (9, 19), (1, 17), (6, 13), (7, 12), (7,$
4080 $21), (3, 17), (9, 12), (3, 26), (5, 23), (9, 21), (8, 25), (3, 19), (5, 16), (4, 18), (9, 14), (5, 25),$
4081 $(1, 21), (4, 11), (5, 18), (9, 16), (8, 20), (1, 14), (2, 13), (1, 23), (2, 22), (3, 14), (5, 11), (4,$
4082 $13), (3, 23), (4, 22), (8, 13), (8, 22), (1, 16), (0, 18), (2, 15), (0, 27), (6, 24), (3, 16), (5, 13),$
4083 $(4, 24), (8, 15), (0, 11), (8, 24), (1, 18), (0, 20), (2, 17), (2, 26), (7, 25), (3, 18), (4, 17), (4,$
4084 $26), (8, 17), (1, 11), (5, 27), (8, 26), (9, 25), (0, 22), (2, 19), (6, 10), (6, 19), (7, 18), (3, 11),$
4085 $(4, 10), (7, 27), (4, 19), (8, 10), (5, 20), (1, 13), (0, 15), (9, 18), (9, 27), (6, 12), (7, 20), (4,$
4086 $12), (4, 21), (9, 11), (0, 17), (2, 14), (0, 26), (2, 23), (6, 14), (6, 23), (7, 22), (8, 14), (9, 13),$
4087 $(3, 27), (5, 24), (8, 23), (9, 22), (0, 19), (2, 16), (7, 15), (6, 25), (7, 24), (3, 20), (5, 17), (9,$
4088 $15), (0, 12), (5, 26), (9, 24), (0, 21)\}$

4089 Q: Is there a path between node 27 and node 25?

4090 A:

4091 Let's construct a graph with the nodes and edges first:

4092 • **TASK INFO:** connectivity, hard, 0-Instruct, Edge Set
4093 • **MODEL:** claude-3-5-sonnet-20241022
4094 • **ACCURACY:** 1
4095 • **GROUND TRUTH:** True
4096 • **ANSWER:** Let me help you find if there's a path between node 27 and node 25.4097 Looking at the edge set, I can see that: - Node 27 is connected to nodes 3, 5, 7, and 9 - Node
4098 25 is connected to nodes 6, 7, 8, and 94099 We can find a path from node 27 to node 25: $27 \rightarrow 7 \rightarrow 25$ (direct connection through node
4100 7)4101 Since we can find at least one path between node 27 and node 25 (through node 7), there is
4102 definitely a path between these two nodes.

4103 The answer is yes.

4104

4105

4106

4107

4108

4109

4110

4111

4112

4113

4114

4115

4116

4117

4118

4119

4120

4121

4122

4123

4124

4125

4126

4127

4128

4129

4130

4131

4132

4133

4134

4135

4136

4137

4138

4139

4140

4141

4142

4143

4144

4145

4146

4147

4148

4149

4150

4151

4152

4153

4154

4155

4156

4157

Connectivity

- **QUERY:** To determine if there is a path between two nodes in an undirected graph, we can use a Breadth-First Search (BFS) algorithm. BFS is an algorithm that starts at one node and explores all of its neighbors before moving on to the next level of neighbors. By exploring each node in the graph, the algorithm can determine if there is a path between two nodes.

Determine if there is a path between two nodes in the graph.

Graph: Edge Set is $\{(0, 7), (3, 8), (5, 8), (3, 7), (6, 8), (1, 8), (5, 7), (6, 7), (1, 7), (4, 8), (4, 7), (2, 8)\}$

Q: Is there a path between node 5 and node 7?

A:

- **TASK INFO:** connectivity, easy, 0-Algorithm, Edge Set

- **MODEL:** Mistral

- **ACCURACY:**

1

- **GROUND TRUTH:**True

- **ANSWER:** yes, there is a path between node 5 and node 7. one possible path is: 5 \rightarrow 8 \rightarrow 7
here's the code for the bfs algorithm in python:

```
““ from collections import deque
def bfs(graph, start, end):
    visited = set()
    queue = deque([start])
    while queue:
        current = queue.popleft()
        if current == end:
            return true
        if current not in visited:
            visited.add(current)
            for neighbor in graph[current]:
                queue.append(neighbor)
    return false
# example usage
graph =
0: [4, 3],
1: [7, 4],
2: [8],
3: [],
4: [0, 1, 7],
5: [8],
6: [7, 8],
7: [0, 1, 6, 3, 5],
8: [2, 6, 5, 3]
print(bfs(graph, 5, 7)) # output: true ““
```

in this code, ‘graph’ is a dictionary where the keys are the nodes and the values are lists of their neighbors. the ‘bfs’ function takes in the graph, the start node, and the end node, and returns ‘true’ if there is a path between the two nodes, and ‘false’ otherwise. the function uses a queue to keep track of the nodes to be visited, and a set to keep track of the visited nodes to avoid visiting the same node multiple times. the function loops through the queue until it finds the end node or the queue is empty, and returns the result.

Connectivity

- **QUERY:** Determine if there is a path between two nodes in the graph. Graph: GraphML is

```
...  
<node id="1"/>  
<node id="2"/>  
...  
<edge source="4" target="5"/>  
<edge source="4" target="6"/>  
<edge source="4" target="7"/>  
</graph></graphml>
```

Q: Is there a path between node 1 and node 0?

A:

Let's think step by step:

- **TASK INFO:** connectivity, easy, 0-CoT, GraphML

- **MODEL:** Llama3.1

- **ACCURACY:** 0

- **GROUND TRUTH:** True

- **ANSWER:** the first step is to convert the given graphml into a format that can be used in the java code. we can use the graphml to xml function from the graphml library to do this. the second step is to create a graph from the xml string. we can use the graphmlreader class to do this. the third step is to find the nodes with id 1 and 0. we can use the getnodes method of the graph to do this. the fourth step is to check if there is a path between the two nodes. we can use the haspath method of the graph to do this. the fifth step is to return the result. we can use the print function to do this.

```
““java import org.graphstream.graph.graph;  
import org.graphstream.graph.implementations.singlegraph;  
import org.graphstream.graph.implementations.graphmlreader;  
import org.graphstream.graph.implementations.defaultgraph;  
public class main  
public static void main(string[] args)  
string graphml = "<?xml version='1.0' encoding='utf-8'?><graphml  
xmlns=http://graphml.graphdrawing.org/xmlns\xmlns:xsi=http://www.w3.org/2001/XMLSchema-  
instance\xsi:schemalocation=http://graphml.graphdrawing.org/xmlns  
http://graphml.graphdrawing.org/xmlns/1.0/graphml.xsd><graph  
edge-de-  
fault=undirected><node id=0/><node id=5/><node id=6/><node id=7/><node  
id=1/><node id=2/><node id=3/><node id=4/><edge source=0target=5/><edge  
source=0target=6/><edge source=0target=7/><edge source=5target=1/><edge  
source=5target=2/><edge source=5target=3/><edge source=6target=1/><edge  
source=6target=2/><edge source=6target=3/><edge source=7target=1/><edge  
source=7target=2/><edge source=7target=3/></graph></graphml>";  
graph graph = new singlegraph("graph");  
graph.read(graphml);  
string node1 = "1";  
string node0 = "0";  
boolean ispath = graph.haspath(node1, node0);  
system.out.println(ispath);  
””
```

this will print: false. there is no path between node 1 and node 0.

please note that this is a very simple implementation and does not handle any exceptions that might occur. in a real-world application, you would want to add error handling code.

4212 **Diameter**

4213 • **QUERY:** Given a graph, your task is to determine the diameter of this graph. Graph:
4214 Adjacency List is {0: [1], 1: [0, 2, 4, 5, 6, 7, 8, 11, 12], 2: [1, 3, 9], 3: [2], 4: [1], 5:
4215 [1], 6: [1], 7: [1, 10], 8: [1], 9: [2], 10: [7], 11: [1], 12: [1]}

4216 Q: What is the diameter of this graph?

4217 A:

- 4218 • **TASK INFO:** diameter, medium, 0-shot, Adjacency List
- 4219 • **MODEL:** Phi-4
- 4220 • **ACCURACY:** 0
- 4221 • **GROUND TRUTH:** 4.0
- 4222 • **ANSWER:**

4223 3

4224

4225

4226

4227

4228

4229

4230

4231

4232

4233

4234

4235

4236

4237

4238

4239

4240

4241

4242

4243

4244

4245

4246

4247

4248

4249

4250

4251

4252

4253

4254

4255

4256

4257

4258

4259

4260

4261

4262

4263

4264

4265

4266

Diameter

4267

- **QUERY:** Given a graph, your task is to determine the diameter of this graph. Graph: Adjacency List is {0: [1], 1: [0, 2, 4, 5, 6, 7, 8, 11, 12], 2: [1, 3, 9], 3: [2], 4: [1], 5: [1], 6: [1], 7: [1, 10], 8: [1], 9: [2], 10: [7], 11: [1], 12: [1]}

4270

Q: What is the diameter of this graph?

4271

A:

4272

- **TASK INFO:** diameter, medium, 0-shot, Adjacency List
- **MODEL:** gemini-2.0-flash-001
- **ACCURACY:** 1
- **GROUND TRUTH:** 4.0
- **ANSWER:**

4278

To find the diameter of the graph, we need to compute the shortest path between all pairs of nodes and then find the maximum of these shortest path lengths. The given graph has 13 nodes (0 to 12).

4281

Here's how we can determine the shortest paths:

4282

* **Node 0:** Only connected to Node 1, distance 1. * **Node 1:** The central node, connected to 0, 2, 4, 5, 6, 7, 8, 11, 12. * **Node 2:** Connected to 1 and 3, 9. * **Node 3:** Connected to 2. * **Node 4, 5, 6, 8, 11, 12:** Only connected to 1. * **Node 7:** Connected to 1 and 10. * **Node 9:** Connected to 2. * **Node 10:** Connected to 7.

4285

Let's analyze some key distances:

4286

* Distance(0, x): 2 for x in 2, 4, 5, 6, 7, 8, 9, 11, 12, otherwise infinity

4287

* Distance(0, 3): 3

4288

* Distance(0, 10): 3

4289

* Distance(1, x): 1 for x in 0, 2, 4, 5, 6, 7, 8, 11, 12

4290

* Distance(1, 3): 2

4291

* Distance(1, 9): 2

4292

* Distance(1, 10): 2

4293

* Distance(2, x):

4294

* 1 for x in 1, 3, 9

4295

* 2 for x in 0, 4, 5, 6, 7, 8, 11, 12

4296

* 3 for x in 10

4297

* Distance(3, x):

4298

* 1 for x in 2

4299

* 2 for x in 1, 9

4300

* 3 for x in 0, 4, 5, 6, 7, 8, 11, 12

4301

* 4 for x in 10

4302

* Distance(9, x):

4303

* 1 for x in 2

4304

* 2 for x in 1, 3

4305

* 3 for x in 0, 4, 5, 6, 7, 8, 11, 12

4306

* 4 for x in 10

4307

* Distance(10, x):

4308

* 1 for x in 7

4309

* 2 for x in 1

4310

* 3 for x in 0, 2, 4, 5, 6, 8, 9, 11, 12

4311

* 4 for x in 3

4312

Now, let's find the maximum shortest path:

4313

* Distance(3, 10) = 4

4314

* Distance(9, 10) = 4

4315

It appears 4 is the maximum distance.

4316

The diameter is 4.

4320

Diameter

4321

4322

4323

4324

4325

4326

4327

4328

4329

4330

4331

4332

4333

4334

4335

4336

4337

4338

4339

4340

4341

4342

4343

4344

4345

4346

4347

4348

4349

4350

4351

4352

4353

4354

4355

4356

4357

4358

4359

4360

4361

4362

4363

4364

4365

4366

4367

4368

4369

4370

4371

4372

4373

- **QUERY:** To calculate the diameter of the graph, you can use BFS based on the following tips
 1. identify all nodes in the graph.
 2. For each node in the graph , perform BFS to compute the shortest path from that node to all other nodes.
 3. calculate the shortest path from node u to all other nodes.
 4. Find the longest shortest path.
 5. Repeat the process and update the diameter of the graph.
 6. Return the diameter of the graph.

Given a graph, your task is to determine the diameter of this graph.

And the graph representation of Edge Set is :

$\{(0, 1), (1, 2), (0, 4), (0, 3), (1, 8), (0, 6), (0, 2), (2, 5), (4, 7)\}$

Q: What is the diameter of this graph?

A: Identify all nodes: The graph has nodes 0 to 8. Perform BFS from node 0. The longest shortest path is 2 edges (to node 5, 7 or 8). Perform BFS from node 1. The longest shortest path is 3 edges (to node 7). Perform BFS from node 2. The longest shortest path is 3 edges (to node 7). Perform BFS from node 3. The longest shortest path is 3 edges (to node 5, 7 or 8). Perform BFS from node 4. The longest shortest path is 3 edges (to node 5 or 8). Perform BFS from node 5. The longest shortest path is 4 edges (to node 7). Perform BFS from node 6. The longest shortest path is 3 edges (to node 5, 7, or 8). Perform BFS from node 7. The longest shortest path is 4 edges (to node 8). Perform BFS from node 8. The longest shortest path is 4 edges (to node 7). Based on all the results above, the maximum shortest path is 4 edges. So the diameter is 4.0.

...

Given a graph, your task is to determine the diameter of this graph. Graph: Edge Set is

$\{(7, 17), (4, 12), (3, 16), (5, 10), (9, 14), (0, 14), (1, 12), (7, 10), (6, 8), (7, 13), (6, 17), (3, 9), (3, 6), (0, 1), (5, 15), (11, 16), (1, 8), (6, 7), (4, 7), (12, 14), (3, 11), (3, 17), (9, 12), (1, 4), (10, 13), (11, 15), (2, 15)\}$

Q: What is the diameter of this graph?

A:

- **TASK INFO:** diameter, medium, Algorithm, Edge Set
- **MODEL:** Mistral
- **ACCURACY:** 0
- **GROUND TRUTH:** 6.0
- **ANSWER:** identify all nodes: the graph has nodes 0 to 17. perform bfs from node 0. the longest shortest path is 3 edges (to node 14). perform bfs from node 1. the longest shortest path is 3 edges (to node 12). perform bfs from node 2. the longest shortest path is 3 edges (to node 15). perform bfs from node 3. the longest shortest path is 3 edges (to node 16, 9, 17 or 6). perform bfs from node 4. the longest shortest path is 2 edges (to node 12). perform bfs from node 5. the longest shortest path is 3 edges (to node 15). perform bfs from node 6. the longest shortest path is 2 edges (to node 7, 17 or 3). perform bfs from node 7. the longest shortest path is 3 edges (to node 17, 13, 10, 5 or 4). perform bfs from node 8. the longest shortest path is 2 edges (to node 1, 6 or 17). perform bfs from node 9. the longest shortest path is 3 edges (to node 14). perform bfs from node 10. the longest shortest path is 3 edges (to node 7, 13). perform bfs from node 11. the longest shortest path is 3 edges (to node 16, 17 or 3). perform bfs from node 12. the longest shortest path is 2 edges (to node 4, 14 or 1). perform bfs from node 13. the longest shortest path is 3 edges (to node 7, 10). perform bfs from node 14. the longest shortest path is 2 edges (to node 0, 4, 12 or 9). perform bfs from node 15. the longest shortest path is 3 edges (to node 2, 5 or 11). perform bfs from node 16. the longest shortest path is 3 edges (to node 3, 11, 17 or 11). perform bfs from node 17. the longest shortest path is 3 edges (to node 3, 6, 7 or 13). based on all the results above, the longest shortest path is 3 edges. so the diameter is 3.0.

4374

4375

4376

4377

4378

4379

4380

4381

4382

4383

4384

4385

4386

4387

4388

4389

4390

4391

4392

4393

4394

4395

4396

4397

4398

4399

4400

4401

4402

4403

4404

4405

4406

4407

4408

4409

4410

4411

4412

4413

4414

4415

4416

4417

4418

4419

4420

4421

4422

4423

4424

4425

4426

4427

Diameter

- **QUERY:** To calculate the diameter of the graph, you can use BFS based on the following tips
 1. identify all nodes in the graph.
 2. For each node in the graph , perform BFS to compute the shortest path from that node to all other nodes.
 3. calculate the shortest path from node u to all other nodes.
 4. Find the longest shortest path.
 5. Repeat the process and update the diameter of the graph.
 6. Return the diameter of the graph.

Given a graph, your task is to determine the diameter of this graph. And the graph representation of Edge List is :

...

Q: What is the diameter of this graph?

...

Given a graph, your task is to determine the diameter of this graph. Graph: Edge List is

0 3

1 2

1 3

1 5

1 6

2 4

2 6

3 6

4 5

4 6

Q: What is the diameter of this graph?

A:

- **TASK INFO:** diameter, easy, Algorithm, Edge List
- **MODEL:** gpt-4o-mini
- **ACCURACY:** 1
- **GROUND TRUTH:** 3.0
- **ANSWER:**

To determine the diameter of the graph represented by the given edge list, we will follow the outlined steps:

1. **Identify all nodes**: The nodes present in the edge list are 0, 1, 2, 3, 4, 5, and 6. Thus, the set of nodes is {0, 1, 2, 3, 4, 5, 6}.

2. **Perform BFS from each node**: We will conduct a BFS for each node to compute the shortest paths to all other nodes.

- **From node 0**: Shortest paths are {0: 0, 3: 1} → max distance = 1

- **From node 1**: Shortest paths are {1: 0, 2: 1, 3: 1, 5: 1, 6: 1, 4: 2} → max distance = 2

- **From node 2**: Shortest paths are {2: 0, 1: 1, 4: 1, 5: 2, 6: 1, 3: 2} → max distance = 2

- **From node 3**: Shortest paths are {3: 0, 1: 1, 6: 1, 2: 2, 4: 2, 5: 2} → max distance = 2

- **From node 4**: Shortest paths are {4: 0, 2: 1, 5: 1, 6: 1, 1: 2, 3: 2} → max distance = 2

- **From node 5**: Shortest paths are {5: 0, 1: 1, 4: 1, 2: 2, 6: 2, 3: 3} → max distance = 3

- **From node 6**: Shortest paths are {6: 0, 1: 1, 2: 1, 3: 1, 4: 1, 5: 2} → max distance = 2

3. **Find longest shortest path**: The longest shortest path discovered in the BFS runs is from node 5 to node 3, which has a length of 3.

4. **Update diameter**: The diameter is updated to 3 as the maximum of the discovered maximum paths is 3.

5. **Return the diameter**: The diameter of the graph is thus recorded.

Final Answer: The diameter of this graph is **3**.

4428 Triangle

- **QUERY:** Given a graph, your task is to determine how many triangles in this graph. Graph: Graph Modelling Language is

```

4429
4430   graph [
4431     node [
4432       id 0
4433       label "0"
4434     ]
4435     ...
4436     edge [
4437       source 1
4438       target 4
4439     ]
4440     edge [
4441       source 1
4442       target 5
4443     ]
4444     edge [
4445       source 1
4446       target 6
4447     ]
4448     edge [
4449       source 2
4450       target 6
4451     ]
4452     ]
4453
4454
4455
4456
4457
4458
4459
4460
4461
4462
4463
4464
4465
4466
4467
4468
4469
4470
4471
4472
4473
4474
4475
4476
4477
4478
4479
4480
4481

```

Q: How many triangles are in this graph?

A:

Let's break down this problem:

- **TASK INFO:** triangle, easy, LTM, Graph Modelling Language
- **MODEL:** Qwen-2.5
- **ACCURACY:** 0
- **GROUND TRUTH:** 1
- **ANSWER:**

a triangle in a graph is a set of three nodes where each node is connected to the other two. in other words, if nodes a, b, and c form a triangle, then there must be an edge between a and b, b and c, and c and a.

looking at the given graph, we can see that all nodes are connected to node 1. however, there is no direct connection between any of the other nodes. therefore, no three nodes form a triangle.

so, the answer is 0 triangles. you are an ai assistant. you will be given a task. you must generate a detailed0 answer.

4536 Triangle

4537

4538 • **QUERY:** Given a graph, your task is to determine how many triangles this graph.

4539 And the graph representation of Edge List is :

4540 0 1

4541 ...

4542 8 1

4543 Let's construct a graph with the nodes and edges first.

4544 Q: How many triangles are in this graph?

4545 A: The graph contains 3 nodes that form a triangle (0, 1, and 2), resulting in 1 triangle. So the

4546 number of triangles is 1.

4547 Given a graph, your task is to determine how many triangles in this graph. Graph: Edge List

4548 is

4549 1 0

4550 2 0

4551 2 1

4552 3 1

4553 4 1

4554 2 4

4555 1 5

4556 5 2

4557 6 1

4558 1 7

4559 8 1

4560 8 4

4561 7 9

4562 1 10

4563 10 4

4564 Let's construct a graph with the nodes and edges first.

4565

4566 Q: How many triangles are in this graph?

4567 A:

4568 • **TASK INFO:** triangle, medium, Instruct, Edge List

4569 • **MODEL:** claude-3-5-sonnet-20241022 SF

4570

4571 • **ACCURACY:** 1

4572 • **GROUND TRUTH:** 5

4573 • **ANSWER:**

4574 Let me help identify the triangles in this graph.

4575 Looking at the edge list, I'll find sets of three nodes where all three nodes are connected to

4576 each other.

4577 Let's check the triangles:

4578 1. Triangle (0, 1, 2): - Edge 1-0 exists - Edge 2-0 exists - Edge 2-1 exists

4579 2. Triangle (1, 2, 4): - Edge 1-2 exists - Edge 2-4 exists - Edge 1-4 exists

4580 3. Triangle (1, 2, 5): - Edge 1-2 exists - Edge 2-5 exists - Edge 1-5 exists

4581 4. Triangle (1, 4, 8): - Edge 1-4 exists - Edge 4-8 exists - Edge 1-8 exists

4582 5. Triangle (1, 4, 10): - Edge 1-4 exists - Edge 4-10 exists - Edge 1-10 exists

4583 After checking all possible combinations, I found 5 triangles in the graph.

4584 The number of triangles is 5.

4585

4586

4587

4588

4589

4590

Triangle

4591

- **QUERY:** Given a graph, your task is to determine how many triangles in this graph.

4592

Graph: Adjacency Set is {0: {8, 1, 3, 6}, 1: {0, 3, 5}, 2: {3, 4, 5, 7}, 3: {0, 1, 2, 4, 7}, 4: {2, 3, 6, 7, 8}, 5: {1, 2}, 6: {0, 8, 4, 7}, 7: {2, 3, 4, 6}, 8: {0, 4, 6}}

4593

Q: How many triangles are in this graph?

4594

A:

4595

Let's think step by step:

4596

- **TASK INFO:** triangle, easy, 0-CoT Adjacency Set

4597

- **MODEL:** Mistral

4598

- **ACCURACY:** 1

4599

- **GROUND TRUTH:** 8

4600

- **ANSWER:**

4601

1. we know that a triangle has 3 vertices.

4602

2. to find the number of triangles, we will count the number of edges that are part of a triangle twice (since each edge is shared by two triangles).

4603

3. to count the edges, we can use the formula for the degree sum of a graph: sum of degrees = 2 * number of edges. the sum of the degrees of all vertices in the graph is 36.

4604

4. since there are 8 vertices in the graph, the average degree of each vertex is $36 / 8 = 4.5$. however, since vertices cannot have a fractional degree, we round down to 4.

4605

5. this means that each vertex has 4 edges, and since each edge connects two vertices, we have $4 * 8 / 2 = 16$ edges.

4606

6. since each edge is part of 2 triangles, the number of triangles is $16 / 2 = 8$.

4607

so, there are 8 triangles in the given graph.

4608

4609

4610

4611

4612

4613

4614

4615

4616

4617

4618

4619

4620

4621

4622

4623

4624

4625

4626

4627

4628

4629

4630

4631

4632

4633

4634

4635

4636

4637

4638

4639

4640

4641

4642

4643

4644

4645

4646

4647

4648

4649

4650

4651

4652

4653

BFS order

- **QUERY:** Given a graph, your task is to determine the BFS traversal order of this graph starting at node 7.

[[0 1 1 1 1 0 1 0 0]

...

[0 1 0 0 0 0 0 0 0]]

...

Given a graph, your task is to determine the bfs traversal order of this graph starting at node 1.

And the graph representation of: Adjacency Matrix is

[[0 1 1 0 0 0 0 0 0 0 0 0 0]

[1 0 1 1 1 1 0 0 0 0 0 0 0]

[1 1 0 1 0 1 0 0 0 1 0 0 0]

[0 1 1 0 1 0 1 1 1 0 1 0 1]

[0 1 0 1 0 0 0 1 0 0 1 0 0]

[0 1 1 0 0 0 0 0 0 0 0 0 0]

[0 1 0 1 0 0 0 0 1 0 0 0 1]

[0 0 0 1 1 0 0 0 0 1 0 0 0]

[0 0 0 1 0 0 1 0 0 0 0 1 0]

[0 0 1 0 0 0 0 1 0 0 0 1 0]

[0 0 0 1 1 0 0 0 0 0 0 0 0]

[0 0 0 0 0 0 0 0 1 1 0 0 0]

[0 0 0 1 0 0 1 0 0 0 0 0 0]]

Let's construct a graph with the nodes and edges first.

Q: Give the bfs traversal order starting from node 1.

A:

- **TASK INFO:** bfsorder, medium, Instruct, Adjacency Matrix

- **MODEL:** gpt-4o

- **ACCURACY:** 1

- **STARTING NODE:** 1

- **ANSWER:** We begin the BFS traversal from node 1. Here is the breakdown of the traversal:

1. Start at node 1. The first node in the BFS traversal is 1. 2. Visit the neighbors of node 1. The neighbors of node 1 are nodes 0, 2, 3, 4, 5, and 6. We enqueue all these nodes. 3. Visit the next node in the queue, which is node 0. Node 0 only has node 1 as a neighbor, which has already been visited, so we move to the next in queue. 4. Visit node 2. The neighbors of node 2 are nodes 0, 1, 3, 5, and 9. Nodes 0, 1, and 5 are already visited or enqueued, so we enqueue node 3 and 9. 5. Visit node 3. The neighbors of node 3 are nodes 1, 2, 4, 6, 7, 8, 10, and 12. We enqueue nodes 4, 6, 7, 8, 10, and 12. 6. Visit node 4. Node 4's neighbors are nodes 1, 3, 7, and 10. All these nodes are either visited or enqueued. 7. Visit node 5. Node 5's neighbors are nodes 1 and 2, which are already visited. 8. Visit node 6. Node 6's neighbors are nodes 1, 3, 8, and 12. Node 8 is already enqueued, while 12 is already enqueued, and nodes 1 and 3 are visited. 9. Visit node 9. Node 9's neighbors are nodes 2, 7, and 11. Nodes 2 is visited, while we enqueue nodes 7 and 11. 10. Visit node 7. Node 7's neighbors are nodes 3, 4, and 9. These nodes have been visited or enqueued. 11. Visit node 10. Node 10's neighbors are nodes 3, 4. These are already visited. 12. Visit node 8. Node 8's neighbors are nodes 3 and 6. These are already visited. 13. Visit node 12. Neighbors are nodes 3 and 6. These are already visited. 14. Visit the last node in the queue, which is node 11. Node 11's neighbors are nodes 8 and 9. These nodes have already been visited.

Thus, the BFS traversal order starting from node 1 is 1, 0, 2, 3, 4, 5, 6, 9, 7, 10, 8, 12, 11.

4694

4695

4696

4697

4698

4699

4700

4701

4702

4703

4704

4705

4706

4707

4708

4709

4710

4711

4712

4713

4714

4715

4716

4717

4718

4719

4720

4721

4722

4723

4724

4725

4726

4727

4728

4729

4730

4731

4732

4733

4734

4735

4736

4737

4738

4739

4740

4741

4742

4743

4744

4745

4746

4747

4748

4749

4750

4751

BFS order

- **QUERY:** Given a graph, your task is to determine the bfs traversal order of this graph starting at node 7.

And the graph representation of: Edge List is 3 2

4 1

5 2

6 5

7 0

8 2

9 7

10 3

Q: Give the bfs traversal order starting from node 7.

A:

Let's break down this problem:

- **TASK INFO:** bfsorder, medium, LTM, Edge List
- **MODEL:** gpt-4o-mini BAF
- **ACCURACY:** 1
- **STARTING NODE:** 7
- **ANSWER:**

To perform a breadth-first search (BFS) starting from node 7, we first need to construct the graph from the provided edge list. The edge list indicates connections between nodes as follows:

- 3 is connected to 2 - 4 is connected to 1 - 5 is connected to 2 - 6 is connected to 5 - 7 is connected to 0 - 8 is connected to 2 - 9 is connected to 7 - 10 is connected to 3 From this edge list, we can represent the graph as an adjacency list:

“ 0: [7] 1: [4] 2: [3, 5, 8] 3: [2, 10] 4: [1] 5: [2, 6] 6: [5] 7: [0, 9] 8: [2] 9: [7] 10: [3] “

Now, we will perform the BFS traversal starting from node 7:

1. Initialize a queue and a visited set.
2. Enqueue the starting node (7).
3. Dequeue a node, process it, and enqueue its unvisited neighbors.

The BFS traversal process:

- Start with node 7, enqueue it. (Queue: [7])
- Dequeue 7, visit it. (Visited: [7])
- Enqueue its neighbor 0 (Queue: [0])
- Enqueue its other neighbor 9 (Queue: [0, 9])
- Dequeue 0, visit it. (Visited: [7, 0])
- No unvisited neighbors.
- Dequeue 9, visit it. (Visited: [7, 0, 9])
- Enqueue its neighbor 7, but it is already visited.

At this point, the queue is empty, and the BFS is complete.

Thus, the BFS traversal order starting from node 7 is:

A: 7, 0, 9

4752

BFS order

4753

- **QUERY:** To determine the BFS (Breadth-First Search) traversal order, you need to follow these steps: 1. Initialize: Start by choosing a starting node and enqueue it into a queue. 2. Mark visited: Mark the starting node as visited to avoid reprocessing. 3. Traverse: While the queue is not empty: Dequeue a node and add it to the traversal order. For each unvisited neighboring node of the dequeued node, enqueue it and mark it as visited. 4. Continue the process until all reachable nodes are visited.

4758

4759

4760

4761

4762

4763

4764

4765

4766

4767

4768

4769

4770

4771

4772

4773

4774

4775

4776

4777

4778

4779

4780

4781

4782

4783

4784

4785

4786

4787

4788

4789

4790

4791

4792

4793

4794

4795

4796

4797

4798

4799

4800

4801

4802

4803

4804

4805

Given a graph, your task is to determine the bfs traversal order of this graph starting at node 4. And the graph representation of: Edge Set is $\{(11, 36), (5, 25), (32, 3), (4, 33), (14, 31), (0, 14), (5, 22), (4, 30), (11, 17), (0, 26), (18, 1), (11, 35), (12, 0), (1, 27), (10, 2), (11, 7), (0, 16), (0, 13), (0, 19), (10, 20), (1, 23), (21, 5), (0, 34), (16, 24), (1, 29), (28, 4), (9, 6), (0, 15)\}$

Q: Give the bfs traversal order starting from node 4.

A:

- **TASK INFO:**

bfsorder, hard, 0-Algorithm, Edge Set

- **MODEL:** Qwen-3

- **ACCURACY:** 0

- **STARTING NODE:** 4

- **ANSWER:**

To determine the **Breadth-First Search (BFS)** traversal order starting from **node 4***, we must carefully analyze the given **edge set** and build the **adjacency list** of the graph. BFS is a traversal algorithm that explores all nodes at the current depth level before moving on to nodes at the next depth level. It uses a **queue** to manage the nodes to be processed and a **visited set** to avoid revisiting nodes.

—
Step 1: Analyze the Edge Set

The edge set is:

“ $\{(11, 36), (5, 25), (32, 3), (4, 33), (14, 31), (0, 14), (5, 22), (4, 30), (11, 17), (0, 26), (18, 1), (11, 35), (12, 0), (1, 27), (10, 2), (11, 7), (0, 16), (0, 13), (0, 19), (10, 20), (1, 23), (21, 5), (0, 34), (16, 24), (1, 29), (28, 4), (9, 6), (0, 15)\}$ ”

We can construct the **adjacency list** by iterating through each edge and adding both directions (since the graph is undirected).

—
Step 2: Build the Adjacency List

From the edge set, we find the neighbors of **node 4***: - (4, 33) → node 4 is connected to node 33 - (4, 30) → node 4 is connected to node 30 - (28, 4) → node 4 is connected to node 28

So, **node 4's neighbors are 33, 30, and 28**.

Similarly, we can find the neighbors for other nodes, but for the BFS starting at node 4, we only need to consider the nodes reachable from it.

—
Step 3: Perform BFS

We initialize: - **Queue**: [4] - **Visited Set**: 4 - **Traversal Order**: []

Now, we follow the BFS algorithm step-by-step:

1. **Dequeue 4** → Add to traversal order → **[4]** - Neighbors: 33, 30, 28 → all unvisited - Enqueue: [33, 30, 28] - Mark visited: 4, 33, 30, 28

2. **Dequeue 33** → Add to traversal order → **[4, 33]** - Neighbors: only 4 (already visited) - Queue: [30, 28]

3. **Dequeue 30** → Add to traversal order → **[4, 33, 30]** - Neighbors: only 4 (already visited) - Queue: [28]

4. **Dequeue 28** → Add to traversal order → **[4, 33, 30, 28]** - Neighbors: only 4 (already visited) - Queue: empty

Final Result

All reachable nodes from node 4 have been visited in the order: “ 4 → 33 → 30 → 28 ”

Final Answer

\$\$ \{4, 33, 30, 28\} \$\$

4806

BFS order

4807

- **QUERY:** Given a graph, your task is to determine the bfs traversal order of this graph starting at node 7.

4808

And the graph representation of: GraphML is <?xml version='1.0' encoding='utf-8'?> <graphml xmlns="http://graphml.graphdrawing.org/xmlns" xmlns:xsi="http://www.w3.org/2001/XMLSchema-instance" xsi:schemaLocation="http://graphml.graphdrawing.org/xmlns http://graphml.graphdrawing.org/xmlns/1.0/graphml.xsd"><graph edgedefault="undirected"><node id="0"/> <node id="1"/> <node id="2"/>

...

<edge source="5" target="18"/> <edge source="8" target="18"/> <edge source="9" target="13"/> <edge source="9" target="16"/> <edge source="16" target="19"/> </graph></graphml>

4809

Q: Give the bfs traversal order starting from node 7.

4810

A:

4811

Let's construct a graph with the nodes and edges first:

4812

- **TASK INFO:** bfsorder, hard, 0-Instruct, GraphML

4813

- **MODEL:** claude-3-5-sonnet-20241022 SF

4814

- **ACCURACY:** 1

4815

- **STARTING NODE:** 7

4816

- **ANSWER:**

4817

Let me help you find the BFS traversal order starting from node 7.

4818

1) Starting at node 7, we first visit its adjacent nodes: - Node 7 is connected to nodes 0 and 5

4819

2) Next level (visiting neighbors of 0 and 5): From node 0: - Connected to 1, 2, 3, 4, 6, 19

4820

From node 5: - Connected to 12, 15, 16, 18

4821

3) Next level (visiting unvisited neighbors of previous level): From the previous nodes' connections: - Node 1 connects to 14 - Node 2 connects to 9 - Node 4 connects to 8, 10, 11, 17, 20 - Node 9 connects to 13

4822

Following BFS rules, visiting level by level: - First: 7 - Second: 0, 5 - Third: 1, 2, 3, 4, 6, 19, 12, 15, 16, 18 - Fourth: 14, 9, 8, 10, 11, 17, 20, 13

4823

The BFS traversal order starting from node 7 is

4824

7,0,5,1,2,3,4,6,19,12,15,16,18,14,9,8,10,11,17,20,13

4825

4826

4827

4828

4829

4830

4831

4832

4833

4834

4835

4836

4837

4838

4839

4840

4841

4842

4843

4844

4845

4846

4847

4848

4849

4850

4851

4852

4853

4854

4855

4856

4857

4858

4859

4860

BFS order

4861

- **QUERY:** Given a graph, your task is to determine the bfs traversal order of this graph starting at node 2.

4863

And the graph representation of: Adjacency Set is

4864

```
{0: {8, 2, 4, 6}, 1: {8, 3, 4, 5}, 2: {0, 7}, 3: {1, 4, 6, 7}, 4: {0, 1, 3, 5, 6, 8}, 5: {1, 4, 6}, 6: {0, 3, 4, 5, 8}, 7: {2, 3}, 8: {0, 1, 4, 6}}
```

4866

Q: Give the bfs traversal order starting from node 2.

4867

A:

4869

Let's break down this problem:

4870

- **TASK INFO:** bfsorder, easy, LTM, Adjacency Set
- **MODEL:** Qwen-2.5
- **ACCURACY:** 0
- **STARTING NODE:** 2
- **ANSWER:**

4875

1. **identify the starting node and the adjacency set:** - we start at node 2. - the adjacency set is given as: {0: {8, 2, 4, 6}, 2: {0, 7}, 4: {0, 1, 3, 5, 6, 8}, 6: {0, 3, 4, 5, 8}, 8: {0, 1, 4, 6}, 1: {8, 3, 4, 5}, 3: {1, 4, 6, 7}, 5: {1, 4, 6}, 7: {2, 3}} 2. **perform bfs traversal:** - **step 1:** start at node 2. - **step 2:** add all adjacent nodes of 2 to the queue and mark them as visited. - node 2 is adjacent to node 0 and node 7. - add 0 and 7 to the queue. - **step 3:** dequeue the first node in the queue (node 0) and add all its adjacent nodes (8, 2, 4, 6) to the queue (excluding nodes already visited). - add 8, 4, and 6 to the queue. - **step 4:** dequeue the next node in the queue (node 7) and add its adjacent nodes (2, 3) to the queue (excluding nodes already visited). - add 3 to the queue. - **step 5:** dequeue the next node in the queue (node 8) and add its adjacent nodes (0, 1, 4, 6) to the queue (excluding nodes already visited). - add 1 to the queue. - **step 6:** dequeue the next node in the queue (node 4) and add its adjacent nodes (0, 1, 3, 5, 6, 8) to the queue (excluding nodes already visited). - add 5 to the queue. - **step 7:** dequeue the next node in the queue (node 6) and add its adjacent nodes (0, 3, 4, 5, 8) to the queue (excluding nodes already visited). - no new nodes are added as all are already visited. - **step 8:** dequeue the next node in the queue (node 3) and add its adjacent nodes (1, 4, 6, 7) to the queue (excluding nodes already visited). - no new nodes are added as all are already visited. - **step 9:** dequeue the next node in the queue (node 1) and add its adjacent nodes (8, 3, 4, 5) to the queue (excluding nodes already visited). - no new nodes are added as all are already visited. - **step 10:** dequeue the next node in the queue (node 5) and add its adjacent nodes (1, 4, 6) to the queue (excluding nodes already visited). - no new nodes are added as all are already visited.

4895

3. **list the order of nodes visited:** - the order of nodes visited in bfs starting from node 2 is: 2, 0, 7, 8, 4, 6, 3, 1, 5

4896

therefore, the bfs traversal order starting from node 2 is: 2, 0, 7, 8, 4, 6, 3, 1, 5.

4897

4898

4899

4900

4901

4902

4903

4904

4905

4906

4907

4908

4909

4910

4911

4912

4913

4914

4915

4916

4917

4918

4919

4920

4921

4922

4923

4924

4925

4926

4927

4928

4929

4930

4931

4932

4933

4934

4935

4936

4937

4938

4939

4940

4941

4942

4943

4944

4945

4946

4947

4948

4949

4950

4951

4952

4953

4954

4955

4956

4957

4958

4959

4960

4961

4962

4963

4964

4965

4966

4967

4968

4969

4970

4971

4972

4973

4974

4975

4976

4977

4978

4979

4980

4981

4982

4983

4984

4985

4986

4987

4988

4989

4990

4991

4992

4993

4994

4995

4996

4997

4998

4999

5000

5001

5002

5003

5004

5005

5006

5007

5008

5009

5010

5011

5012

5013

5014

5015

5016

5017

5018

5019

5020

5021

5022

5023

5024

5025

5026

5027

5028

5029

5030

5031

5032

5033

5034

5035

5036

5037

5038

5039

5040

5041

5042

5043

5044

5045

5046

5047

5048

5049

5050

5051

5052

5053

5054

5055

5056

5057

5058

5059

5060

5061

5062

5063

5064

5065

5066

5067

5068

5069

5070

5071

5072

5073

5074

5075

5076

5077

5078

5079

5080

5081

5082

5083

5084

5085

5086

5087

5088

5089

5090

5091

5092

5093

5094

5095

5096

5097

5098

5099

5100

5101

5102

5103

5104

5105

5106

5107

5108

5109

5110

5111

5112

5113

5114

5115

5116

5117

5118

5119

5120

5121

5122

5123

5124

5125

5126

5127

5128

5129

5130

5131

5132

5133

5134

5135

5136

5137

5138

5139

5140

5141

5142

5143

5144

5145

5146

5147

5148

5149

5150

5151

5152

5153

5154

5155

5156

5157

5158

5159

5160

5161

5162

5163

5164

5165

5166

5167

5168

5169

5170

5171

5172

5173

5174

5175

5176

5177

5178

5179

5180

5181

5182

5183

5184

5185

5186

5187

5188

5189

5190

5191

5192

5193

5194

5195

5196

5197

5198

5199

5200

5201

5202

5203

5204

5205

5206

5207

5208

5209

5210

5211

5212

5213

5214

5215

5216

5217

5218

5219

5220

5221

5222

5223

5224

5225

5226

5227

5228

5229

5230

5231

5232

5233

5234

5235

5236

5237

5238

5239

5240

5241

4968

Cycle

- **QUERY:** To determine whether or not there is a cycle in an undirected graph, you can use a depth-first search algorithm to traverse the graph. If the algorithm ever returns to a node it has already visited, then it has detected a cycle in the graph.

Given a graph representation, your task is determining whether the graph has a cycle

```

4970      Graph:          GraphML      is      <?xml      version='1.0'      encoding='utf-
4971      8'?>          <graphml      xmlns="http://graphml.graphdrawing.org/xmlns"
4972      xmlns:xsi="http://www.w3.org/2001/XMLSchema-instance"
4973      xsi:schemaLocation="http://graphml.graphdrawing.org/xmlns
4974      http://graphml.graphdrawing.org/xmlns/1.0/graphml.xsd"><graph      edgede-
4975      fault="undirected"><node id="0"/>
4976
4977      <node id="1"/>
4978      <node id="2"/>
4979      <node id="3"/>
4980      <node id="4"/>
4981      <node id="5"/>
4982      <node id="6"/>
4983      <node id="7"/>
4984      <node id="8"/>
4985      <node id="9"/>
4986
4987      <edge source="0" target="1"/>
4988      <edge source="0" target="2"/>
4989      <edge source="0" target="3"/>
4990      <edge source="0" target="5"/>
4991      <edge source="0" target="6"/>
4992      <edge source="0" target="8"/>
4993      <edge source="0" target="9"/>
4994      <edge source="1" target="4"/>
4995      <edge source="2" target="7"/>
4996
4997      </graph></graphml>
4998
4999  Q: Is there a cycle in this graph?
5000
5001  A:
5002  • TASK INFO: cycle, medium, 0-Algorithm, GraphML
5003  • MODEL: claude-3-5-sonnet-20241022
5004  • ACCURACY: 1
5005  • GROUND TRUTH: False
5006  • ANSWER:
5007
5008  Let me analyze this graph:
5009  1. The graph has 10 nodes (0-9) 2. Looking at the edges: - Node 0 connects to nodes 1, 2,
5010  3, 5, 6, 8, and 9 - Node 1 connects to nodes 0 and 4 - Node 2 connects to nodes 0 and 7 -
5011  Nodes 3, 5, 6, 8, and 9 only connect to node 0 - Node 4 only connects to node 1 - Node 7
5012  only connects to node 2
5013
5014  In this graph, there is no cycle. The graph forms a star-like structure with node 0 as the
5015  center, and some nodes (1 and 2) having additional connections to nodes 4 and 7 respectively.
5016  However, there is no way to start at any node and follow edges to return to the starting point
5017  without using the same edge twice. The structure is essentially tree-like.
5018
5019
5020
5021

```

Cycle

- **QUERY:** Given a graph representation, your task is to determine whether the graph has a cycle
And the graph representation of GraphML is :

...

Q: Is there a cycle in this graph? A: No, there is no cycle in this graph.

...

Given a graph representation, your task is determining whether the graph has a cycle

Graph: GraphML is

...

```
<edge source="4" target="6"/>
<edge source="5" target="6"/>
</graph></graphml>
```

Q: Is there a cycle in this graph?

A:

- **TASK INFO:** cycle, easy, CoT, GraphML

- **MODEL:** Qwen-2.5

- **ACCURACY:** 0

- **GROUND TRUTH:** False

- **ANSWER:**

the edges (6,5), (5,6) form a cycle, so yes, there is a cycle in this graph. given the graph representation in graphml format:

```
“xml <?xml version='1.0' encoding='utf-8'?> <graphml xmlns="http://graphml.graphdrawing.org/xmlns"
xmlns:xsi="http://www.w3.org/2001/
```

```
xmlschema-instance" xsi:schemalocation="http://graphml.graphdrawing.org/xmlns
http://graphml.graphdrawing.org/xmlns/1.0/graphml.xsd" > <graph edgedefault="undirected">
```

```
<node id="0"/>
```

```
<node id="6"/>
```

```
<node id="5"/>
```

```
<node id="1"/>
```

```
<node id="4"/>
```

```
<node id="3"/>
```

```
<node id="2"/>
```

```
<edge source="0" target="6"/>
```

```
<edge source="6" target="5"/>
```

```
<edge source="6" target="1"/>
```

```
<edge source="6" target="4"/>
```

```
<edge source="6" target="3"/>
```

```
<edge source="6" target="2"/>
```

```
</graph>
```

```
</graphml>
```

“

we need to determine if there is a cycle in the graph.

analysis: - node 6 is connected to nodes 0, 5, 1, 4, 3, and 2. - the connections from node 6 to nodes 5, 1, 4, 3, and 2 do not form a cycle by themselves. - however, the connection from node 6 to node 5 and back to node 6 forms a cycle.

conclusion: the edges (6, 5) and (5, 6) form a cycle.

answer:

q: is there a cycle in this graph?

a: yes, there is a cycle in this graph. the cycle is formed by the edges (6, 5) and (5, 6).

5076

Cycle

5077

- **QUERY:** Given a graph representation, your task is determining whether the graph has a cycle

5078

Graph: Edge Set is $\{(4, 6), (3, 10), (0, 2), (9, 14), (0, 8), (1, 3), (0, 17), (13, 14), (2, 17), (3, 9), (3, 6), (3, 15), (0, 1), (0, 7), (0, 4), (0, 16), (0, 13), (3, 5), (3, 11), (3, 17), (0, 3), (0, 12), (2, 3), (0, 15), (7, 8)\}$

5079

Q: Is there a cycle in this graph?

5080

A:

5081

Let's think step by step:

5082

- **TASK INFO:** cycle, medium, 0-CoT, Edge Set

5083

- **MODEL:** gpt-4o-mini

5084

- **ACCURACY:** 1

5085

- **GROUND TRUTH:** True

5086

- **ANSWER:**

5087

To determine whether the graph represented by the given edge set has a cycle, we can employ Depth First Search (DFS) or a Union-Find algorithm.

5088

1. **Initialization**: Start from any vertex and initiate a search (DFS or Union-Find).

5089

2. **Tracking Visits**: Keep a record of visited nodes. For DFS, maintain a parent reference to detect back edges.

5090

3. **Finding Cycles**: - During traversal, if you find a visited vertex that is not the parent of the current vertex, a cycle exists. - If using Union-Find, detect cycles when trying to union two vertices that are already in the same set.

5091

For the provided edge set, we systematically traverse each edge.

5092

Edges:

5093

- (4, 6)

5094

- (3, 10)

5095

- (0, 2)

5096

- (9, 14)

5097

- (0, 8)

5098

- (1, 3)

5099

- (0, 17)

5100

- (13, 14)

5101

- (2, 17)

5102

- (3, 9)

5103

- (3, 6)

5104

- (3, 15)

5105

- (0, 1)

5106

- (0, 7)

5107

- (0, 4)

5108

- (0, 16)

5109

- (0, 13)

5110

- (3, 5)

5111

- (3, 11)

5112

- (3, 17)

5113

- (0, 3)

5114

- (0, 12)

5115

- (2, 3)

5116

- (0, 15)

5117

- (7, 8)

5118

Analysis: From the edges: - The edge (3, 6) and (3, 5) suggests multiple connections around vertex

5119

3. - The edge (3, 17) connects back to vertex 3, which confirms presence of a cycle.

5120

Conclusion: Yes, the graph has a cycle.

5121

5122

5123

5124

5125

5126

5127

5128

5129

5130

Cycle

5131

- **QUERY:** To determine whether or not there is a cycle in an undirected graph, you can use a depth-first search algorithm to traverse the graph. If the algorithm ever returns to a node it has already visited, then it has detected a cycle in the graph.

5132

Given a graph representation, your task is to determine whether the graph has a cycle

5133

And the graph representation of Adjacency Set is : {3: {4, 5}, 4: {3}, 5: {2, 3}, 1: {0}, 0: {1, 2}, 2: {0, 5}}

5134

Q: Is there a cycle in this graph?

5135

A: DFS traversal visits nodes {0, 1, 2, 5, 3, 4}. At no point does the traversal return to an already visited node that is not the parent. Hence, no cycle is detected.

5136

Given a graph representation, your task is to determine whether the graph has a cycle

5137

And the graph representation of Adjacency Set is : {3: {0, 2, 4, 5}, 5: {3}, 1: {0, 4}, 0: {1, 3}, 4: {1, 3}, 2: {3}}

5138

Q: Is there a cycle in this graph?

5139

A: During DFS, the traversal path includes nodes {0, 1, 4, 3, 5, 2}. A back edge is detected from node 3 to node 4, where the latter is already in recursive stack. So, there is a cycle in this graph.

5140

Given a graph representation, your task is to determine whether the graph has a cycle

5141

And the graph representation of Adjacency Set is : {7: {1, 3, 5}, 1: {7}, 5: {6, 7}, 0: {2}, 2: {0, 4, 6}, 3: {7}, 4: {2}, 6: {2, 5}}

5142

Q: Is there a cycle in this graph?

5143

A: DFS visits nodes {0, 2, 4, 6, 5, 7, 1, 3}. The traversal completes without encountering any back edges, there is no cycle in this graph.

5144

Given a graph representation, your task is to determine whether the graph has a cycle

5145

And the graph representation of Adjacency Set is : {0: {1, 2}, 1: {0, 4}, 2: {0, 6}, 6: {2, 4}, 5: {3}, 3: {5, 7}, 4: {1, 6, 7}, 7: {3, 4}}

5146

Q: Is there a cycle in this graph?

5147

A: While traversing nodes {0, 1, 4, 7, 3, 5, 6, 2}, a back edge from node 2 to node 0 is identified, the latter is already in recursion stack of DFS, so yes, there is a cycle in this graph.

5148

Given a graph representation, your task is to determine whether the graph has a cycle

5149

And the graph representation of Adjacency Set is : {1: {0, 2, 3, 4, 5, 6}, 3: {0, 1, 2, 4, 5, 6}, 2: {0, 1, 3, 4, 5, 6}, 4: {0, 1, 2, 3, 5, 6}, 6: {0, 1, 2, 3, 4, 5}, 0: {1, 2, 3, 4, 5, 6}, 5: {0, 1, 2, 3, 4, 6}}

5150

Q: Is there a cycle in this graph?

5151

A: This graph contains multiple cycles. During DFS, cycles are detected through paths like {3-4-6-3}, {1-2-3-1}, and {4-5-6-4}. Multiple back edges indicate the presence of several cycles.

5152

Given a graph representation, your task is determining whether the graph has a cycle

5153

Graph: Adjacency Set is {0: {1, 2, 3, 4, 5, 6, 18, 20, 30}, 1: {0, 2, 3, 4, 5, 6, 21}, 2: {0, 1, 3, 4, 5, 6, 7, 24, 25}, 3: {0, 1, 2, 32, 4, 5, 6, 28}, 4: {0, 1, 2, 3, 5, 6, 14, 23}, 5: {0, 1, 2, 3, 4, 6, 10, 11, 31}, 6: {0, 1, 2, 3, 4, 5, 8, 9, 12, 13, 17, 19, 22, 26, 27}, 7: {2}, 8: {6}, 9: {6}, 10: {5}, 11: {5}, 12: {6, 15}, 13: {16, 6}, 14: {4}, 15: {12}, 16: {13}, 17: {6}, 18: {0}, 19: {6}, 20: {0}, 21: {1}, 22: {29, 6}, 23: {4}, 24: {2}, 25: {2}, 26: {6}, 27: {6}, 28: {3}, 29: {22}, 30: {0}, 31: {5}, 32: {3}}

5154

Q: Is there a cycle in this graph?

5155

A:

- **TASK INFO:** cycle, hard, Algorithm, Adjacency Set
- **MODEL:** o4-mini-2025-04-16
- **ACCURACY:** 1
- **GROUND TRUTH:** True
- **ANSWER:**

5156

The subgraph induced by nodes 0 through 6 is a complete graph (each of those nodes connects to every other), which immediately contains many 3-node cycles (for example, 0-1-2-0). Therefore, this graph definitely has a cycle. Yes, there is a cycle in this graph

5157

5158

5159

5160

5161

5162

5163

5164

5165

5166

5167

5168

5169

5170

5171

5172

5173

5174

5175

5176

5177

5178

5179

5180

5181

5182

5183

5184

5185

5186

5187

5188

5189

5190

5191

5192

5193

5194

5195

5196

5197

5198

5199

5200

5201

5202

5203

5204

5205

5206

5207

5208

5209

5210

5211

5212

5213

5214

5215

5216

5217

5218

5219

5220

5221

5222

5223

5224

5225

5226

5227

5228

5229

5230

5231

5232

5233

5234

5235

5236

5237

5238

5239

5240

5241

5242

5243

5244

5245

5246

5247

5248

5249

5250

5251

5252

5253

5254

5255

5256

5257

5258

5259

5260

5261

5262

5263

5264

5265

5266

5267

5268

5269

5270

5271

5272

5273

5274

5275

5276

5277

5278

5279

5280

5281

5282

5283

5284

5285

5286

5287

5288

5289

5290

5291

5292

5293

5294

5295

5296

5297

5298

5299

5300

5301

5302

5303

5304

5305

5306

5307

5308

5309

5310

5311

5312

5313

5314

5315

5316

5317

5318

5319

5320

5321

5322

5323

5324

5325

5326

5327

5328

5329

5330

5331

5332

5333

5334

5335

5336

5337

5338

5339

5340

5341

5342

5343

5344

5345

5346

5347

5348

5349

5350

5351

5352

5353

5354

5355

5356

5357

5358

5359

5360

5361

5362

5363

5364

5365

5366

5367

5368

5369

5370

5371

5372

5373

5374

5375

5376

5377

5378

5379

5380

5381

5382

5383

5384

5385

5386

5387

5388

5389

5390

5391

5392

5393

5394

5395

5396

5397

5398

5399

5400

5401

5402

5403

5404

5405

5406

5407

5408

5409

5410

5411

5412

5413

5414

5415

5416

5417

5418

5419

5420

5421

5422

5423

5424

5425

5426

5427

5428

5429

5430

5431

5432

5433

5434

5435

5436

5437

5438

5439

5440

5441

5442

5443

5444

5445

5446

5447

5448

5449

5450

5451

5452

5453

5454

5455

5456

5457

5458

5459

5460

5461

5462

5463

5464

5465

5466

5467

5468

5469

5470

5471

5472

5473

5474

5475

5476

5477

5478

5479

5480

5481

5482

5483

5484

5485

5486

5487

5488

5489

5490

5491

5492

5493

5494

5495

5496

5497

5498

5499

5500

5501

5502

5503

5504

5505

5506

5507

5508

5509

5510

5511

5238

Shortest path

5239

- **QUERY:** Given a graph representation, your task is to compute shortest path between the specified two nodes

5240

And the graph representation of Adjacency List is : {0: [8, 4, 3, 2, 5, 1, 6], 8: [0], 4: [0], 3: [0], 2: [0], 5: [0], 1: [0], 6: [0]}

5241

Q: Give the shortest path from node 5 to node 8.

5242

A: The shortest path from node 5 to node 8 is 5,0,8.

5243

Given a graph representation, your task is to compute shortest path between the specified two nodes

5244

And the graph representation of Adjacency List is : {0: [1], 1: [0, 2, 3, 4, 5, 6, 8], 2: [1, 7], 3: [1], 4: [1], 5: [1], 6: [2], 7: [2], 8: [1]}

5245

Q: Give the shortest path from node 3 to node 7.

5246

A: The shortest path from node 3 to node 7 is 3,1,2,7.

5247

Given a graph representation, your task is to compute shortest path between the specified two nodes

5248

And the graph representation of Adjacency List is : {3: [1, 7, 4, 6], 1: [3, 2, 7, 6, 5], 8: [0, 4, 2, 6, 5, 7], 0: [8, 6, 2, 7], 6: [0, 5, 4, 8, 7, 1, 3], 7: [3, 5, 0, 6, 1, 8], 5: [7, 6, 2, 8, 1], 4: [6, 8, 3], 2: [1, 8, 5, 0]}

5249

Q: Give the shortest path from node 4 to node 2.

5250

A: The shortest path from node 4 to node 2 is 4,8,2.

5251

Given a graph representation, your task is to compute shortest path between the specified two nodes

5252

And the graph representation of Adjacency List is : {0: [6, 7], 6: [0], 7: [0, 1, 3], 1: [5, 7], 5: [1], 2: [4], 4: [2, 3], 3: [4, 7]}

5253

Q: Give the shortest path from node 6 to node 5.

5254

A: The shortest path from node 6 to node 5 is 6,0,7,1,5.

5255

Given a graph representation, your task is to compute shortest path between the specified two nodes

5256

And the graph representation of Adjacency List is : {0: [1, 2, 4, 5], 1: [0, 2, 3, 6], 2: [0, 1, 3, 5], 3: [1, 2, 4], 4: [3, 0], 5: [0, 2, 6], 6: [1, 5]} Q: Give the shortest path from node 6 to node 0.

5257

A: The shortest path from node 6 to node 0 is 6,1,0.

5258

Given a graph representation, your task is to compute shortest path between the specified two nodes.

5259

And the graph representation of: Adjacency List is {0: [1, 2], 1: [0, 2, 3, 5, 6, 7], 2: [1, 0, 3, 4, 5], 3: [2, 1, 4, 7], 4: [2, 3, 6], 5: [1, 2], 6: [4, 1], 7: [1, 3]}

5260

Q: Give the shortest path from node 3 to node 2.

5261

A:

- **TASK INFO:** shortest path, easy, k-shot, Adjacency List
- **MODEL:** Qwen-2.5
- **ACCURACY:** 0
- **STARTING AND ENDING NODE:** 3, 2
- **ANSWER:**

5262

the shortest path from node 3 to node 2 is 3,1,2.

5263

5264

5265

5266

5267

5268

5269

5270

5271

5272

5273

5274

5275

5276

5277

5278

5279

5280

5281

5282

5283

5284

5285

5286

5287

5288

5289

5290

5291

5292

Shortest path

5293

5294

5295

5296

5297

5298

5299

5300

5301

5302

5303

5304

5305

5306

5307

5308

5309

5310

5311

5312

5313

5314

5315

5316

5317

5318

5319

5320

5321

5322

5323

5324

5325

5326

5327

5328

5329

5330

5331

5332

5333

5334

5335

5336

5337

5338

5339

5340

5341

5342

5343

5344

5345

- **QUERY:** Given a graph representation, your task is to compute shortest path between the specified two nodes.

And the graph representation of: GraphML is <?xml version='1.0' encoding='utf-8'?> <graphml xmlns="http://graphml.graphdrawing.org/xmlns" xmlns:xsi="http://www.w3.org/2001/XMLSchema-instance" xsi:schemaLocation="http://graphml.graphdrawing.org/xmlns http://graphml.graphdrawing.org/xmlns/1.0/graphml.xsd"><graph edgedefault="undirected"><node id="0"/>

<node id="1"/>

<node id="2"/>

<node id="3"/>

<node id="4"/>

<node id="5"/>

<node id="6"/>

<edge source="0" target="1"/>

<edge source="0" target="2"/>

<edge source="0" target="3"/>

<edge source="0" target="6"/>

<edge source="3" target="4"/>

<edge source="3" target="5"/>

</graph></graphml>

Q: Give the shortest path from node 2 to node 1.

A:

Let's construct a graph with the nodes and edges first:

- **TASK INFO:**

shortest path, easy, 0-Instruct, GraphML

- **MODEL:** Qwen-2.5

- **ACCURACY:** 0

- **STARTING AND ENDING NODE:** 2, 1

- **ANSWER:**

- nodes: 0, 1, 2, 3, 4, 5, 6 - edges: (0, 1), (0, 2), (0, 3), (0, 6), (3, 4), (3, 5)

now, we want to find the shortest path from node 2 to node 1.

we can use the breadth-first search (bfs) algorithm to find the shortest path in an unweighted graph.

bfs traversal of the graph starting from node 2:

1. start at node 2 2. visit node 0 (since it's directly connected to node 2) 3. visit nodes 1, 3, and 6 (all directly connected to node 0)

since node 1 is one of the visited nodes, the shortest path from node 2 to node 1 is:

2 -> 0 -> 1

you are an ai assistant. user will provide you with a task. your goal is to complete the task as faithfully as you can. you will ask for clarification in cases where the task is not clear. you will not make any assumptions and you will not introduce any information not provided in the input.

5346

Shortest path

5347

5348

5349

- **QUERY:** Given a graph representation, your task is to compute shortest path between the specified two nodes

5350

And the graph representation of Adjacency Set is : {0: {1, 2, 3, 4, 5, 6, 8}, 8: {0}, 4: {0}, 3: {0}, 2: {0}, 5: {0}, 1: {0}, 6: {0}}

5351

Let's construct a graph with the nodes and edges first.

5352

Q: Give the shortest path from node 5 to node 8.

5353

A: To find the shortest path from node 5 to node 8, let's explore the graph: Node 5 is directly connected to node 0 (via the edge 0 5). Node 0 is directly connected to node 8 (via the edge 0 8). Thus, the shortest path from node 5 to node 8 is 5,0,8.

5354

...

5355

Given a graph representation, your task is to compute shortest path between the specified two nodes.

5356

And the graph representation of: Adjacency Set is

5357

{3: {8, 9, 6}, 8: {1, 2, 3, 4}, 4: {8, 9, 6, 7}, 6: {1, 2, 3, 4}, 1: {8, 9, 10, 6}, 2: {8, 9, 10, 6}, 10: {0, 1, 2}, 9: {0, 1, 2, 3, 4}, 7: {4}, 0: {9, 10, 5}, 5: {0}}

5358

Let's construct a graph with the nodes and edges first.

5359

Q: Give the shortest path from node 6 to node 5.

5360

A:

- **TASK INFO:** shortest path, medium, Instruct, Adjacency Set

5361

- **MODEL:** claude-3-5-sonnet-20241022

5362

- **ACCURACY:** 1

5363

- **STARTING AND ENDING NODE:** 6, 5

5364

- **ANSWER:**

5365

Let me help find the shortest path from node 6 to node 5 in this graph.

5366

Let's analyze the possible paths: 1. Node 6 is connected to nodes 1, 2, 3, and 4 2. To reach node 5, we need to go through node 0 (as node 5 is only connected to node 0) 3. To reach node 0, we can go through either node 9 or node 10 4. From node 6: - We can reach node 1 or node 2, which both connect to nodes 9 and 10 - Through node 9 or 10, we can reach node 0 - From node 0, we can reach node 5

5367

The shortest path would be:

5368

6 → 1 → 9 → 0 → 5

5369

or

5370

6 → 2 → 9 → 0 → 5

5371

(both paths have the same length)

5372

The shortest path is 6,1,9,0,5

5373

5374

5375

5376

5377

5378

5379

5380

5381

5382

5383

5384

5385

5386

5387

5388

5389

5390

5391

5392

5393

5394

5395

5396

5397

5398

5399

5400

Shortest path

5401

• **QUERY:**

5402

Given a graph representation, your task is to compute shortest path between the specified two nodes. And the graph representation of: Edge List is

5403

0 1

5404

2 0

5405

3 0

5406

0 4

5407

2 5

5408

6 1

5409

7 0

5410

8 2

5411

4 8

5412

9 0

5413

9 4

5414

10 0

5415

11 4

5416

Q: Give the shortest path from node 1 to node 2. A: Let's think step by step:

5417

- **TASK INFO:** shortest path,medium,0-CoT,Edge List

5418

- **MODEL:** o4-mini-2025-04-16

5419

- **ACCURACY:** 1

5420

- **STARTING AND ENDING NODE:** 1, 2

5421

- **ANSWER:** We can use a breadth-first search starting from node 1:

5422

1. Start at node 1. Neighbors are 0, 6, 2. Visit node 0 (distance 1). Its neighbors are 1, 2, 3, 4, 7, 9, 10. We discover node 2 here. 3. We stop as soon as we reach node 2.

5423

Reconstructing the path gives $1 \rightarrow 0 \rightarrow 2$.

5424

The shortest path from node 1 to node 2 is 1,0,2.

5425

5426

5427

5428

5429

5430

5431

5432

5433

5434

5435

E.6 MORE FINDINGS FROM EVALUATION RESULTS

5436

5437

5438

Finding ④: Serialization exhibits task-dependent effects, with both open-source and closed-source models excelling at concise and structured representations. From Tables 18 and 21, the formats most suitable for open-source and closed-source models vary across tasks such as Diameter calculation, Triangle counting, Shortest path and Cycle detection. In open-source models, nearly every task exhibits a preference for a distinct format. In contrast, closed-source models tend to perform well with formats such as *Adjacency List (AL)* and *Adjacency Set (AS)*, yet *Graph Markup Language (GMaL)* also achieves superior performance in certain tasks. Taking the Cycle detection benchmark as an example, the *Edge Set (ES)* format outperforms other alternatives, whereas in closed-source models, formats like *Graph Markup Language (GMaL)* demonstrate marked advantages. Such task-specific preferences for serialization formats further highlight the importance and significance of GRAPHOMNI.

5439

5440

5441

5442

5443

5444

5445

5446

5447

5448

5449

5450

5451

5452

5453

Finding ⑤: Complex multi-step prompts can negatively impact the performance of closed-source models. In the Triangle counting task, open-source models performed very well with more examples in *Instruct* and *k-shot* scenario, while closed-source models excelled using minimal prompting strategies such as *0-Algorithm*, which avoid elaborate reasoning steps or intermediate explicit guidance (Tables 17, 20 in Appendix E.1). This pattern suggests that complex or abstract multi-step prompts can confound closed-source models in certain challenging tasks.

5454
5455

E.7 ANALYSIS ON EFFICIENCY VIA NUMBER OF OUTPUT TOKENS

5456
5457
5458
5459
5460
5461
5462

To assess inference efficiency, we measure the total number of output tokens each model produces—tokenized consistently with the OpenAI GPT-3.5-turbo tokenizer¹—and analyze how token counts vary across four key dimensions: difficulty levels (Table 23), task categories (Table 24), serialization formats (Table 25), and prompt schemes (Table 26). The average token counts under each condition are reported in these tables, together with the main results of accuracy, providing a comprehensive view of the trade-offs between output verbosity and model performance across our benchmark.

5463
5464

E.7.1 OVERALL ANALYSIS

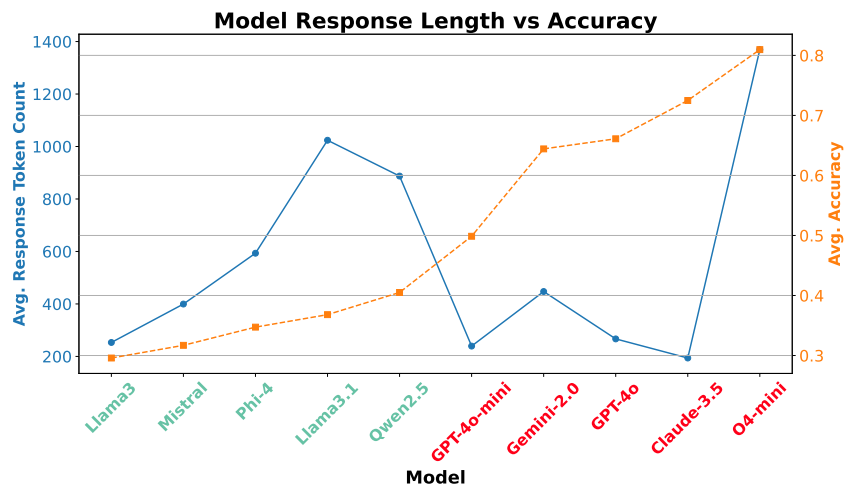
5465
5466
5467
5468
5469
5470
5471
5472
5473
5474
5475
5476
5477
5478
5479
54805481
5482
5483
5484

Figure 32: **Average output tokens versus overall accuracy across all graph-theoretic tasks.** Models are ordered by the average performance. Models in **Green** are open-source models while others in **Red** are closed-source ones.

5485
5486
5487
5488
5489
5490
5491
5492
5493

Figure 32 highlights two distinct patterns. **Closed-source models**—GPT-4o, Claude-3.5, and Gemini-2.0—achieve the highest accuracy while keeping total output below roughly 300 tokens, showing tight control over generation length. **o4-mini**, a reasoning-focused model stands out: its final answers remain short (about 100 tokens), but it adds a lengthy chain-of-thought (up to 1.6 K tokens), yielding strong accuracy with markedly larger overall output. **Open-source models** display a different trend. Llama-3.1 and Qwen-2.5 match the best accuracies only when they generate much longer responses, whereas Llama-3 and Mistral remain shorter and less accurate. These contrasts persist across difficulty levels, task categories, serialization formats, and prompt schemes, as detailed in Tables 23–26.

5494

E.7.2 ANALYSIS CONCERNING DIFFICULTY OF TASK

5495
5496
5497
5498
5499

Table 23: **Average output tokens per model at each difficulty level (Easy, Medium, Hard).** Orange / Blue / Light purple highlights indicate the largest/second-largest/third-largest number of output tokens.

Difficulty	Llama-3 (8B)	Llama-3.1 (8B)	Mistral (7B)	Phi-4 (14B)	Qwen-2.5 (7B)	Claude-3.5	GPT-4o	GPT-4o-mini	Gemini-2.0	o4-mini		Average
										Answer	Reasoning	
easy	210.51	1050.08	375.91	517.31	881.82	198.82	257.17	248.50	440.26	143.87	841.68	469.63
hard	292.46	994.80	419.36	644.85	873.01	182.71	263.71	217.44	411.54	70.25	1660.83	548.27
medium	267.18	1018.81	408.88	632.09	903.56	197.35	278.82	246.52	481.29	120.70	1367.97	538.47
Average	256.72	1021.23	401.38	598.08	886.13	192.96	266.57	237.49	444.37	111.61	1290.16	-

5504
5505
5506
5507

Table 23 presents the token output across different models under varying levels of task difficulty. Overall, most models exhibit small variation in output length as task difficulty increases. However, a

¹Note that the number of the reasoning of o4-mini is obtained from the metadata of each API call.

5508 notable exception is the reasoning model, which demonstrates a distinct pattern: as task difficulty
 5509 rises, the number of tokens in the final answer tends to decrease, while the length of the reasoning
 5510 process correspondingly increases.

5512 E.7.3 ANALYSIS CONCERNING TASK TYPE

5514 **Table 24: Average output tokens per model for each graph-theoretic task.**
 5515 Orange / Blue / Light purple highlights indicate the largest/second-largest/third-largest number of
 5516 output tokens.

5518 Task type	Llama-3 (8B)	Llama-3.1 (8B)	Mistral (7B)	Phi-4 (14B)	Qwen-2.5 (7B)	Claude-3.5	GPT-4o	GPT-4o-mini	Gemini-2.0	o4-mini		Average
										Answer	Reasoning	
BFS order	288.58	897.44	394.37	582.88	859.08	243.48	511.06	435.15	638.90	269.69	1666.66	617.03
Connectivity	176.60	919.75	375.53	565.78	630.62	133.71	154.63	130.19	137.39	96.13	547.11	351.59
Cycle detection	266.47	828.07	362.82	477.68	735.21	176.49	132.92	125.41	118.81	100.38	564.12	353.49
Diameter calculation	269.48	878.37	391.86	502.67	792.25	236.41	259.02	285.96	513.27	81.00	1839.11	549.95
Shortest path	286.65	1839.88	525.77	946.46	1491.21	127.57	149.54	187.84	351.89	91.59	735.50	612.17
Triangle counting	231.02	768.90	347.19	489.85	802.21	246.97	424.23	295.00	925.66	80.55	2156.73	615.30
Average	253.13	1022.07	399.59	594.22	885.10	194.11	271.90	243.26	447.66	119.89	1251.54	-

5524 Further insights can be drawn from Table 24, which reveals a clear correlation between output
 5525 tokens and task type. Specifically, tasks such as Connectivity and Cycle detection consistently
 5526 yield significantly shorter outputs compared to other tasks, as they are relatively easier compared
 5527 to others. Among open-source models, the Shortest path task results in the longest outputs,
 5528 whereas for closed-source models, the BFS order and Triangle counting task generate the highest
 5529 average token counts. In the case of the reasoning model, the token output associated with the
 5530 reasoning process increases markedly with the complexity and difficulty of the task—particularly
 5531 when considering task accuracy. For instance, in the Triangle counting task, the reasoning
 5532 component alone produces an average of over 2000 tokens, highlighting the model’s tendency to
 5533 elaborate more extensively as task complexity increases.

5535 E.7.4 ANALYSIS CONCERNING SERIALIZATION FORMATS

5537 **Table 25: Average output tokens per model under different serialization formats.**
 5538 Orange / Blue / Light purple highlights indicate the largest/second-largest/third-largest number
 5539 of output tokens.

5541 Serialization format	Llama-3 (8B)	Llama-3.1 (8B)	Mistral (7B)	Phi-4 (14B)	Qwen-2.5 (7B)	Claude-3.5	GPT-4o	GPT-4o-mini	Gemini-2.0	o4-mini		Average
										Answer	Reasoning	
Adjacency List	260.58	958.19	393.76	505.19	792.85	199.83	280.26	234.54	455.60	123.91	1118.90	483.96
Adjacency Matrix	288.42	897.05	400.13	555.10	862.35	198.44	291.62	243.48	536.80	105.28	1535.59	537.66
Adjacency Set	256.95	962.41	390.89	509.12	787.49	199.17	284.96	237.48	497.91	119.09	1144.19	489.97
Edge List	239.61	930.70	383.71	526.96	805.14	195.93	267.44	261.68	445.74	117.61	1260.25	494.07
Edge Set	246.07	914.69	405.22	511.70	823.50	203.51	285.23	269.78	497.43	114.47	1282.32	504.90
Graph Modelling Language	267.75	853.42	335.60	544.70	787.79	181.31	221.91	180.38	339.59	114.18	1238.94	460.51
GraphML	212.87	1650.01	487.76	1000.29	1351.85	179.31	235.97	248.29	358.25	114.39	1195.50	639.50
Average	253.18	1023.78	399.58	593.29	887.28	193.93	266.77	239.38	447.33	115.56	1253.67	-

5548 Table 25 presents the influence of different graph serialization formats on the number of output
 5549 tokens generated by various models. Overall, more complex formats—such as GMaL and Adjacency
 5550 Matrix—tend to induce longer outputs, whereas simpler formats—such as Adjacency List and Edge
 5551 List—are associated with significantly shorter outputs. Among the evaluated models, open-source
 5552 models such as Llama-3.1 and Qwen-2.5 consistently produce a higher number of tokens across most
 5553 formats. This effect is particularly pronounced for Llama-3.1 under the GMaL format, where its
 5554 output length reaches a peak. In contrast, closed-source models generally yield more concise outputs,
 5555 with Claude-3.5 being especially compact. An exception is observed in o4-mini, whose output length
 5556 is substantially higher due to the inclusion of intermediate reasoning steps.

5558 E.7.5 ANALYSIS CONCERNING PROMPT SCHEMES

5559 Table 26 further examines the impact of different prompting strategies on model output. Prompts
 5560 that involve reasoning or instruction (e.g., CoT, Instruct, and 0-Instruct) significantly increase output
 5561 length, a trend that is particularly salient in open-source models. For instance, under the 0-Instruct
 5562 prompt, both Llama-3.1 and o4-mini produce extended outputs. In contrast, prompts with no

5562 Table 26: **Average output tokens per model for each prompt scheme.**
 5563 Orange / Blue / Light purple highlights indicate the largest/second-largest/third-largest number of
 5564 output tokens.
 5565

Prompt Scheme	Llama-3 (8B)	Llama-3.1 (8B)	Mistral (7B)	Phi-4 (14B)	Qwen-2.5 (7B)	Claude-3.5	GPT-4o	GPT-4o-mini	Gemini-2.0	o4-mini	Average
										Answer	Reasoning
0-Algorithm	283.43	1071.04	484.71	434.10	953.42	206.22	305.95	237.04	684.95	123.07	1223.52
0-CoT	308.61	1114.37	346.42	145.13	763.46	221.08	385.55	386.72	558.95	156.72	1223.45
0-Instruct	308.80	1151.98	391.51	643.39	690.56	204.07	334.83	370.93	544.26	137.55	1229.01
Algorithm	202.15	964.36	456.40	815.85	946.63	215.10	245.75	225.96	349.02	120.56	1313.74
CoT	192.88	916.17	378.05	851.34	1042.81	164.95	154.63	203.33	253.13	92.06	1271.55
Instruct	212.82	987.20	355.99	917.42	1043.12	176.66	169.42	210.20	255.77	119.57	1302.98
LTM	303.64	1116.18	405.24	361.22	694.98	205.71	347.82	339.98	579.05	142.44	1239.87
K-Shot	160.98	760.10	440.39	1024.57	1009.45	170.52	196.37	39.37	270.99	67.35	1277.14
o-shot	305.27	1133.08	337.44	146.16	841.05	181.03	260.59	140.92	529.71	80.78	1201.01
Average	253.18	1023.83	399.57	593.24	887.27	193.93	266.77	239.38	447.32	115.56	1253.59

5567
 5568 instruction (0-shot) or few-shot examples (K-Shot) tend to yield shorter outputs. Closed-source
 5569 models exhibit relatively stable output lengths across prompt types, suggesting stronger control over
 5570 generation behavior.
 5571

E.7.6 COST-ACCURACY TRADEOFF ANALYSIS

5572 Table 27: Per-Query Inference Cost Analysis. Costs are calculated based on current
 5573 API pricing (as of November 2025) with average input tokens of 933 per query.
 5574 **Bold orange** / Underlined blue / Light purple highlights indicate lowest/second-lowest/third-
 5575 lowest cost in each category.
 5576

Model	Input Cost (\$)	Output Cost (\$)	Total Cost (\$)
<i>Open-Source Models</i>			
Llama-3.1 (8B)	0.000019	<u>0.000031</u>	0.000049
Mistral (7B)	0.000187	0.000080	0.000267
Phi-4 (14B)	<u>0.000056</u>	0.000084	<u>0.000140</u>
Qwen-2.5 (7B)	0.000037	0.000089	0.000126
<i>Closed-Source Models</i>			
Claude-3.5	0.002799	0.002894	0.005694
GPT-4o	0.002333	0.002666	0.004998
GPT-4o-mini	<u>0.000140</u>	0.000142	<u>0.000282</u>
Gemini-2.0	0.000093	0.000178	0.000271
o4-mini	0.001026	0.006168	0.007194

5600 Table 27 presents per-query inference costs based on current API pricing. Cost varies by three orders
 5601 of magnitude across models, ranging from \$0.000049 (Llama-3/Llama-3.1) to \$0.007194 (o4-mini)
 5602 per query. Open-source models uniformly cost less than \$0.0003 per query, while closed-source
 5603 models span from \$0.000271 (Gemini-2.0) to \$0.007194 (o4-mini).
 5604

5605 Figure 33 visualizes the cost-(mean) accuracy tradeoff on all tasks. o4-mini achieves the highest
 5606 accuracy (80.96%) but incurs the highest cost. Notably, no model dominates across all metrics.
 5607 The optimal choice depends on application requirements: open-source models for cost-sensitive
 5608 deployments with relaxed accuracy constraints, Gemini-2.0 or GPT-4o-mini for balanced cost-
 5609 performance, Claude-3.5 or GPT-4o for high-accuracy applications, and o4-mini when maximizing
 5610 accuracy justifies premium costs. For full benchmark evaluation (241,726 queries), total costs range
 5611 from \$11.85 (Llama-3) to \$1,739 (o4-mini), a 147× difference that has significant implications for
 5612 large-scale graph reasoning deployments.
 5613

F DETAILED RELATED WORKS

5614 Integrating LLMs with graph-structured data merges linguistic reasoning capabilities with structural
 5615 representation insights. While comprehensive discussions on LLM-graph integration can be found in

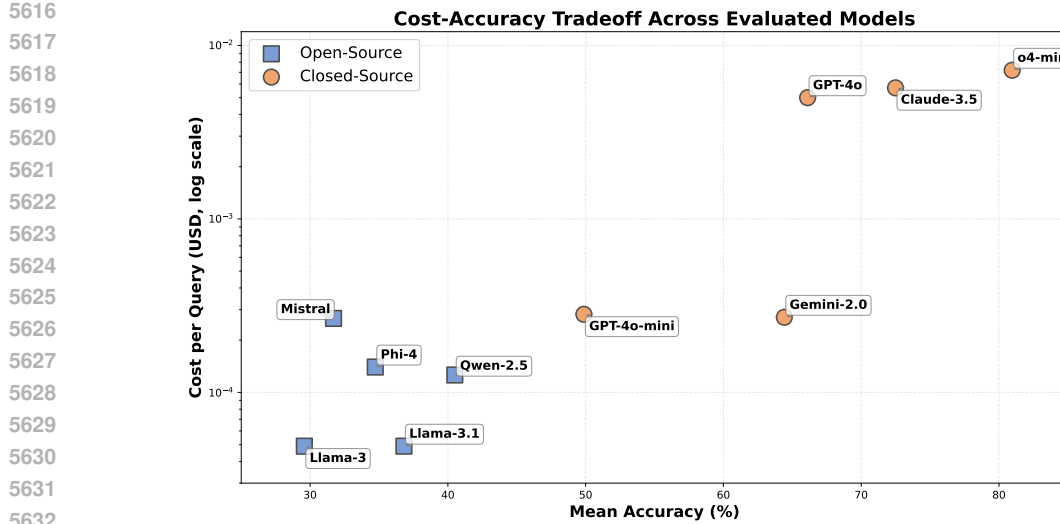


Figure 33: Cost-accuracy tradeoff across evaluated models on average. Each point represents a model’s mean accuracy versus per-query inference cost (log scale).

Appendix F.1, recent benchmarks specifically targeting LLM applications for graph reasoning, such as LLM4DyG (Zhang et al., 2024b), GraphTMI (Das et al., 2024), GraphInstruct (Luo et al., 2024b), and MAGMA (Taylor et al., 2024), have highlighted substantial progress and persistent limitations. These benchmarks reveal issues including narrow graph diversity, scalability constraints, and pronounced sensitivity to input formatting. Studies on graph pattern comprehension and multi-hop reasoning (Dai et al., 2024; Wang et al., 2023; Jin et al., 2024b) further emphasize brittleness under complex or noisy data conditions. Empirical analyses conducted by GPT4Graph (Guo et al., 2024a) and GraphWiz (Chen et al., 2024a) underscore performance gaps relative to specialized graph models and highlight computational inefficiencies. Additionally, recent contributions through transformer scaling studies (Sanford et al., 2024), comprehensive benchmarks like GraphFM (Xu et al., 2024) and GLBench (Li et al., 2024d), and specialized datasets (Yan et al., 2023; Fatemi et al., 2024) have provided valuable yet often limited insights. ProGraph (Li et al., 2024b) offers innovation but introduces extra computational overhead due to external dependencies. A detailed summary of these benchmark-related works is available as follows.

F.1 LLM APPLICATIONS ON GRAPH DATA

The intersection of LLMs and graph-structured data has emerged as an active research domain, combining the nuanced contextual reasoning abilities of LLMs with the structural representational power of traditional Graph Neural Networks (GNNs). Initial studies addressed fundamental challenges such as reducing sensitivity to prompt formulation (Sclar et al., 2024) and enabling zero-shot cross-dataset transferability (Li et al., 2024c). These foundational efforts have supported the development of generative models that jointly leverage textual and structural graph information, creating unified semantic embeddings for enhanced performance (Wang et al., 2024b; Fang et al., 2025b; Li et al., 2024a; Kong et al., 2024).

Subsequent research built upon these foundations by focusing on enhancing the robustness of LLMs when applied to graph tasks (Guo et al., 2024b) and advancing techniques for effectively translating complex graph structures into natural language, notably through methods like graph-syntax trees (Zhao et al., 2023). Recent advancements have directly embedded graph reasoning capabilities within LLM architectures, significantly extending their application beyond purely textual domains (Hu et al., 2023). In this context, specific methodologies have been developed, embedding graph learning modules and leveraging instruction tuning for improved alignment between structural data and LLM input modalities (Chai et al., 2023; Tang et al., 2024).

Parallel efforts have provided extensive overviews of the evolving field through comprehensive surveys (Li et al., 2023; Jin et al., 2024a), highlighting foundational concepts such as Graph Foundation

5670 Models that employ dedicated graph vocabularies for effective cross-domain learning (Mao et al.,
 5671 2024). Concurrently, advances in parameter-efficient encoding techniques, exemplified by GraphTo-
 5672 ken (Perozzi et al., 2024), and retrieval-augmented frameworks such as G-Retriever (He et al., 2024),
 5673 have further refined the processing and utilization of graph structures. Moreover, assistant-based
 5674 frameworks employing instruction-tuning strategies, including LLaGA (Chen et al., 2024b) and
 5675 InstructGraph (Wang et al., 2024a), demonstrated significant potential for enabling LLMs to produce
 5676 high-quality graph-structured outputs through preference-aligned interactions.

5677 Complementing these directions, significant innovations have emerged within graph representation
 5678 learning, exemplified by models like OpenGraph (Xia et al., 2024) and MuseGraph (Tan et al.,
 5679 2024), which integrate scalable transformers, data augmentation, and graph-specific instruction
 5680 tuning for robust zero-shot performance and general graph mining applications. Additional methods
 5681 employing compact node identifiers (Luo et al., 2024a) and attributed random walks for fine-tuning
 5682 (Tan et al., 2023) have notably improved inference efficiency, collectively illustrating a coherent
 5683 evolution towards integrated frameworks that effectively harness the combined strengths of LLMs
 5684 and graph-centric approaches.

5685 F.2 BENCHMARKS ON LLM APPLICATION TO GRAPH DATA

5686 Recent benchmarks assessing LLM capabilities on graph reasoning tasks have significantly advanced
 5687 understanding yet still present important limitations. Benchmarks such as LLM4DyG (Zhang et al.,
 5688 2024b), which emphasizes spatial-temporal dynamics, typically neglect the complexity inherent to
 5689 static graph structures. Similarly, GraphTMI (Das et al., 2024), exploring various graph input modalities
 5690 (text, motif, image), has exposed inherent trade-offs between token efficiency and representational
 5691 expressiveness, potentially impacting scalability.

5692 Other benchmarks, including GraphInstruct (Luo et al., 2024b) and MAGMA (Taylor et al., 2024),
 5693 incorporate traditional graph reasoning tasks with explanatory strategies but remain limited by
 5694 small-scale graph sizes and lack comprehensive coverage across diverse graph structures. Studies
 5695 specifically targeting graph pattern recognition and natural-language-based graph problem-solving
 5696 (Dai et al., 2024; Wang et al., 2023) have further revealed pronounced sensitivity to input formats,
 5697 resulting in brittleness under complex or noisy conditions. Additionally, frameworks designed to
 5698 mitigate multi-hop reasoning inaccuracies through graph-centric reasoning chains (Jin et al., 2024b)
 5699 and examinations of generalization beyond memorized patterns (Zhang et al., 2024a) continue to
 5700 illustrate significant unresolved challenges.

5701 Empirical assessments conducted by initiatives such as GPT4Graph (Guo et al., 2024a) and instruction-
 5702 tuned benchmarks like GraphWiz (Chen et al., 2024a) highlight persistent performance gaps com-
 5703 pared to specialized graph neural architectures, accompanied by elevated computational demands.
 5704 More recent contributions, including scaling analyses of transformer models (Sanford et al., 2024),
 5705 comprehensive benchmarks like GraphFM (Xu et al., 2024) and GLBench (Li et al., 2024d), and
 5706 specialized datasets such as CS-TAG (Yan et al., 2023) and encoding studies (Fatemi et al., 2024),
 5707 have substantially enriched the literature but remain constrained by challenges related to homogeneity,
 5708 training inefficiencies, and limited scalability. While innovative, solutions such as ProGraph (Li et al.,
 5709 2024b), employing programming-based integration and external API retrieval, introduce additional
 5710 computational overhead and dependencies.

5711 G LIMITATIONS AND FUTURE DIRECTIONS OF GRAPHOMNI

5712 While GRAPHOMNI significantly advances the evaluation of large language models (LLMs) on
 5713 graph-theoretic tasks, several considerations highlight opportunities for future enhancement:

- 5714 • **Diversity of Tasks:** The benchmark presently includes key canonical tasks, which may not
 5715 fully represent the diversity of graph-related problems encountered in practice. Expanding
 5716 the task set to include dynamic, temporal, or heterogeneous graph challenges could
 5717 offer deeper insights into model performance. Future work should focus on defining and
 5718 integrating tasks that capture evolving network structures and multi-relational data.
- 5719 • **Generalizability of Findings:** GRAPHOMNI evaluates LLMs under controlled experimental
 5720 conditions, which might not entirely reflect performance in less structured, real-world
 5721 environments.

environments. Future work could include testing the generalizability of models across various practical conditions, such as noisy data, incomplete graphs, or domain-specific variations, to better understand the robustness and applicability of LLMs.

Addressing these aspects will further enhance the robustness, applicability, and inclusivity of GRAPHOMNI, fostering wider adoption and deeper insights into LLM performance.

H ADDITIONAL ABLATION STUDIES

H.1 PERFORMANCE VS. TIME COMPLEXITY OF TASKS

H.1.1 TIME COMPLEXITY ANALYSIS

The time complexities are determined based on well-established algorithms in graph theory (we are aware more efficient algorithms are available, especially for Diameter calculation and Triangle counting, but we use the most naive implementations since they typically reflect how LLMs approach these tasks):

- **Connectivity:** $O(V + E)$ — Determined via a single breadth-first search (BFS) or depth-first search (DFS) traversal starting from one node to check reachability to another node.
- **Cycle detection:** $O(V + E)$ — Implemented using DFS with back-edge detection; each node and edge is visited at most once.
- **BFS order:** $O(V + E)$ — Standard breadth-first traversal visits each node once and examines each edge once.
- **Shortest path:** $O(V + E)$ for unweighted graphs using BFS, or $O(E + V \log V)$ for weighted graphs using Dijkstra’s algorithm. Since our benchmark uses unweighted graphs, we report $O(V + E)$.
- **Diameter calculation:** $O(V(V + E))$ — Requires computing all-pairs shortest paths, typically achieved by running BFS from each node, resulting in $O(V)$ BFS operations each costing $O(V + E)$.
- **Triangle counting:** $O(V^3)$ naively by checking all triplets of nodes, or $O(V \cdot d_{\text{avg}}^2)$ with neighbor-based enumeration where d_{avg} is the average degree. For dense graphs or without optimizations, this remains the most computationally intensive task.

H.1.2 ALIGNMENT ANALYSIS

Tables 28, 29, and 30 demonstrate partial alignment between computational complexity and LLM difficulty. At the extremes, correspondence is clear: Triangle counting ($O(V^3)$) achieves only 15.45% accuracy (closed-source, Hard) and 6.77% (open-source, Hard), while Connectivity ($O(V + E)$) reaches 91.90% and 75.97% respectively. Similarly, Diameter calculation ($O(V(V + E))$) yields 40.09% (closed-source) and 21.33% (open-source), ranking as the second-hardest task both algorithmically and empirically.

However, among tasks with identical $O(V + E)$ complexity, performance diverges substantially. Connectivity maintains 91.90% accuracy on hard instances, while BFS order collapses to 27.15%, a 64.75 percentage point gap despite equivalent asymptotic complexity. This divergence indicates that computational complexity alone does not determine LLM difficulty.

H.1.3 FACTORS BEYOND COMPUTATIONAL COMPLEXITY

Three task characteristics account for this divergence. First, **output structure** critically impacts performance: binary decisions (Connectivity, Cycle detection) achieve 91.90% and 79.24%, while sequence generation (BFS order) and numerical enumeration (Triangle counting, Diameter calculation) fall to 27.15%, 15.45%, and 40.09% respectively. Second, **error propagation** varies by task type—sequence tasks suffer cascading failures where single errors invalidate entire outputs, as evidenced by BFS order’s severe 62.52% performance drop. Third, **reasoning scope** distinguishes task difficulty: local reasoning tasks (Connectivity, Cycle detection) degrade minimally (4.31%,

2.74%), while global reasoning tasks requiring complete graph traversal (Diameter calculation, BFS order) drop sharply (41.34%, 62.52%).

Table 30 quantifies these effects: open-source models degrade 16.93% on average from Easy to Hard, while closed-source models drop 26.26%. Crucially, this degradation correlates more strongly with reasoning scope and output structure than with algorithmic complexity—BFS order ($O(V + E)$) degrades more severely than Diameter calculation ($O(V(V + E))$), demonstrating that maintaining sequential dependencies in textual representations poses greater challenges than computational intensity per se.

H.1.4 CONCLUSION

Our analysis reveals that computational complexity establishes a baseline for LLM difficulty, as evidenced by Triangle counting and Diameter calculation ranking as both algorithmically expensive and empirically challenging. However, output structure and reasoning scope play equally critical roles. The 64.75 percentage point gap between Connectivity and BFS order—both $O(V + E)$ tasks—demonstrates that LLMs struggle disproportionately with maintaining long-range sequential dependencies, performing combinatorial enumeration, and generating outputs under strict ordering constraints. These limitations manifest independently of algorithmic complexity and persist across all evaluated models (Tables 28–30), indicating fundamental constraints in how current LLM architectures encode and manipulate graph-structured information through natural language representations.

Table 28: Open-Source LLM Performance Across Tasks Ranked by Computational Complexity (Mean Accuracy %). **Bold orange** / Underlined blue / Light purple highlights indicate best/second-best/third-best performance in each difficulty level.

Task	Time Complexity	Easy (5–10 nodes)					Hard (20–30 nodes)						
		Llama-3.1	Mistral	Phi-4	<u>Qwen-2.5-7B</u>	<u>Qwen-2.5-7B</u>	Qwen-3	Llama-3.1	Mistral	Phi-4	<u>Qwen-2.5-7B</u>	Qwen-2.5-7B	Qwen-3
Triangle	$O(V^3)$	14.97	11.87	12.88	36.57	18.56	41.36	4.95	2.55	4.38	4.73	4.45	19.54
Diameter	$O(V(V+E))$	41.27	28.55	42.81	78.50	45.08	77.56	18.63	6.97	17.71	29.59	15.27	39.83
BFS order	$O(V+E)$	18.69	13.75	33.03	71.41	21.46	65.87	0.63	0.34	2.65	22.03	1.38	29.53
Shortest path	$O(V+E)$	38.75	31.18	42.61	90.03	47.46	77.69	23.03	12.21	26.60	72.53	28.31	64.28
Cycle	$O(V+E)$	55.49	55.44	45.25	74.02	62.19	90.30	52.40	51.64	40.64	68.40	58.88	86.81
Connectivity	$O(V+E)$	79.53	79.90	56.29	90.24	88.10	97.17	74.58	74.77	48.39	84.09	81.19	92.89

Table 29: Closed-Source LLM Performance Across Tasks Ranked by Computational Complexity (Mean Accuracy %). **Bold orange** / Underlined blue / Light purple highlights indicate best/second-best/third-best performance in each difficulty level.

Task	Time Complexity	Easy (5–10 nodes)				Hard (20–30 nodes)			
		Claude-3.5	GPT-4o	Gemini-2.0	o4-mini	Claude-3.5	GPT-4o	Gemini-2.0	o4-mini
Triangle	$O(V^3)$	43.41	36.32	50.33	84.54	15.92	12.81	15.55	17.53
Diameter	$O(V(V+E))$	83.71	63.99	79.14	98.88	56.70	45.60	23.45	34.61
BFS order	$O(V+E)$	91.42	81.48	90.31	95.46	26.80	21.58	27.77	32.45
Shortest path	$O(V+E)$	94.35	92.17	81.75	95.08	87.88	74.98	78.16	88.63
Cycle	$O(V+E)$	82.56	85.08	62.30	97.97	80.10	82.96	58.30	95.61
Connectivity	$O(V+E)$	98.38	95.63	92.61	98.23	96.99	90.59	87.99	92.02

Table 30: Aggregate Performance Comparison by Model Category and Task Complexity with Performance Degradation. Accuracy (%) with color intensity indicating performance level. Δ shows Easy→Hard performance drop.

Task	Time Complexity	Open-Source			Closed-Source		
		Easy	Hard	Δ	Easy	Hard	Δ
Triangle	$O(V^3)$	22.70	6.77	-15.93	53.65	15.45	-38.20
Diameter	$O(V(V+E))$	52.30	21.33	-30.97	81.43	40.09	-41.34
BFS order	$O(V+E)$	37.37	9.43	-27.94	89.67	27.15	-62.52
Shortest path	$O(V+E)$	54.62	37.83	-16.79	90.84	82.41	-8.43
Cycle	$O(V+E)$	63.78	59.76	-4.02	81.98	79.24	-2.74
Connectivity	$O(V+E)$	81.87	75.97	-5.90	96.21	91.90	-4.31
Mean		52.11	35.18	-16.93	82.30	56.04	-26.26

5832 **H.2 SCALING BEYOND 50 NODES**
58335834 To address scale concerns, we extend evaluation to 50–100 node graphs on representative models
5835 (Qwen-2.5-72B and o4-mini). Table 31 compares performance against the 20–30 node Hard split.5836 Performance degrades uniformly as graph size increases, but the fundamental patterns remain un-
5837 changed. Task difficulty ranking stays identical: Triangle counting and BFS order remain
5838 hardest, while Connectivity and Cycle detection remain most stable. Relative model perfor-
5839 mance gaps persist at similar magnitudes across scales. Critically, no new failure modes emerge, i.e.,
5840 the same challenges identified in smaller graphs (combinatorial enumeration, sequential dependencies,
5841 serialization sensitivity) simply intensify.5842 These results confirm that our 5–30 node design captures the essential reasoning challenges. Larger
5843 graphs amplify these challenges quantitatively but reveal no new qualitative phenomena, validating
5844 our focus on controlled-scale evaluation where reasoning capability, rather than resource constraints,
5845 determines performance.5846 Table 31: Results on 50–100 node graphs (EEH = Extremely Extra Hard). Results on the 20–30 node
5847 Hard split are shown in parentheses for comparison. **Bold orange** / Underlined blue highlights
5848 indicate best/second-best performance.

5851 Task	5852 Difficulty	5853 Open-source Model	5854 Closed-source Model
		5855 Qwen-2.5 (72B)	5856 o4-mini
5857 BFS order	5858 EEH	<u>8.19±2.03</u> (22.03)	10.23±2.07 (32.45)
5859 Connectivity	5860 EEH	<u>62.00±4.90</u> (84.09)	81.86±8.24 (92.02)
5861 Cycle	5862 EEH	<u>37.78±4.11</u> (68.40)	74.81±4.90 (95.61)
5863 Diameter	5864 EEH	<u>8.89±2.39</u> (29.59)	40.44±3.76 (34.61)
5865 Shortest path	5866 EEH	<u>33.28±6.09</u> (72.53)	68.51±11.04 (88.63)
5867 Triangle	5868 EEH	<u>2.36±0.67</u> (4.73)	2.85±0.71 (17.53)

5869 **H.3 ROBUSTNESS CHECK UNDER PROMPT NOISE (PERTURBATION)**5870 To address concerns about robustness to natural language variation, we conduct a supplementary
5871 evaluation examining model sensitivity to paraphrased prompts. In our main evaluation, we deliber-
5872 ately use deterministic phrasing within each prompt scheme to isolate the effects of our three core
5873 dimensions, i.e., graph types, serialization formats, and prompt schemes, without confounding factors
5874 from linguistic variation. This controlled design allows us to systematically attribute performance
5875 differences to structural representation choices (serialization formats) and reasoning guidance strate-
5876 gies (prompt schemes) rather than to incidental phrasing variations. However, real-world applications
5877 inevitably encounter diverse linguistic expressions of the same semantic content, and robustness to
5878 such variation is a practical concern. We therefore design a controlled perturbation framework to
5879 assess whether our conclusions remain stable under realistic linguistic variation.5880 **H.3.1 DESIGN OF THE STUDY**5881 **Task and Sample Selection.** We choose to conduct this robustness analysis on BFS order. This
5882 choice is motivated by three considerations: (1) it is among the most challenging tasks in our
5883 benchmark, exhibiting substantial performance gaps across models and difficulty levels; (2) it
5884 requires complex structured output (a full node ordering), making it potentially more sensitive to
5885 prompt variations that might affect the model’s understanding of output format requirements; and (3)
5886 given limited time and budget constraints, concentrating on a single representative hard task allows
5887 for deeper analysis. From the full BFS order dataset, we subsample 4,000 instances to balance
5888 coverage across graph types, serialization formats, prompt schemes, and difficulty levels.5889 **Perturbation Design.** Our perturbation framework defines *noisy prompts* as semantically equivalent
5890 (so it is still a problem with the same answer) but syntactically diverse variants of the original prompts.



Figure 34: Example of algorithm explanation perturbation. The original formal, numbered description (left) is transformed into conversational phrasing (right) while preserving algorithmic correctness. Highlighted changes show systematic replacement of technical terms with colloquial alternatives. Word-level changes: 47.9%.

And they are generated through systematic paraphrasing of natural-language components while maintaining the absolute structural preservation of graph data. The design adheres to three core principles:

1. *Semantic Equivalence*: All perturbations preserve the semantic content and task requirements through lexical substitution, syntactic restructuring, and stylistic variation. So it is designed to test linguistic invariance.
2. *Structural Preservation*: Graph representations remain character-for-character identical across all perturbations. This ensures that performance variation reflects model sensitivity to linguistic expression rather than changes in the underlying graph structure. In this way, the nature of the problem does not change much, and the ground truth results will still be the same.
3. *Comprehensive Coverage*: Perturbations span all nine prompt types in our framework (Algorithm, CoT, k-shot, Instruct, LTM, and their variants) and all seven serialization formats (Adjacency Matrix, Adjacency List, Adjacency Set, Edge List, Edge Set, GMoL, GMaL).

Perturbation Methodology. We construct task-specific variation pools for each perturbable component. For prompts containing algorithmic explanations, we develop multiple human-authored paraphrases that express the same procedural steps using different vocabulary, sentence structures, and explanatory styles. Figure 34 illustrates a representative example: the original formal description uses a numbered list structure with technical terminology (“Initialize”, “enqueue”, “dequeue”, “Mark visited”), while the perturbed version adopts a conversational flow with colloquial alternatives (“First”, “pick your”, “put it in”, “take out”, “Mark it as visited so we don’t check it again”). The transformation achieves 47.9% word-level change while maintaining algorithmic correctness and semantic equivalence.

For few-shot answer components, we generate variations that maintain identical logical reasoning and final answers while modifying transitional phrases and technical terminology. Figure 35 demonstrates this approach: the original example uses formal procedural terms (“Dequeue”, “neighbors”, “enqueue”, “visited”) that are systematically replaced with more natural alternatives (“Extract from queue”, “neighboring nodes”, “insert into queue”, “seen”). This achieves 17.5% word-level change through 29 replacements with 82.5% similarity, preserving the reasoning structure while varying linguistic expression. For instructional components, we create alternatives for opening statements, reasoning indicators, and procedural connectives. For task descriptions in minimal prompts, we paraphrase the task specification itself.

The perturbation process employs delimiter-based component extraction to precisely identify natural language elements while avoiding graph data. Specifically, we identify boundaries between natural language answers and graph representations (e.g., “And the graph representation of [format] is”)



Figure 35: Example of few-shot answer perturbation. The original formal reasoning (left) is paraphrased with natural language variation (right) while maintaining identical logical structure and final answer. Color-coded highlights show systematic terminology replacement (e.g., “Dequeue” → “Extract from queue”, “visited” → “seen”). Word-level changes: 17.5%.

to ensure that variations are applied exclusively to linguistic content. For each prompt, we randomly sample variations from component-specific pools matched to the prompt’s (prompt scheme, serialization format) combination, apply targeted string replacement using bounded pattern matching, and verify post-perturbation that all graph representations remain unchanged through format-specific validation procedures.

Quality Assurance. To guarantee structural preservation, we implement multi-level verification: format-specific validation for each of the seven serialization types (e.g., character-level comparison of matrix blocks, structural validation for GML/GraphML, exact content matching for list and set formats), automated testing on representative samples spanning all prompt-serialization combinations, and per-instance validation confirming preservation before evaluation. Our implementation achieves 100% graph structure preservation across all perturbations while successfully modifying 87.9% of prompts of the samples (with the remaining 12.1% representing cases where random sampling selects the original phrasing).

Summary. This framework enables systematic evaluation of whether model performance and our main conclusions remain stable under realistic linguistic variation, providing evidence for the robustness of our findings beyond the specific phrasings used in the primary benchmark.

H.3.2 EXPERIMENTAL RESULTS AND ANALYSIS

Experimental Setting. We evaluate two representative models from our main benchmark: **o4-mini** (top-performing closed-source reasoning model) and **Qwen-2.5-72B** (strongest open-source model). These models provide coverage of both closed-source and open-source categories and exhibited the highest performance in our main evaluation. We report results aggregated across prompt schemes and serialization formats separately, as well as fine-grained breakdowns per model, to assess whether our main conclusions about representation sensitivity remain stable under linguistic perturbation.

Overall Results. Tables 32 and 33 present results averaged across both models. Several key patterns emerge:

Preservation of relative performance patterns. The relative rankings of prompt schemes and serialization formats remain largely stable between original and perturbed conditions. For prompt schemes (Table 32), Algorithm, CoT, and Instruct consistently rank among the top three performers in Easy mode under both conditions, while 0-Shot maintains strong performance in Medium and Hard modes. For serialization formats (Table 33), AL and AS consistently dominate across all difficulty levels

5994 in both original and perturbed settings, with AL achieving 92.26% to 93.41% (Easy), 83.44% to
 5995 83.56% (Medium), and 48.27% to 50.33% (Hard). The persistence of these rankings confirms that
 5996 our main finding holds under linguistic variation, as no single configuration works universally, but
 5997 certain formats consistently outperform others.

5998 *Evidence of real perturbation effects.* While relative patterns are preserved, absolute performance
 5999 values shift measurably between conditions. For example, CoT improves from 85.26% to 90.98%
 6000 in Easy mode, while K-Shot shows variation from 80.48% to 78.36%. These changes confirm that
 6001 our perturbations introduce meaningful variation rather than being trivial paraphrases. We note that
 6002 performance differences may be partially attributable to the subsampling from the full dataset to
 6003 4,000 instances, though the consistency of relative patterns suggests this effect is limited.

Task	Difficulty	0-Algorithm	0-CoT	0-Instruct	0-Shot	Algorithm	CoT	Instruct	K-Shot	LTM
Original	E	84.71 \pm 8.99	78.36 \pm 10.06	82.32 \pm 9.07	83.22 \pm 9.08	85.82 \pm 7.12	85.26 \pm 7.45	86.86 \pm 6.13	80.48 \pm 8.52	83.88 \pm 8.58
	M	65.82 \pm 12.78	64.46 \pm 12.61	64.97 \pm 11.99	66.90 \pm 13.59	66.29 \pm 10.15	61.97 \pm 11.01	62.31 \pm 9.35	54.18 \pm 14.67	65.48 \pm 11.94
	H	32.22\pm10.81	<u>31.87\pm9.64</u>	29.42 \pm 9.90	31.69 \pm 10.66	26.93 \pm 8.37	22.67 \pm 5.51	20.90 \pm 6.63	20.26 \pm 8.55	29.18 \pm 10.15
Perturbed	E	84.98 \pm 14.09	75.50 \pm 14.08	85.54 \pm 9.64	79.13 \pm 15.83	85.82 \pm 4.49	90.98\pm7.83	78.21 \pm 16.30	78.36 \pm 10.79	<u>87.59\pm10.59</u>
	M	70.78 \pm 16.77	70.58 \pm 11.78	60.24 \pm 18.49	76.93\pm13.23	66.22 \pm 14.67	58.44 \pm 10.42	<u>70.90\pm11.63</u>	54.65 \pm 16.17	68.73 \pm 14.16
	H	<u>34.26\pm19.27</u>	28.38 \pm 12.29	27.46 \pm 14.77	41.06\pm15.69	26.93 \pm 12.75	22.38 \pm 9.41	18.75 \pm 7.55	21.27 \pm 12.25	32.37 \pm 12.90

6005 Table 32: Performance of Prompt Schemes with perturbed prompt (Mean \pm 95% CI Margin of All
 6006 Models). Averaged over **o4mini** and **Qwen-2.5-72B**. **Bold orange** / Underlined blue / Light purple
 6007 highlights indicate best/second-best/third-best performance in each difficulty level.

Task	Difficulty	AL	AM	AS	EL	ES	GMaL	GMoL
Original	E	92.26\pm3.71	75.24 \pm 10.67	91.88\pm3.76	82.28 \pm 7.11	82.17 \pm 6.40	<u>85.68\pm4.64</u>	74.51 \pm 8.09
	M	83.44\pm5.82	46.03 \pm 13.79	<u>79.44\pm6.32</u>	59.84 \pm 7.94	53.39 \pm 7.86	<u>67.04\pm6.66</u>	56.01 \pm 10.77
	H	48.27\pm6.14	7.46 \pm 2.72	<u>48.23\pm6.57</u>	20.74 \pm 3.70	15.56 \pm 2.76	26.95 \pm 3.29	23.46 \pm 5.37
Perturbed	E	93.41\pm5.30	74.08 \pm 15.27	<u>87.40\pm7.19</u>	80.64 \pm 15.75	81.91 \pm 8.49	<u>85.60\pm8.14</u>	77.67 \pm 12.33
	M	<u>83.56\pm11.24</u>	52.54 \pm 14.98	83.93\pm7.28	61.40 \pm 11.35	57.99 \pm 11.80	<u>62.85\pm10.07</u>	60.51 \pm 14.09
	H	50.33\pm10.84	6.97 \pm 6.66	<u>50.02\pm13.24</u>	22.52 \pm 8.83	24.93 \pm 11.77	19.24 \pm 6.17	22.38 \pm 8.42

6015 Table 33: Performance of Serialization Formats with perturbed prompt (Mean \pm 95%
 6016 CI Margin of All Models). Averaged over **o4-mini** and **Qwen-2.5-72B**.
 6017 **Bold orange** / Underlined blue / Light purple highlights indicate best/second-best/third-best
 6018 performance in each difficulty level.

6023 **Fine-Grained Results.** Tables 34–37 break down results per model, revealing differential robustness
 6024 characteristics:

6025 *o4-mini exhibits high robustness.* The closed-source reasoning model shows remarkable stability
 6026 across perturbations (Tables 34 and 35). For serialization formats, AL maintains 98.54% to 97.89%
 6027 (Easy), 91.75% to 92.20% (Medium), and 54.24% to 56.08% (Hard), with minimal changes in
 6028 ranking. For prompt schemes, the relative ordering remains nearly identical between conditions,
 6029 with only minor absolute shifts (e.g., 0-Algorithm improves from 95.84% to 97.64% in Easy mode).
 6030 This stability suggests that o4-mini’s reasoning capabilities are relatively invariant to surface-level
 6031 linguistic variation, consistent with its design for robust multi-step reasoning.

6032 *Qwen-2.5-72B shows greater sensitivity.* The open-source model exhibits larger absolute performance
 6033 shifts and wider confidence intervals under perturbation (Tables 36 and 37). For example, in
 6034 serialization formats, performance on AS varies from 86.68% to 77.64% (Easy) and 47.74% to
 6035 52.59% (Hard), with substantially increased variance (e.g., Hard mode: 10.30 to 27.65). Similarly,
 6036 prompt scheme performance shows notable fluctuation (e.g., CoT: 75.10% to 85.22% in Easy, 47.82%
 6037 to 46.85% in Medium). However, crucially, the *relative rankings* remain consistent: AL and AS
 6038 continue to outperform other serializations, and Algorithm/CoT/Instruct remain competitive prompt
 6039 schemes. This indicates that while open-source models may be more sensitive to phrasing variations,
 6040 our comparative conclusions about which representations work better are robust.

6041 **Summary.** Our robustness analysis demonstrates that the main conclusions of GRAPHOMNI remain
 6042 stable under realistic linguistic perturbation. While absolute performance values shift measurably,

6048

6049

Task	Difficulty	0-Algorithm	0-CoT	0-Instruct	0-Shot	Algorithm	CoT	Instruct	K-Shot	LTM
Original	E	95.84±2.29	94.66±3.43	<u>96.53±1.96</u>	94.66±2.76	97.02±2.05	95.42±1.58	96.32±2.16	93.90±2.26	94.80±2.51
	M	<u>83.06±6.30</u>	80.88±5.51	80.34±7.04	84.08±5.94	77.28±5.58	76.12±6.47	73.74±6.33	79.73±6.15	79.12±6.32
	H	37.88±12.33	<u>38.07±11.51</u>	35.77±13.43	39.31±14.47	26.98±10.81	26.26±7.98	21.48±7.40	31.85±11.55	34.45±12.51
Perturbed	E	97.64±1.76	95.54±2.69	<u>97.39±1.95</u>	96.36±3.85	95.20±4.17	95.92±2.65	94.71±3.32	93.37±2.53	95.48±2.82
	M	89.42±4.41	81.41±4.49	75.27±8.19	<u>86.36±7.86</u>	74.24±8.63	68.37±11.29	71.33±9.88	78.26±6.93	78.76±9.51
	H	41.10±19.67	33.05±16.53	33.75±16.26	50.55±15.98	27.23±13.65	24.28±10.70	27.30±6.95	<u>35.71±12.20</u>	34.86±17.31

6055

Table 34: Performance of Prompt Schemes with perturbed prompt (Mean±95% CI Margin of All Models) on **o4-mini**. **Bold orange** / Underlined blue / Light purple highlights indicate best/second-best/third-best performance in each difficulty level.

Task	Difficulty	AL	AM	AS	EL	ES	GMaL	GMoL
Original	E	98.54±0.63	96.06±1.47	<u>97.09±1.40</u>	95.74±1.14	95.25±1.00	94.71±1.51	90.83±2.72
	M	91.75±1.49	74.71±1.86	<u>87.20±4.62</u>	74.92±2.89	69.10±2.66	<u>79.63±3.63</u>	78.31±1.97
	H	54.24±5.95	12.83±1.73	<u>48.72±8.78</u>	27.49±2.78	19.01±3.80	31.11±4.72	33.74±4.02
Perturbed	E	97.89±1.76	96.99±2.15	<u>97.17±2.64</u>	95.29±2.12	95.20±2.90	94.20±2.81	93.39±2.76
	M	92.20±2.48	73.15±5.68	<u>87.22±7.43</u>	76.96±6.46	67.16±7.90	72.84±6.68	77.57±5.61
	H	56.08±10.23	13.51±12.75	<u>47.74±7.90</u>	31.36±12.84	28.68±9.58	24.25±7.84	33.20±11.99

6070

Table 35: Performance of Serialization Formats with perturbed prompt (Mean±95% CI Margin of All Models) on **o4-mini**. **Bold orange** / Underlined blue / Light purple highlights indicate best/second-best/third-best performance in each difficulty level.

Task	Difficulty	0-Algorithm	0-CoT	0-Instruct	0-Shot	Algorithm	CoT	Instruct	K-Shot	LTM
Original	E	73.58±13.66	62.07±9.30	68.10±9.70	71.78±13.48	74.62±7.41	<u>75.10±10.29</u>	77.39±6.59	67.06±8.88	72.95±12.65
	M	48.57±16.95	48.03±17.71	49.59±16.46	49.73±19.69	55.31±16.14	47.82±15.08	50.88±13.11	28.64±7.72	<u>51.84±18.43</u>
	H	<u>26.56±17.71</u>	25.67±14.87	23.07±13.88	24.07±14.43	26.88±13.67	19.08±10.17	20.32±11.63	8.68±3.39	23.92±15.94
Perturbed	E	72.33±25.53	52.11±15.51	71.71±14.31	61.91±26.30	72.70±16.55	85.22±16.18	55.11±29.20	60.84±12.59	<u>78.39±21.24</u>
	M	52.14±27.47	57.94±21.58	42.71±35.28	<u>65.93±25.51</u>	58.20±27.85	46.85±13.95	70.40±23.79	27.10±14.46	58.70±25.48
	H	28.39±32.49	23.71±18.80	20.12±26.21	31.56±26.38	26.62±22.75	20.16±17.12	11.43±10.14	1.05±2.06	<u>29.87±20.35</u>

6083

Table 36: Performance of Prompt Schemes with perturbed prompt (Mean±95% CI Margin of All Models) on **Qwen-2.5-72B**. **Bold orange** / Underlined blue / Light purple highlights indicate best/second-best/third-best performance in each difficulty level.

Task	Difficulty	AL	AM	AS	EL	ES	GMaL	GMoL
Original	E	<u>85.98±4.51</u>	54.42±8.08	86.68±5.68	68.82±6.28	69.09±2.97	<u>76.65±3.28</u>	58.20±3.92
	M	75.13±8.68	17.35±3.83	<u>71.69±9.52</u>	44.76±6.41	37.67±4.27	<u>54.44±4.82</u>	33.70±3.43
	H	<u>42.30±9.52</u>	2.08±0.76	47.74±10.30	13.99±2.60	12.10±2.53	22.80±2.67	13.17±2.23
Perturbed	E	87.65±10.82	51.17±21.97	<u>77.64±11.01</u>	47.66±34.42	68.62±11.31	<u>75.94±14.67</u>	59.99±20.12
	M	<u>74.92±21.42</u>	29.36±22.16	80.64±12.64	45.83±16.54	47.68±22.05	<u>50.00±17.76</u>	38.57±23.07
	H	<u>43.85±19.81</u>	1.25±2.45	52.59±27.65	13.67±9.54	<u>21.18±21.98</u>	13.59±8.54	11.57±6.71

6097

Table 37: Performance of Serialization Formats with perturbed prompt (Mean±95% CI Margin of All Models) on **Qwen-2.5-72B**. **Bold orange** / Underlined blue / Light purple highlights indicate best/second-best/third-best performance in each difficulty level.

6101

6102 confirming that perturbations introduce real variation rather than trivial paraphrases, the relative
6103 performance patterns across prompt schemes and serialization formats are preserved. Specifically,
6104 the finding that no single configuration works universally, but that certain serialization-prompt
6105 combinations consistently outperform others, holds across both original and perturbed conditions.
6106 The differential sensitivity between models (o4-mini showing higher robustness than Qwen-2.5-72B)
6107 provides an additional dimension for understanding model capabilities. These results validate the
6108 reliability of our benchmark findings while highlighting that prompt perturbation represents a valid
6109 and interesting dimension for future investigation. Importantly, our extensible framework design
6110 readily accommodates such extensions: future work could systematically incorporate perturbation
6111 as an additional evaluation axis alongside graph types, serialization formats, and prompt schemes,
6112 enabling deeper exploration of linguistic robustness in graph reasoning tasks.

6113 THE USE OF LARGE LANGUAGE MODELS

6114 We declare that we only use LLM to aid or polish writing in this paper. Of course, we use LLMs to
6115 do inference in our experiment since we need to evaluate them on GRAPHOMNI.

6116
6117
6118
6119
6120
6121
6122
6123
6124
6125
6126
6127
6128
6129
6130
6131
6132
6133
6134
6135
6136
6137
6138
6139
6140
6141
6142
6143
6144
6145
6146
6147
6148
6149
6150
6151
6152
6153
6154
6155